

UNCLASSIFIED

AD NUMBER
AD486499
NEW LIMITATION CHANGE
TO Approved for public release, distribution unlimited
FROM Distribution authorized to U.S. Gov't. agencies and their contractors; Administrative/Operational Use; Jan 1966. Other requests shall be referred to Army Electronics Command, Fort Monmouth, NJ.
AUTHORITY
USAEC ltr, 14 Mar 1969

THIS PAGE IS UNCLASSIFIED

JANSKY & BAILEY RESEARCH and ENGINEERING DEPARTMENT



#86499

TROPICAL PROPAGATION RESEARCH

Semiannual Report Number 7

1 July 1965 - 31 December 1965

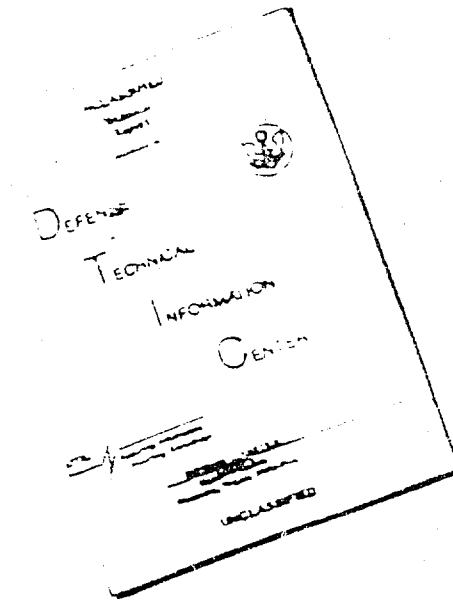
Prepared for
U. S. ARMY ELECTRONICS COMMAND
Fort Monmouth, New Jersey

Signal Corps Contract
DA 36-039 SC-90889

Sponsored by
ADVANCED RESEARCH PROJECTS AGENCY
Office of Secretary of Defense

ATLANTIC  RESEARCH

DISCLAIMER NOTICE



THIS DOCUMENT IS BEST
QUALITY AVAILABLE. THE COPY
FURNISHED TO DTIC CONTAINED
A SIGNIFICANT NUMBER OF
PAGES WHICH DO NOT
REPRODUCE LEGIBLY.

REPRODUCED FROM
BEST AVAILABLE COPY

TROPICAL PROPAGATION RESEARCH

Semiannual Report Number 7

1 July 1965 - 31 December 1965

Jansky & Bailey
Research and Engineering Division
of
Atlantic Research Corporation
Alexandria, Virginia


Prepared for
U. S. ARMY ELECTRONICS COMMAND

Sponsored by
ADVANCED RESEARCH PROJECTS AGENCY
Office of Secretary of Defense

ARPA Order Number:	371
Program Code Number:	2860
Contract Number:	DA 36-039 SC-90889

Approved by


Frank T. Mitchell, Jr.
Division Director


L. G. Sturgill
Project Director

ACKNOWLEDGMENT

This extensive radio propagation study program in Thailand has been possible only through the invaluable support of several organizations there. Jansky & Bailey particularly wishes to express its gratitude for the cooperation and assistance received from the Joint Thai - U. S. Military Research and Development Center in conducting the field measurements described in this report.

ABSTRACT

This is the seventh semiannual report on a research program involving theoretical and experimental studies of the propagation of radio waves in tropically vegetated environments. The over-all purpose of this program is to provide basic information about radio propagation phenomena that can be used to improve communications equipment and techniques for military forces in Southeast Asia and other areas with similar environments. The first comprehensive series of measurements of propagation and environmental data has been obtained in a "wet-dry" tropically vegetated area in Thailand in the vicinity of the town of Pak Chong. Propagation measurements have been made at discrete test frequencies in the 100-kc to 10-gc range.

A major portion of this program is concerned with the collection and analysis of basic data on radio propagation in relation to the physical characteristics of the natural environment that influence propagation losses. These characteristics include terrain features, climate, vegetation, and radio noise. The quantitative effects of the environment upon radio propagation losses are being studied through correlation analysis. The information thus obtained will be used to develop a comprehensive model that will permit practical predictions of range performance of tactical mobile communications equipment in any tropical environment.

The field measurements originally planned in the 100-kc to 425-mc frequency range at Pak Chong were essentially completed during this reporting period. This

report summarizes the results of these measurements and presents certain tentative conclusions which can be drawn from the work thus far.

A part of the field measurement program, not yet completed, has been devoted to measurements of line-of-sight propagation in the 400-mc to 10-gc frequency range over a well-defined, vegetated obstacle. This report presents the initial results of these measurements, including results from conjunctive measurements of the radio refractive index profile which were made with a balloon-borne wiresonde system.

CONTENTS

	<u>Page</u>
ACKNOWLEDGMENT	
ABSTRACT	1
1. INTRODUCTION	1-1
2. SUMMARY OF TEST PROGRAM TO DATE	2-1
2.1 Environment	2-3
2.1.1 Foliage	2-3
2.1.2 Terrain	2-6
2.1.3 Climate	2-13
2.2 Types of Measurements	2-16
2.3 Major Variables	2-21
2.4 Foliage Effect	2-25
2.5 Terrain Effect	2-31
2.6 Data Variability	2-35
2.6.1 Height and Time Variation	2-35
2.6.2 Vehicular Data	2-37
2.7 Polarization Comparison	2-44
3. FIXED-POINT DATA	3-1
3.1 Basic Fixed-Point Data	3-2
3.2 Smooth Curves for Basic Transmission Loss	3-7
3.3 Wet-Dry Comparisons	3-49
3.4 Height-Gain Profile Summary	3-78
3.5 Foliage Factor	3-90
3.5.1 Vertical Polarization Below 25 mc	3-90
3.5.2 Horizontal Polarization	3-99
4. VEHICULAR DATA	4-1
4.1 L_p vs Distance	4-4
4.2 Data Variability	4-11
5. CLIMATOLOGICAL DATA	5-1
6. 10-GC MEASUREMENT PROGRAM	6-1
6.1 Path Characteristics	6-2
6.2 Theoretical Knife-Edge Diffraction	6-8
6.3 Line-of-Sight Data	6-13
6.4 Diurnal Fading Data	6-19

CONTENTS, continued

	<u>Page</u>
6.5 Measurement Equipments and Techniques . . .	6-24
6.5.1 Conversion of Measurements to L_p . . .	6-26
6.5.2 Mounting of Antennas	6-28
6.5.3 Determination of Antenna Gain	6-29
6.5.4 Antennas	6-29
6.5.5 Transmitting Equipment	6-30
6.5.6 Receiving Equipment	6-31
7. REFRACTIVITY MEASUREMENTS	7-1
7.1 Measurement Setup, In-Foliage Measurements .	7-2
7.2 Measurement Setup, Out-of-Foliage Measurements	7-3
7.3 Sample Diurnal Plots	7-4
8. MEETINGS AND CONFERENCES	8-1
9. PROJECT PERSONNEL	9-1
APPENDIX A Vegetation Survey Report	A-1
REFERENCES	
DOCUMENT CONTROL DATA - R&D, DD Form 1473	
DISTRIBUTION LIST	

ILLUSTRATIONS

Figure		Page
2.1	Sample Floristic Profile	2-4
2.2	Sample Floristic Profile, Plan View	2-5
2.3	Composite Distribution of Tree Heights from All Plots	2-7
2.4	View of Typical Foliage	2-8
2.5	View of Typical Foliage	2-8
2.6	Aerial View of Transmitter Site	2-10
2.7	Aerial View of Terrain	2-10
2.8	Radial Points and Field Points in Sector A . .	2-11
2.9	Radial Points and Field Points in Sector B . .	2-12
2.10	Terrain Profile of Path Between Transmitter and Field Point FPA-8	2-14
2.11	Terrain Profile of Path Between Transmitter and Field Point FPB-8	2-15
2.12	Typical Field Point	2-17
2.13	Variation of Basic Transmission Loss with Receiving Antenna Height $L_b = F_B(25.5, 40, V, d, H_r)$	2-18
2.14	Typical Measurement Trail, Dry Season	2-20
2.15	Comparison of L_b vs Distance for Various Receiving Antenna Heights $L_b = F_A(f, H_t, V, d, H_r)$	2-24
2.16	Foliage Factor (F.F.)	2-27
2.17	Comparison Between Measured Results and Egli Model $L_b = F_A(25.5, 13-80, V, d, 13-80)$	2-29
2.18	Comparison Between Measured Results and Egli Model $L_b = F_A(100, 13-80, V, d, 13-80)$	2-30

ILLUSTRATIONS. continued

<u>Figure</u>		<u>Page</u>
2.19	Comparison Between Measured Results and NBS Model Including $G(H)$ Functions $L_b = F_A(25.5, 80, V, d, 80)$	2-33
2.20	Best Fit to Measured Results $L_b = F_A(25.5, 80, V, d, 80)$	2-34
2.21	Best Fit 10 db Below Measured Results $L_b = F_A(25.5, 80, V, d, 80)$	2-35
2.22	Example of Vehicular Raw Data $F_A(25.5, 40, V, 1.0-1.2, 7)$	2-38
2.23	Example of Vehicular Raw Data $F_A(250, 80, V, 0.8-1.0, 7)$	2-40
2.24	Statistical Distribution of L_b $L_b = F_A(25.5, 80, V, 0.4-0.6, 7)$	2-42
2.25	Comparison Between Vehicular Data and Measured F.P. Data $L_b = F_A(25.5, 80, V, d, 7)$	2-43
2.26	Standard Deviation of Vehicular Data $L_b = F_A(25.5, 80, V, d, 7)$	2-45
2.27	L_b for Vertical Polarization Minus L_b for Horizontal Polarization at 25.5 mc	2-46
2.28	L_b for Vertical Polarization Minus L_b for Horizontal Polarization at 400 mc	2-48
3.1	Measured Data Summary $L_b = F_{A,B}(0.105, 80, V, d, 17)$	3-8
3.2	Measured Data Summary $L_b = F_{A,B}(0.300, 80, V, d, 17)$	3-9
3.3	Measured Data Summary $L_b = F_{A,B}(0.880, 80, V, d, 17)$	3-10
3.4	Measured Data Summary $L_b = F_{A,B}(2.0, 80, V, d, 17)$	3-11

ILLUSTRATIONS, continued

<u>Figure</u>		<u>Page</u>
3.20	Measured Data Summary $L_b = F_{A,B}(0.105, 80, V, d, 80)$	3-27
3.21	Measured Data Summary $L_b = F_{A,B}(0.300, 80, V, d, 80)$	3-28
3.22	Measured Data Summary $L_b = F_{A,B}(0.880, 80, V, d, 80)$	3-29
3.23	Measured Data Summary $L_b = F_{A,B}(2.0, 80, V, d, 80)$	3-30
3.24	Measured Data Summary $L_b = F_{A,B}(6.0, 40, V, d, 80)$	3-31
3.25	Measured Data Summary $L_b = F_{A,B}(12.0, 20, V, d, 80)$	3-32
3.26	Measured Data Summary $L_b = F_{A,B}(25.5, 80, V, d, 80)$	3-33
3.27	Measured Data Summary $L_b = F_{A,B}(50.0, 80, V, d, 80)$	3-34
3.28	Measured Data Summary $L_b = F_{A,B}(100.0, 80, V, d, 80)$	3-35
3.29	Measured Data Summary $L_b = F_{A,B}(250.0, 80, V, d, 80)$	3-36
3.30	Measured Data Summary $L_b = F_{A,B}(400.0, 80, V, d, 80)$	3-37
3.31	Measured Data Summary $L_b = F_{A,B}(2.0, 80, H, d, 80)$	3-38
3.32	Measured Data Summary $L_b = F_{A,B}(6.0, 80, H, d, 80)$	3-39
3.33	Measured Data Summary $L_b = F_{A,B}(12.0, 80, H, d, 80)$	3-40
3.34	Measured Data Summary $L_b = F_{A,B}(25.5, 80, H, d, 80)$	3-41

ILLUSTRATIONS, continued

<u>Figure</u>		<u>Page</u>
3.35	Measured Data Summary $L_b = F_{A,B}(50.0, 80, H, d, 80)$	3-42
3.36	Measured Data Summary $L_b = F_{A,B}(100.0, 80, H, d, 80)$	3-43
3.57	Measured Data Summary $L_b = F_{A,B}(250.0, 80, H, d, 80)$	3-44
3.38	Measured Data Summary $L_b = F_{A,B}(400.0, 80, H, d, 80)$	3-45
3.39	Smoothed Fixed-Point Data $L_b = F_{A,B}(0.105, 80, V, d, 17)$	3-50
3.40	Smoothed Fixed-Point Data $L_b = F_{A,B}(0.300, 80, V, d, 17)$	3-51
3.41	Smoothed Fixed-Point Data $L_b = F_{A,B}(0.880, 80, V, d, 17)$	3-52
3.42	Smoothed Fixed-Point Data $L_b = F_{A,B}(2.0, 80, V, d, 17)$	3-53
3.43	Smoothed Fixed-Point Data $L_b = F_{A,B}(6.0, 40, V, d, 17)$	3-54
3.44	Smoothed Fixed-Point Data $L_b = F_{A,B}(12.0, 20, V, d, 17)$	3-55
3.45	Smoothed Fixed-Point Data $L_b = F_{A,B}(25.5, 10, V, d, 11)$	3-56
3.46	Smoothed Fixed-Point Data $L_b = F_{A,B}(50.0, 13, V, d, 20)$	3-57
3.47	Smoothed Fixed-Point Data $L_b = F_{A,B}(100.0, 13, V, d, 11)$	3-58
3.48	Smoothed Fixed-Point Data $L_b = F_{A,B}(250.0, 13, V, d, 11)$	3-59
3.49	Smoothed Fixed-Point Data $L_b = F_{A,B}(400.0, 13, V, d, 11)$	3-60

ILLUSTRATIONS, continued

<u>Figure</u>		<u>Page</u>
3.50	Composite of Smoothed Fixed-Point Data, Vertical Polarization, Low Antennas	3-61
3.51	Composite of Smoothed Fixed-Point Data, Vertical Polarization, High Antennas	3-62
3.52	Composite of Smoothed Fixed-Point Data, Hori- zontal Polarization, Low Antennas	3-63
3.53	Composite of Smoothed Fixed-Point Data, Hori- zontal Polarization, High Antennas	3-64
3.54	Smoothed Fixed-Point Data $L_b = F_{A,B}(2.0, 80, H, d, 80)$	3-65
3.55	Smoothed Fixed-Point Data $L_b = F_{A,B}(6.0, 80, H, d, 80)$	3-66
3.56	Smoothed Fixed-Point Data $L_b = F_{A,B}(12.0, 80, H, d, 80)$	3-67
3.57	Smoothed Fixed-Point Data $L_b = F_{A,B}(25.5, 80, H, d, 80)$	3-68
3.58	Smoothed Fixed-Point Data $L_b = F_{A,B}(50.0, 80, H, d, 80)$	3-69
3.59	Smoothed Fixed-Point Data $L_b = F_{A,B}(100.0, 80, H, d, 80)$	3-70
3.60	Smoothed Fixed-Point Data $L_b = F_{A,B}(250.0, 80, H, d, 80)$	3-71
3.61	Smoothed Fixed-Point Data $L_b = F_{A,B}(400.0, 80, H, d, 80)$	3-72
3.62	Height Gain, Vertical Polarization	3-86
3.63	Height Gain, Horizontal Polarization	3-87
3.64	Foliage Factor (F.F.) for Vertical Polarization	3-92

ILLUSTRATIONS, continued

<u>Figure</u>		<u>Page</u>
4.1	Example of Rapid and Slow Variations of Vehicular Data $L_b = F_B(100.0, 80, V, d, 7)$	4-2
4.2	Summary of Basic Transmission Loss vs Distance for Vehicular Data $L_b = F_A(f, 13, V, d, 7)$	4-5
4.3	Summary of Basic Transmission Loss vs Distance for Vehicular Data $L_b = F_A(f, 13, H, d, 7)$	4-6
4.4	Median Basic Transmission Loss Near the Antenna $L_b = F_A(100.0, 80, V, d, 7)$	4-10
4.5	(Part A) Median Basic Transmission Loss from Vehicular Data $L_b = F_A(100.0, 80, V, d, 7)$	4-15
4.5	(Part B) Median Basic Transmission Loss from Vehicular Data $L_b = F_A(100.0, 80, V, d, 7)$	4-16
4.5	(Part C) Median Basic Transmission Loss from Vehicular Data $L_b = F_A(100.0, 80, V, d, 7)$	4-17
5.1	Rainfall Measurement Points	5-5
5.2	Climatological Data	5-6
6.1	Line-of-Sight Profile for Area A	6-3
6.2	Physical Characteristics of Obstacle	6-7
6.3	Knife-Edge Path with First Fresnel Zone Clearance	6-8
6.4	$A(v)$ and $\phi(v)$ vs v for Perfect Knife Edge	6-12
6.5	Measured Knife Edge Loss at 550 mc	6-14
6.6	Measured Knife Edge Loss at 1.0 gc	6-15

ILLUSTRATIONS, continued

<u>Figure</u>		<u>Page</u>
6.7	Measured Knife Edge Loss at 2.5 gc	6-16
6.8	Measured Knife Edge Loss at 5.0 gc	6-17
6.9	Measured Knife Edge Loss at 10.0 gc	6-18
6.10	Diurnal Variation of L_b at 550 mc	6-21
6.11	Diurnal Variation of L_b at 1.0 gc	6-22
6.12	Diurnal Variation of L_b at 10.0 gc	6-23
6.13	Transmitter Basic Block Diagram	6-25
6.14	Receiver Basic Block Diagram	6-25
7.1	Diurnal Variation of Refractivity Profile (30-31 July 1965)	7-6
7.2	Diurnal Variation of Refractivity Profile (1-2 August 1965)	7-7
A.1	Map of Proposed Measurement Location	A-4

1. INTRODUCTION

This is the seventh semiannual report on the theoretical and experimental research program on the propagation of radio waves in a tropically vegetated environment being conducted by the Jansky & Bailey Research and Engineering Department of Atlantic Research Corporation. This program is sponsored by the Advanced Research Projects Agency, Department of Defense, and is directed by the U. S. Army Electronics Command, Fort Monmouth, New Jersey.

The experimental phase of the program is carried out in a large, tropically vegetated area in Thailand. Measured data on radio transmission loss is taken at discrete test frequencies from 0.1 to 10,000 mc for transmission distances up to 30 miles and varying heights of transmitting and receiving antennas of both horizontal and vertical polarizations. The data is measured in both the wet and dry seasons. In addition to conducting the propagation measurements, project field personnel maintained extensive records on such aspects of the physical environment as climatic data, terrain profiles, vegetation characteristics, and ambient radio noise.

These data are then reduced and analyzed with the objective of separating the effects of the various environmental parameters on path loss. The knowledge gained is to be used to develop a comprehensive model for the prediction of radio path loss characteristics for any tropical environment.

The field measurement program is divided into two tasks, or subprograms. The first task involves the

7

measurements in the frequency range of 0.1 to 400 mc. The second task involves measurements in the frequency range of 400 to 10,000 mc. The measurement techniques and equipments used are described in detail in the respective Primary Field Test Plans.

The field measurements in the 0.1-to-400-mc range, conducted in a wet-dry vegetated area near Pak Chong, were nearly completed during this period. These measurements were made in two sectors of the Pak Chong measurement area, designated Sectors A and B. About one half of the measurements in the 400-to-10,000-mc range have been completed.

Throughout this report a number of hypotheses concerning propagation in foliated environments are presented. The development, testing, and modification of these hypotheses are important steps in the development of a theory for propagation in foliated environments. Some of these hypotheses have evolved from an examination of a limited data base. Others have evolved from a preliminary analysis of the much larger reduced data base which only recently has come into being. The evidence in favor of some of these hypotheses is strong even at this time. For others, the present evidence is not as strong, and in some cases further validation of these hypotheses and the details of the phenomena suggested by these hypotheses can be obtained from additional experimentation within the foliage and can be obtained with short antenna separation distances.

The most important of these hypotheses are summarized below. As analysis proceeds it is likely that some of these hypotheses will be dropped, others modified, and new ones added.

1. Hypothesis: The foliage factor (i.e., the difference in propagation loss between that which is observed in the presence of foliage and that which is expected in the absence of foliage) is independent of distance for frequencies from 0.1 to 400 mc and all distances beyond 0.2 mile. At 100 mc, the distance independence for the foliage factor has been observed to hold at least to within 350 feet of the antenna.
2. Hypothesis: If the antenna is within $\lambda/2$ of the foliage, there is a foliage effect which is inversely proportional to the antenna-to-foliage separation. This is called the antenna-to-foliage coupling factor.
3. Hypothesis: For frequencies of 1 mc and below there is no foliage effect other than the antenna proximity effect mentioned in Hypothesis 2. For frequencies of 1 mc and above there is an additional foliage effect which increases at a rate of $9 \log f_{mc}$ for vertical polarization and $15 \log f_{mc}$ for horizontal polarization. This is called the vegetation attenuation factor.
4. Hypothesis: There is no significant statistical difference between the data collected in Sector A and the data collected in Sector B.
5. Hypothesis: There is no significant statistical difference between the data collected in the wet and dry seasons.
6. Hypothesis: On the average, loss increases with distance at the rate of $40 \log d$ with the following exceptions for which the increase is less:
 - (1) Vertical polarization below 1 mc.

- (2) Horizontal polarization with low antennas at 100 mc and above.
- (3) Horizontal polarization with high antennas at 250 mc and above.

7. Hypothesis: There is no height gain for vertical polarization below 12 mc. There is only a slight height gain for vertical polarization at 12 mc. For all other vertical polarization cases and for all horizontal polarization cases, a height gain of $20 \log h$ or better can be expected. In particular:

<u>Freq. (mc)</u>	<u>Pol.</u>	<u>Height Gain Type</u>	<u>Advantage in Changing One Antenna Height From 10' to 80'</u>
2-100	H	$20 \log h$	18 db
25-50	V	$20 \log h$	18 db
250-400	H	αh	23 db
100-400	V	αh	22 db

where h is antenna height in feet and α is considered a constant.

8. Hypothesis: Within the foliage, propagation loss has two distinctive types of variation: a rapid variation associated with the presence of foliage, and a less rapid variation associated with the presence of terrain. It is important to study the following characteristics of each of these variations.

- (1) Type of statistical distribution the amplitudes follow.
- (2) The standard deviation as a measure of total data variation.
- (3) Average length of one cycle of variation measured in feet.

9. Hypothesis: Propagation loss within foliage does not vary significantly with time for short time intervals in the distance ranges out to 15 miles and the frequency range from 100 kc to 400 mc.

Section 2 of this report summarizes the results of the field measurements in the 0.1 to 400-mc range thus far obtained. Section 3 is devoted to the analysis and discussion of the data obtained from the stationary antenna measurements, that is, measurements in which only the antenna heights are varied. Section 4 is concerned exclusively with data from the vehicular measurements. The climatological data obtained from the Pak Chong area is summarized in Section 5.

In Section 6, the results from the data thus far obtained from the measurements above 400 mc are discussed. Measurements of the vertical radio refractivity profile, up to about 1000 feet above ground, are carried out as a part of the 400- to 10,000-mc measurements. The results of the radio refractivity measurements are presented in Section 7. Sections 8 and 9 are devoted to Conferences, and Project Personnel, respectively.

Appendix A is a report by Edward N. Gladish on vegetative aspects of a survey of potential second measurement sites in which he participated. Mr. Gladish is a forestry consultant to Atlantic Research Corporation.

2. SUMMARY OF TEST PROGRAM TO DATE

In summary, the over-all objective of the current propagation measurement program is to improve existing knowledge of radio frequency propagation characteristics in foliated environments such as those found in Southeast Asia. This improved propagation knowledge will be used in turn to aid in the development of improved tactical communication capabilities in these extremely adverse types of environment.

Although the measurement program consists of a large number of point-to-point measurements, the ultimate interest is not in point-to-point conditions per se but rather in the full range of propagation possibilities within a dynamic tactical situation. Since there is always a high degree of statistical uncertainty in a tactical communications situation, it is important to know the full range of possibility for each system variable. A complete knowledge of the statistical distributions of the important parameters is essential to a realistic assessment of reliability of communications in foliated environments. Only through a proper understanding of the propagation mechanism in such environments can systems planners hope to provide improved tactical communications.

Two measurement programs of interest are being conducted in Thailand. The first, which covers the frequency range from 100 kc to 400 mc, is referred to as the 400-mc program. The second, which covers the 550-mc to 10-gc range, is referred to as the 10-gc program. The 10-gc program consists of two basic types of measurements. The first type involves propagation measurements over line-of-sight paths

of approximately 3 miles which traverse a foliated obstacle. The detailed effects of the foliated obstacle are studied by changing the heights of the transmitting and receiving antennas so that propagation conditions vary from complete obstruction up to more than first Fresnel zone clearance. Data from these tests has been analyzed. The results are presented in Section 6 of this report. The measured result for the foliated environment agree very well with theoretical results for nonfoliated environments. As part of the 10-gc line-of-sight experiments, meteorological measurements for use in the computation of radio refractive index are being made from ground-based towers at heights up to 80 feet and by means of wiresonde at altitudes up to 1000 feet.

The second task under the 10-gc program consists of short-range propagation measurements at various heights within the foliage. The purpose of these tests is to obtain and analyze basic propagation data which will be useful in the design and evaluation of ground-based short-range surveillance and intrusion detection systems as well as of communications systems.

The next portion of Section 2 is devoted to a review of the type of environment in which the measurements in the vicinity of Pak Chong are being made. The remainder of Section 2 will be devoted to a detailed summary of the 400-mc project only, since most of the 10-gc data is presented for the first time in Section 6 of this report.

2.1 Environment

2.1.1 Foliage

A rather detailed study has been made of the foliage in a number of sample plots within the Pak Chong measurement areas.¹ Figure 2.1 illustrates the floristic profile in one of these plots. As can be seen from Figure 2.1, trees reach heights of more than 40 meters. The average tree height, however, is about 10 meters. In addition to the trees shown in Figure 2.1, there is a relatively dense undergrowth which extends to a height of approximately 6 meters. Figure 2.2, a plan view of the sample plot shown in Figure 2.1, illustrates that the trees do not form a solid canopy.

The Pak Chong area in which propagation measurements are being made is considered a wet-dry tropical region; i.e., although the vegetation remains green for the entire year, there is a distinct wet season and a distinct dry season. Table 1, which summarizes the foliage statistics for nine sample plots, may be considered as a characterization of a typical wet-dry tropical region. The size of the sample plot in most cases was 10 meters by 40 meters. However, in two cases the sample plot was 10 meters by 60 meters. Table 1 shows the density of the trees, which varied from 314 trees to 475 trees per acre. The table also gives the basal area of the trees. Basal area is the total cross-sectional area of trees in one acre at a height of

1. Christensen, Kelley, Anan Nalampoon, and Sommart Sukhawong, Environmental Description 1 of the Jansky & Bailey Test Site at Khao Yai, Thailand, 66-015 Joint Thai - U. S. Military Research and Development Center; January 1966.

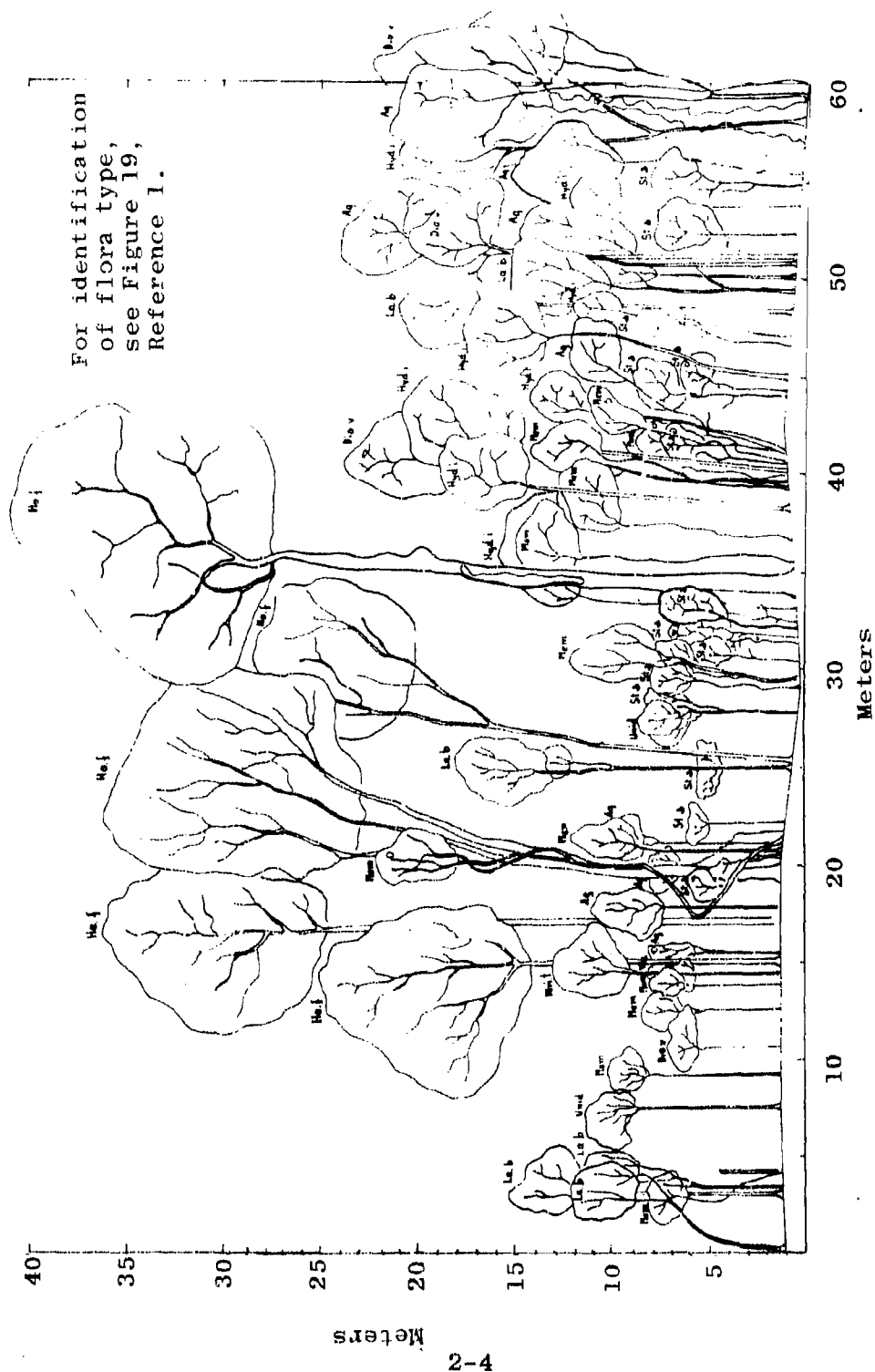


Figure 2.1 Sample Floristic Profile

Numbers are arbitrary
sample numbers. See
Figure 19, Reference 1.

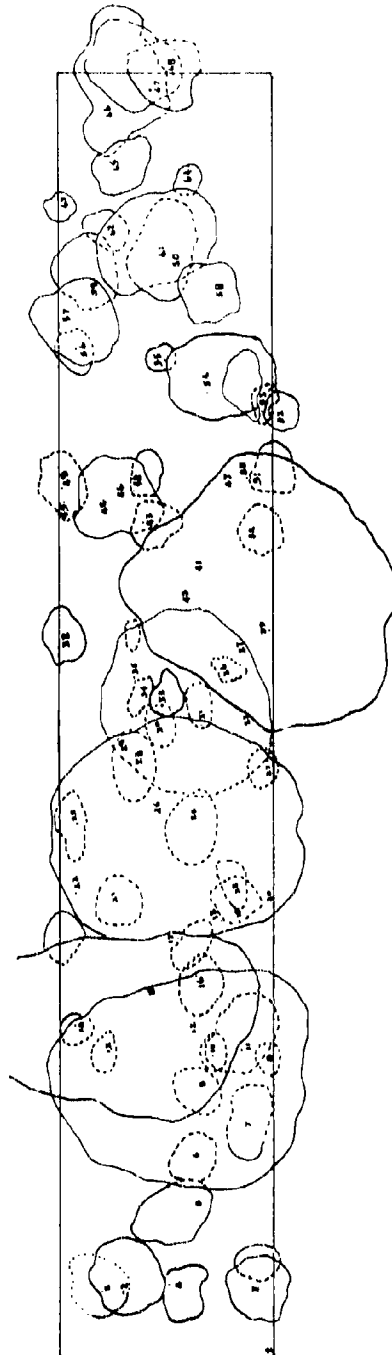


Figure 2.2 Sample Floristic Profile, Plan View

about 1.5 meters. Finally, Table 1 shows the median height of trees in each sample plot. The median height varied considerably from plot to plot. The range is from 5.5 meters to 14 meters; the over-all average is slightly over 10 meters.

Table 1
FOLIAGE SUMMARY

<u>Plot No.</u>	<u>Plot Area (meters²)</u>	<u>Trees/Acre</u>	<u>Basal Area Feet²/Acre</u>	<u>Median Ht. (meters)</u>
1	400	354	55.9	8.6
2	400	364	45.7	5.5
3	400	314	68.0	12.0
4	400	475	74.2	8.5
5	600	337	109.0	14.0
6	400	354	175.0	11.0
7	400	405	130.0	10.0
8	400	334	165.0	11.0
9	600	458	175.0	10.0
Average		377	110.9	10.1

It is interesting to note that statistical distribution of the tree heights plotted in Figure 2.3 is log normal with a median of 10 meters. Figures 2.4 and 2.5 show typical examples of the actual foliage as seen at eye level.

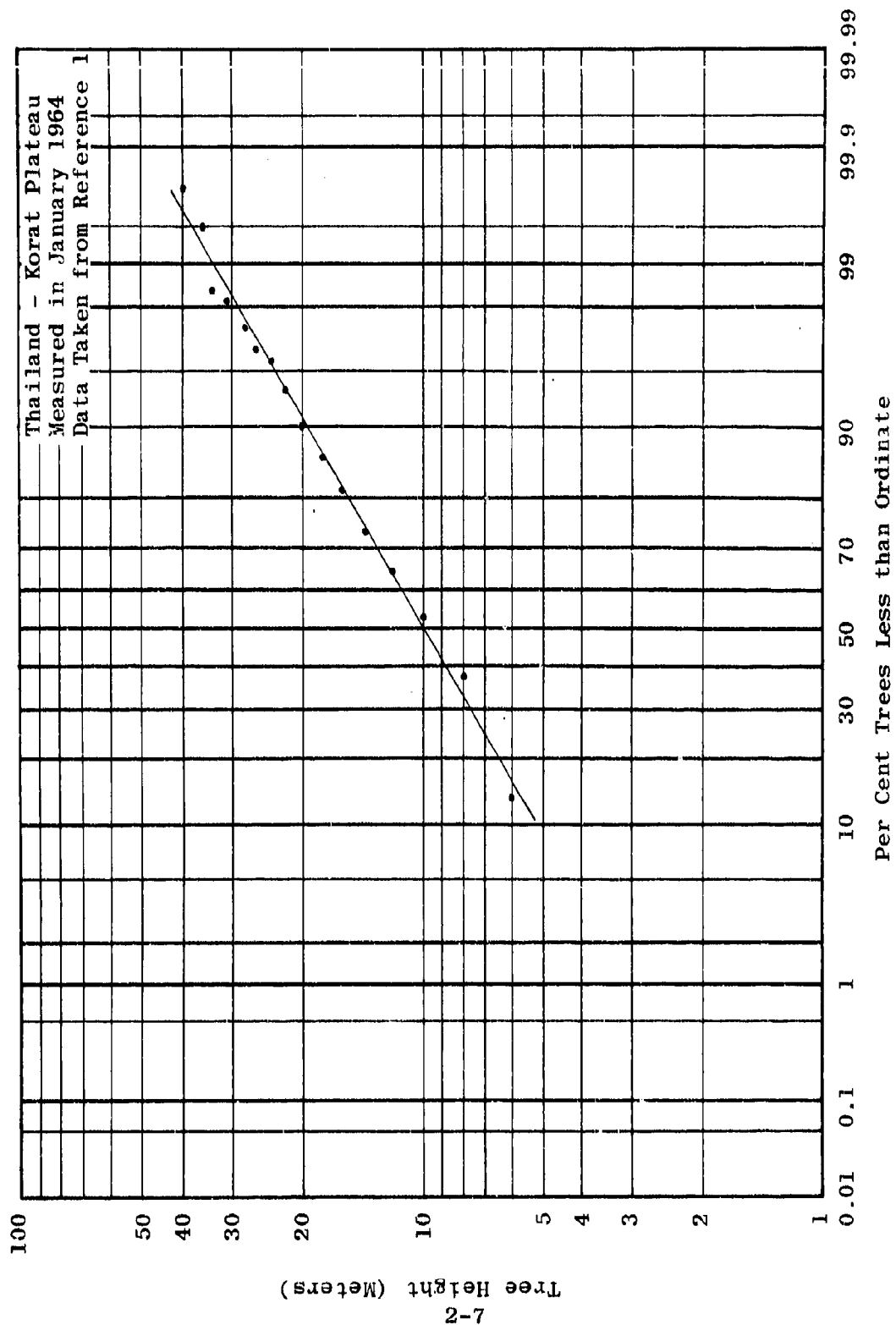


Figure 2.3 Composite Distribution of Tree Heights from All Plots



Figure 2.4 View of Typical Foliage



Figure 2.5 View of Typical Foliage

2.1.2 Terrain

A measurement area about 30 miles in extent has been established in the Pak Chong area. Propagation measurements are made by transmitting from a base camp and making measurements of received field strengths at various remote points within the foliage. Figure 2.6 is an aerial photograph of the base camp. The transmitting antennas are in the foliage just to the left of Figure 2.6. The transmitters are in the building complex at the left of the figure. Measurement trails extend from the transmitting site along the path which is just barely perceptible in the center of Figure 2.6. Figure 2.7 is an aerial view of the terrain in which the measurements are made. This figure shows the relatively rugged nature of the terrain.

Two measurement sectors have been established. The first, denoted as Sector A, extends in a southeasterly direction from the transmitting site. A trail which has been established through this sector is shown in Figure 2.8. Points along the trail, designated as A1 through A41 on Figure 2.8, have been calibrated in terms of radial distance from the transmitting site. Points at intervals of 0.2 mile have been surveyed and marked within 3 miles of the transmitting site. Beyond 3 miles, points have been calibrated at 0.5-mile intervals. Certain calibrated points along the trail have been designated FP or field points. Detailed measurements are made at these FP locations. Vehicular recordings of field strength are made between FP locations.

Sector B, which runs in a southwesterly direction from the transmitter site, is shown in Figure 2.9. As shown in Figure 2.9, radial distance from the transmitter site has



Figure 2.6 Aerial View of Transmitter Site



Figure 2.7 Aerial View of Terrain

been calibrated throughout this sector in the same manner used in Sector A.

The eighth fixed measuring point in Sector A, designated FPA-8, is an example of the measurement area terrain. Figure 2.10 shows the terrain profile between FPA-8 and the transmitting antenna site. Figure 2.10 also shows a distinct terrain obstacle in the path at a distance of slightly more than 1 mile. In addition, at this particular measuring point, there are several smaller terrain obstacles. This presence of a predominant terrain obstacle between 1 and 2 miles is common to most of the fixed measuring points. Therefore, in most cases, measurements taken beyond 1 mile would involve a diffracted mode of propagation in the absence of foliage. For distances of less than 1 mile, the mode of propagation in the absence of foliage would be line of sight. Figure 2.11 shows the terrain profile between FPA-8 and the transmitter site. In the case of Sector B, terrain obstacles are similar, but the terrain is somewhat rougher.

2.1.3 Climate

A detailed summary of the climatological data which has been recorded during the course of measurements at Pak Chong is presented in Section 5 of this report. The foliage remains green throughout the year, but there are two distinct seasons. One season, designated as wet, extends from about May 15 to November 15. During this season, rainfall is frequent and heavy. The foliage grows rapidly, and the floor of the jungle remains moist throughout the wet season.

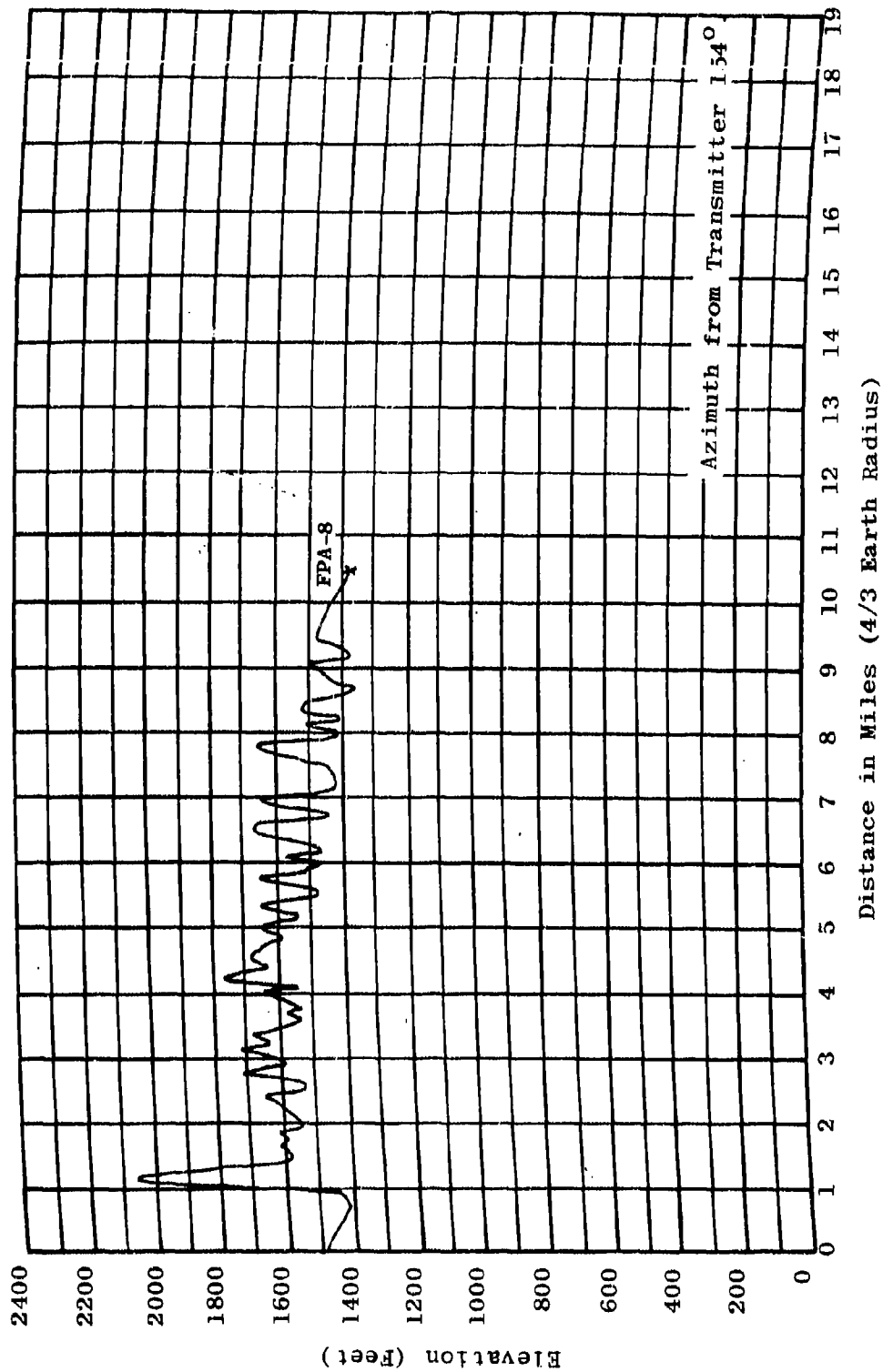


Figure 2.10 Terrain Profile of Path Between Transmitter and Field Point FPA-8

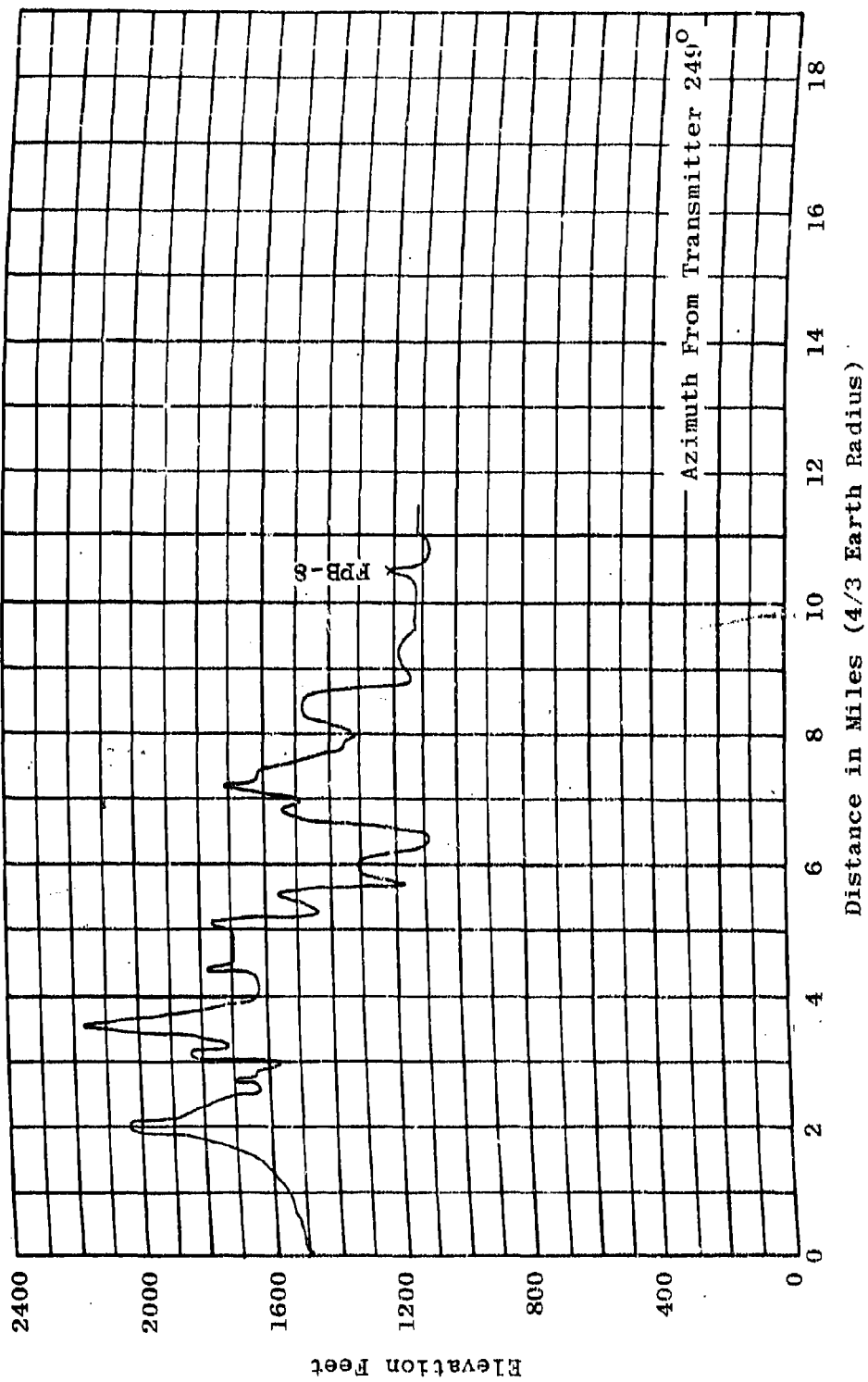


Figure 2.11 Terrain Profile of Path Between Transmitter and Field Point FPB-8

During the dry season, which extends from November 15 until May 15, foliage growth stops. Foliage remains on the trees but dries out. The floor of the jungle also dries out. Although there are significant amounts of rain during the dry season, the average rainfall during the dry season is lower than that for the wet season.

Average daytime temperatures vary from about 70°F to about 85°F. Temperatures tend to be higher in the dry season and lower in the wet season. Average daytime relative humidities vary from 50 per cent to about 80 per cent and tend to be lower in the dry season and higher in the wet season.

2.2 Types of Measurements

Two types of propagation measurements are being carried out in the 400-mc project. The first type is detailed point-to-point measurements which are made at each of the fixed points in Sectors A and B. A telescoping tower is erected at each fixed point. Figure 2.12 shows such a tower. Field strengths are recorded as the tower is lowered from about 80 feet to 11 feet. The type of data produced by these fixed-point measurements is shown in Figure 2.13. The continuous field strength recordings which were obtained as height varies are segmented into height increments of approximately 5 feet, and the median observed field strength is obtained for each increment. These medians are then translated into units of basic transmission loss. These median basic-transmission-loss data points for a typical sequence of measurements are shown plotted on Figure 2.13.

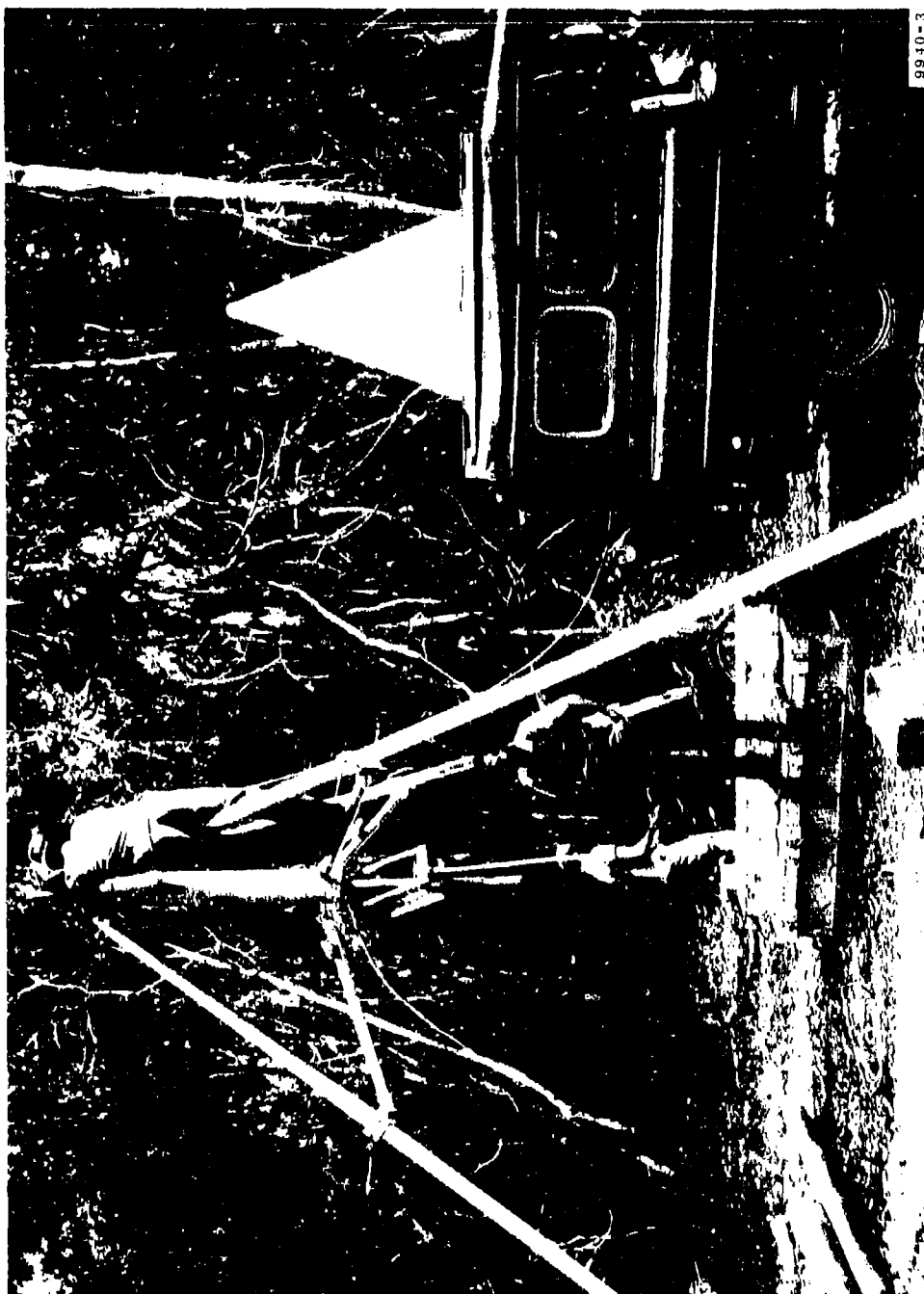


Figure 2.12 Typical Field Point

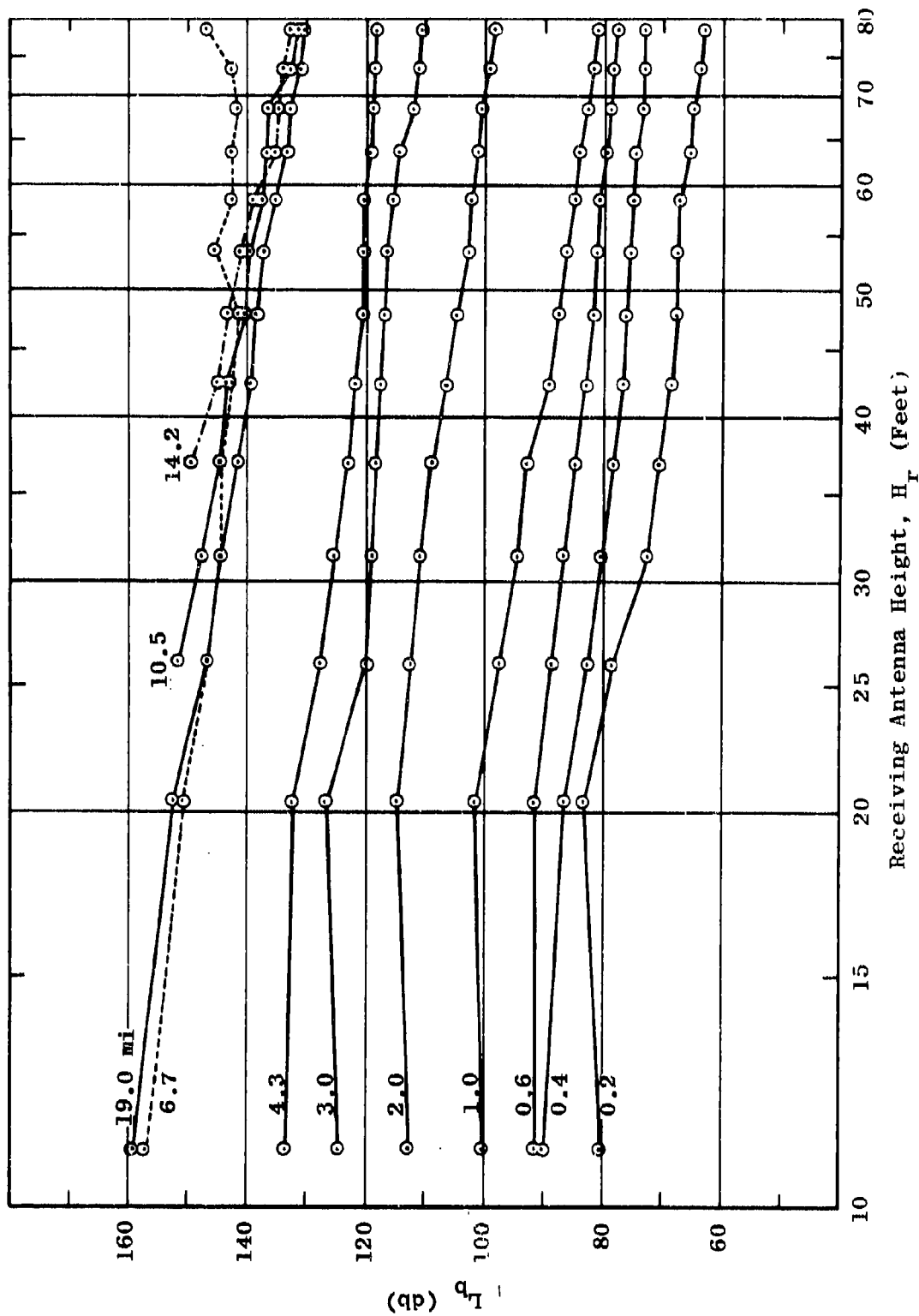


Figure 2.13 Variation of Basic Transmission Loss with Receiving Antenna Height
 $L_b = F_B(25.5, 40, V, d, H_r)$

Each of the curves on Figure 2.13 corresponds to a single height profile made at one of the fixed measuring points.

It has been found convenient to use the following systematic method of identifying the various sets and families of curves similar to the one shown in Figure 2.13.

$$L_b = F(f, H_t, P, d, H_r)$$

The above format, which is used to identify each L_b graph, relates the basic transmission loss derived from measurements to five basic variables: frequency, in megacycles, f ; transmitting antenna height, in feet, H_t ; polarization, horizontal or vertical, P ; distance in miles, d ; and receiving antenna height, in feet, H_r . The identification used on Figure 2.13 is

$$L_b = F_B(25.5, 40, V, d, H_r)$$

This identification indicates that the receiving antenna height and distance were varied while the other three variables remained fixed at the values indicated. The subscript "B" denotes Sector B data. A subscript "A" identifies data from Sector A.

In addition to the propagation measurements which are made at each fixed point, continuous recordings of field strength are made as a vehicle proceeds along a trail from one fixed point to the next. Figure 2.14 shows a typical measurement trail in the dry season. The vehicle shown in

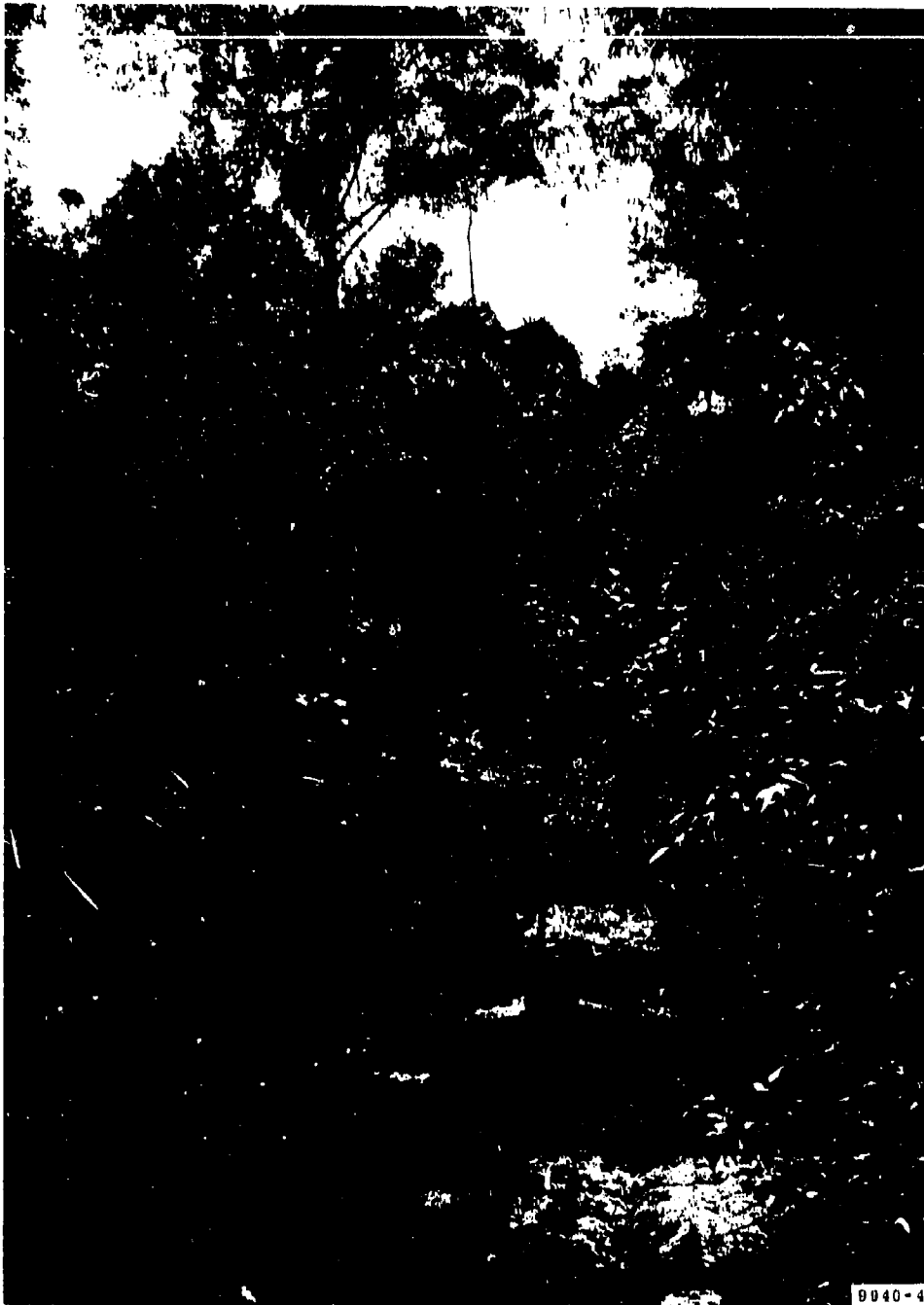


Figure 2.14 Typical Measurement Trail, Dry Season

Figure 2.12 is typical of those used for the vehicular recordings. The data obtained at the fixed receiving points is known as fixed-point or FP data. The continuous recordings of field strength along each measurement trail are referred to in this report as vehicular data.

2.3 Major Variables

In reviewing and analyzing measurement results, it is important to keep in mind the key variables and the ranges over which they are considered. Table 2 summarizes the span of measurement variables for the frequency range from 105 kc to 400 mc. Measurements are made at 11 frequencies within this range. They are made over two sectors which differ slightly in terrain characteristics. The vehicular data is gathered continuously with distance beginning at 0.2 mile. There are 28 measuring points distributed between Sector A and Sector B. Most of these points are interconnected by measurement trails. However, some of the measuring points are not accessible by trail and require the use of a helicopter to transport measuring equipment:

FPA-11, FPA-12, FPB-8.5, FPB-9.5, FPB-11, and FPB-12. In general, three transmitting antenna heights are used, as shown in Table 2. One, at about 13 feet, ensures that the antenna is well submerged in foliage. The second, at about 40 feet, corresponds roughly to treetop height for a majority of the trees. The third, at about 80 feet, corresponds to a height well above most of the trees. These three transmitting antenna heights are not used for vertical polarization in the frequency range from 105 kc to 12 mc. A vertical ground-based antenna is used in this frequency range. For these lower frequencies no significant variation of field

Table 2

MEASUREMENT VARIABLES
(105 kc to 400 mc)

Frequency: 0.105, 0.300, 0.880, 2, 6, 12, 25.5, 50, 100,
(mc) 250, 400

Sectors: A and B

Distances: For vehicular measurements - continuous
(miles)

For fixed point measurements -

FPA-1	0.2	FPB-1	0.2
FPA-2	0.45	FPB-2	0.45
FPA-3	0.7	FPB-3	0.7
FPA-4	1.0	FPB-4	1.0
FPA-5	2.0	FPB-5	2.0
FPA-5.5	3.0	FPB-5.5	3.0
FPA-6	4.0	FPB-6	4.3
FPA-7	7.0	FPB-7	6.7
FPA-8	10.5	FPB-8	10.5
FPA-9	14.0	FPB-8.5	11.4
FPA-10	17.0	FPB-9	14.2
FPA-11	23.54	FPB-9.5	15.3
FPA-12	30.00	FPB-10	19.0
		FPB-11	21.6
		FPB-12	28.9

Trans. In foliage - 13 feet
Antenna Treetop - 40 feet
Heights: Out of foliage - 80 feet

Receiving Vehicular - 7 feet
Antenna Fixed points - continuous from 11 to 80 feet
Heights:

Polarizations: Horizontal and vertical

strength with antenna height is expected, and, in fact, none occurs. Figure 2.15 compares the basic transmission loss observed for various receiving antenna heights in the lower frequency ranges. As Figure 2.15 shows, there is no significant variation with antenna height below 12 mc.

Returning to Table 2, receiving antenna heights for the vehicular measurements are nominally 7 feet. For the fixed-point measurements, receiving antenna height is varied continuously from 11 to 80 feet. The polarizations used are both horizontal and vertical. No intensive study of cross-polarization effects has been made to date. However, since limited experimentation indicates that significant cross-polarization components can exist, it is recommended that a more detailed study of this effect be included in the present measuring program.

Measurements currently are being made in only one type of foliage. To establish a model which contains foliage characteristics as a parameter, it will be necessary to examine at least one other type of significantly different foliated area. Two measurement programs, one in a New Guinea rain forest in 1945,² and the other in Panama,³ give strong evidence that significantly different foliated areas have decidedly different propagation characteristics. The Panama data, collected by Herbstreit and Crichlow³ in 1943, included propagation measurements made at 2, 6, 44 and 99 mc over distances up to 1 mile.

2. H. C. T. Whale, "Ground Aerials," M. Sc. Thesis; 1945.
3. J. W. Herbstreit and W. Q. Crichlow, "Measurement of Factors Affecting Jungle Radio Communications," Office of Chief Signal Officer, Operational Research Branch, ORB-2-3; November 1943.

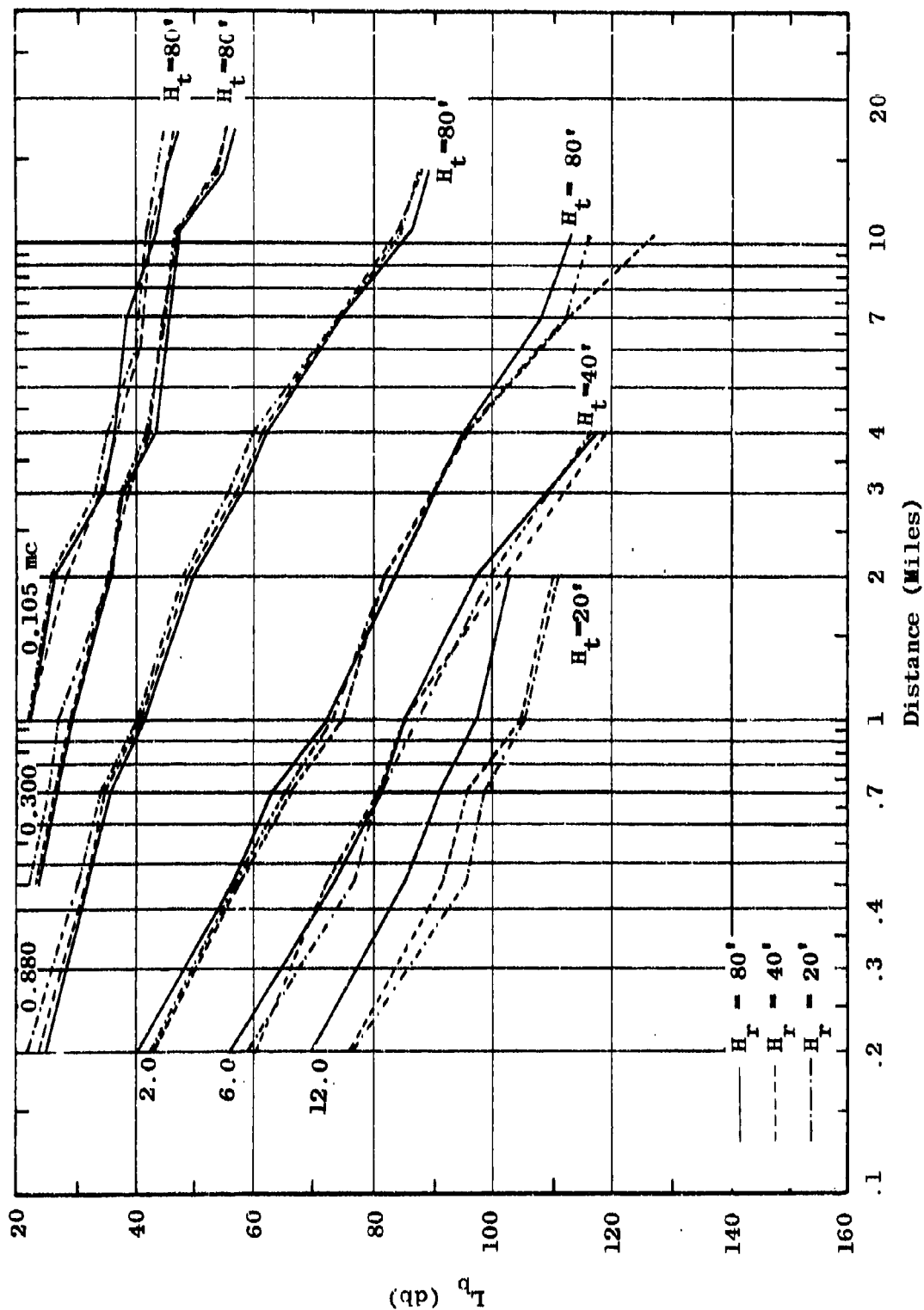


Figure 2.15 Comparison of L_p vs Distance for Various Receiving Antenna Heights
 $L_p = F_A(f, H_t, V, d, H_r)$

7

The Panama data exhibits slightly more loss than that observed in Pak Chong at short ranges, and the loss increases at a slightly greater rate than the Pak Chong data. The New Guinea data indicates significantly more loss at short range and increases at a much more rapid rate than either the Panama or Pak Chong data.

2.4 Foliage Effect

To assess the effect of foliage, it is necessary to adopt a model which represents the propagation characteristics to be expected in the absence of foliage. Since the environment includes rough terrain as well as foliage, this means adopting a propagation model for rough terrain. A rather detailed analysis based on a model suggested by John Egli⁴ was presented in Semiannual Report Number 6. The model is given by

$$L_b = 116.57 + 20 \log f + 40 \log d - 20 \log (h_1 h_2) \quad (1)$$

where

- L_b = median basic transmission loss in db
- f = frequency in megacycles
- d = distance in miles
- h_1, h_2 = transmitting and receiving antenna heights, respectively, in feet

4. J. J. Egli, "Radio Propagation Above 40 mc Over Irregular Terrain," Proc. IRE; October 1957.

The model predicts a range of propagation loss which is normally distributed about a median value given by equation 1. The standard deviation predicted by the model is given in Table 3. If this model is adequate, a foliage factor can be deduced by studying the differences between equation 1 and the measured data. This gives the foliage factor shown in Figure 2.16.

Table 3
ROUGH EARTH STATISTICS

Frequency (mc)	Standard Deviation (db)	10% to 90% Range (db)
25	4.6*	12*
50	6.1	16
100	7.7	20
250	9.2	24
400	10.7	28

*Extrapolated

As Figure 2.16 shows, the foliage factor which is obtained in this way is lower for horizontal polarization than for vertical. For both polarizations the foliage factor appears to follow an increasing straight line at all frequencies except 25 mc. Analysis of all data generated thus far on this program indicates that the foliage factor is not a function of distance. Therefore, distance does not appear as a parameter on Figure 2.16. The foliage factor was deduced from measurements made at distances from 0.2 mile to about 20 miles. This leads to the hypothesis that

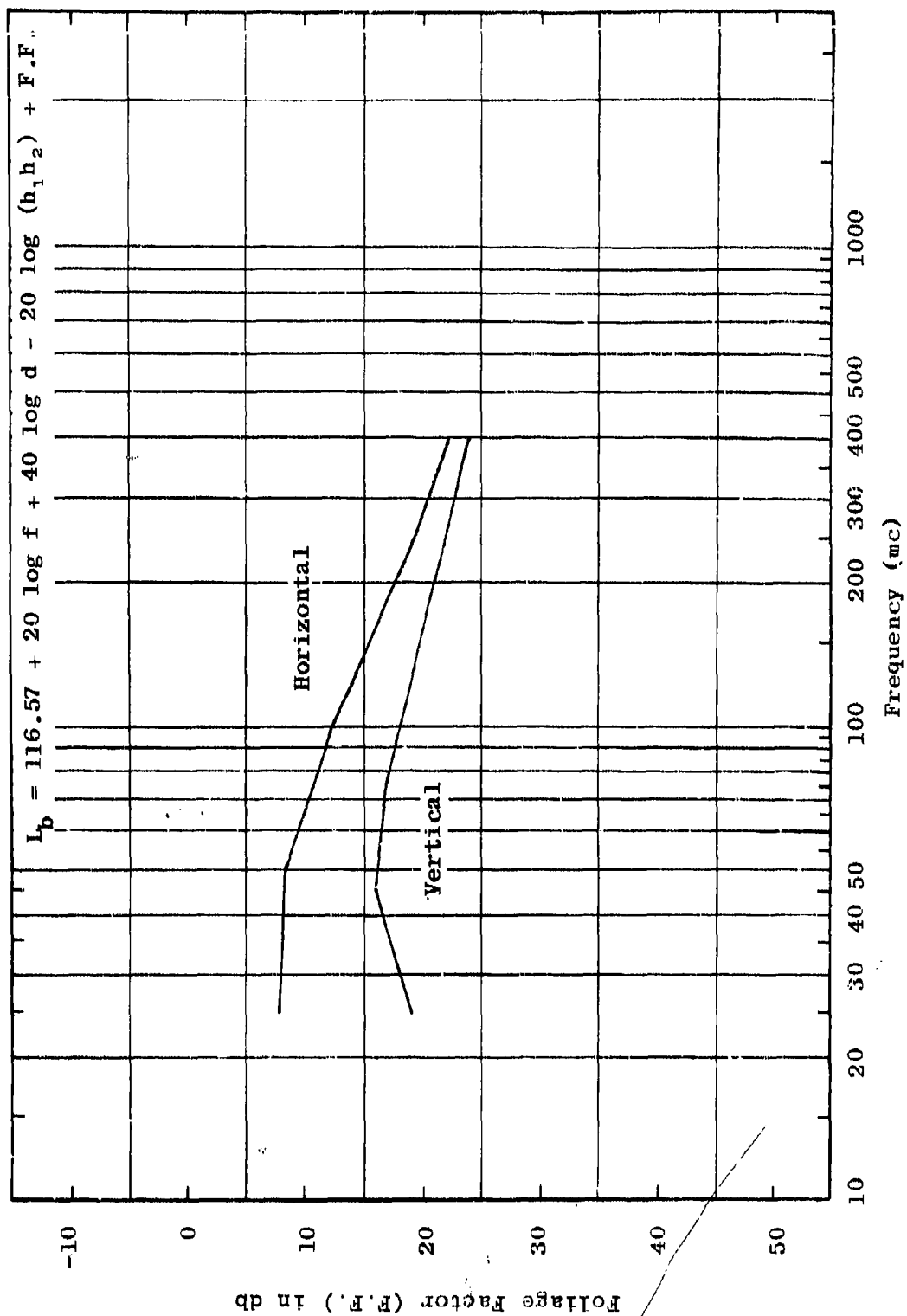


Figure 2.16 Foliage Factor (F.F.)

the foliage effect takes place somewhat closer than 0.2 mile from each antenna. This hypothesis in turn leads to the recommendation that future work be concentrated on the shorter ranges.

The Egli model suggests a 10 to 90 per cent data spread of about 12 db at 25 mc. Figure 2.17 compares the predicted 10 to 90 per cent data range and the total range of measured data at 25 mc. Figure 2.17 suggests that the spread of measured data is comparable to that which is predicted by the theoretical model. Figure 2.17 also shows that the over-all trend of the measured data tends to follow the $40 \log d$ fall-off which is indicated by the Egli model. However, there are distinct deviations from this fall-off at about 2 miles and at about 7 miles. These deviations, seen in Figure 2.17, are attributed to specific terrain characteristics in the sector from which the data came.

Figure 2.18 shows a similar comparison between theoretical and measured results at 100 mc. The data spread increases with increasing frequency, just as the theoretical model predicts. The terrain effect seen in Figure 2.18 is similar to that in Figure 2.17.

The foliage analysis described above was based on a limited data sample consisting of approximately 5000 data points drawn from Sector A. The base of reduced data currently consists of approximately 21,000 samples drawn from both Sectors A and B. The former analysis hypothesized a height-gain factor of $20 \log h$. The most recent analysis, which is discussed in Section 3.4 of this report, indicates that this hypothesis was correct for frequencies of 25 and 50 mc. However, at these frequencies, the height-gain

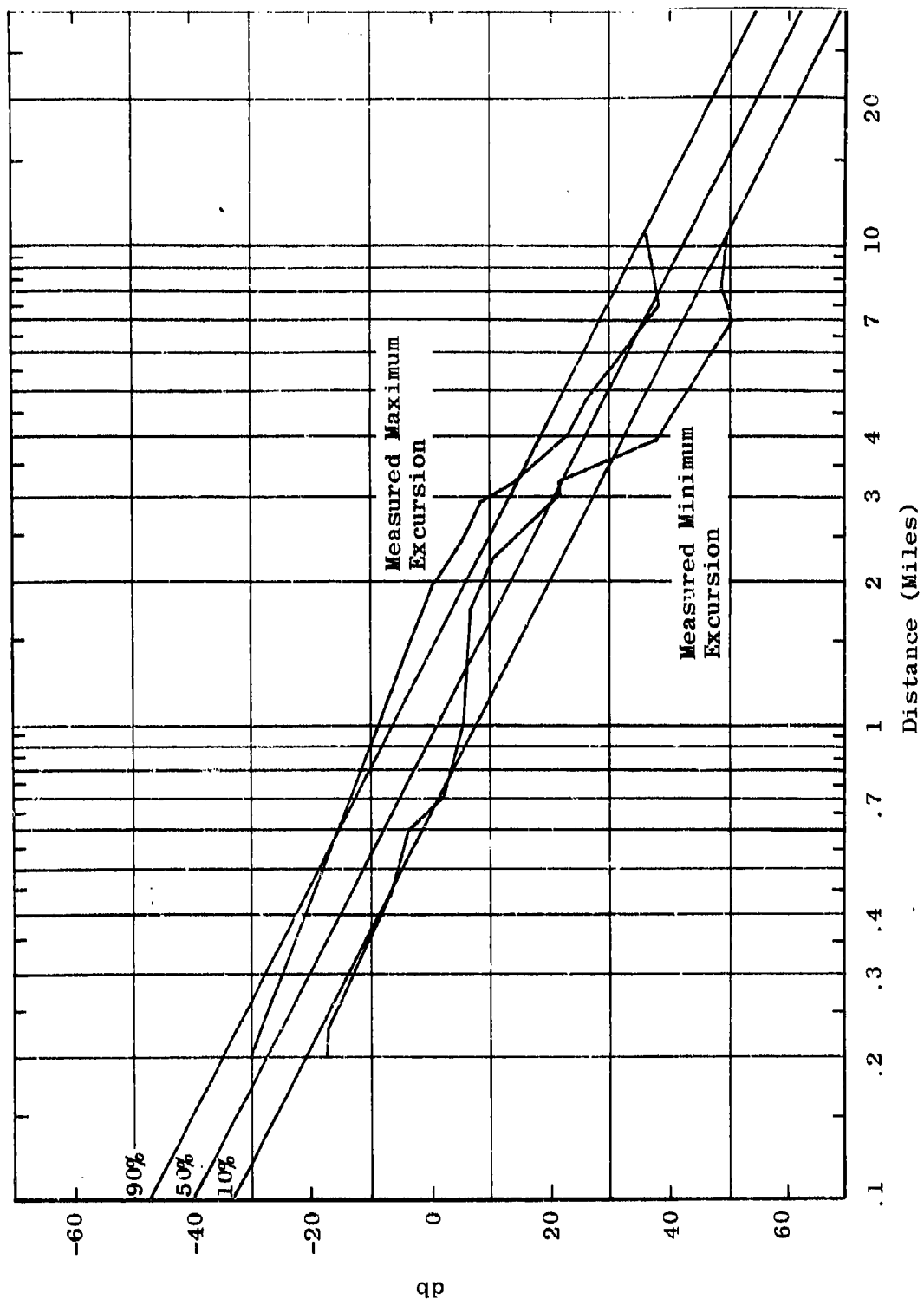


Figure 2.17 Comparison Between Measured Results and Egli Model
 $I_b = F_A(25.5, 13-80, V, d, 13-80)$

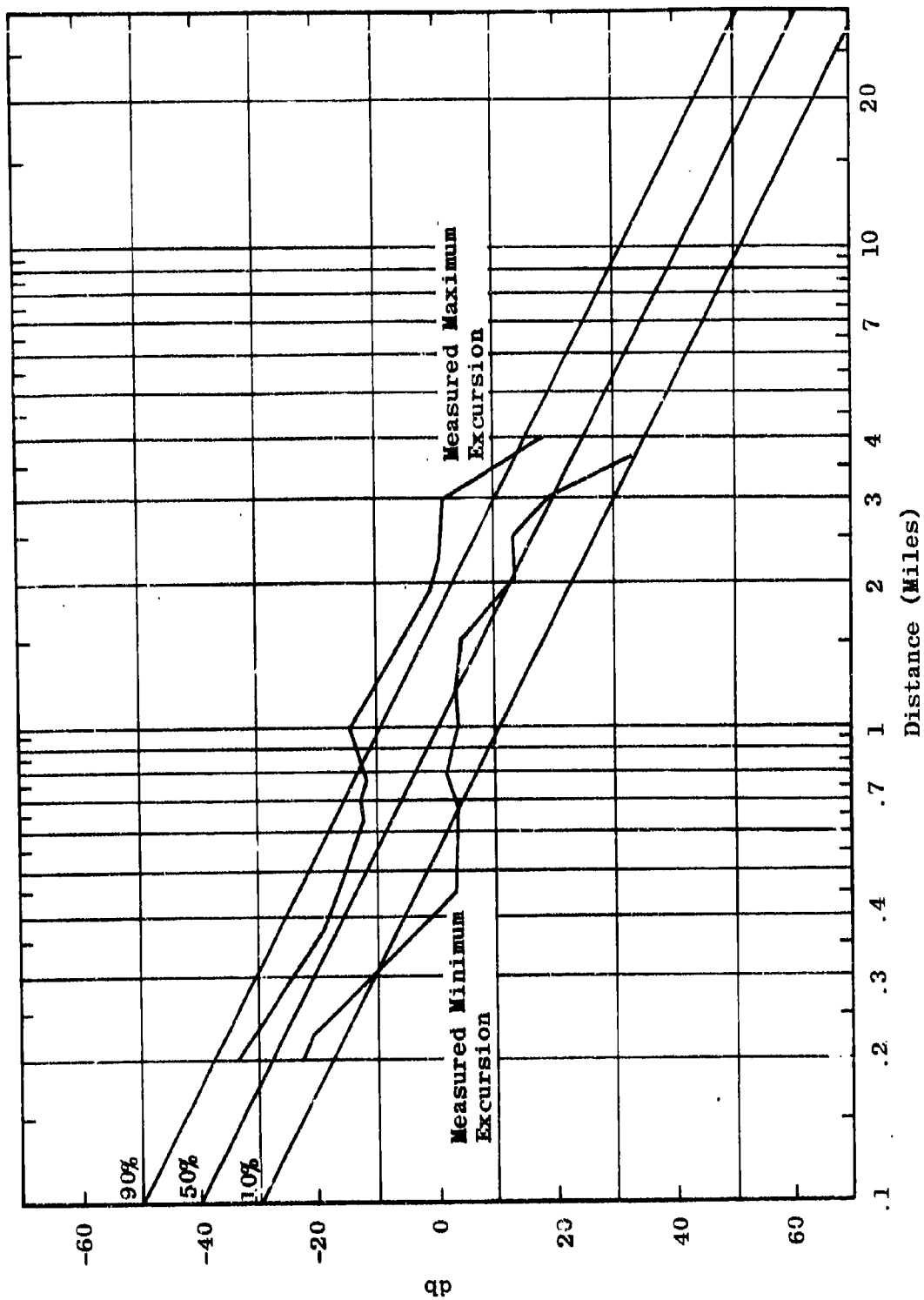


Figure 2.18 Comparison Between Measured Results and Egli Model
 $L_b = F_A(100, 13-80, V, d, 13-80)$

function appears to be quite different. A more detailed analysis of the foliage factor, based on the larger data base which is now available, is currently in progress.

A very preliminary analysis, discussed in Section 3.5, suggests that at the lower frequencies there is a direct foliage effect on the large vertical transmitting antennas. This effect varies according to the antenna's proximity to foliage as measured in wavelengths. For antennas immersed in foliage, this effect is on the order of 20 db at 2 mc and decreases as frequency is increased. In addition, there appears to be a foliage effect on the propagation path which varies from zero at frequencies of 2 mc and below to approximately 8 to 12 db at 25 mc. Under this hypothesis, the foliage effect on the propagation path at frequencies below 50 mc becomes consistent with that observed for frequencies greater than 50 mc.

2.5 Terrain Effect

A pronounced terrain effect becomes apparent from a detailed analysis of the data. The Egli model discussed in the previous section treats propagation as it would appear averaged over many different types of rough terrain. Consideration has been given to more complex terrain models which will more accurately predict at least the gross effects of major terrain obstacles. Single-obstacle

analyses have been considered along with rough-earth analyses based on the four-arc method.^{5,6}

Figure 2.19 compares measured results and a detailed rough-terrain prediction. When a single obstacle would have occurred between the transmitting and receiving antennas in the absence of foliage, knife-edge diffraction theory was used. The points on Figure 2.19 which resulted from knife-edge calculations are marked with a K. When multiple obstacles would have existed in the absence of foliage, rough-earth calculations were used. These points are marked on Figure 2.19 with an R. The correspondence between measured and theoretical results in general was not good.

Height-gain functions, $G(H)$, were used to take into account the possibility of reflections over rough terrain between either of the antennas and their radio horizons. Due to a number of factors, there is some question as to when these factors apply and when they do not. In order to decide whether a detailed study of these functions might be rewarding, the following experiment was made. The rough-earth propagation calculations were repeated, and the $G(H)$ functions were used only in those cases for which their use provided a better fit to the measured data. The results of this experiment at 25 mc are shown in Figure 2.20.

5. K. A. Norton, et al., "The Use of Angular Distance in Estimating Transmission Loss and Fading Range for Propagation Through a Turbulent Atmosphere Over Irregular Terrain," Proc. IRE; October 1955.
6. P. L. Rice, et al., "Transmission Loss Predictions for Tropospheric Communication Circuits," NBS Technical Note 101, Vol. I; May 7, 1965.

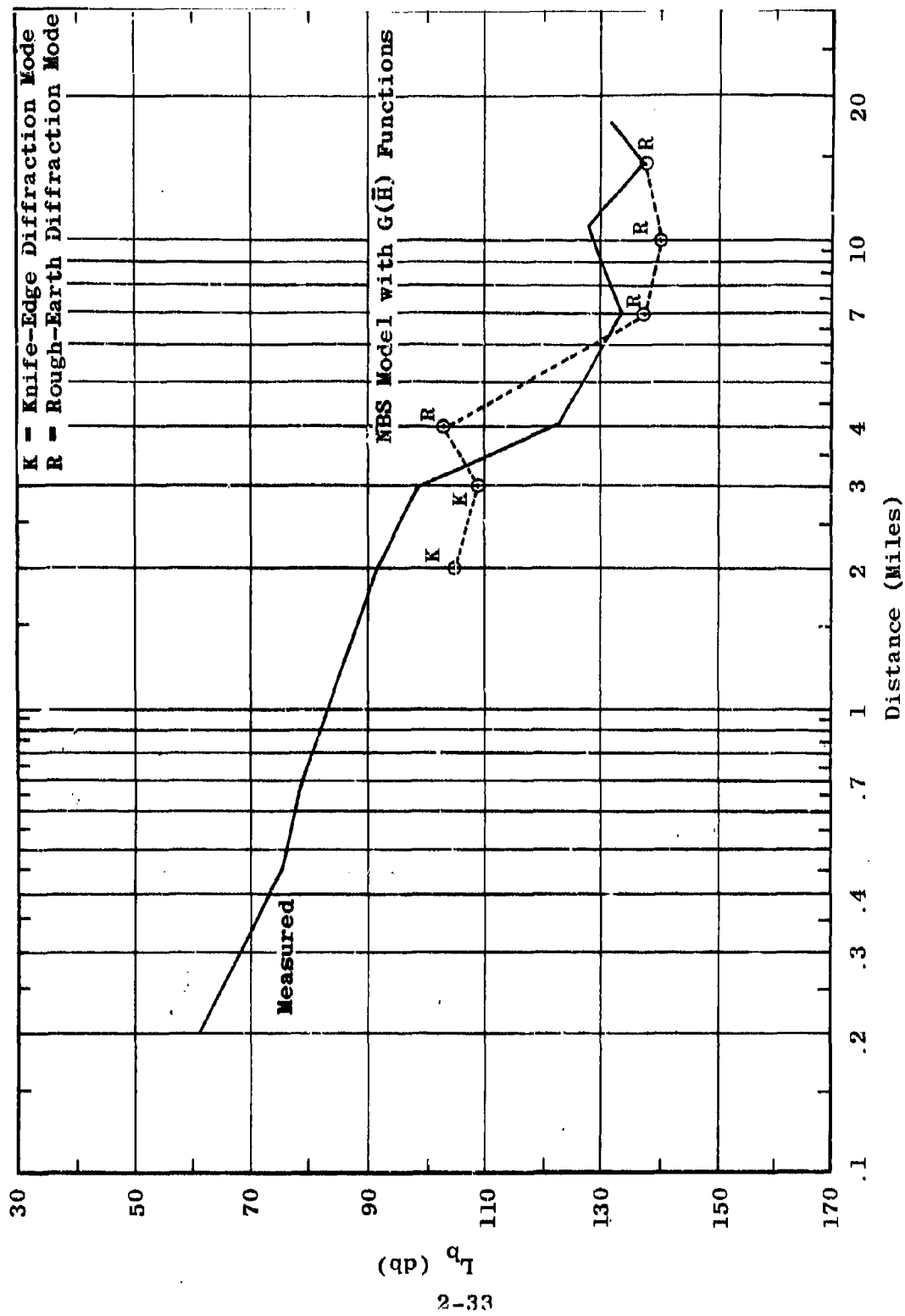


Figure 2.19 Comparison Between Measured Results and NBS Model Including $G(\bar{H})$ Functions
 $L_b = F_A(25.5, 80, V, d, 80)$

The letter T beside a calculated point indicates that the $G(H)$ function was used at the transmitting end but not at the receiving end. For those calculated points marked with an R, the converse is true. For those points marked with both T and R, the $G(H)$ functions were used at both the transmitting and receiving ends. Those computed points for which the $G(H)$ functions were used on neither end are unmarked. As Figure 2.20 shows, the fit at 25 mc is relatively good except for the point at 4 miles.

Since the measured data includes the presence of foliage and the theoretical calculation does not, it is reasonable to assume that the theoretical losses should differ from the measurements by some foliage effect. The attempt in Figure 2.20 was to fit the data with theory as closely as possible. However, hypothesizing a foliage effect, the experiment was repeated in an attempt to find the best theoretical function corresponding to a loss 10 db below that which was measured. The result, which is shown in Figure 2.21, appears to be quite good. Although the results in general have not been exceptionally good, there is enough correlation to justify a continuation of this type of analysis.

2.6 Data Variability

2.6.1 Height and Time Variation

A knowledge of the fine-grain changes in propagation loss with small changes in antenna height, distance and time is essential to an understanding of the propagation mechanism and to an intelligent use of the propagation mechanism for communications.

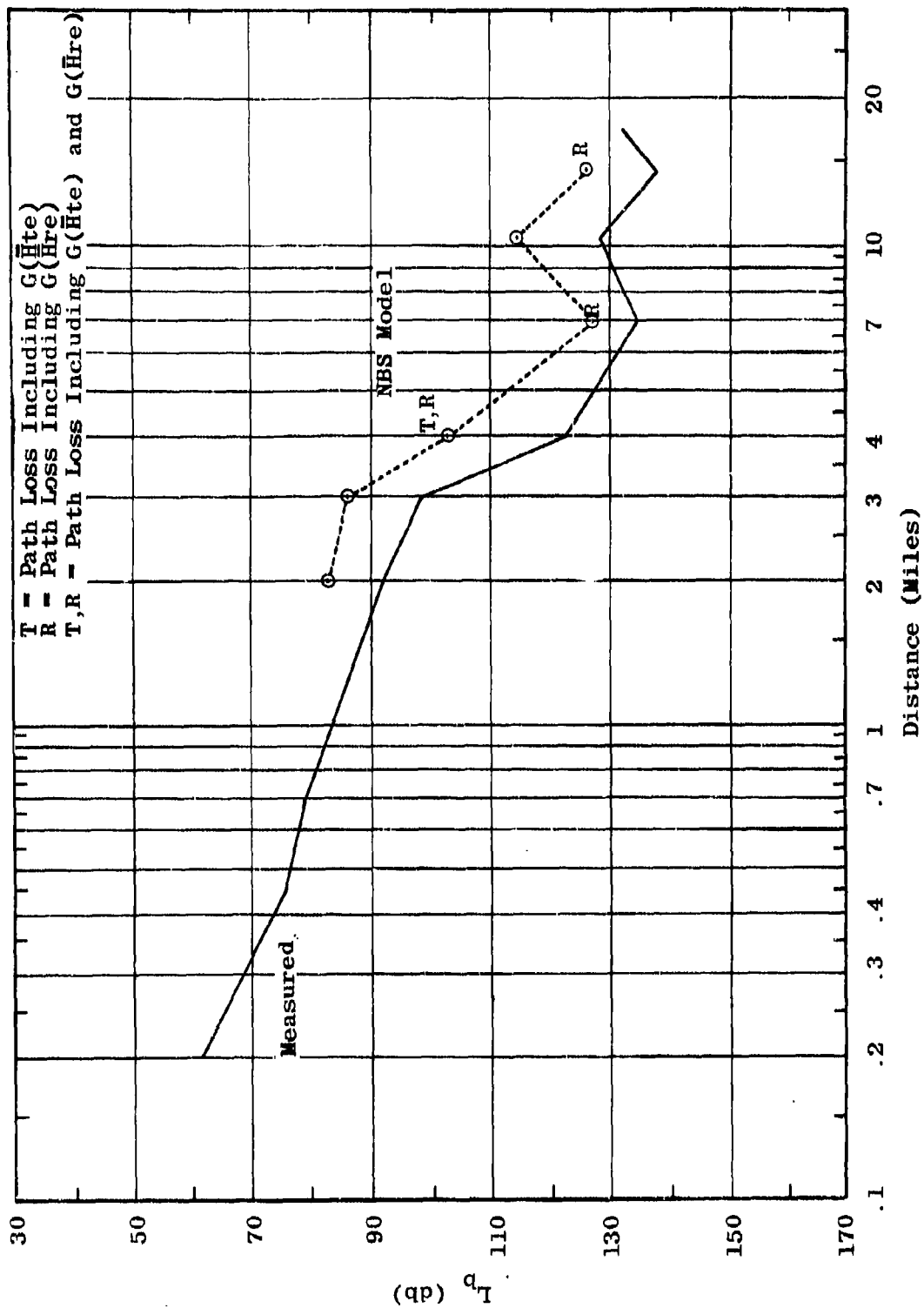


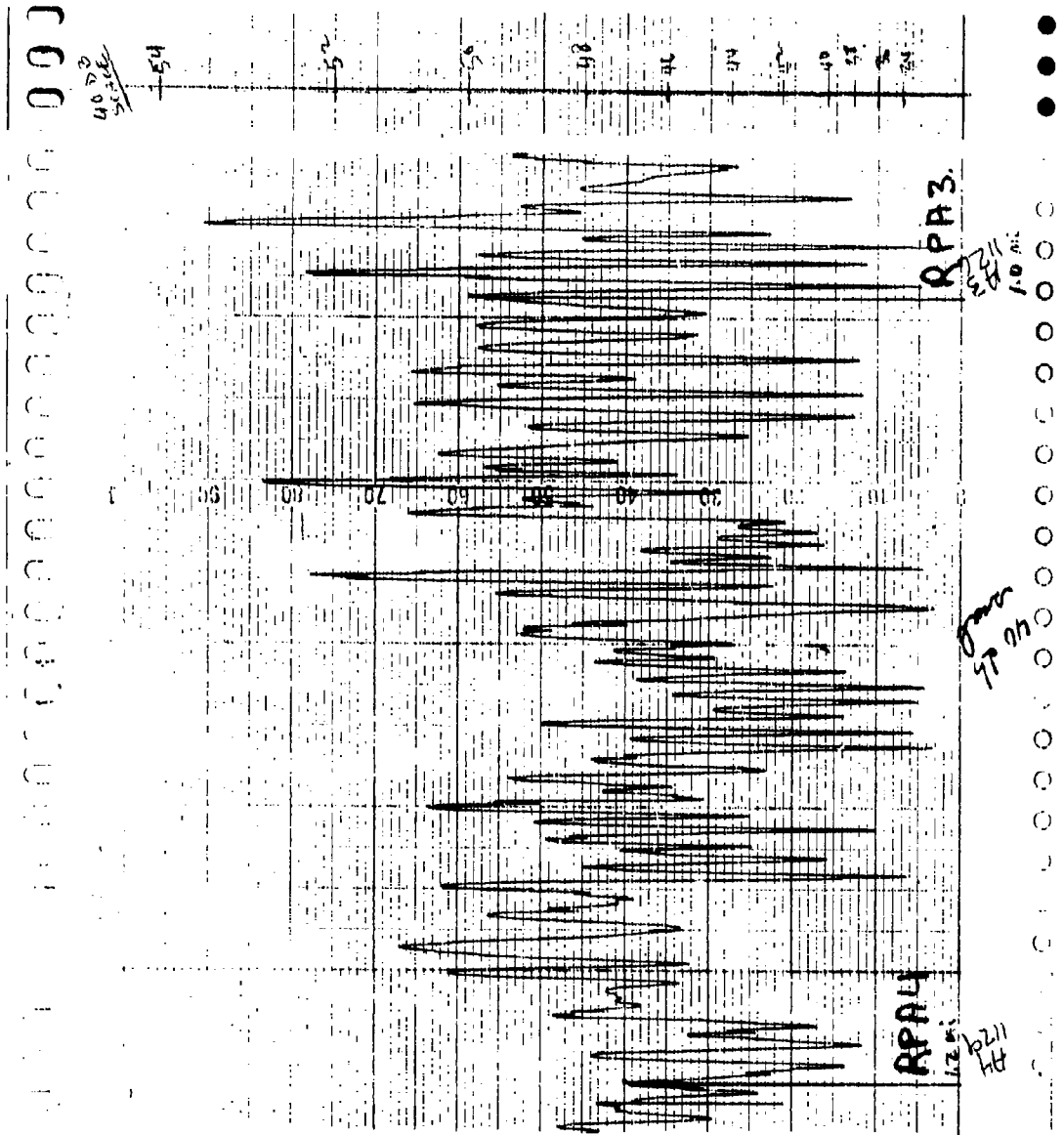
Figure 2.21 Best Fit 10 db Below Measured Results
 $L_b = F_A(25.5, 80, V, d, 80)$

7

The recordings of field strength vs height from 11 feet to 80 feet are broken into height increments of approximately 5 feet. The median field strength is determined within each of these 5-foot height increments. A maximum variation of about 6 db from this median has been noted within any height interval. Variation of 2 db or less from the median within an interval is typical. The fine-grain variability of received field with height tends to be greatest for low antenna heights, i.e., when the antennas are immersed in the foliage. The time variability of recorded field strength over periods of approximately a minute has been very small. The variation is usually a fraction of a decibel.

2.6.2 Vehicular Data

The continuous recordings of field strength vs distance provide a detailed insight into the variability of transmission loss at low antenna heights within the foliage. Figure 2.22 is a typical field-strength recording, taken at 25.5 mc. The trails along which the vehicle moves are calibrated in terms of radial distance from the transmitter at 0.2-mile intervals for distances from 0.2 mile to 3 miles and at 0.5-mile intervals thereafter. Each time the vehicle passes one of these calibration markers, the strip recording is marked. The trails are never exact radials, and thus the actual distance represented on any strip chart is always somewhat greater than the indicated radial distance. The sample shown in Figure 2.22 has distance markings at 1 mile and 1.2 miles. The actual db calibration scale is shown at the right of Figure 2.22.



5978

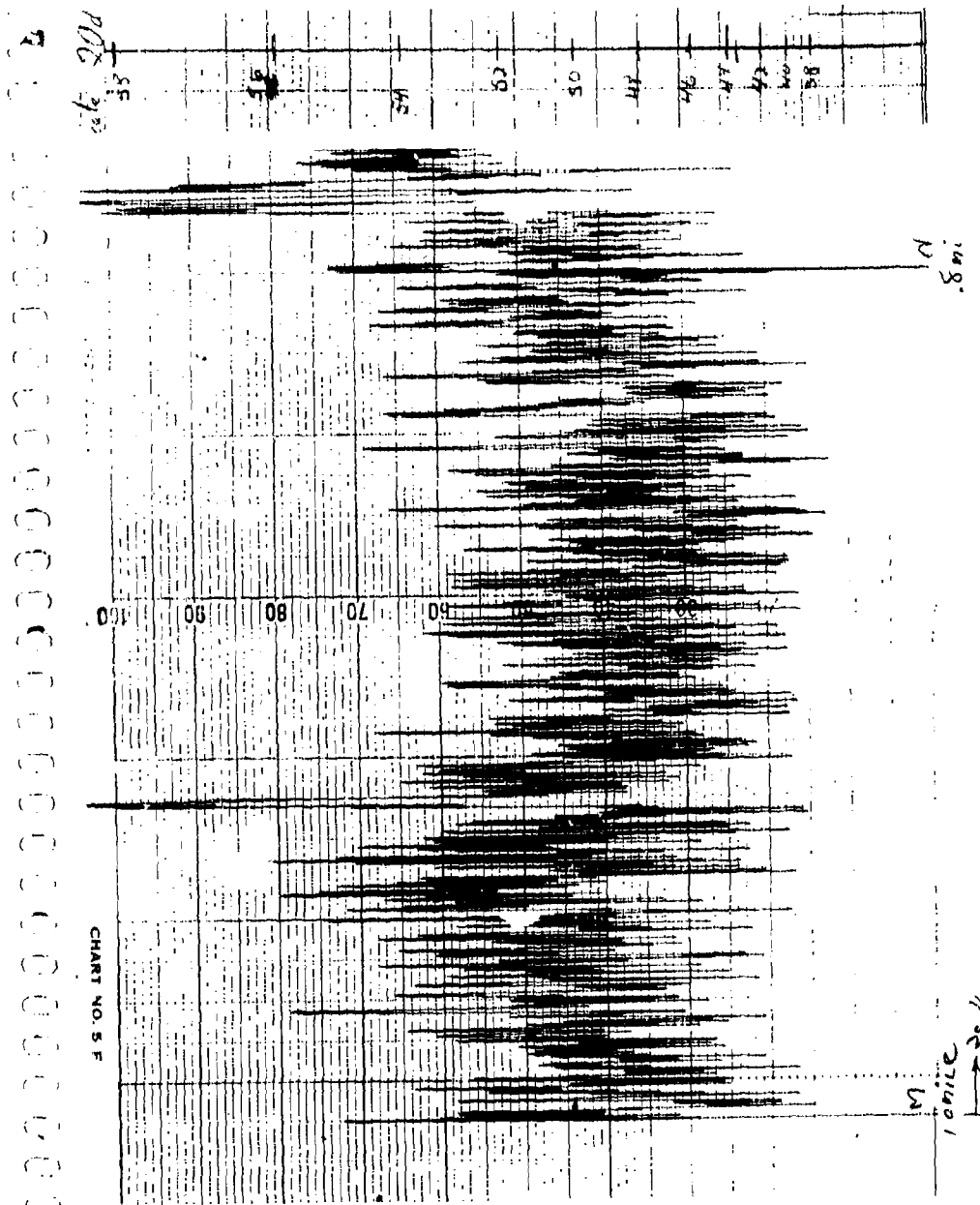
Figure 2.22 Example of Vehicular Raw Data
 $F_A(25.5, 40, V, 1.0-1.2, 7)$

Figure 2.23 provides a similar example of data taken at 250 mc. The frequency with which the data varies increases as radio frequency is increased. Below 25 mc, the frequency of data variation is relatively low as distance changes. However, at 250 and 400 mc the data variation is extremely rapid, as Figure 2.23 indicates. A cursory examination of the data provides a very rough indication of the distance spacings between adjacent maxima and minima shown in Table 4. Table 4 gives the approximate spacings in terms

Table 4
APPROXIMATE SPACING BETWEEN ADJACENT
MAXIMA AND MINIMA

<u>Frequency (mc)</u>	<u>Spacing (ft)</u>	<u>Spacing (wavelengths)</u>
25.5	20	0.52
50.0	15	0.76
100.0	10	1.0
250.0	8	2.0
400.0	4	1.6

of feet as well as wavelengths. The spacings seem to vary from $\lambda/2$ at 25 mc up to about 2λ at 250 mc. These numbers are only approximate, and greater recording resolution is necessary before truly meaningful spacings can be determined. It has been recommended that severe vehicular recordings be made with resolutions which are approximately ten times better than those collected to date.



5981

Figure 2.23 Example of Vehicular Raw Data
 $F_A(250, 80, V, 0.8-1.0, 7)$

In addition to the rapid fluctuations there is a longer-term fluctuation, one cycle of which can be seen in Figure 2.23. This longer-term variation is similar to that which is generally associated with propagation over rough terrain in the absence of foliage. The more rapid variation is typical of that which is generally encountered near or within foliage.

The statistical distribution of signal strength has been analyzed in distance intervals corresponding to 0.2 mile for distances closer than 3 miles, and intervals of 0.5 mile for distances greater than 3 miles. Figure 2.24 provides an example of the distribution which is obtained. In general, a normal statistical distribution seems to fit the data best. There is often a deviation from normality at the ends of the distribution, as can be seen at the high probability end of Figure 2.24. This fall-off is beyond the limits of resolution on the strip chart, however; and thus no significance can be placed on the fall-off at this time.

Figure 2.25 is a sample plot of the medians taken from successive distance intervals along the trail through Sector A. In addition to the medians, the propagation losses which are expected 10 per cent of the time and 90 per cent of the time are plotted on Figure 2.25. For comparison purposes, the dotted curve on Figure 2.25 corresponds to the fixed-point data taken at the same frequency, polarization, and transmitting antenna height. It should be noted that there is a significant difference in receiving antenna heights.

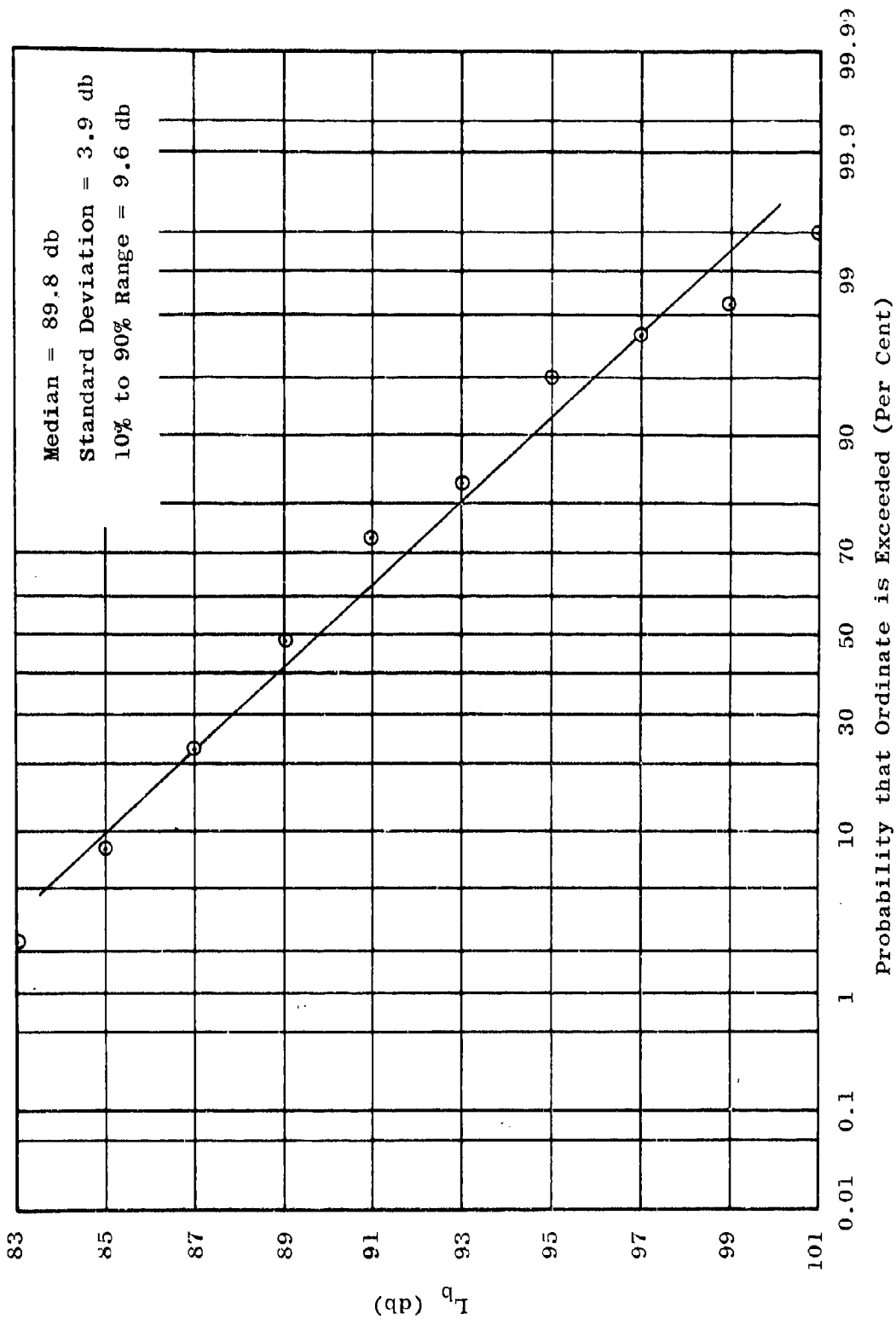


Figure 2.24 Statistical Distribution of L_b
 $L_b = F_A(25.5, 80, V, 0.4-0.6, 7)$

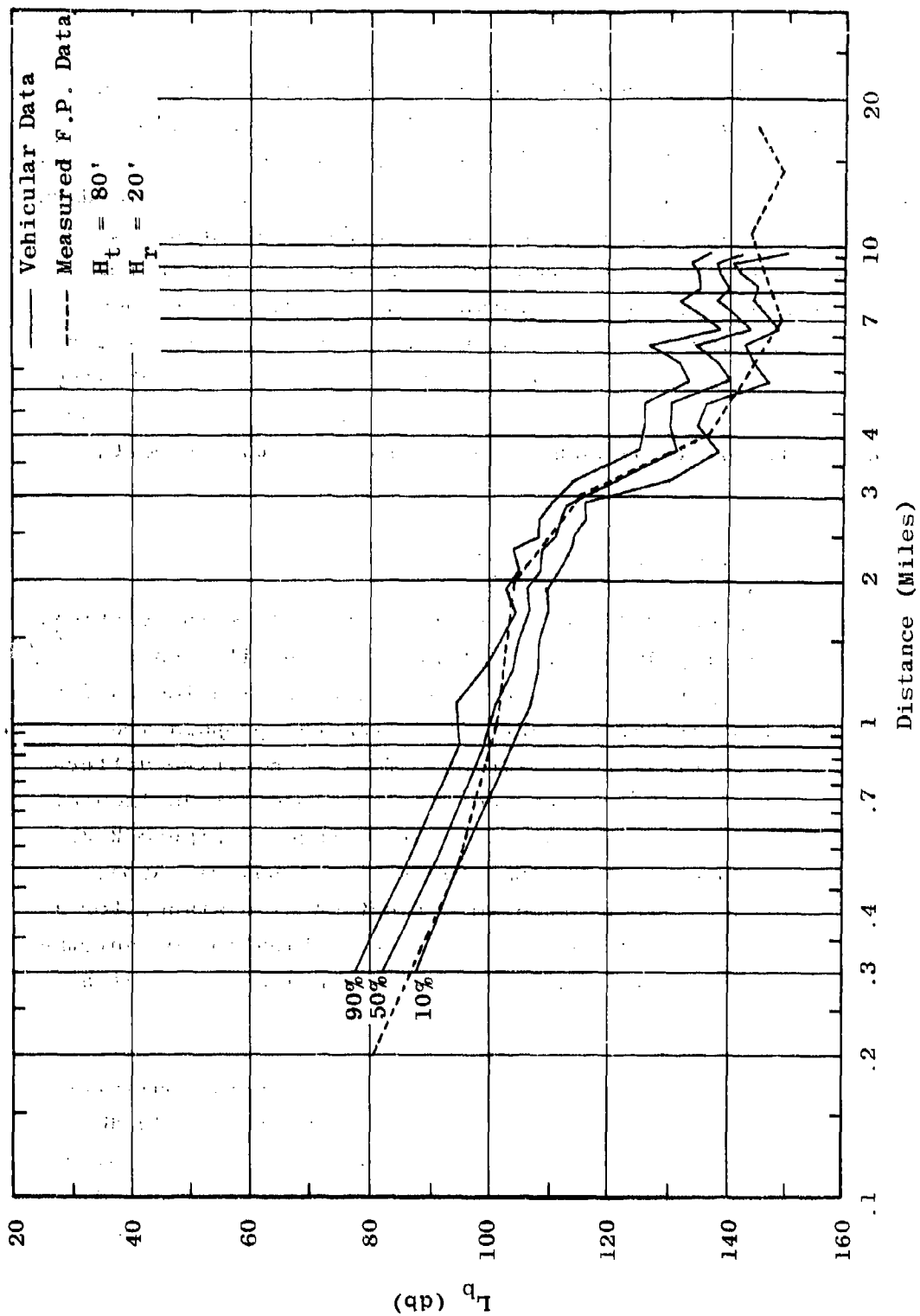


Figure 2.25 Comparison Between Vehicular Data and Measured F.P. Data
 $L_b = F_A(25.5, 80, V, d, 7)$

The standard deviations which were observed in each of the distance intervals plotted on Figure 2.25 are shown in Figure 2.26. The standard deviation varies considerably from one distance interval to the next. The standard deviation ranges from approximately 2 db to about 6.5 db. The over-all tendency seems to be toward a slight increase in standard deviation as distance increases. The standard deviations shown in Figure 2.26 include the effects of the short-term variability and also the longer-term variability. A more recent analysis of the independent effects of these two variations is discussed in Section 4 of this report.

2.7 Polarization Comparison

Figure 2.27 compares propagation loss for vertical and horizontal polarizations at 25 mc. The differences plotted on Figure 2.27 correspond to propagation losses for horizontal polarization subtracted from the propagation losses for vertical polarization. Thus, a positive difference on Figure 2.27 corresponds to less loss for horizontal polarization, whereas a negative difference on Figure 2.27 would correspond to less loss for vertical polarization. The differences are plotted as a function of distance for a combination of low antenna heights, a combination of antenna heights at about treetop level, and a combination of high antenna elevations.

For the low antenna heights, horizontal polarization is favored almost consistently by a factor of 20 db. For the antenna heights at treetop level, horizontal polarization is still favored, but the margin has been reduced to about 10 db. At the upper heights, horizontal polarization

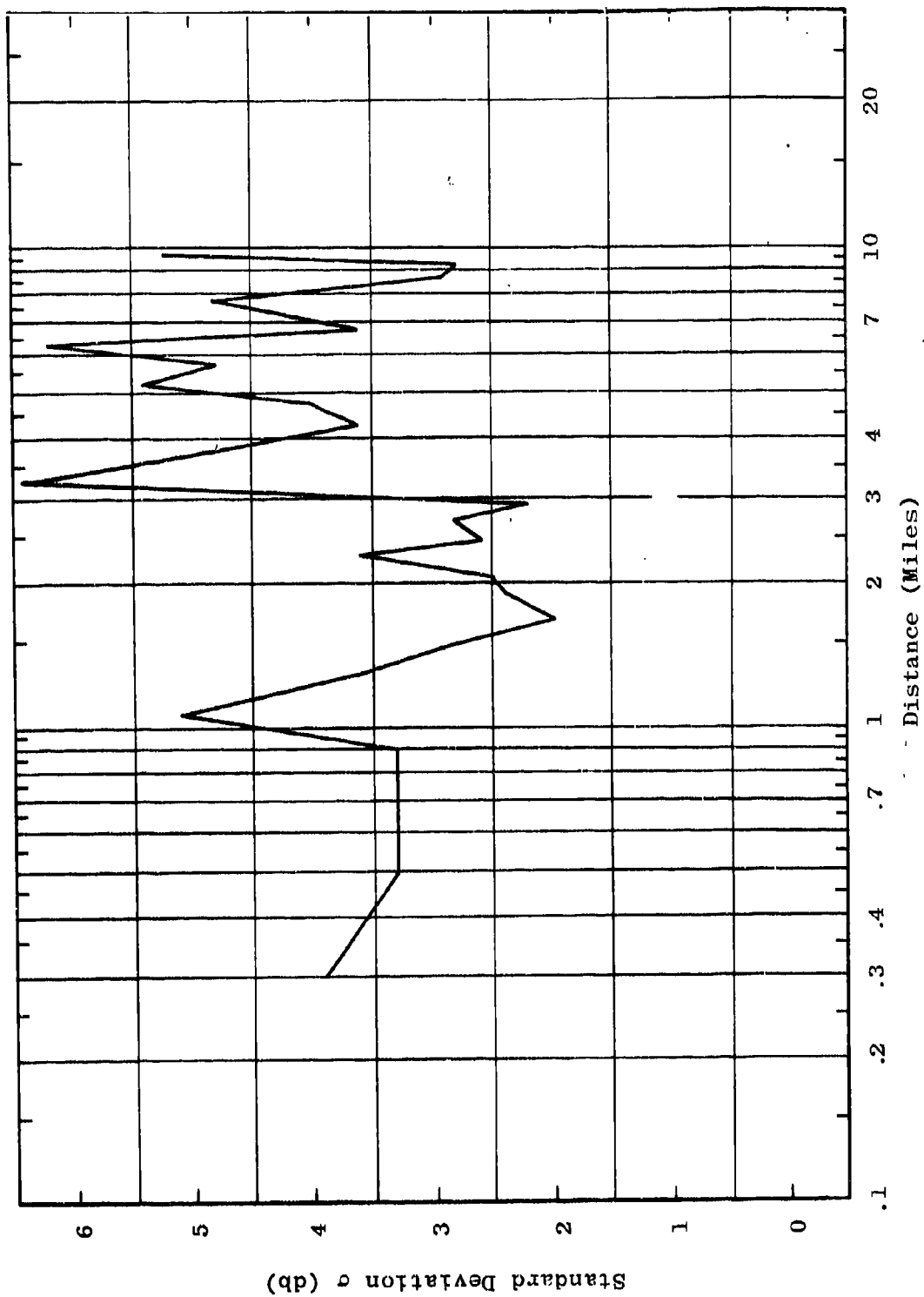


Figure 2.26 Standard Deviation of Vehicular Data
 $L_b = F_A(25.5, 80, V, d, 7)$

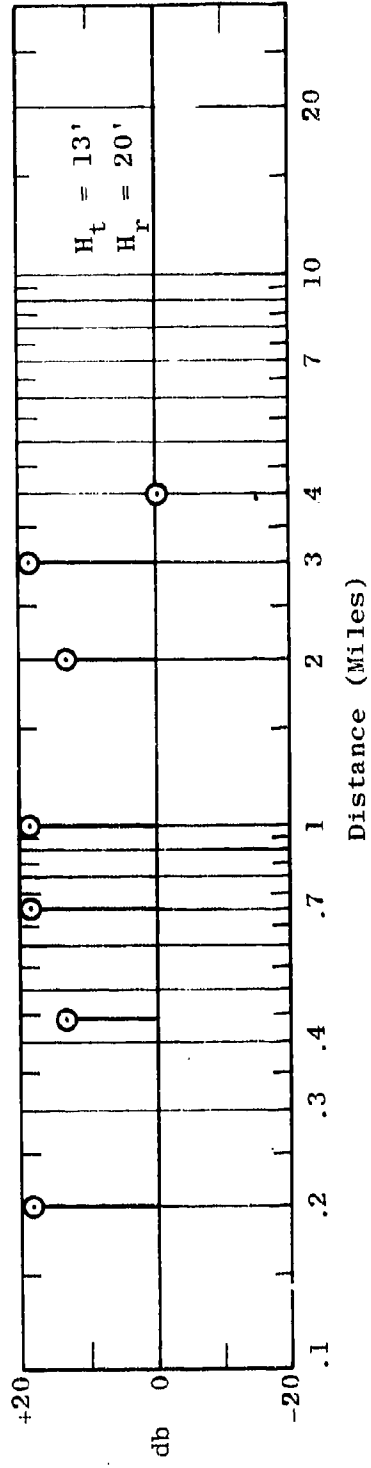
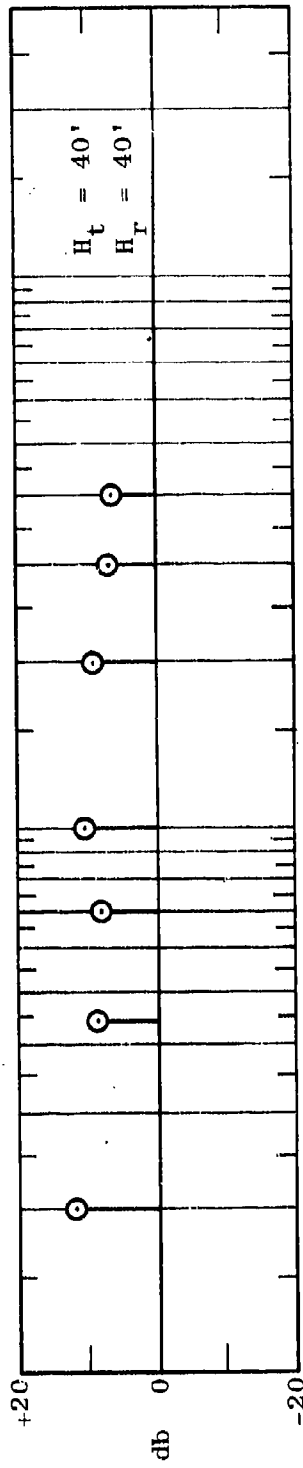
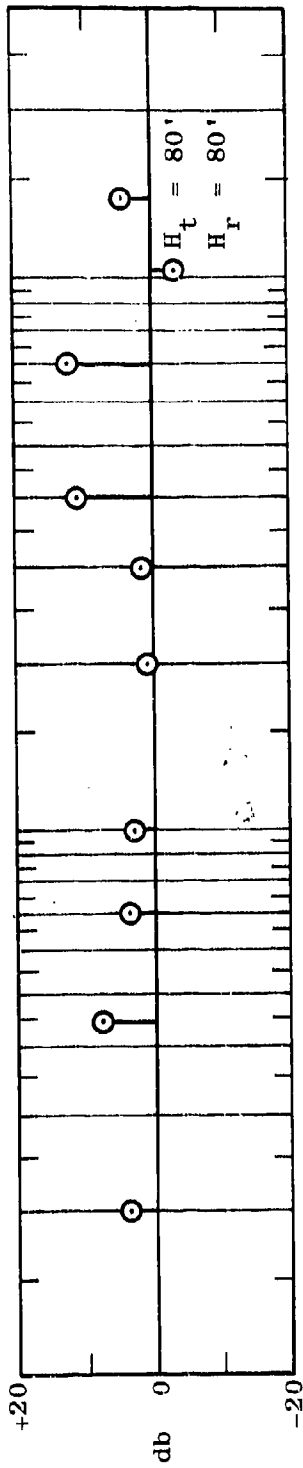


Figure 2.27 L_p for Vertical Polarization Minus L_p for Horizontal Polarization at 25.5 mc

is favored by only a slight margin in most cases. As antenna height is increased, the margin by which horizontal polarization is favored tends to decrease. This is also true as frequency is increased. With increasing frequency the margin by which horizontal polarization is favored begins to decrease even at low antenna heights until at 400 mc, as Figure 2.28 shows, horizontal and vertical polarizations produce equivalent results.

For frequencies of 2, 6 and 12 mc, the measured propagation losses with vertical polarization tend to be much greater than would be expected in the absence of foliage. However, the horizontal polarization losses tend to be significantly lower than would be expected in the absence of foliage. Hence, at these high frequencies a similar tendency to favor horizontal polarization prevails.

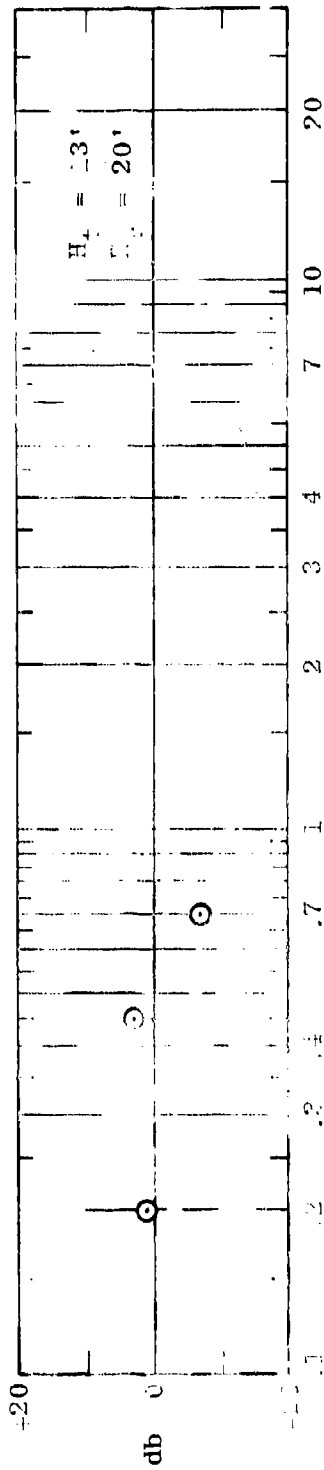
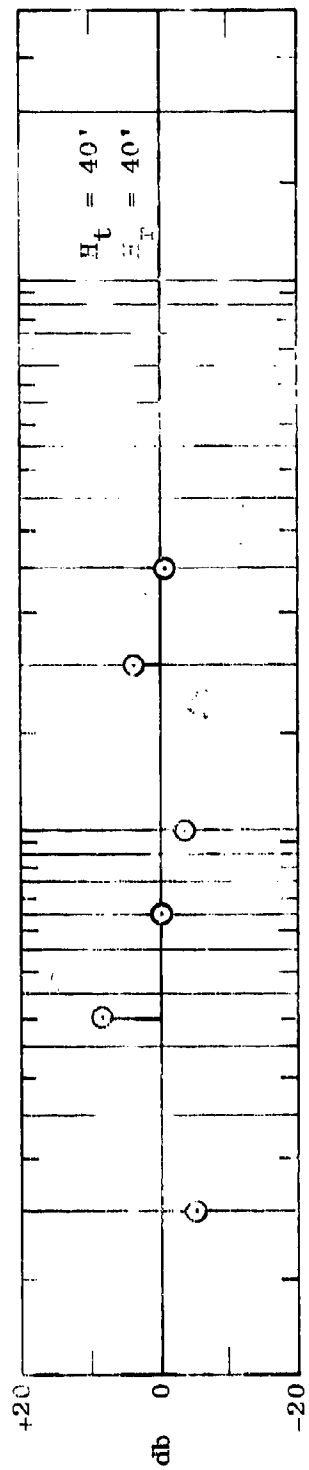
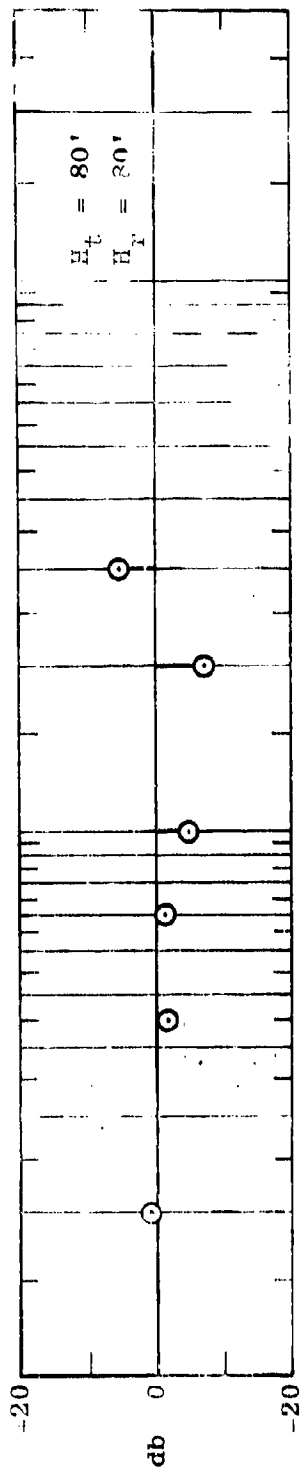


Fig. 2-16. H_t for Vertical Polarization minus H_t for Horizontal Polarization at 40

3. FIXED-POINT DATA

This section discusses the fixed-point data taken at frequencies of 400 mc and below. The data base consists of approximately 21,000 reduced data samples. This is four times the number of reduced data samples available for analysis at the time of Semiannual Report Number 6. Much time during the past 6-month period has been devoted to simply reducing this data into its present form. In addition, a significant amount of time has been spent in automating the data handling procedures to facilitate detailed data analysis. Some data analysis similar to that reported in Semiannual Report Number 6 has been continued. However, the bulk of the detailed data for the 100-kc to 400-mc data will be analyzed during the next 6-month period.

The current stage of data analysis is directed toward achieving three specific goals. The first goal is to characterize in detail the radio propagation characteristics which have been observed through measurement in the Pak Chong area. The second goal is to develop a realistic physical model, with major functional relationships identified, which will allow an extension of the data collected so far to other foliated environments. The third goal, which is auxiliary to the first two, is to carefully appraise the significance of the data and to identify future experiments which have the greatest likelihood of providing needed insight into still-unanswered questions. For example, the existing data provides much information as to the type and quantity of measurements which should be made in significantly different foliated environments to facilitate the development of a physical model which includes foliage parameters as one of its variables.

Section 3.1 examines the data spread between Sectors A and B and between wet and dry seasons as a function of radial distance from the transmitter site. Section 3.2 presents several families of curves which qualitatively represent the propagation characteristics of the particular environment in which the measured data was taken. Section 3.3 presents a rather detailed wet-dry comparison. Section 3.4 presents a study of height gain within vegetation. Section 3.5 reviews the concept of a foliage factor as discussed in Semiannual Report Number 6 and extends the concept to frequencies below 25 mc.

3.1 Basic Fixed-Point Data

This section summarizes the basic propagation loss data gathered at the fixed receiving points in the frequency range from 100 kc to 400 mc. The data is plotted in a format which allows several visual comparisons to be made. Figure 3.1 presents an example of the data format. This figure is a plot of basic transmission loss vs distance for a frequency of 105 kc using vertical antennas at the lowest heights. Basic transmission loss has been normalized by subtracting the quantity $20 \log d$, where d is separation distance measured in miles. Thus, the value of any point along the vertical scale corresponds to basic transmission loss minus $20 \log d$. When this type of scale is used, data which tends to follow a horizontal line with increasing distance actually falls off at a rate of $20 \log d$ (or inverse distance if units of field strength are being used). Data which tends upward with increasing distance on a plot such as that shown on Figure 3.1

actually falls off at a rate less than $20 \log d$ while data which tends downward falls off at a rate greater than $20 \log d$.

Four kinds of points are plotted on Figure 3.1: The black squares represent wet-season measurements made on Sector A; the white squares are dry-season measurements made on Sector A; the black circles denote wet-season measurements made on Sector B; and the white circles represent dry-season measurements made on Sector B.

A comparison of the white points vs the black points on Figure 3.1 gives some indication of the differences between wet and dry seasons. A comparison of the circles regardless of color and the squares regardless of color illustrates the differences between Sector A and Sector B. The curve drawn through the points is intended to help the eye follow the general trend of the data.

In a number of cases, there is more than one sample of the same kind plotted at a particular distance. For example, on Figure 3.1 at 2 miles, there are two wet-season samples for Sector A. At 4 miles, there are three dry-season samples for Sector B. The samples at 4 miles show that the difference between samples of the same type can be as great as the differences between dry- and wet-season samples. Figure 3.1 also shows that no dry-season Sector A samples have been plotted. Dry-season Sector A samples at frequencies of 105, 300 and 880 kc are among the few data points which are not yet a part of the data analysis base.

By comparing the white points on Figure 3.1 with the black points, it can be seen that for distances between 0.2 mile and 1 mile the dry-season data tends to show greater losses than the wet-season data by 1 or 2 db. However, for distances greater than 1 mile, the dry-season data tends to show lower losses than the wet-season data. The differences in either case are not great.

By comparing the square points and the round points, it can be seen that for distances between 0.2 mile and 1 mile, Sector B data tends to have slightly higher losses than Sector A data. However, for distances greater than 1 mile, there appears to be no noticeable difference.

The data fall-off between 0.2 mile and 1 mile appears to be slightly greater than $20 \log d$, but from 1 mile to 10 miles the data fall-off appears to be very close to $20 \log d$. The over-all data spread at any distance does not exceed 5 db, which is indicative of an excellent repeatability.

Figure 3.2 illustrates the slightly greater data spread at 300 kc. The data tends to fall off at a rate slightly less than $20 \log d$ for distances between 0.2 mile and 1 mile and at a rate slightly greater than $20 \log d$ for distances greater than 1 mile. The dry-season data tends to show greater losses than the wet-season data, but not significantly so. Sector A data tends to show lower losses than Sector B data, but again not significantly so. The two most significant deviations occur at 2 miles and 4 miles for wet-season Sector A data. It should be emphasized, however, that the deviation is only 5 db.

The dry-season data for 880 kc (Figure 3.3) again shows more loss than the wet-season data, but the difference is not great enough to be significant. The data fall-off from 0.2 mile to 1 mile is $20 \log d$. From 1 mile to 15 miles the data falls off at a rate which is significantly greater than $20 \log d$. The data begins to show a U-shaped fall-off which is characteristic of all the higher frequency data and is attributed to the specific terrain profiles.

For frequencies above 880 kc (Figures 3.4 through 3.11), a normalizing factor of $40 \log d$ rather than $20 \log d$ is used. Analyses presented in Semiannual Report Number 6 indicate that the data in general tends to fall off at a rate of approximately $40 \log d$ with increasing distance for frequencies of 25 mc and above. Thus, plots of the types shown in Figures 3.1 through 3.11 provide an immediate check against this hypothesis.

Figures 3.4, 3.5 and 3.6 show that the same, small data spread which was characteristic of the lower frequencies prevails at the higher frequencies. However, at 25.5 mc, as Figure 3.7 shows, the data spread becomes significantly greater. This greater data spread is characteristic of all frequencies from 25 mc to 400 mc.

Figures 3.1 through 3.11 show vertical polarization at the lowest antenna heights. Figures 3.12 through 3.19 are concerned with horizontal polarization at the lowest antenna heights. Figures 3.20 through 3.30 illustrate vertical polarization at the highest antenna elevations. Note that again for the kc frequencies,

Figures 3.20 through 3.22, $20 \log d$ has been subtracted from the data whereas $40 \log d$ was subtracted for frequencies in the range 2 mc through 400 mc. Figures 3.31 through 3.38 show horizontal polarization at the highest antenna elevations. The data spread characteristics between Sector A and Sector B and between wet and dry seasons are similar for both polarizations and both sets of antenna heights.

Figure 3.27 presents high antenna data for vertical polarization at 50 mc. The data shown is characteristic of all data at frequencies of 25 mc and above. The data spread for close distances tends to be smaller than the spread of A, the farthest distances. It is significant to note that at distances of about 2 miles the data spread is extremely small. A distance of 2 miles corresponds to a point just past the major terrain obstacle which occurs in both sectors.

Figure 3.27 indicates that there appears to be no consistent difference between sectors or between seasons. The fall-off in data from 0.2 mile to 1 mile is slightly less than $40 \log d$. From 1 mile to about 7 miles the fall-off is much greater than $40 \log d$. The over-all trend in the data is more or less horizontal, indicative of a basic fall-off corresponding to $40 \log d$ with a significant terrain effect superimposed.

Figure 3.23 is interesting in that the wet-season data sample for the Sector B special measurement point at 10.5 miles is almost 10 db above the rest of the data.

Although this point is classed with the Sector B data, it is not in either sector. The terrain is such that there is no major obstacle between the transmitter and this special point except at 10 miles, where an abrupt obstacle exists. A detailed study is being made of this and other special points since they represent significantly different terrain conditions. Such special points are seen in many figures and are easily identified by their position on the distance scale. Points touching the vertical line representing a distance of 10 miles were in fact measured at a sector point 10.5 miles from the transmitter site. The next set of points on these figures, i.e., those which are close to the 10-mile mark without actually touching it, were taken 11.5 miles from the transmitter site.

3.2 Smooth Curves for Basic Transmission Loss

Smooth curves based on Pak Chong measurements have been made for basic transmission loss vs distance. These smooth curves summarize the propagation loss information collected to date. In addition to characterizing propagation within environments of the type found at Pak Chong, these curves can also serve a number of useful analysis purposes. To serve analysis purposes to the greatest extent possible, the data has been smoothed by fitting meaningful functions to the measured data points. The function which was used for frequencies from 105 kc through 25 mc was the smooth-earth surface-wave function for a low ground conductivity.

In order to ease the burden of explanation, two terms will be defined for use in this report. The meanings

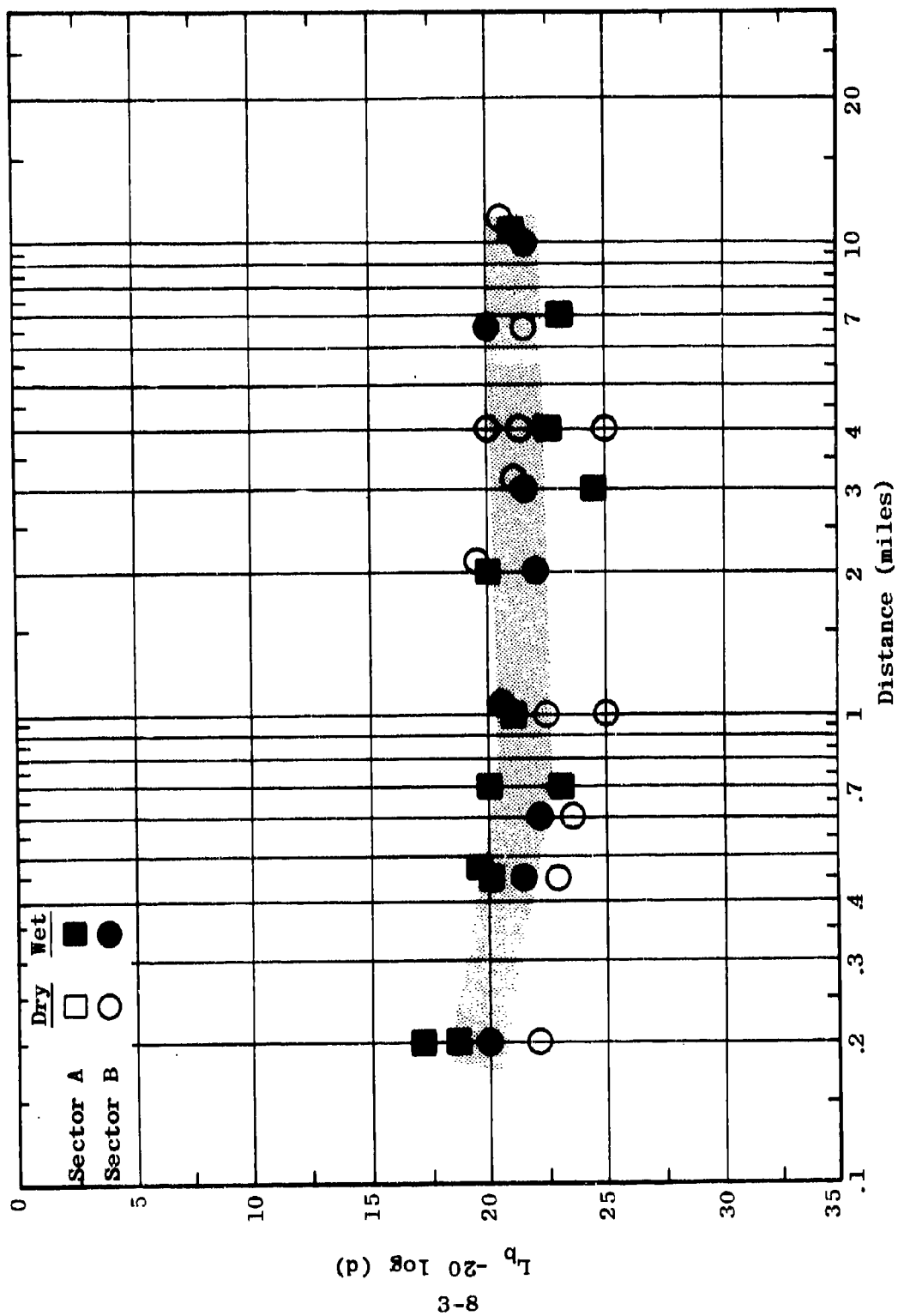


Figure 3.1 Measured Data Summary
 $L_p = F_{A,B}(0.105, 80, V, d, 17)$

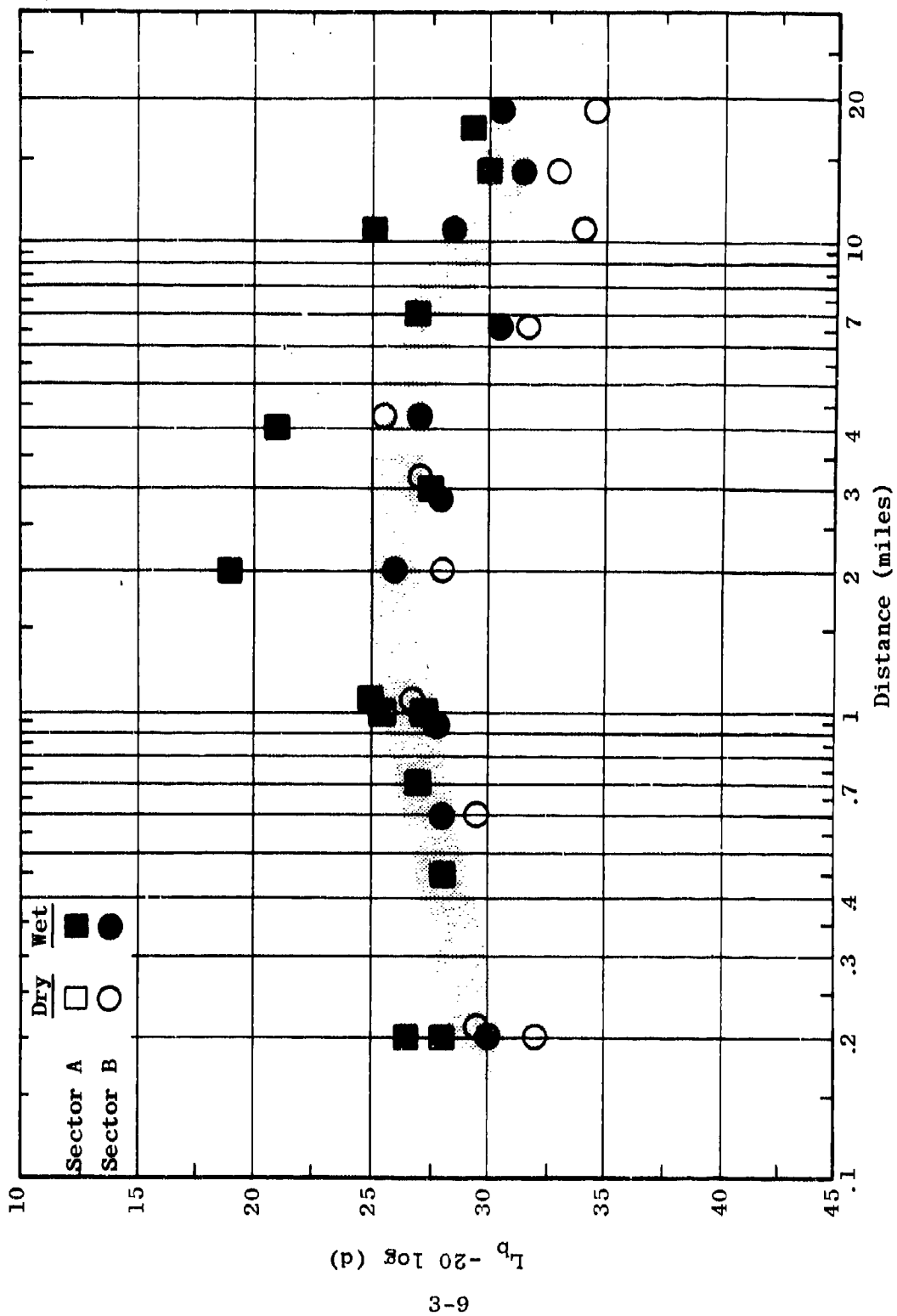


Figure 3.2 Measured Data Summary
 $L_b = F_{A,B}(0.300, 80, V, d, 17)$

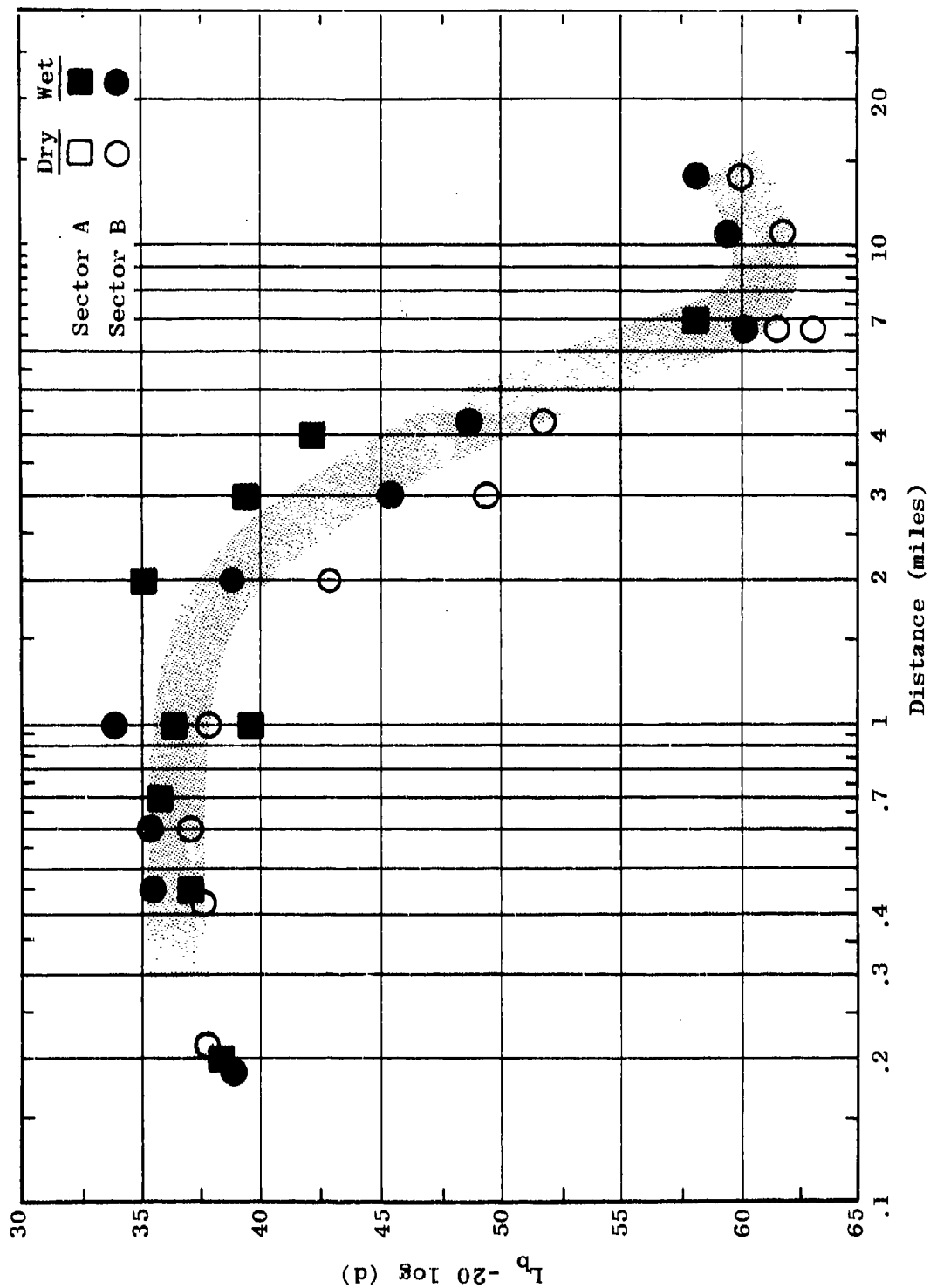


Figure 3.3 Measured Data Summary
 $L_b = F_{A,B}(0.880, 80, V, d, 17)$

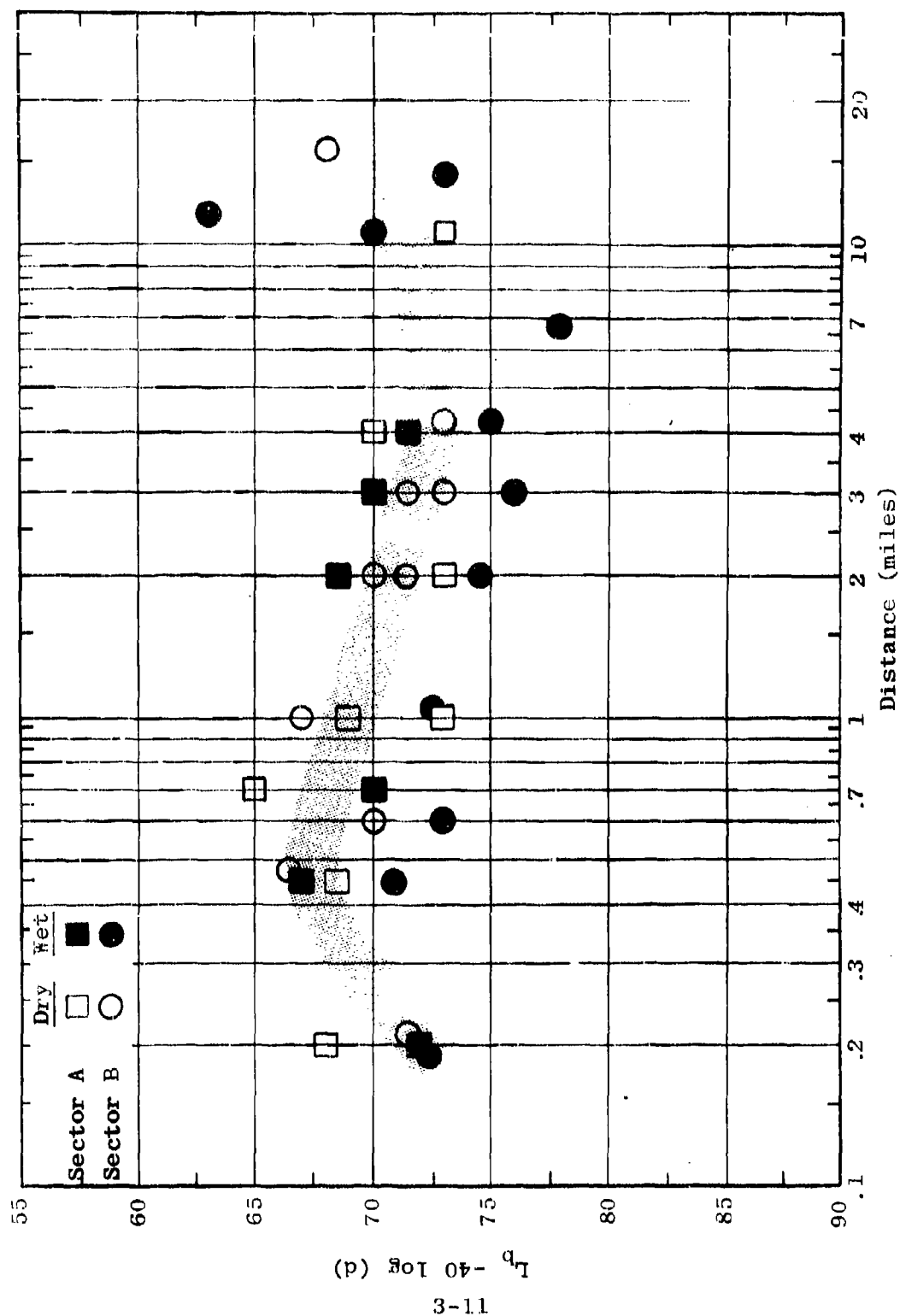


Figure 3.4 Measured Data Summary
 $L_b = F_{A,B}(2.0, 80, V, d, 17)$

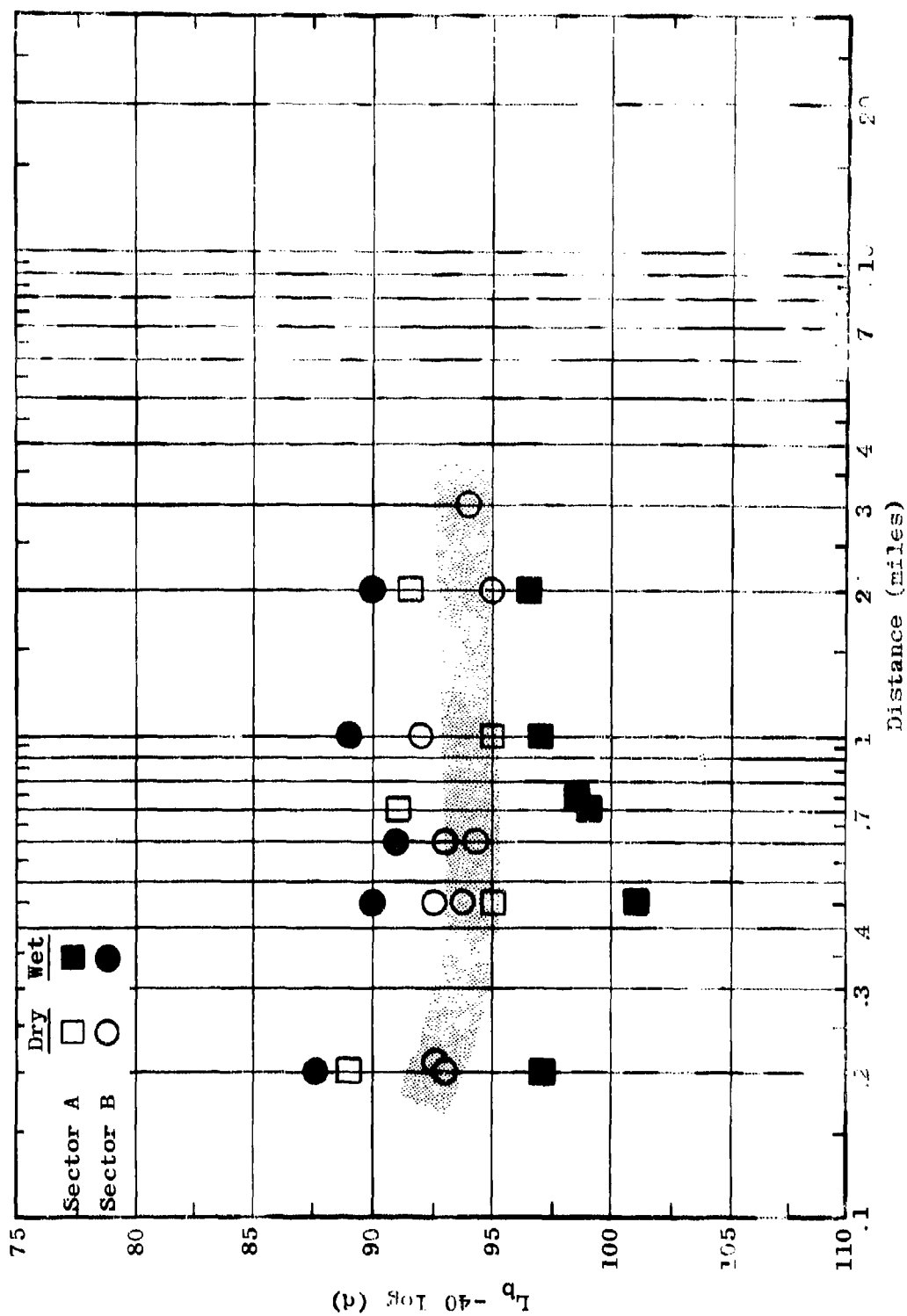


Figure 3.5 Measured Data Summary;
 $L_p = F_{A,B}(S.C., 40, V, d, 17)$

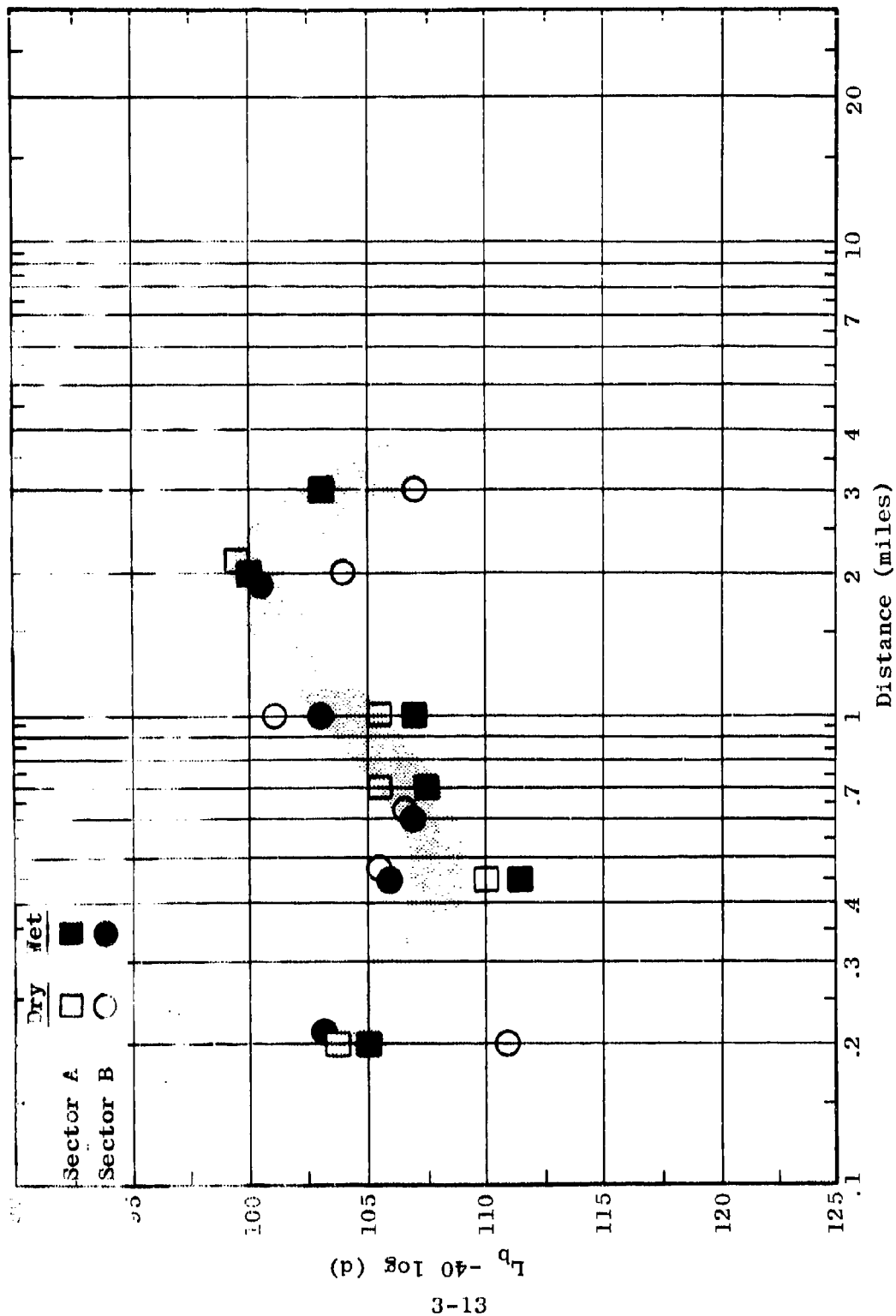


Figure 3.6 Measured Data Summary
 $L_b = F_{A,B}(12.0, 20, V, d, 17)$

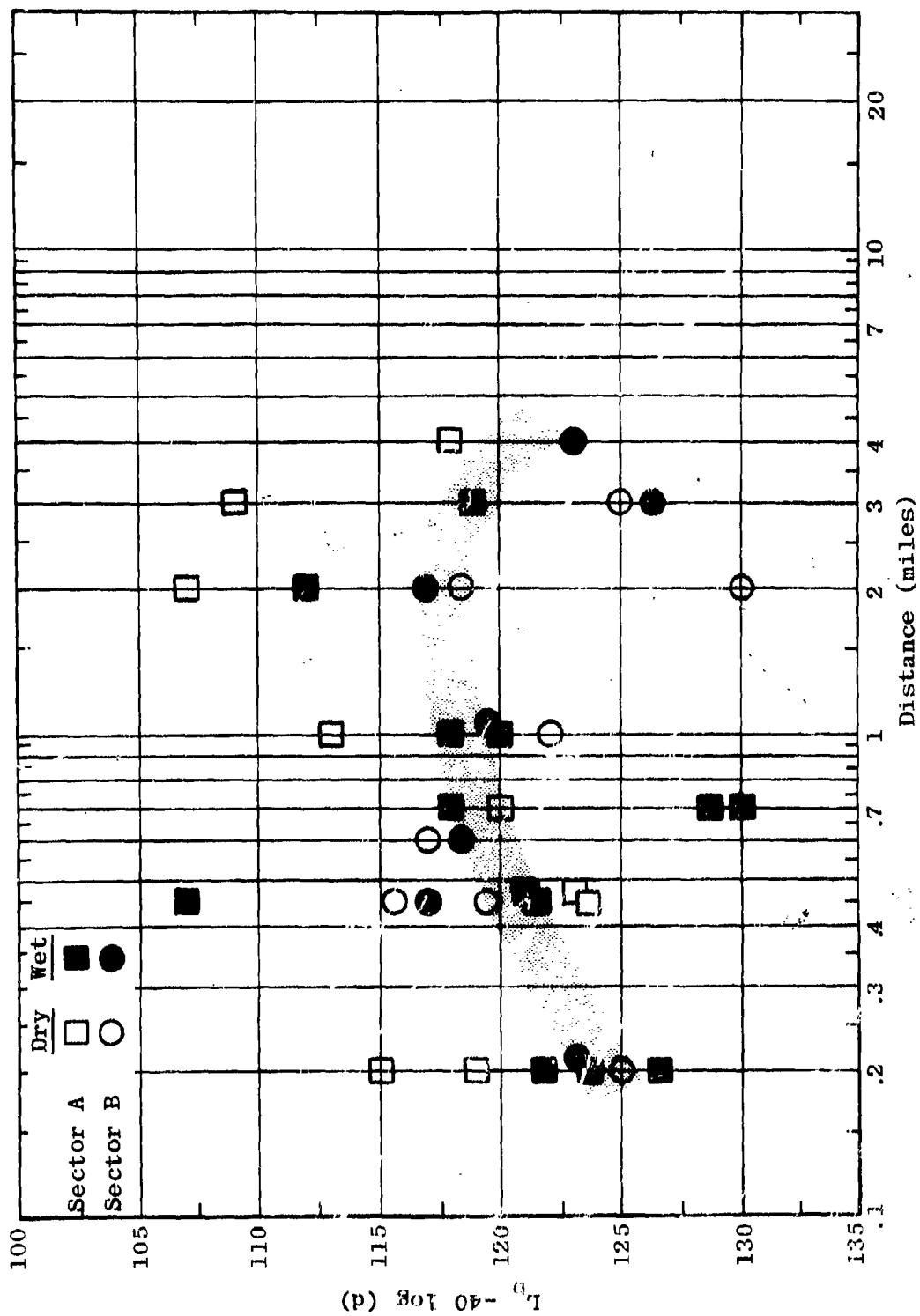


Figure 3.7 Measured Data Summary
 $L_b = F_{A,B}(25.5, 10, V, d, 11)$

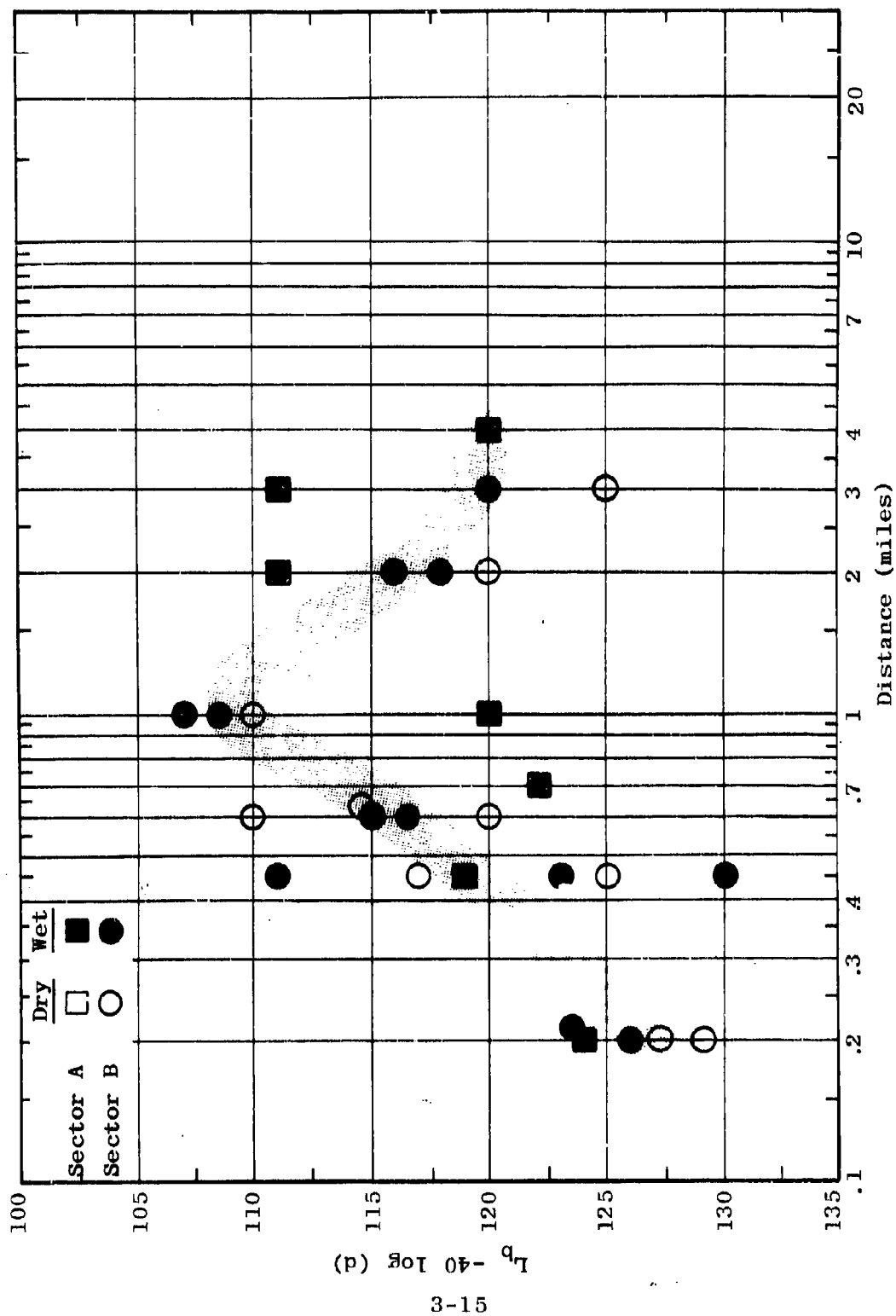


Figure 3.8 Measured Data Summary
 $L_b = F A, B (50.0, 13, V, d, 20)$

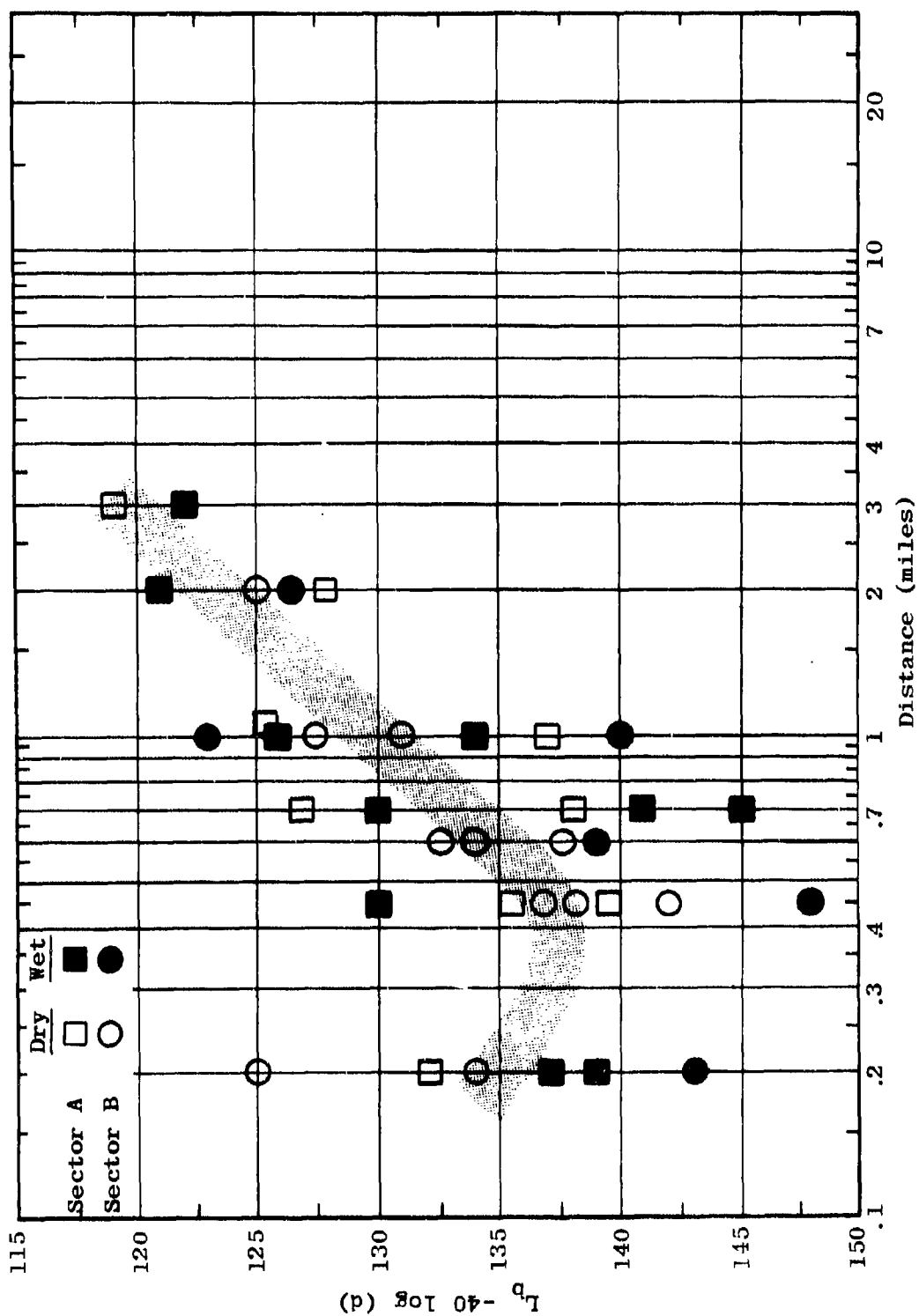


Figure 3.9 Measured Data Summary
 $L_b = F_{A,B}(100.0, 13, V, d, 11)$

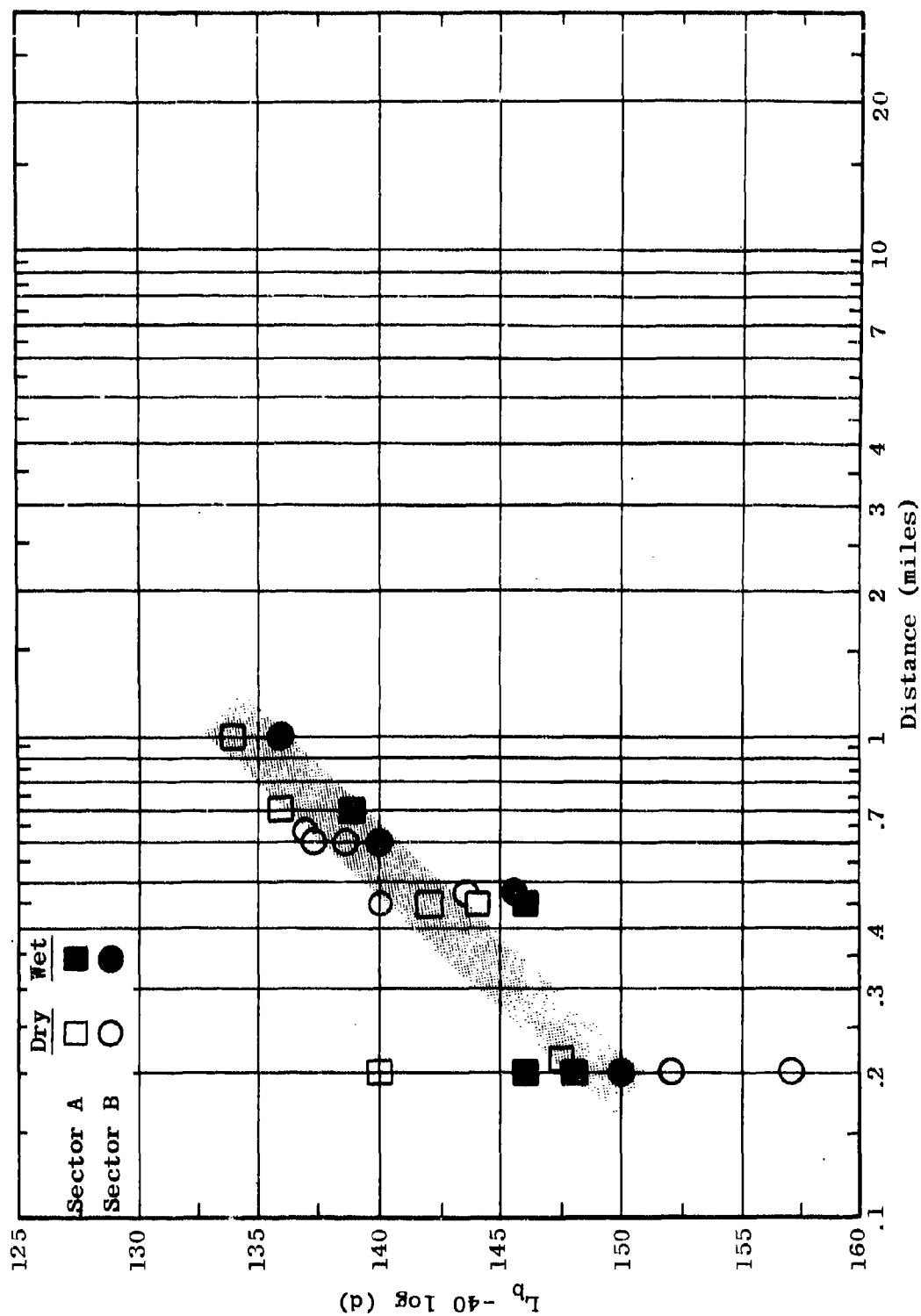


Figure 3.10 Measured Data Summary
 $L_b = F_{A,B}(250.0, 13, V, d, 11)$

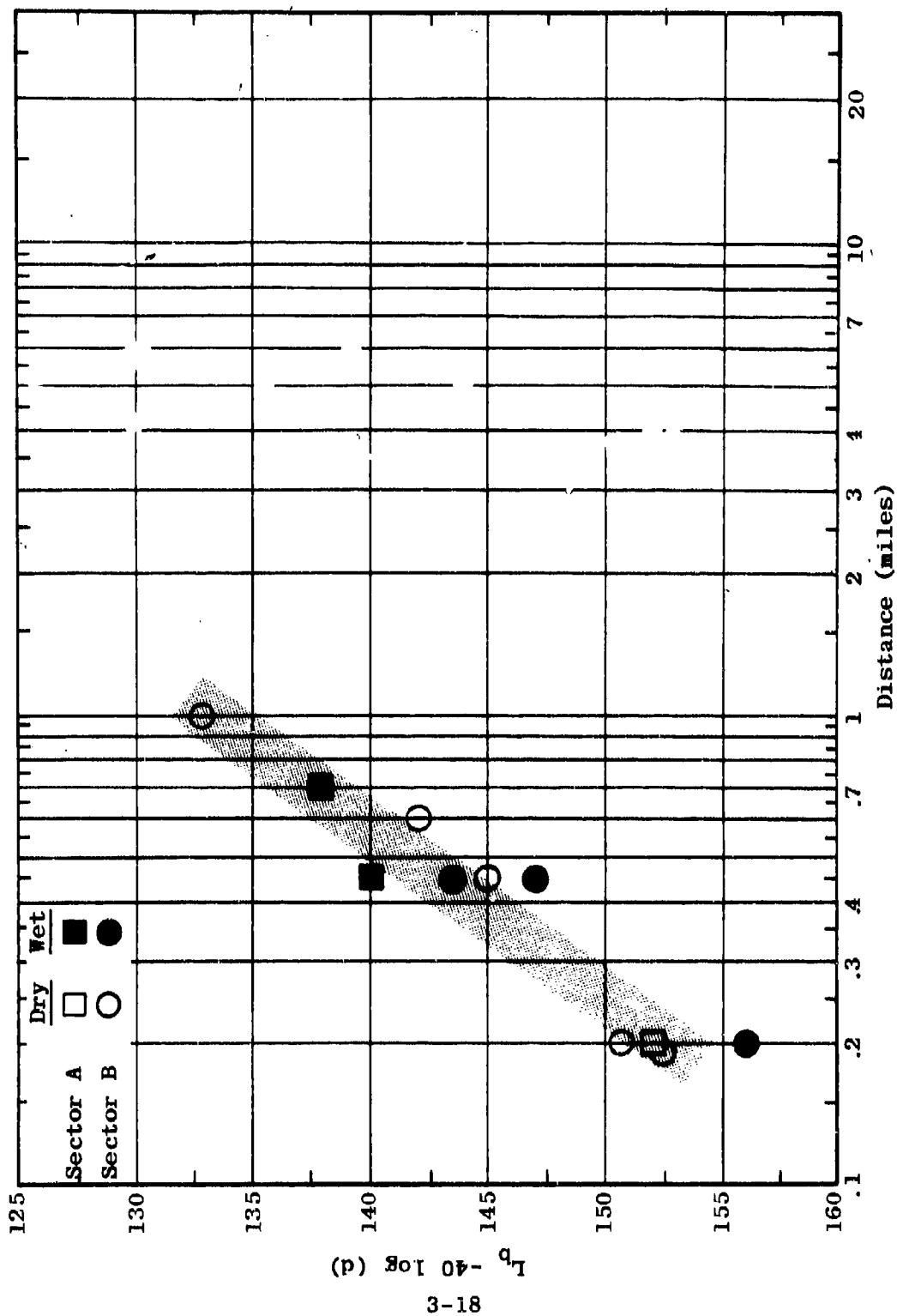


Figure 3.11 Measured Data Summary
 $L_b = F_{A,B}(400.0, 13, V, d, 11)$

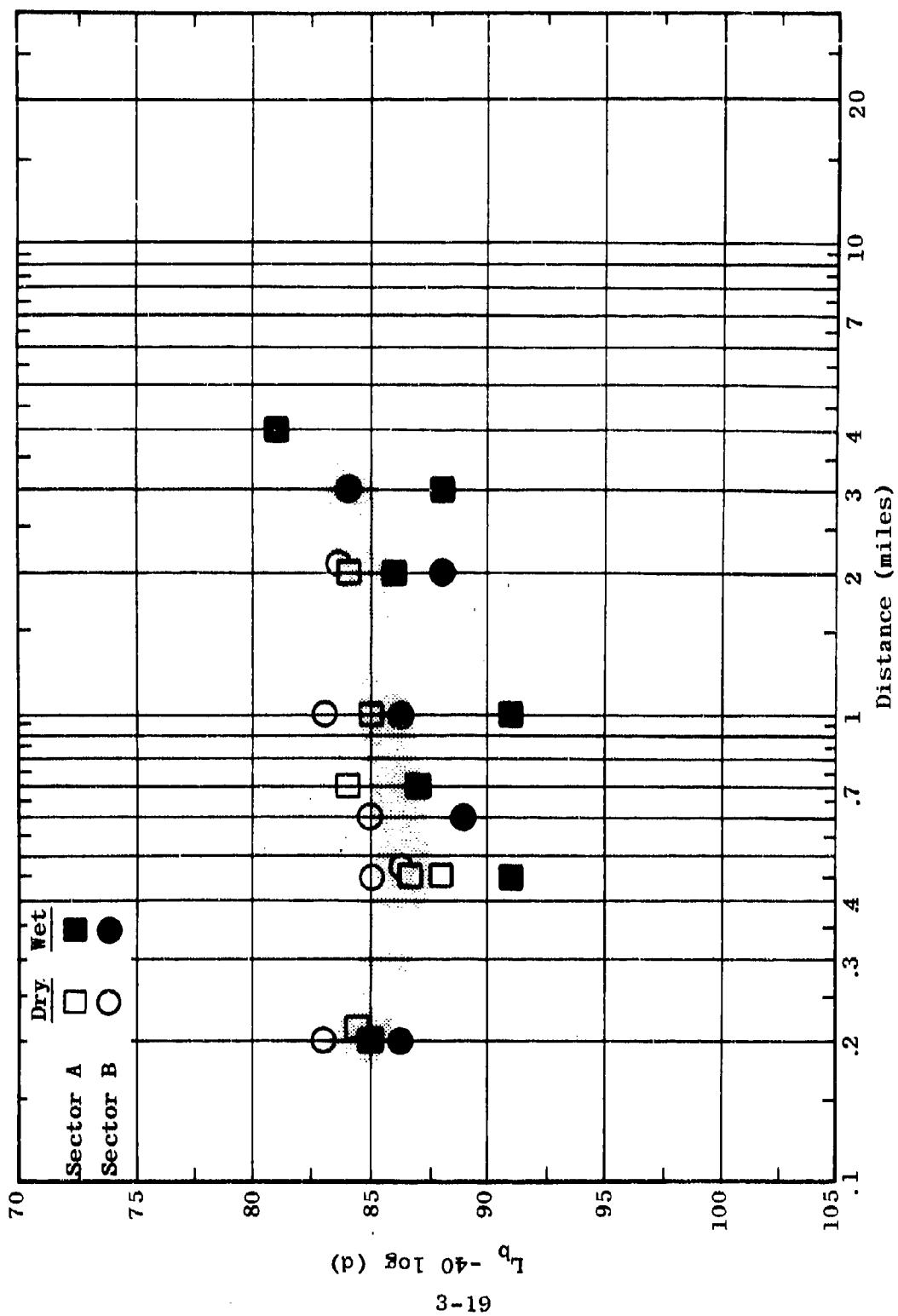


Figure 3.12 Measured Data Summary
 $L_p = F_{A,B}(2.0, 40, H, d, 17)$

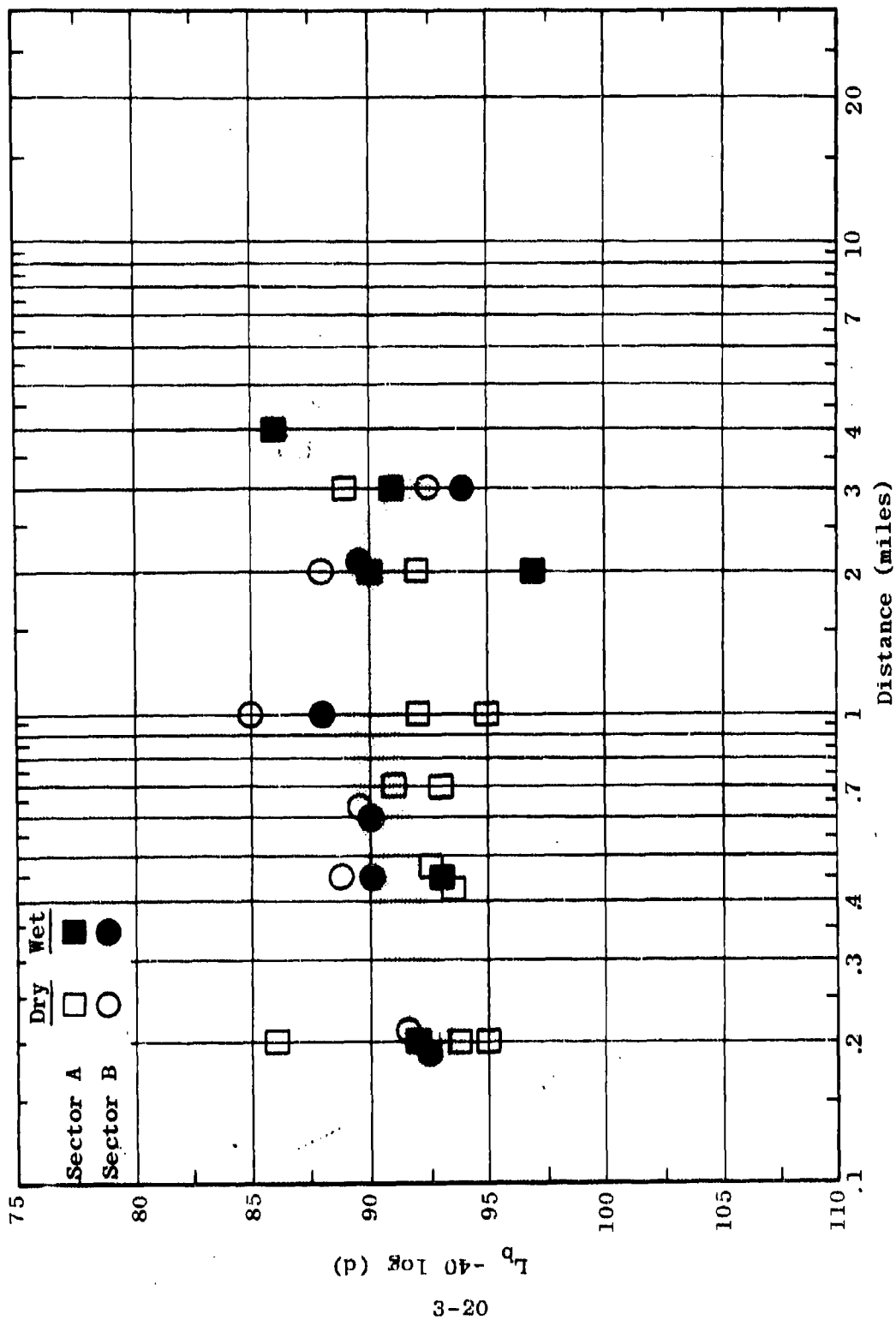


Figure 3.13 Measured Data Summary
 $L_p = F_{A,B}(6.0, 40, H, d, 17)$

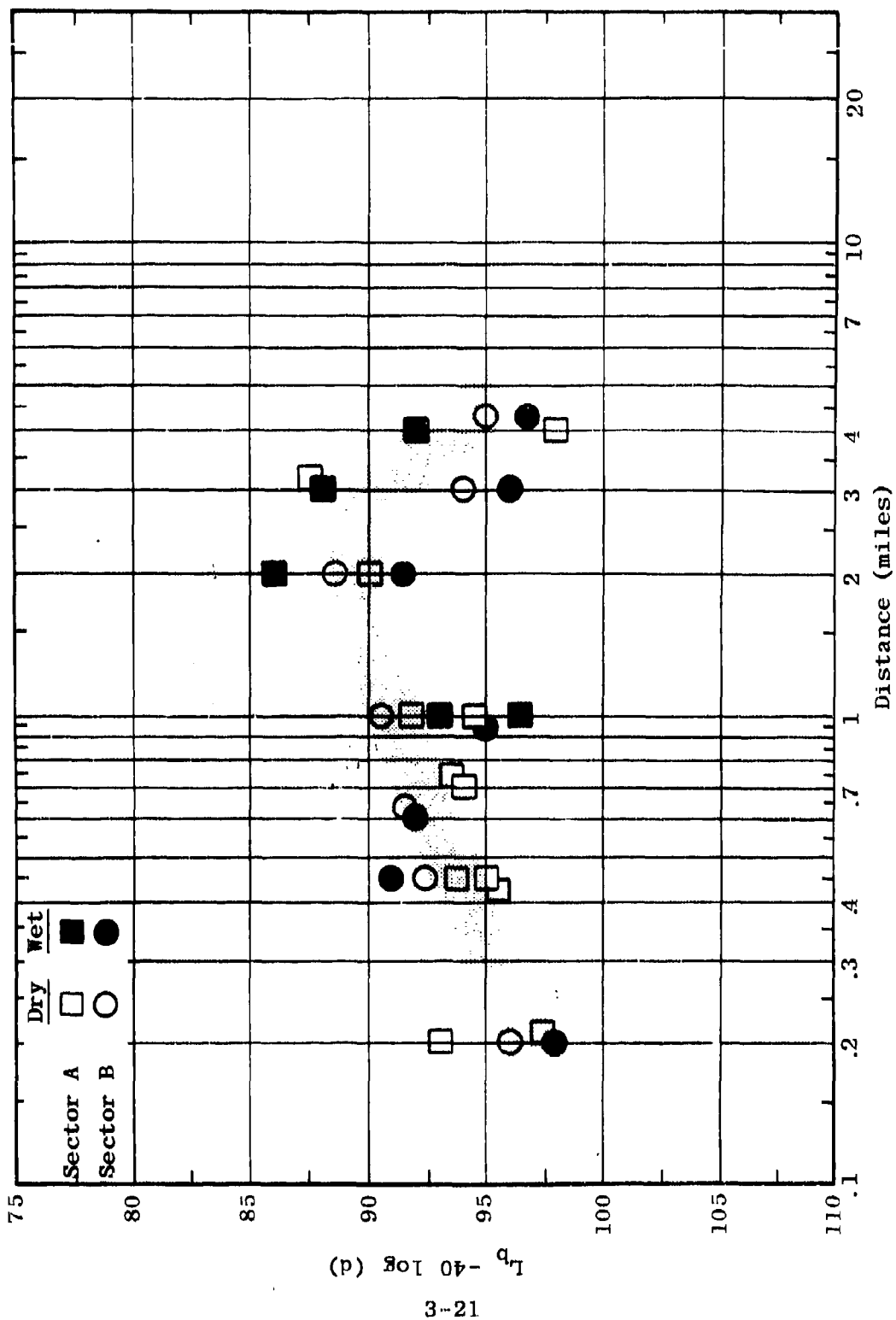


Figure 3.14 Measured Data Summary
 $L_b = F_{A,B}(12.0, 40, H, d, 17)$

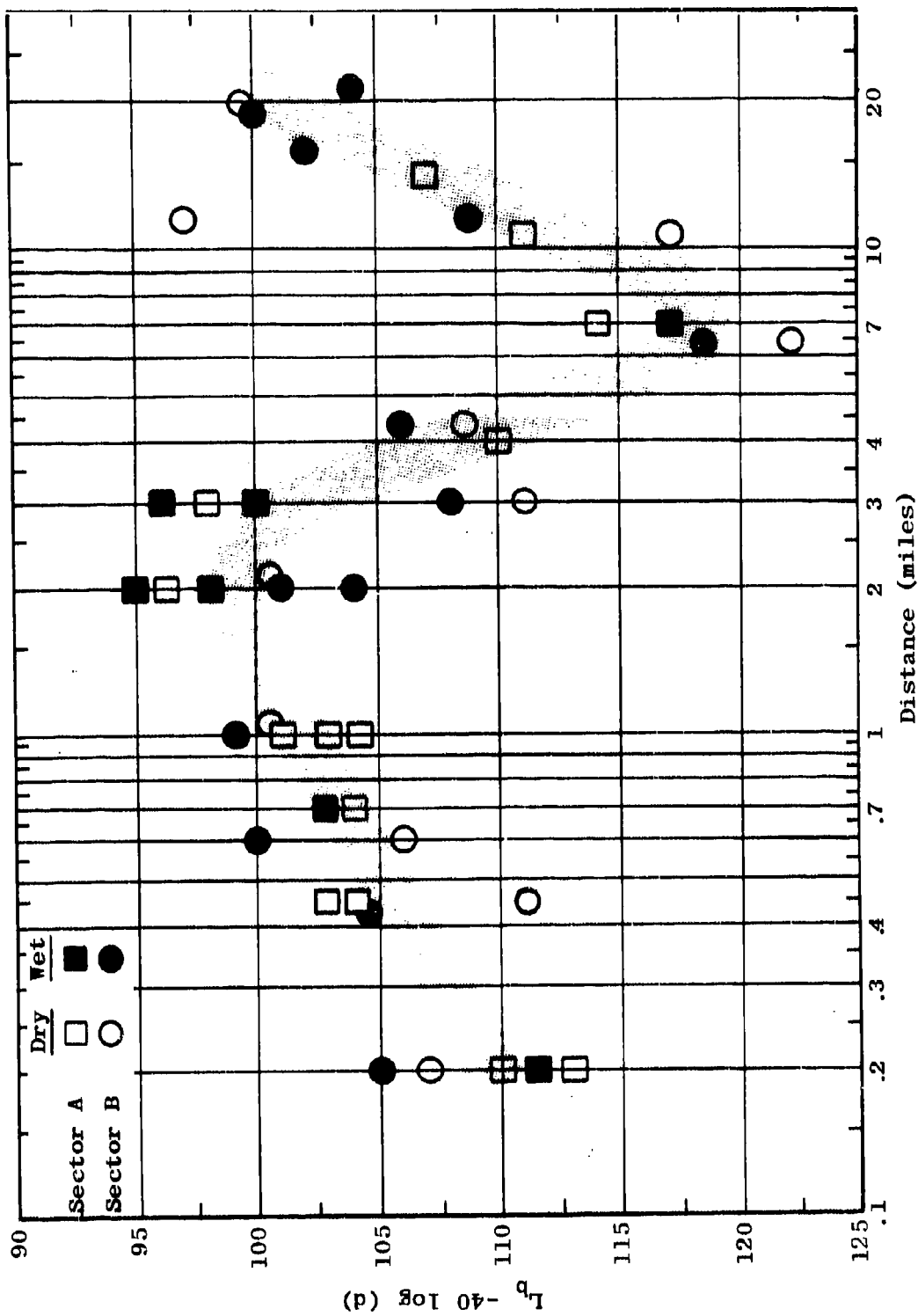


Figure 3.15 Measured Data Summary
 $L_E = F_{A,B}(25.5, 13, H, d, 11)$

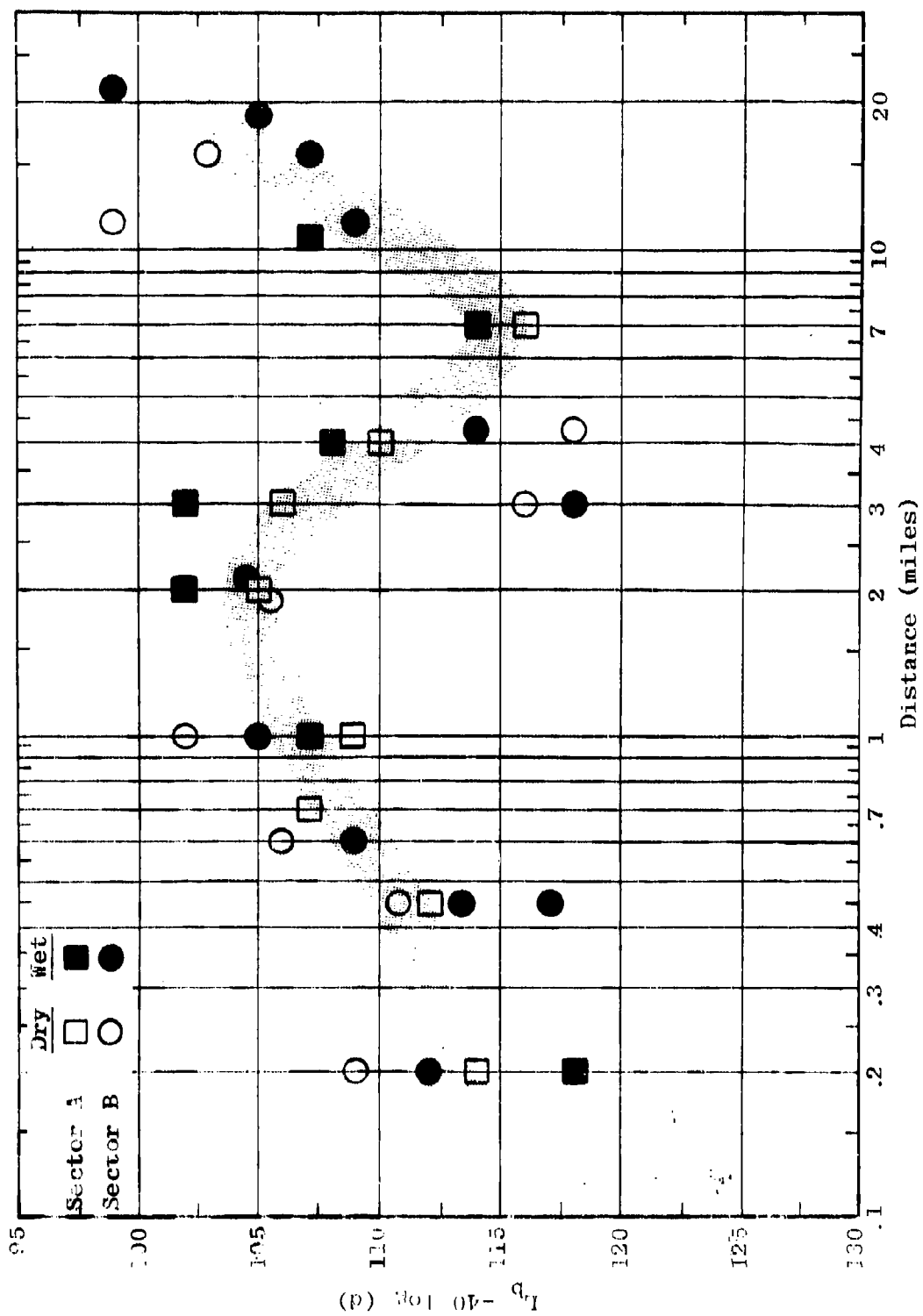


Figure 3.16 Measured Data Summary
 $L_b = F_{A,B}(50.0, 13, H, d, 11)$

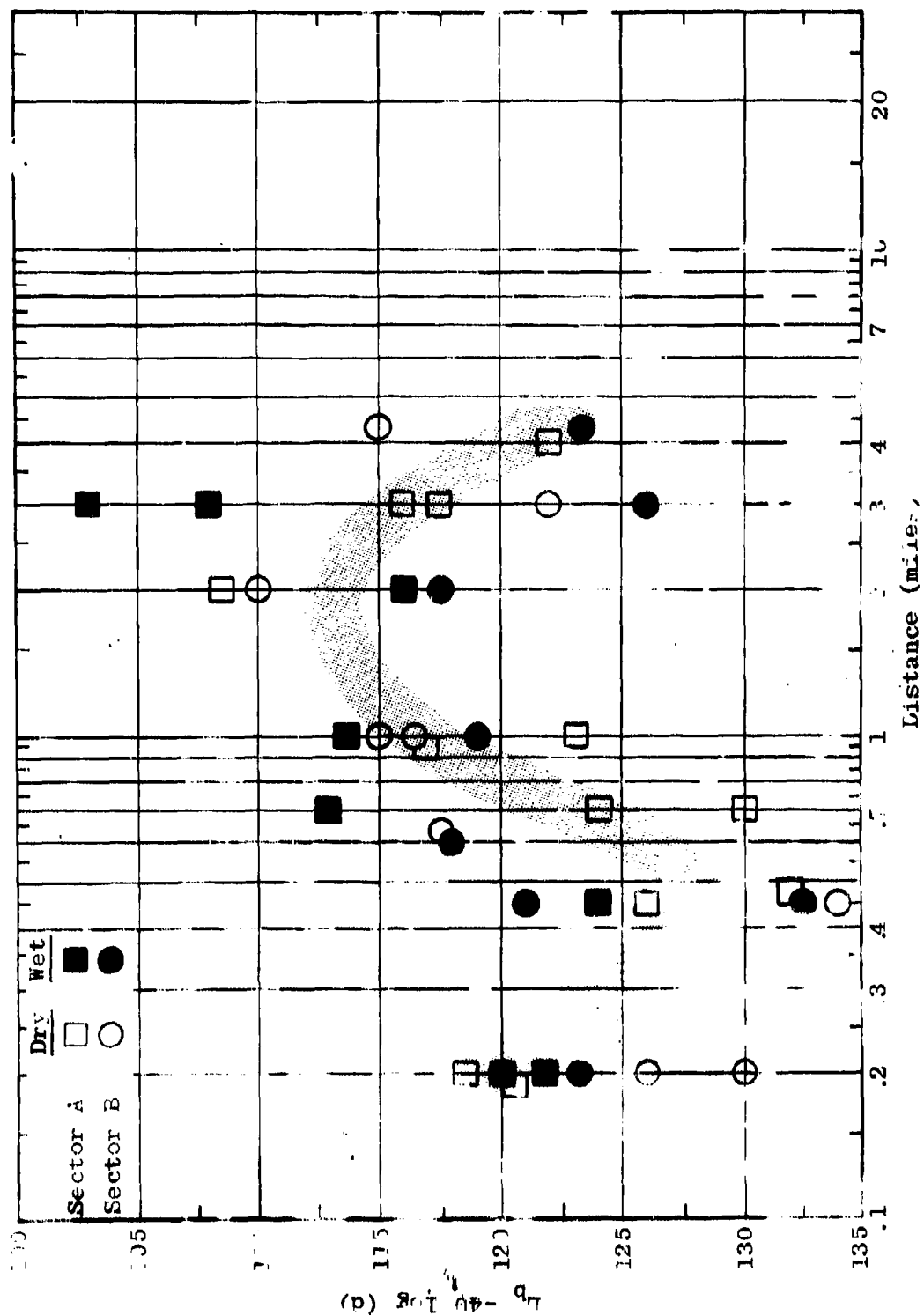


Figure 3.17 Measured Data Summary
 $L_b = F_{A,B} C_{00} 0, 12, 4, d, 11$

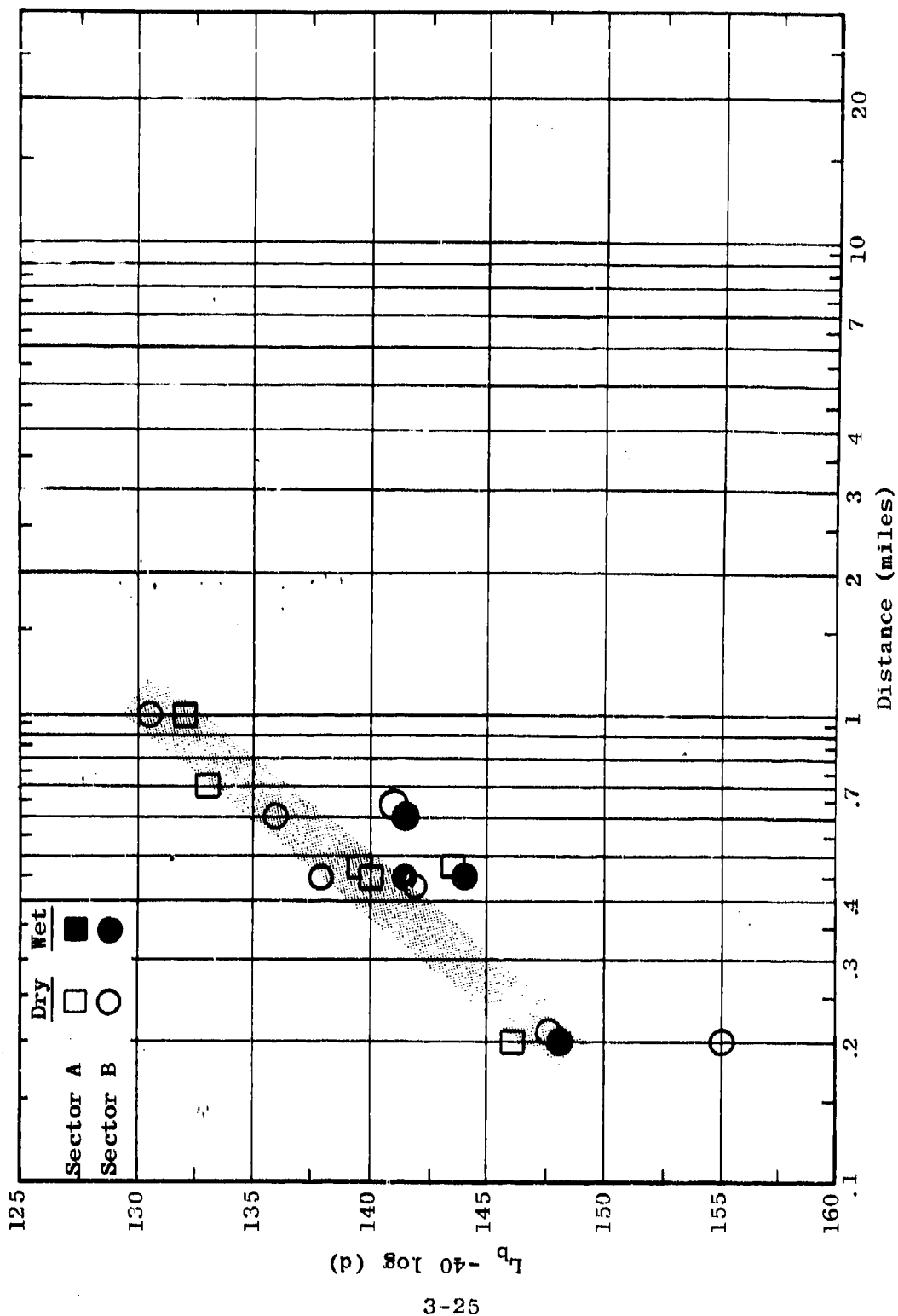


Figure 3.18 Measured Data Summary
 $L_b = F_{A,B}(250.0, 13, H, d, 11)$

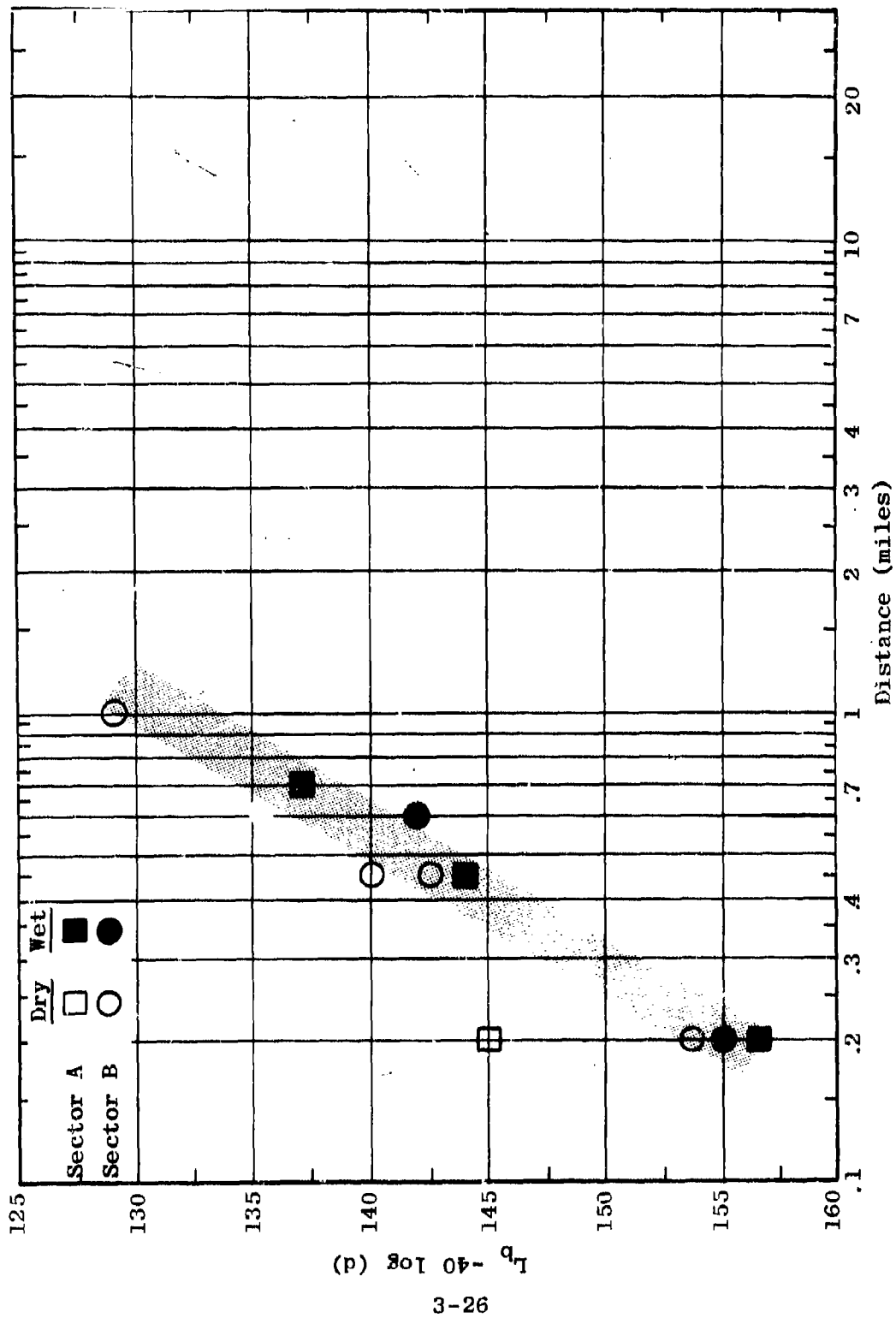


Figure 3.19 Measured Data Summary
 $L_b = F_{A,B}(400.0, 13, H, d, 11)$

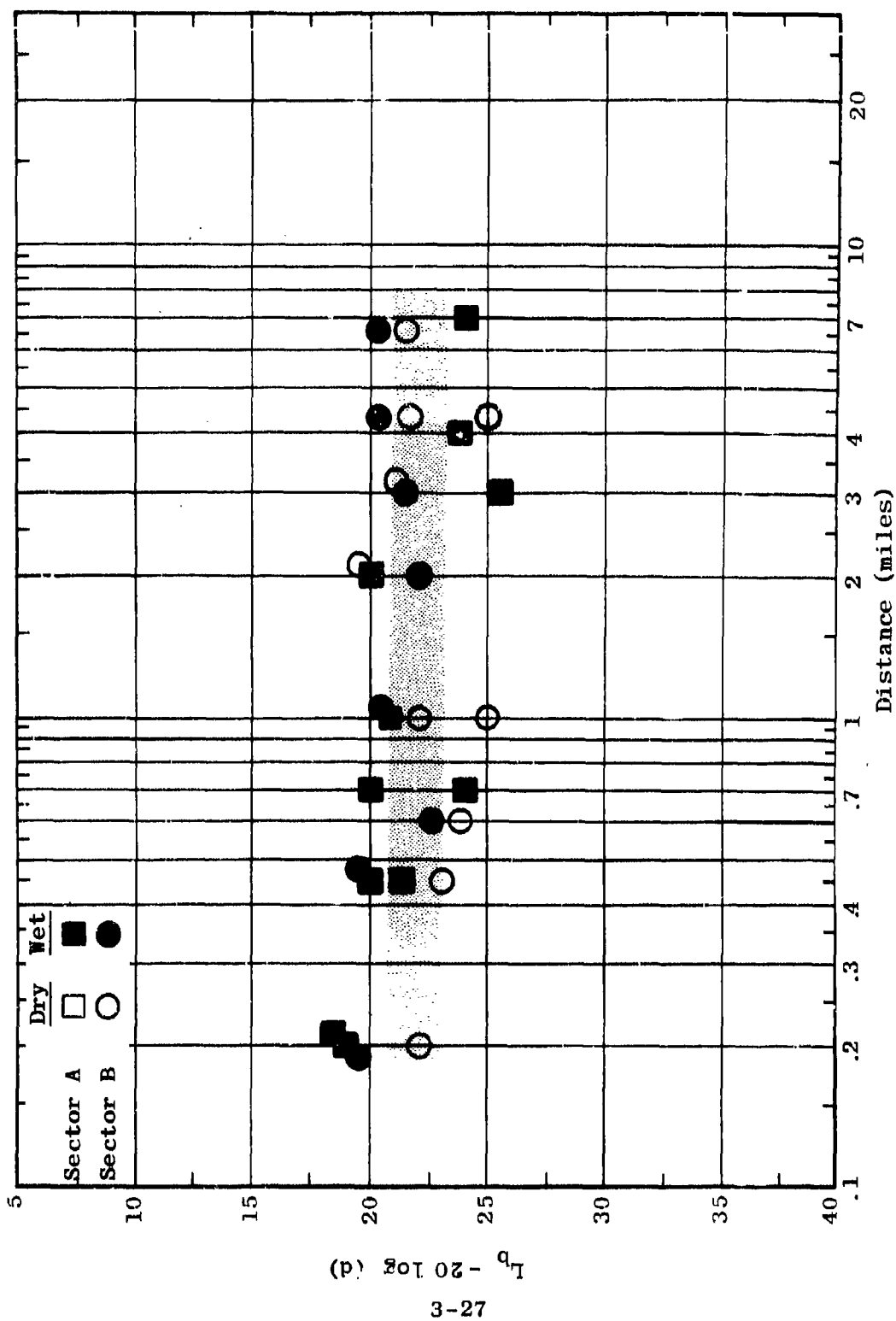


Figure 3.20 Measured Data Summary
 $L_b = F_{A,B}(0.105, 80, V, d, 80)$

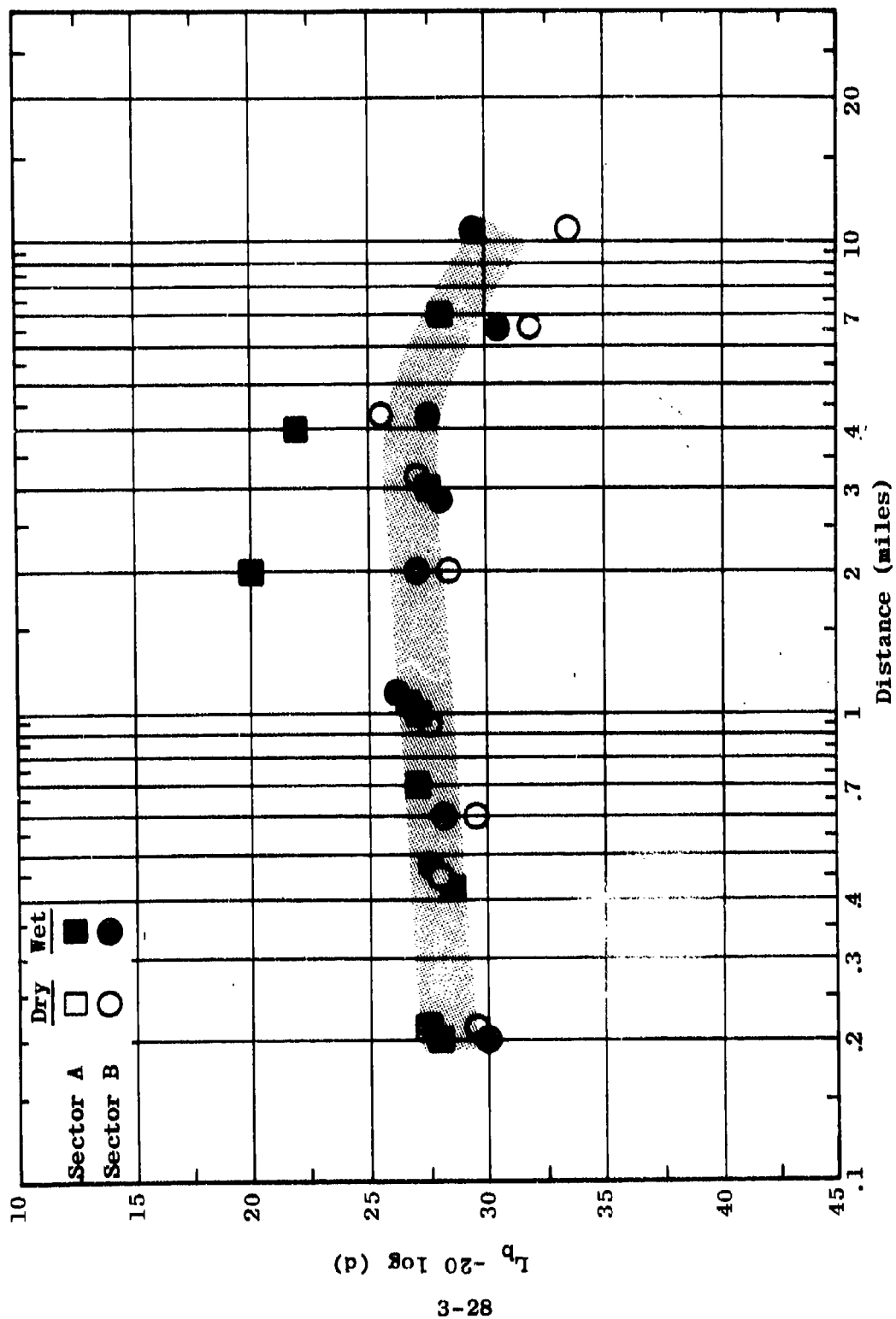


Figure 3.21 Measured Data Summary
 $L_b = F_{A,B} (0.300, 80, V, d, 80)$

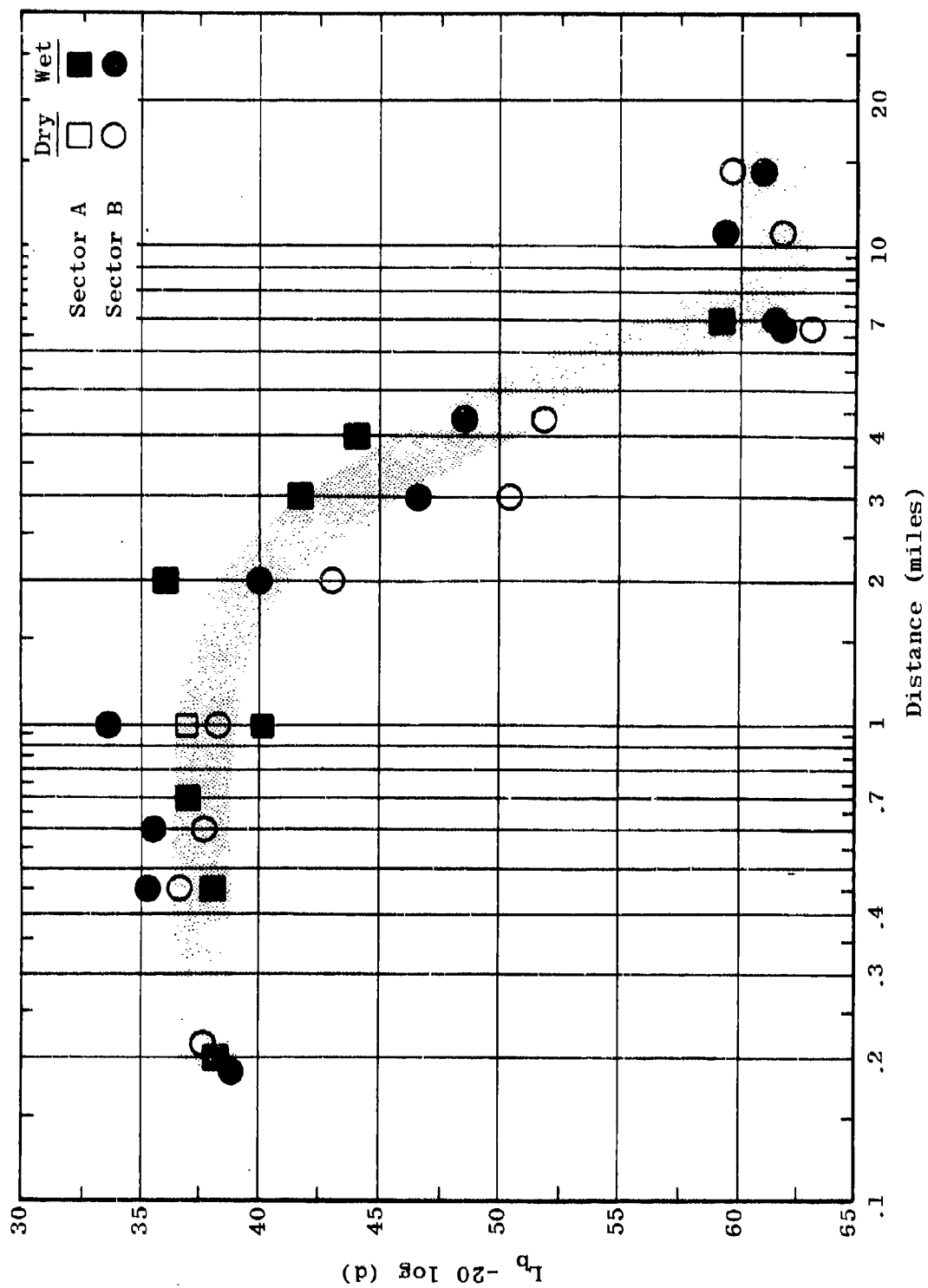


Figure 3.22 Measured Data Summary
 $L_b = F_{A,B}(0.880, 80, V, d, 80)$

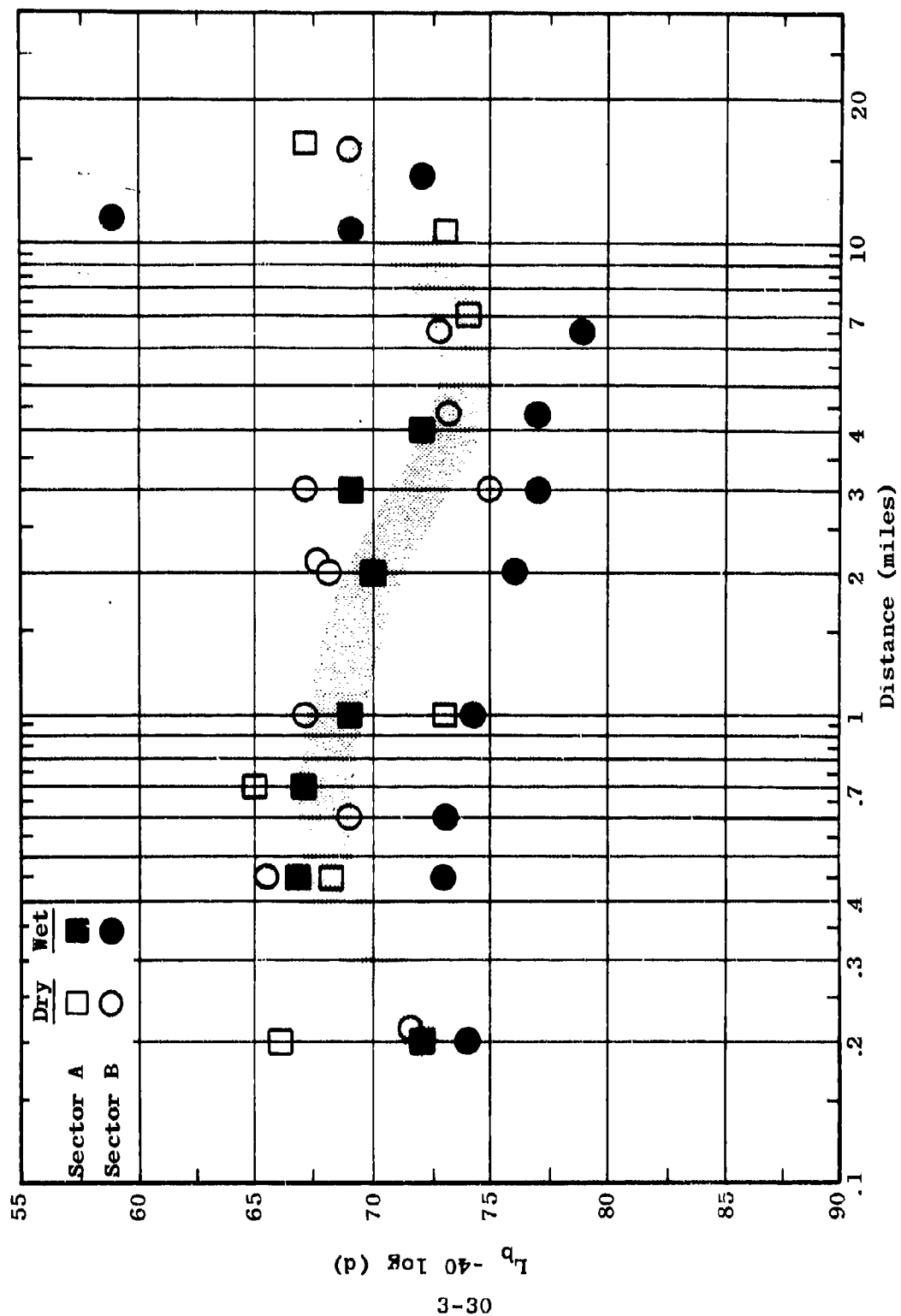


Figure 3.23 Measured Data Summary
 $L_b = F_{A,B}(2.0, 80, V, d, 80)$

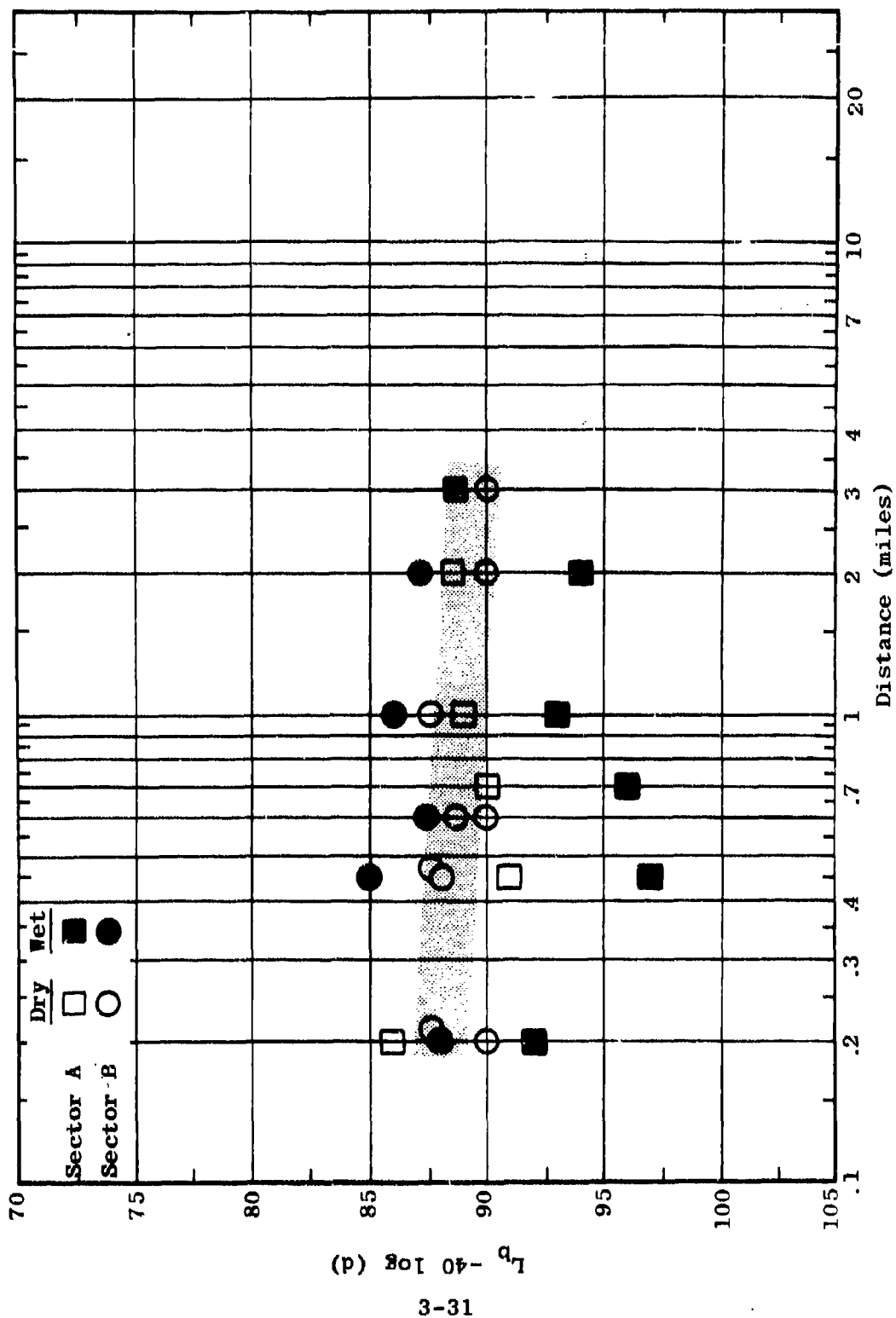


Figure 3.24 Measured Data Summary
 $L_b = F_{A,B}(6.0, 40, V, d, 80)$

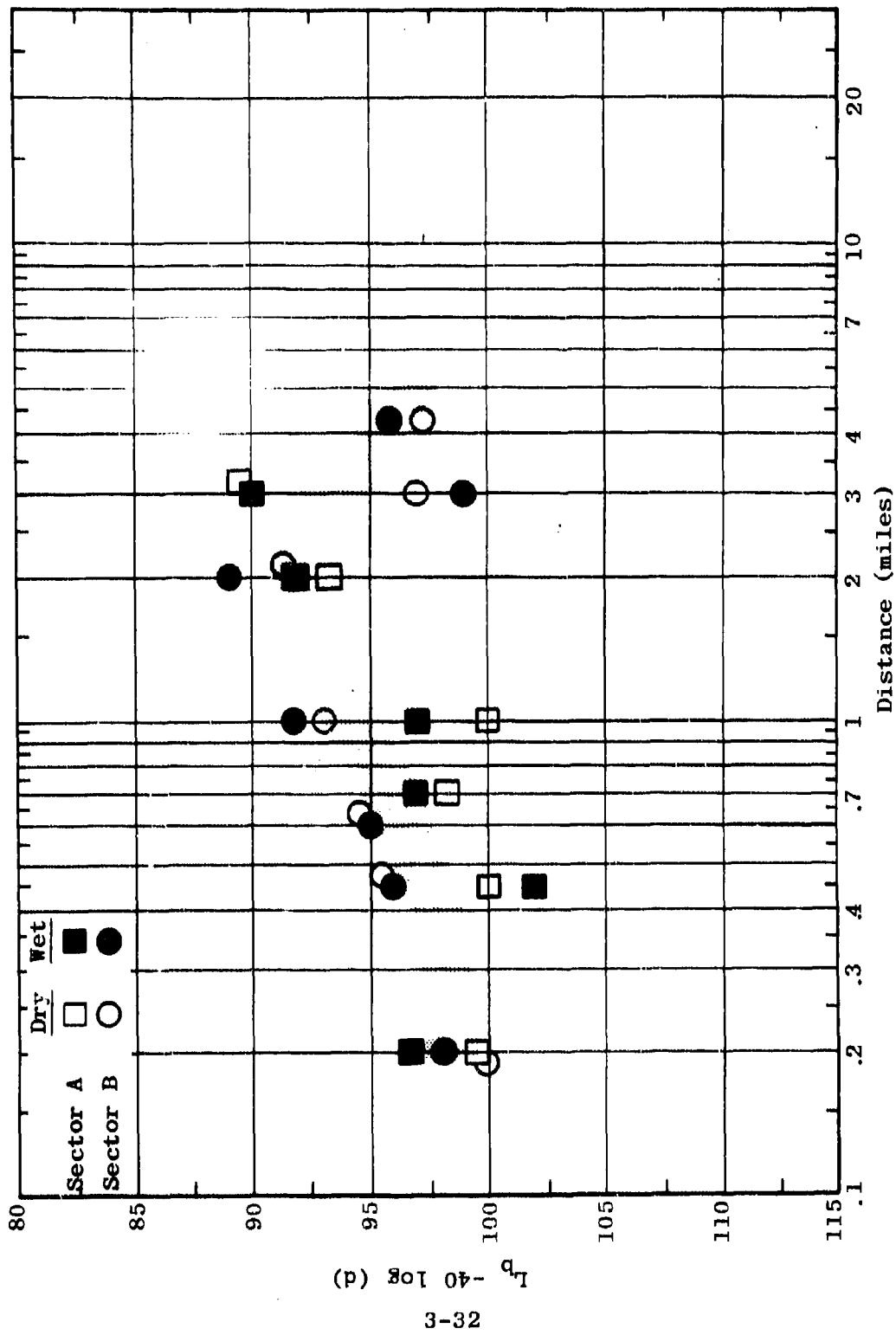


Figure 3.25 Measured Data Summary
 $L_b = F_{A,B}(12.0, 20, V, d, 80)$

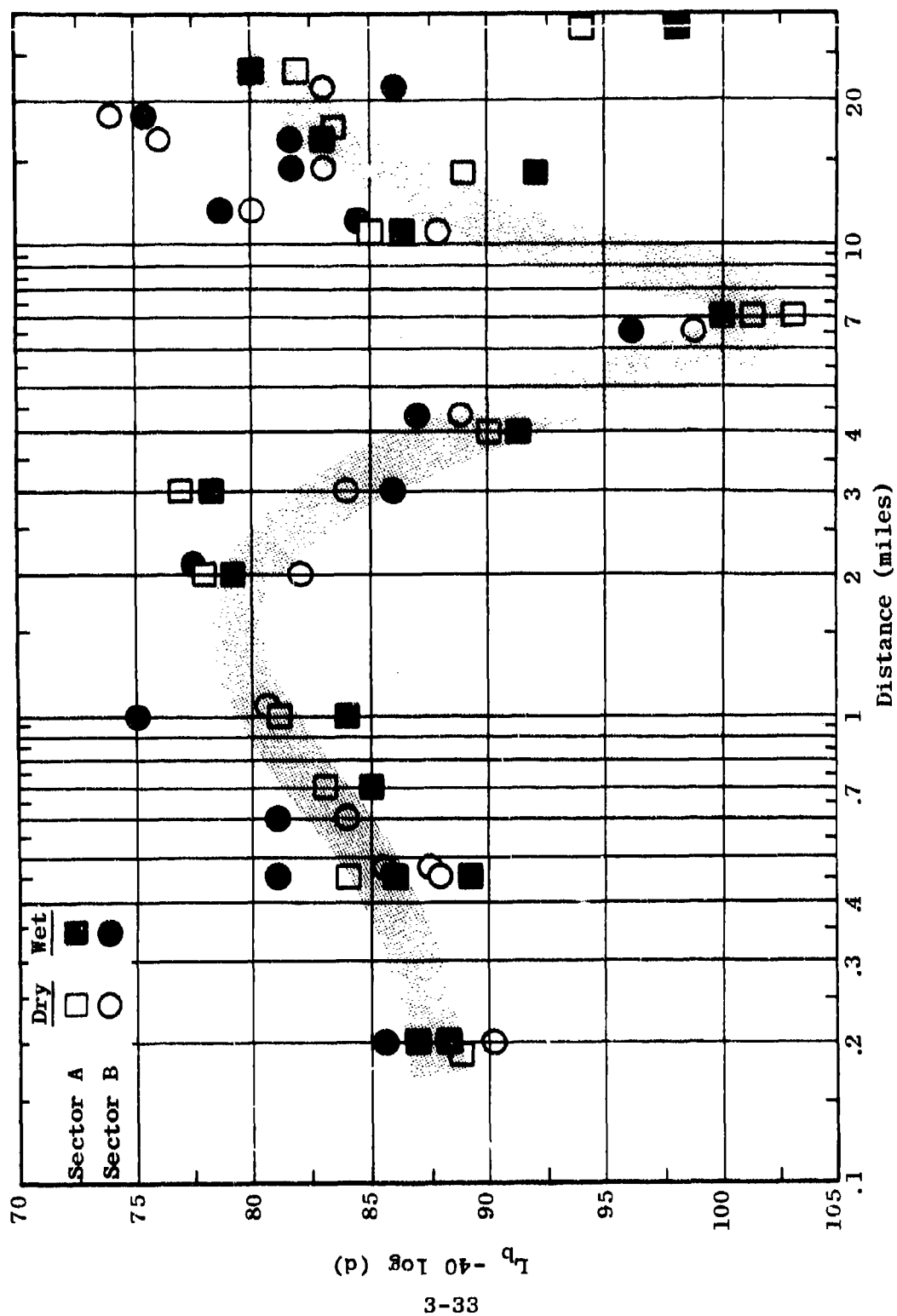


Figure 3.26 Measured Data Summary
 $L_b = F_{A,B}(25.5, 80, V, d, 80)$

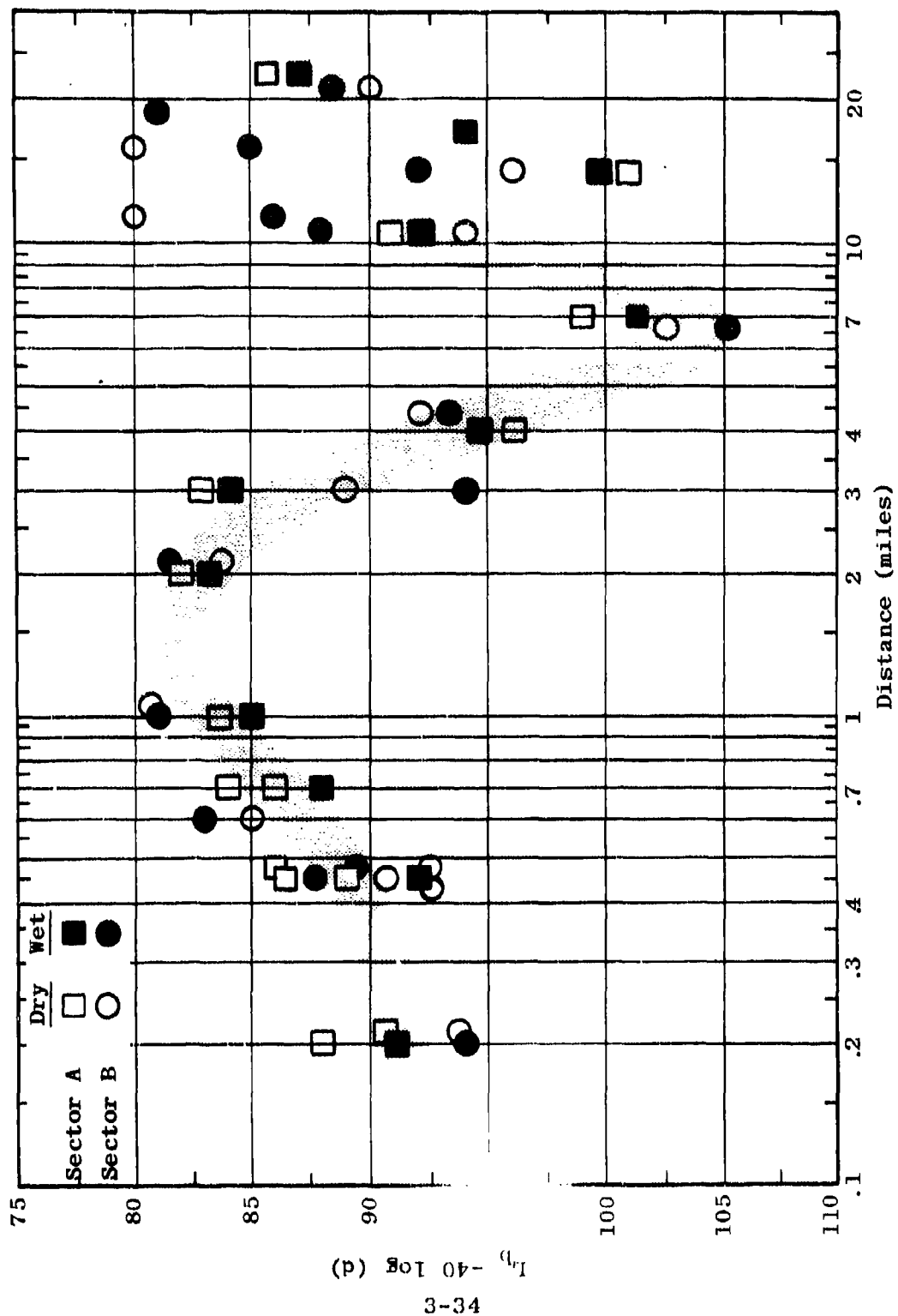


Figure 3.27 Measured Data Summary
 $L_b = F_{A,B}(50.0, 80, V, d, 80)$

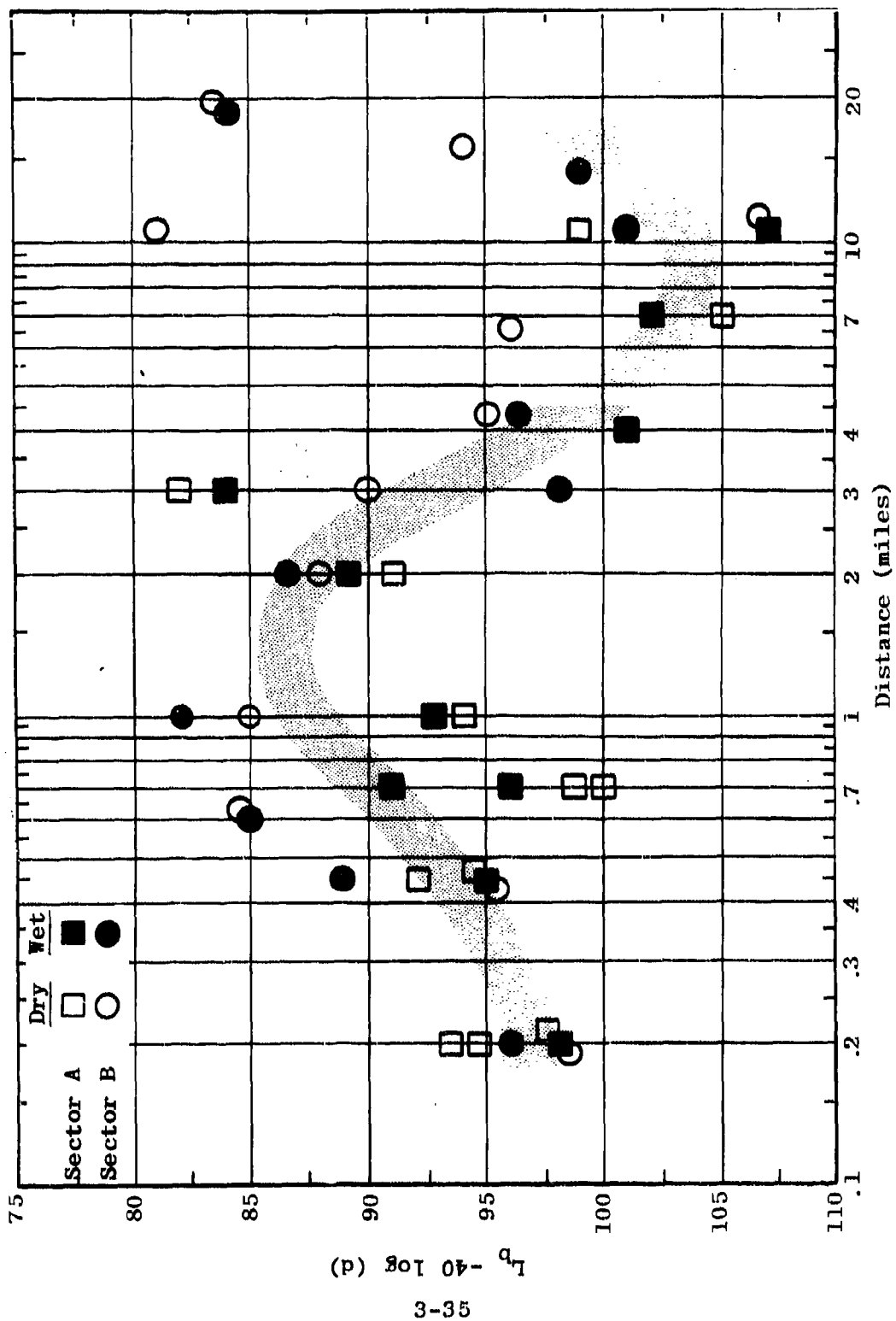


Figure 3.28 Measured Data Summary
 $L_p = F_{A,B}(100.0, 80, V, d, 80)$

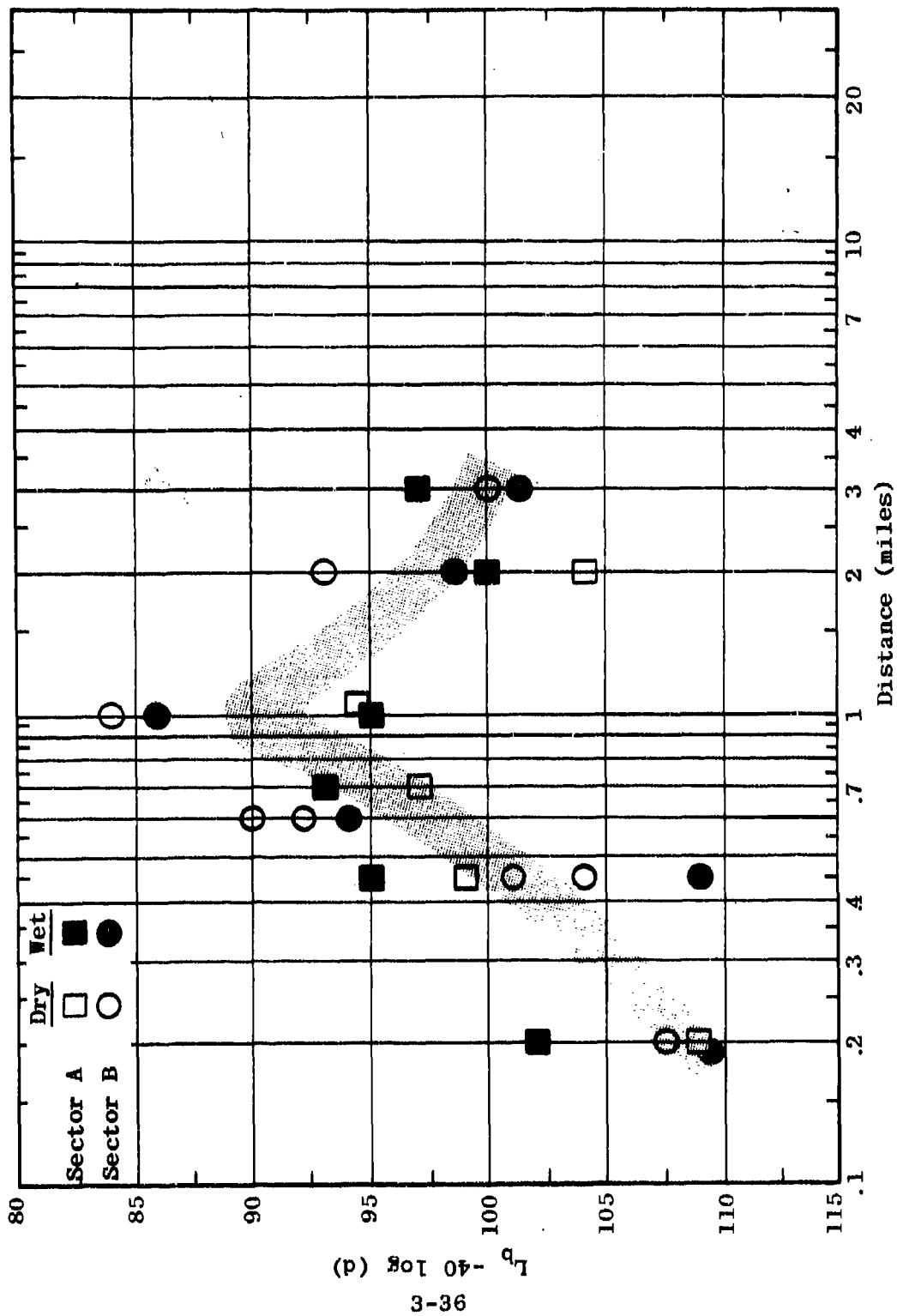


Figure 3.29 Measured Data Summary
 $L_b = F_{A,B}(250.0, 80, V, d, 80)$

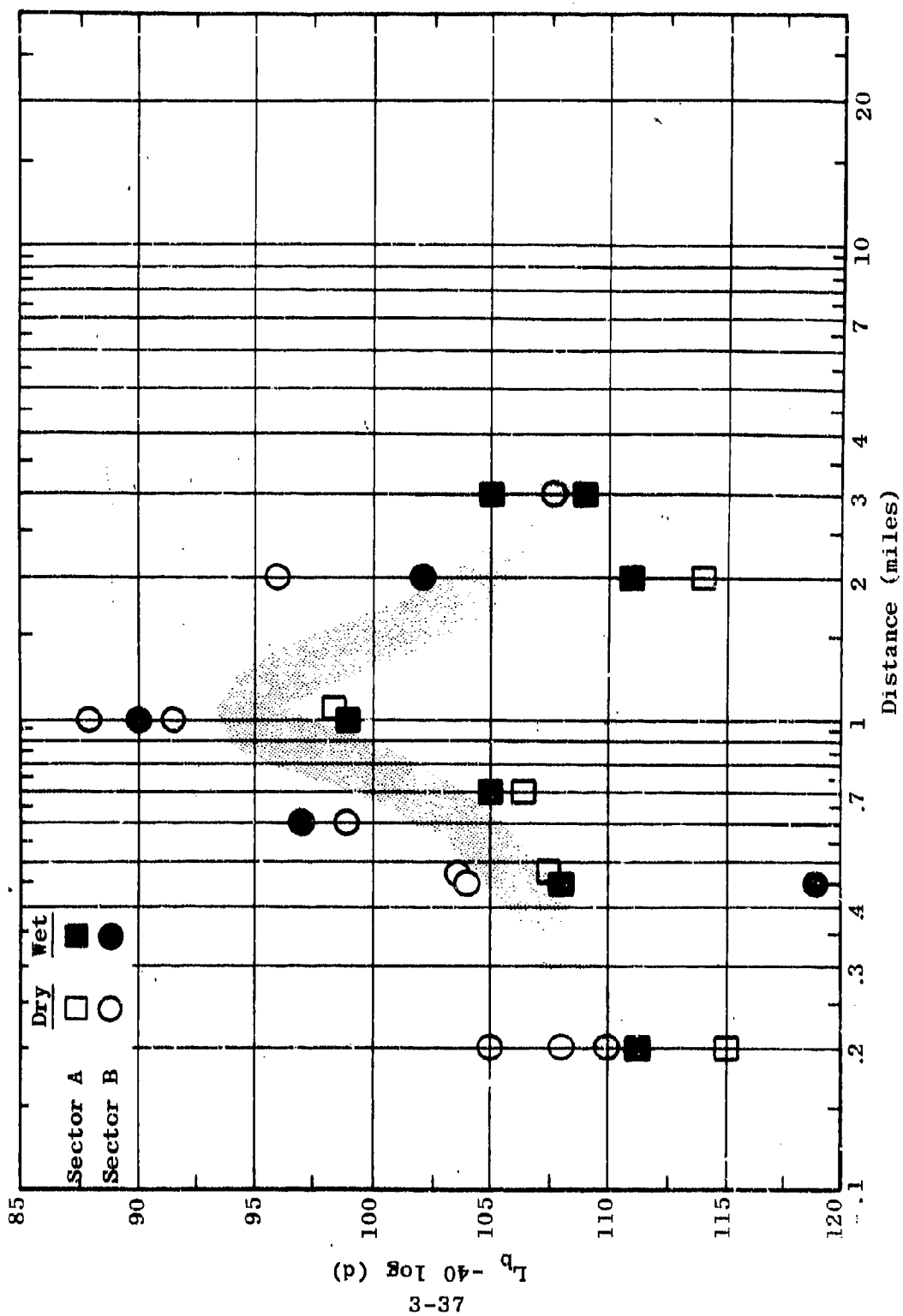


Figure 3.30 Measured Data Summary
 $L_b = F_{A,B}(400.0, 80, V, d, 80)$

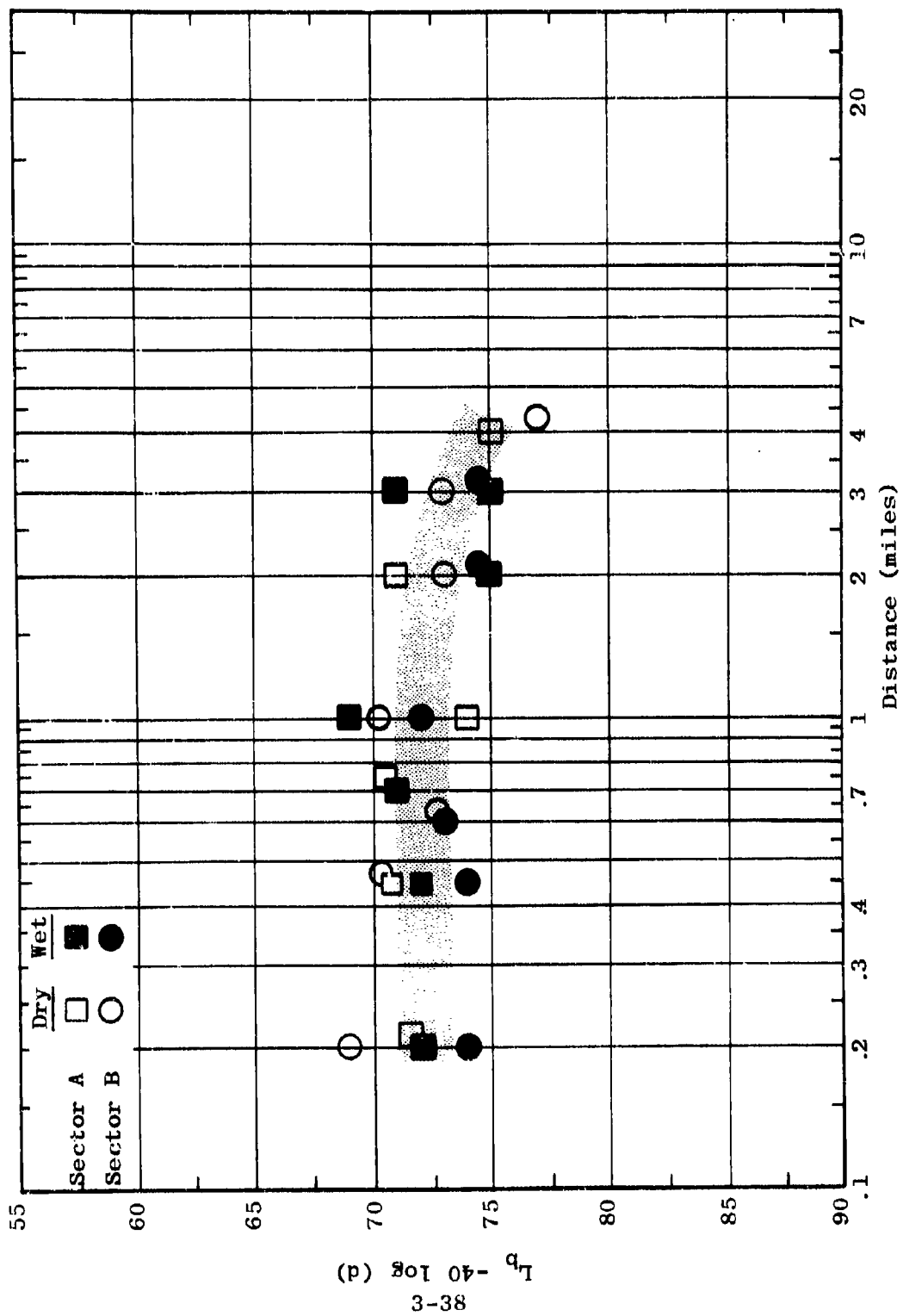


Figure 3.31 Measured Data Summary
 $L_b = F_{A,B}(2.0, 80; H, d, 80)$

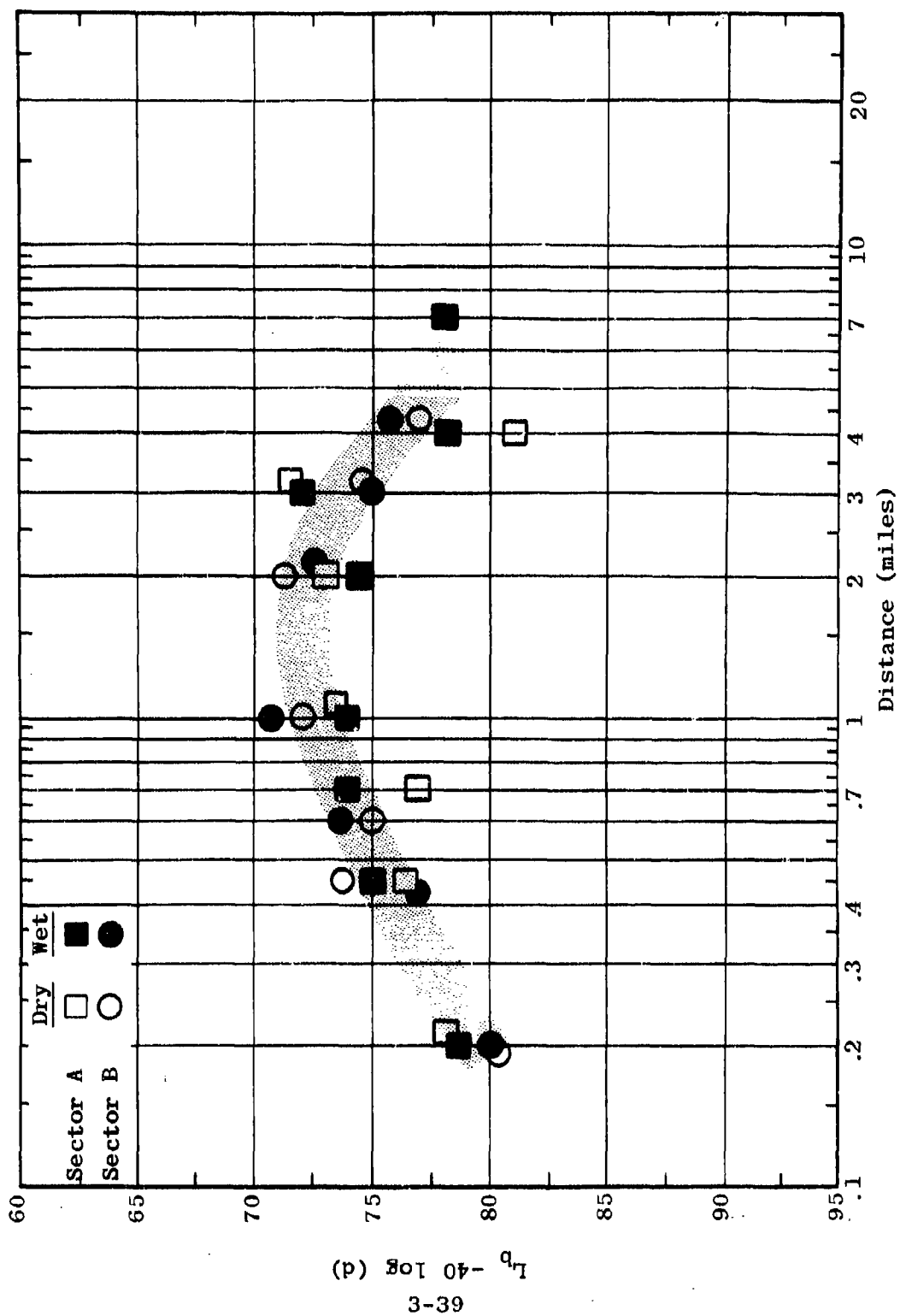


Figure 3.32 Measured Data Summary
 $L_b = F_{A,B}(6.0, 80, H, d, 80)$

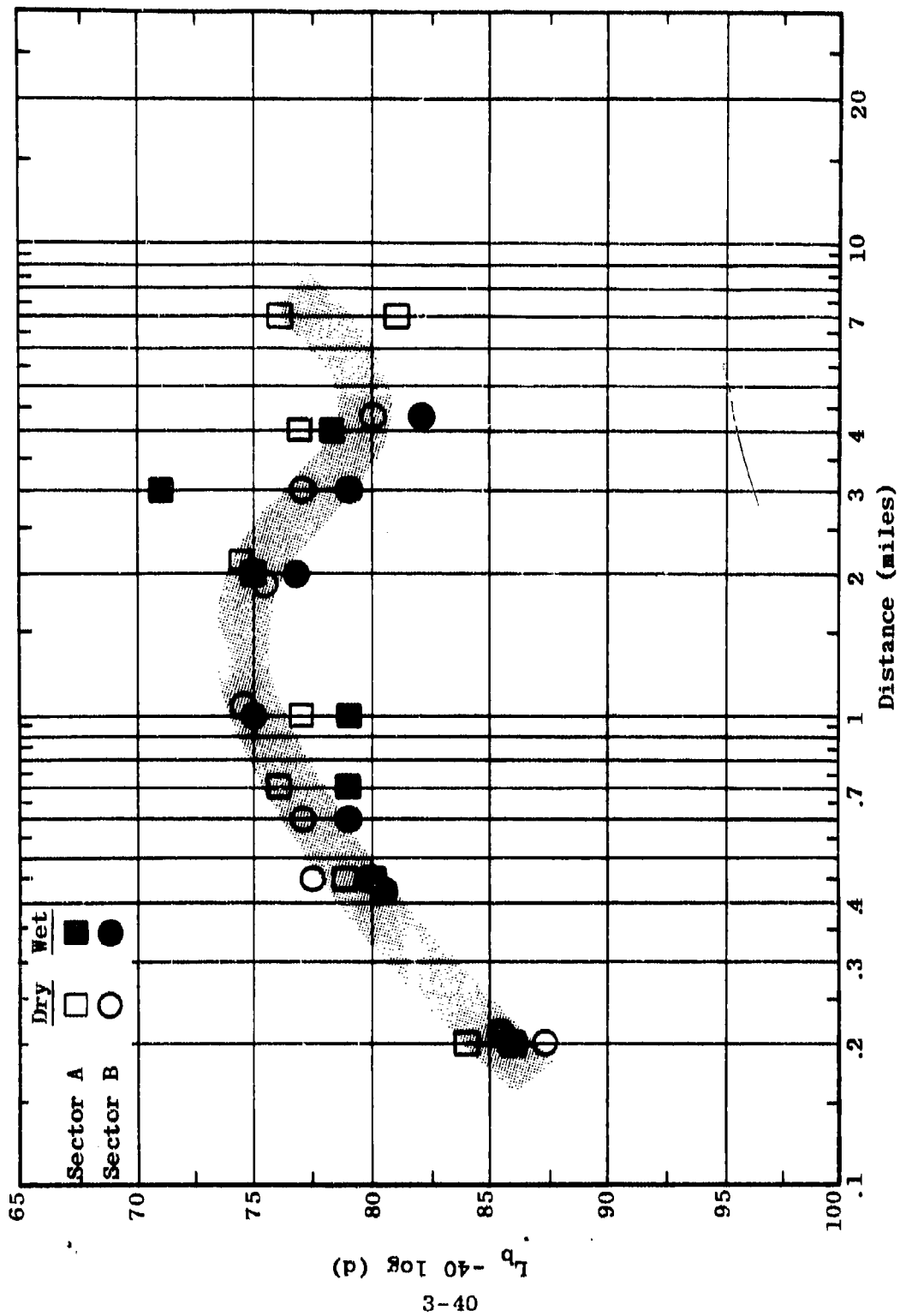


Figure 3.33 Measured Data Summary
 $L_b = F_{A,B}(12.0, 80, H, d, 80)$

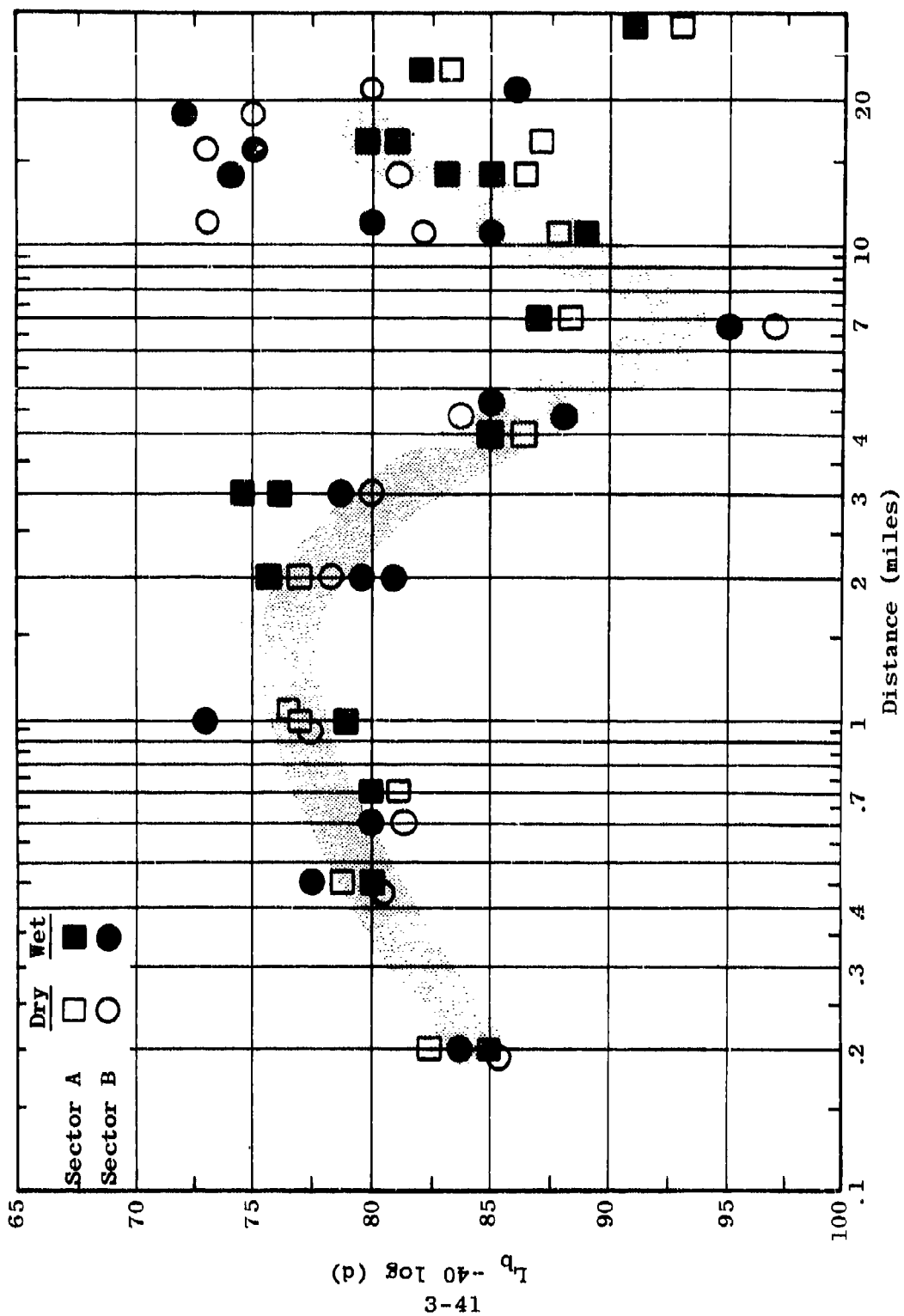


Figure 3.34 Measured Data Summary
 $L_b = F_{A,B} (25.5, 80, H, d, 80)$

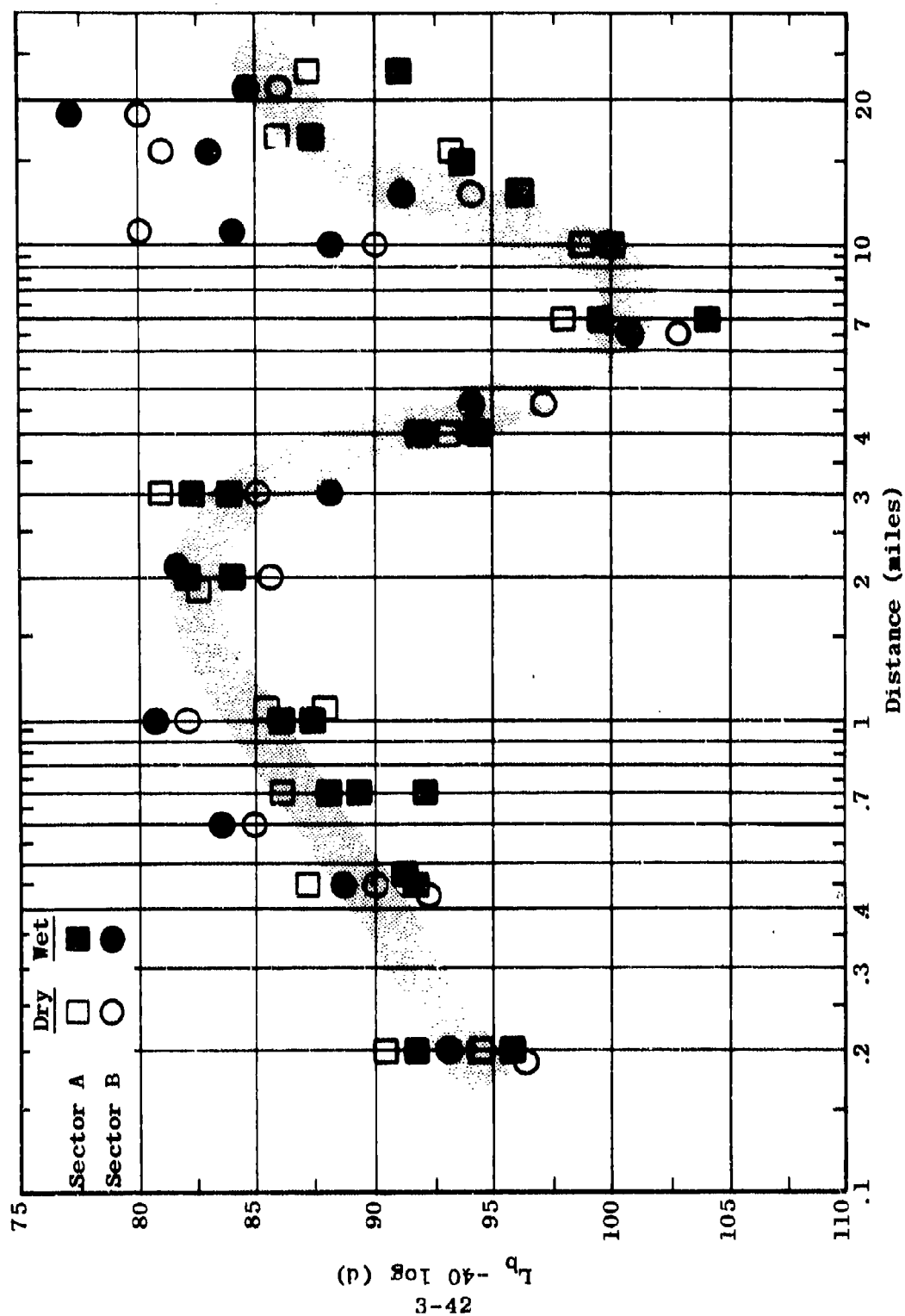


Figure 3.35 Measured Data Summary
 $L_b = F_{A,B}(50.0, 80, H, d, 80)$

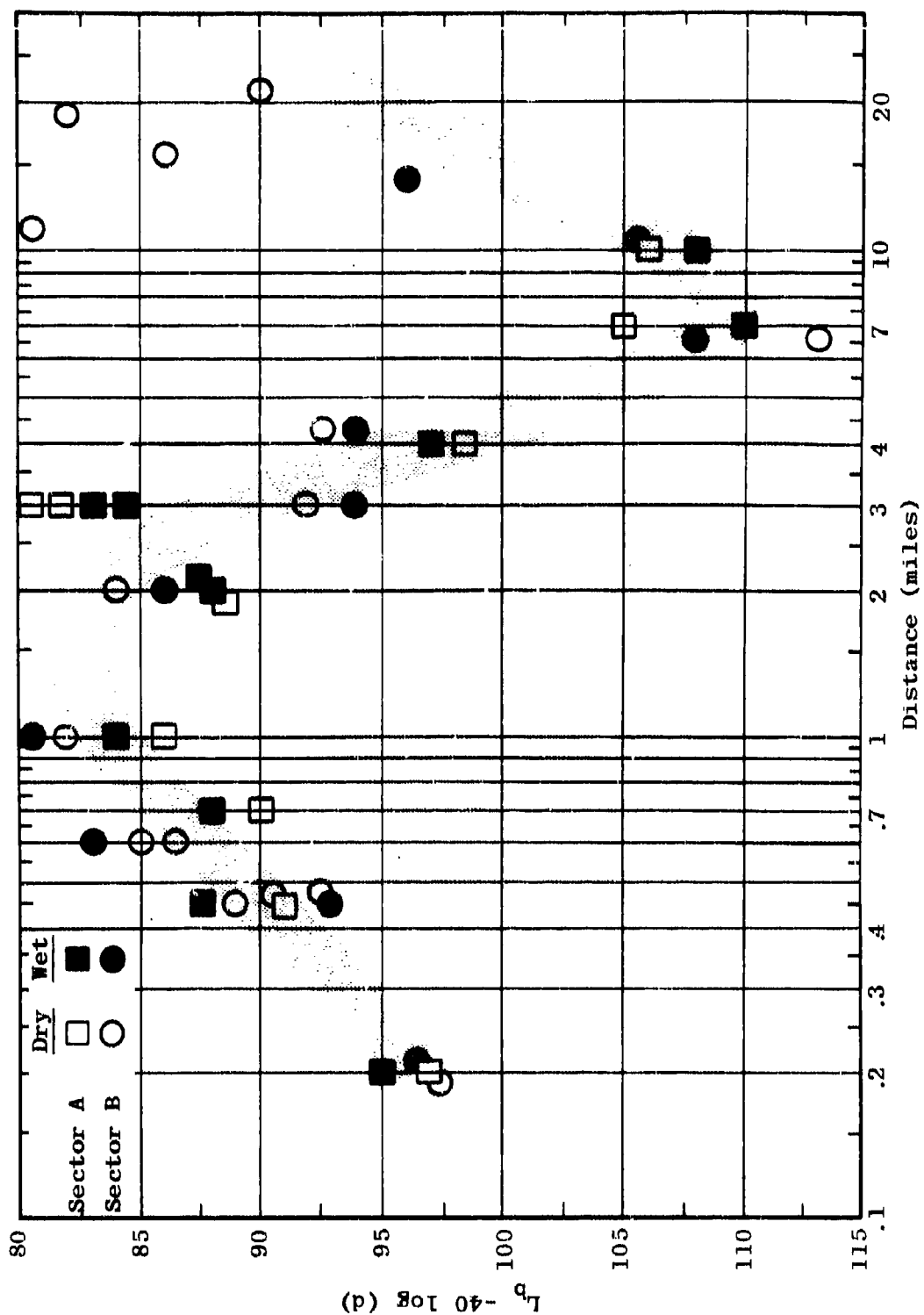


Figure 3.36 Measured Data Summary
 $L_b = F_{A,B}(100.0, 80, H, d, 80)$

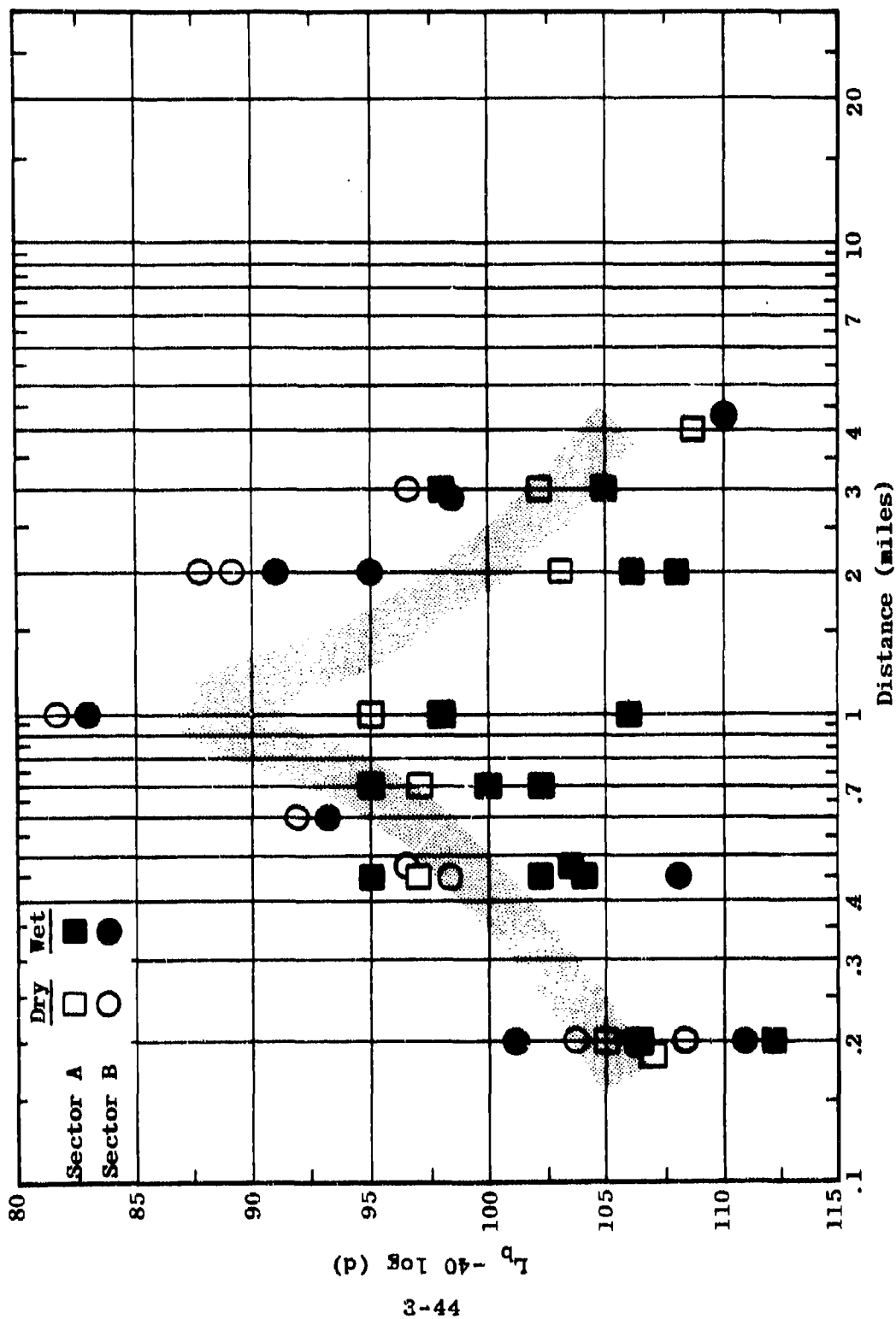


Figure 3.37 Measured Data Summary
 $L_b = F_{A,B}(250.0, 80, H, d, 80)$

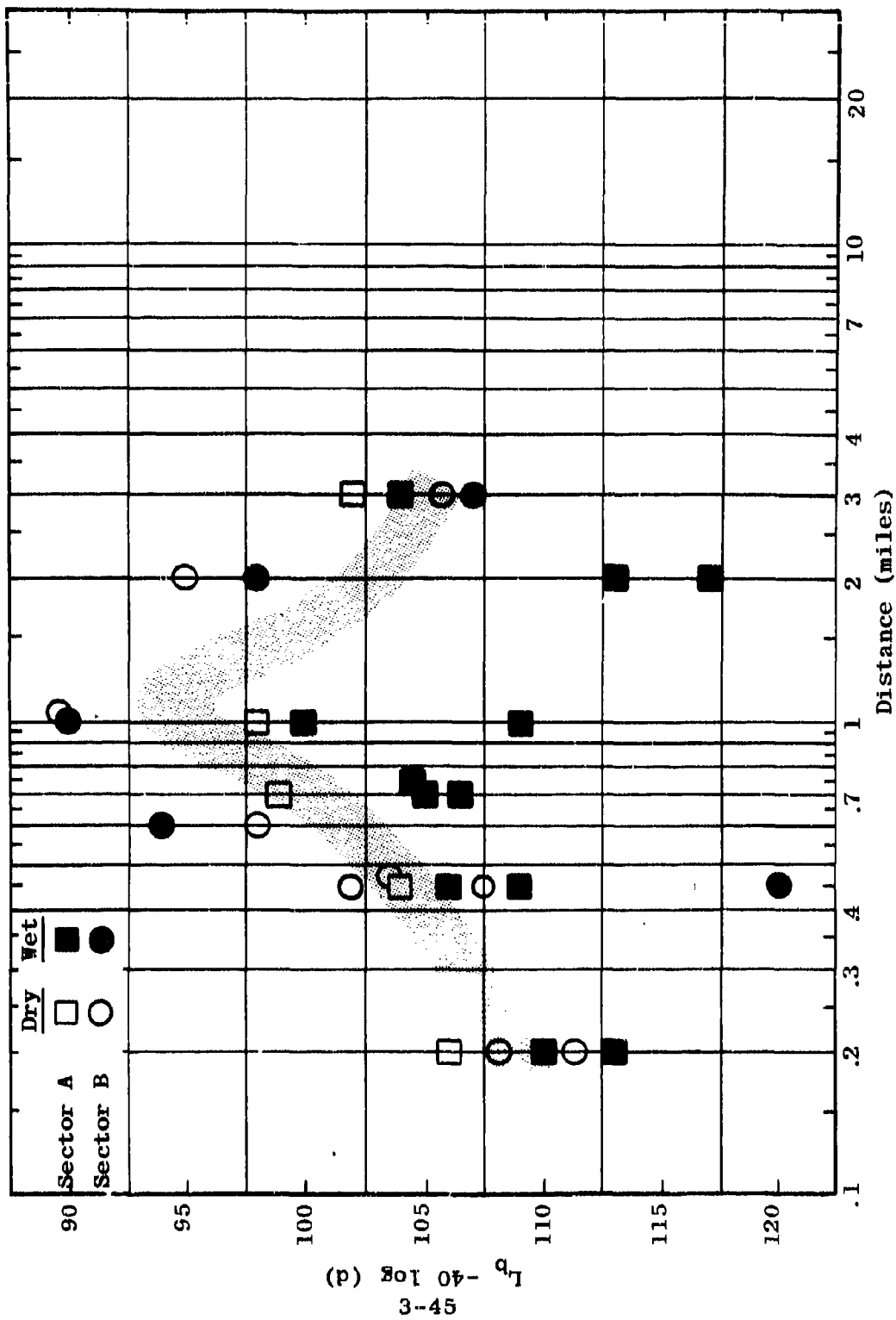


Figure 3.38 Measured Data Summary
 $L_b = F_{A,B}(400.0, 80, H, d, 80)$

of these two terms should be carefully distinguished. The term "theoretical surface-wave path loss values" refers to the actual surface-wave path loss curves expected to hold in the absence of foliage. On the other hand, the term "surface-wave function" will be used to refer to these theoretical curves displaced vertically by any given number of decibels.

Figure 3.39 shows the results of this fit at 105 kc. The solid curve is the surface-wave function, which has been moved vertically in order to best fit the data. As the figure shows, it was necessary to move the theoretical function 10 db in the direction of greater loss to best fit the measured points. The range of measured data at each distance is noted on Figure 3.39 by the vertical bars. The median of the measured points is indicated by the middle tick on each vertical bar. Figure 3.39 also illustrates that the surface-wave function matches the measured data extremely well at 105 kc. In addition, the figure shows that the spread of measured data is very small at this frequency.

Figure 3.40 illustrates a somewhat greater data spread at 300 mc and shows that the surface function plus 8 db fits the measured information reasonably well with the exception of the point at 0.2 mile and several points at about 15 and 20 miles. Figure 3.41 shows a surface-wave function fitted to the 880-kc data. In this case, the fit is not nearly as good as at the lower frequencies. It is interesting to note that it was not necessary to move the theoretical surface-wave curve to achieve a reasonable fit to measured data. The significance of the amount by which the theoretical curve must be moved to best fit the measured

data is discussed in Section 3.5 of this report. Figures 3.42, 3.43 and 3.44 show that the surface-wave function fits the high-frequency data reasonably well with the addition of a factor on the order of 20 db. At 25 mc (Figure 3.45) the surface-wave function begins to match the rough propagation model which was introduced in Semiannual Report Number 6 and is given by

$$L_b = 116.57 + 20 \log f + 40 \log d - 20 \log (h_1 h_2) \quad (2)$$

where

L_b = median basic transmission loss in decibels

f = frequency in megacycles

d = distance in miles

$h_1 h_2$ = transmitting and receiving antenna heights in feet

Figure 3.46 illustrates the result of fitting equation 2 to the measured data for a frequency of 50 mc.

It became obvious that a propagation curve with a $40 \log d$ fall-off would not fit the vertical polarization data for low antenna heights. Therefore, the best straight line was used to summarize the data between 100 mc and 400 mc. As Figure 3.47 shows, a line with a fall-off corresponding to $18 \log d$ was used to summarize the data at 100 mc. The line represents a good fit between 0.45 mile and 3 miles but overestimates the loss by 10 db at 0.2 mile.

7

A curve with a fall-off of $18 \log d$ was used in Figure 3.48 for 250 mc. This curve fits the data well, even at 0.2 mile. As Figure 3.49 shows, a curve with a slope corresponding to $12 \log d$ was used for 400 mc.

In general, the curves shown in Figures 3.39 through 3.49 represent the measured data extremely well and therefore provide an excellent summary in a convenient format of propagation characteristics measured at Pak Chong. These curves are summarized on Figure 3.50. The curves in Figure 3.50, which apply to low antenna heights for vertical polarization, indicate an unusually large gap between 880 kc and 2 mc. The possible significance of this jump is discussed in Section 3.5 of this report. It is also interesting to note that a different type of propagation phenomenon seems to begin at 100 mc. This fact is deduced from the unusually large gap in loss between 50 mc and 100 mc plus the distinctly different slope which the 100-, 250- and 400-mc propagation curves exhibit. This change in propagation phenomena is discussed in Section 3.3 of this report.

A set of propagation curves similar to those shown on Figure 3.50 are presented in Figure 3.51 for high antennas with vertical polarization. For the high antennas, the propagation mechanism appears to be relatively regular. Figure 3.51 shows no distinctive changes in slopes or unusual changes in path loss between frequencies.

Figure 3.52 presents similar information for horizontal polarization and low antenna heights. Figure 3.53 pertains to horizontal polarization with high antennas. Figures 3.54 through 3.61 provide examples of how well the

measured data fits the smoothed curves for horizontal polarization with high antenna heights. It is significant to note that in the frequency range from 2 to 12 mc, the measured losses for vertical polarization were considerably higher than would be expected for unfoliated environments while the measured losses for horizontal polarization appear to be considerably less than would be expected for unfoliated environments. Further discussions of this observation are included in Section 3.5 of this report.

3.3 Wet-Dry Comparisons

The weather cycles in the Pak Chong area are divided into two distinct seasons: a wet season which lasts from approximately May 15 until November 15, and a dry season which lasts from approximately November 15 to May 15. The wet season is characterized by frequent and intense rainfalls, by slightly heavier vegetation, and by the fact that the ground usually remains moist throughout the season. During the dry season, a significant amount of rain continues to fall, and vegetation remains green. However, the vegetation is not quite as heavy, and the ground tends to dry out. Figure 5.2 in Section 5 summarizes weather data which has been collected during cycles.

Complete sets of propagation loss measurements have been made in each of the two seasons. It is of interest to compare propagation loss between these two seasons to determine if there is a significant difference. If there is a significant seasonal difference in propagation characteristics, it is important to learn if this difference is a function of frequency, antenna height, communication

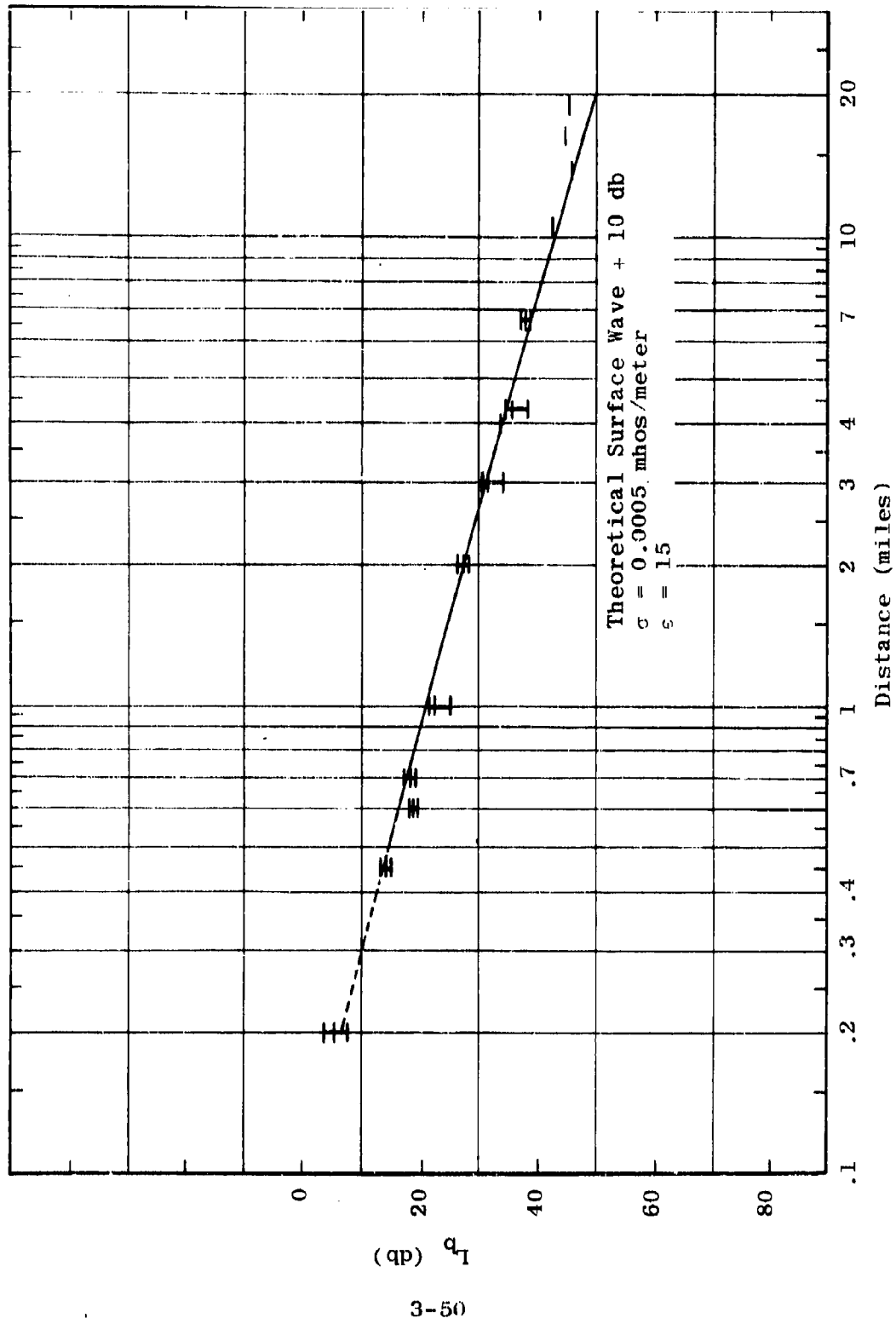


Figure 3.39 Smoothed Fixed-Point Data
 $L_b = F_{A,B}(0.105, 80, V, d, 17)$

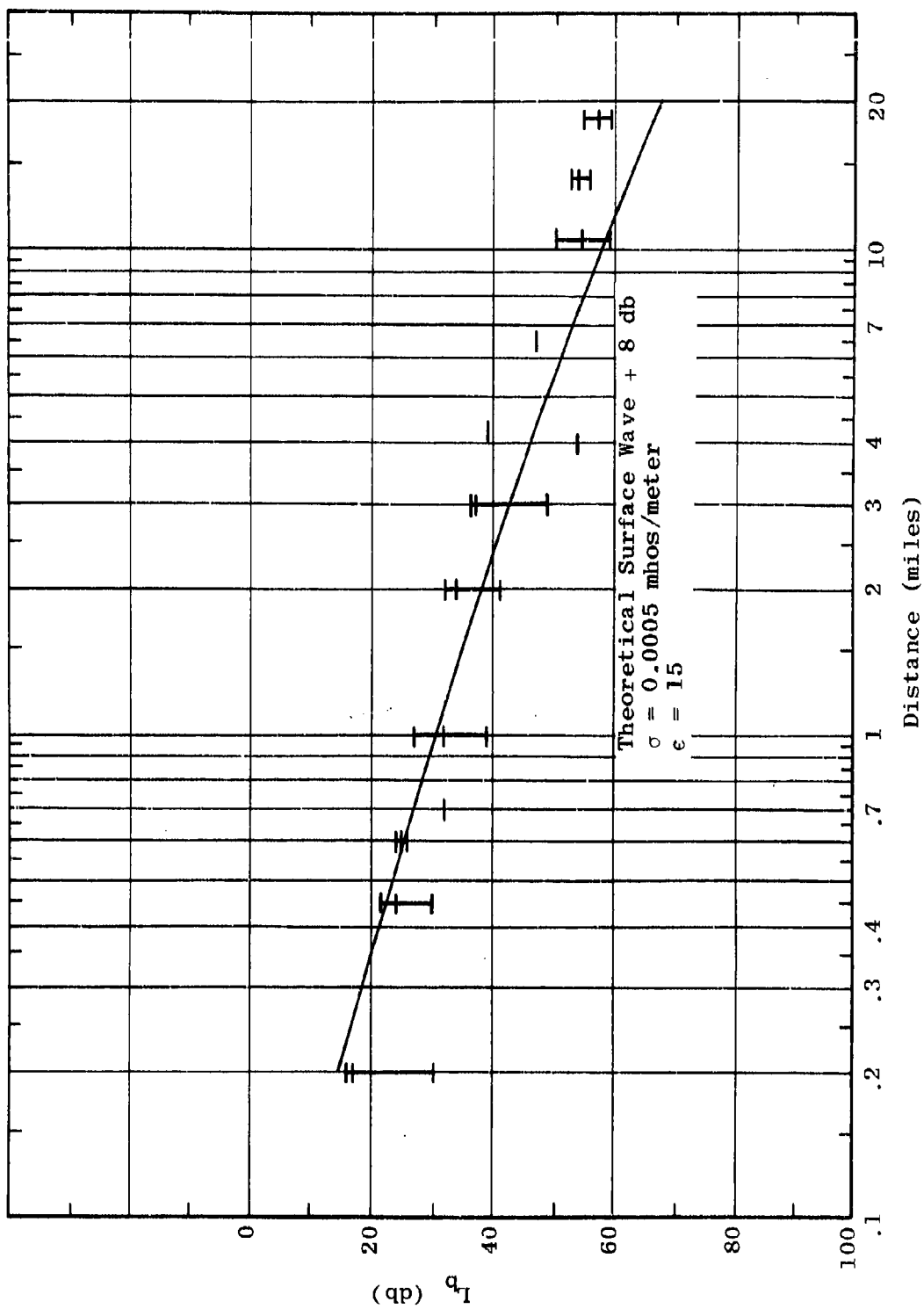


Figure 3.40 Smoothed Fixed-Point Data
 $L_b = F_{A,B}(0.300, 80, V, d, 17)$

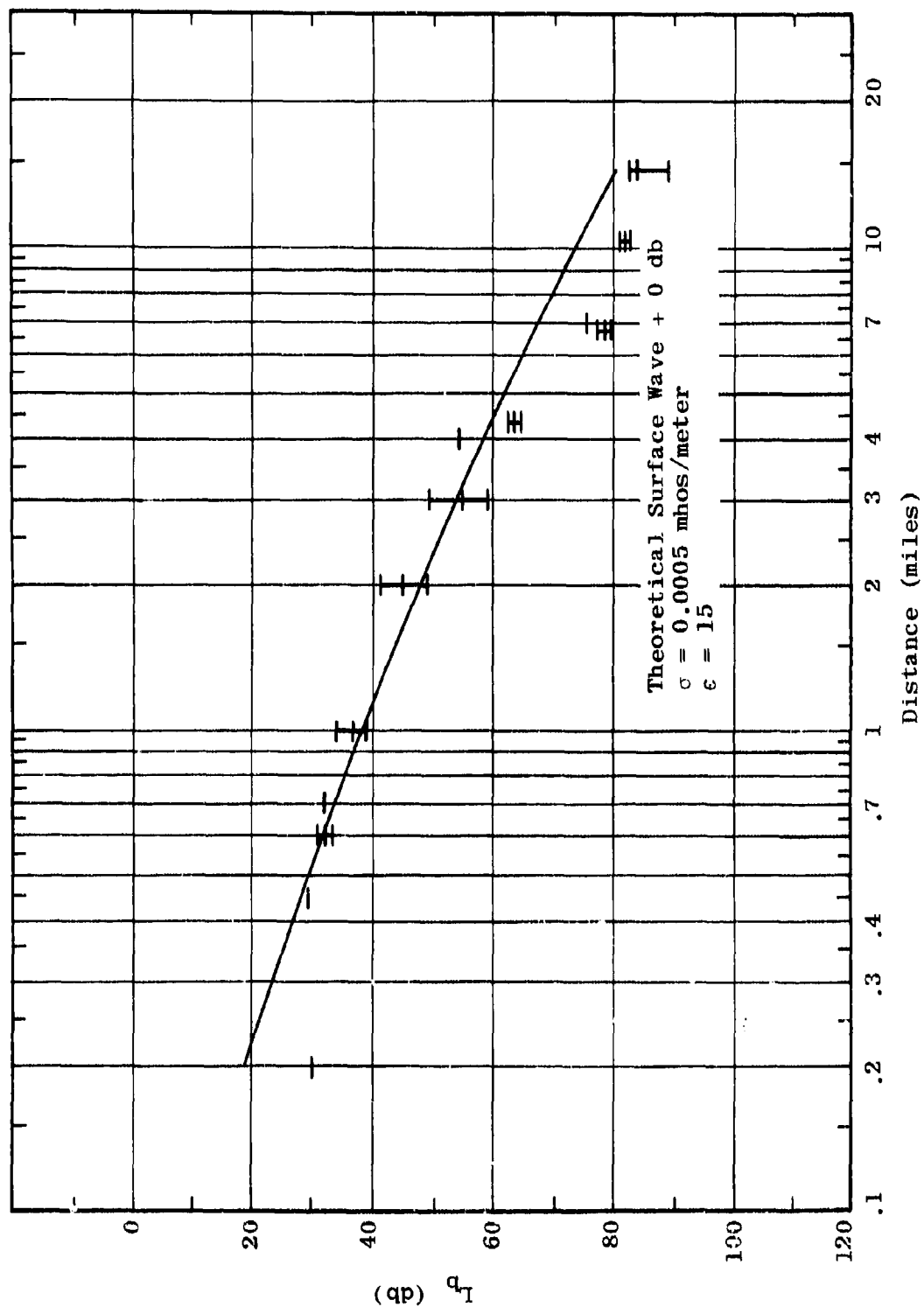


Figure 3.41 Smoothed Fixed-Point Data
 $L_b = F_{A,B}(0.880, 80, V, d, 17)$

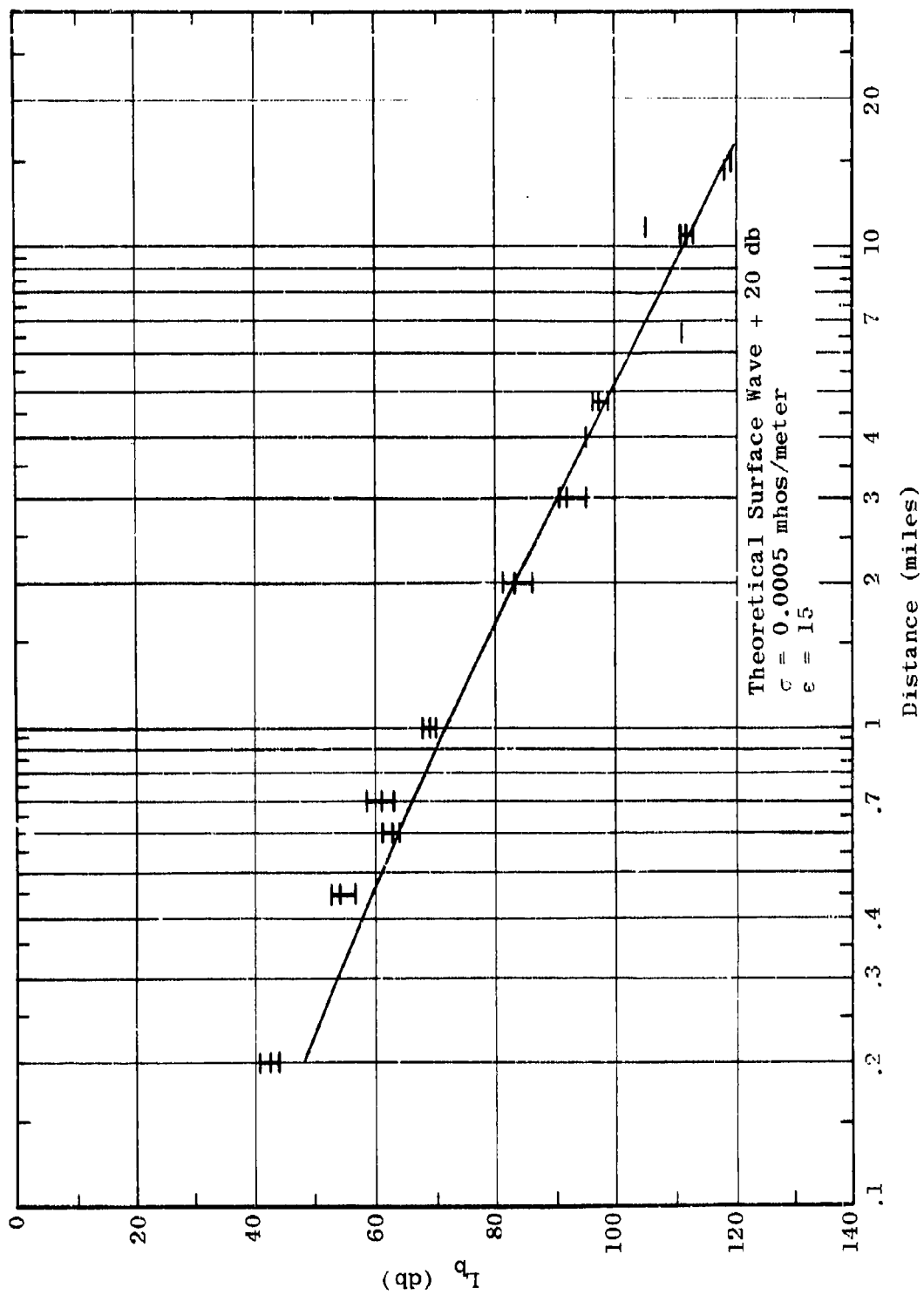


Figure 3.42 Smoothed Fixed-Point Data
 $L_b = F_{A,B}(2.0, 80, v.d, 17)$

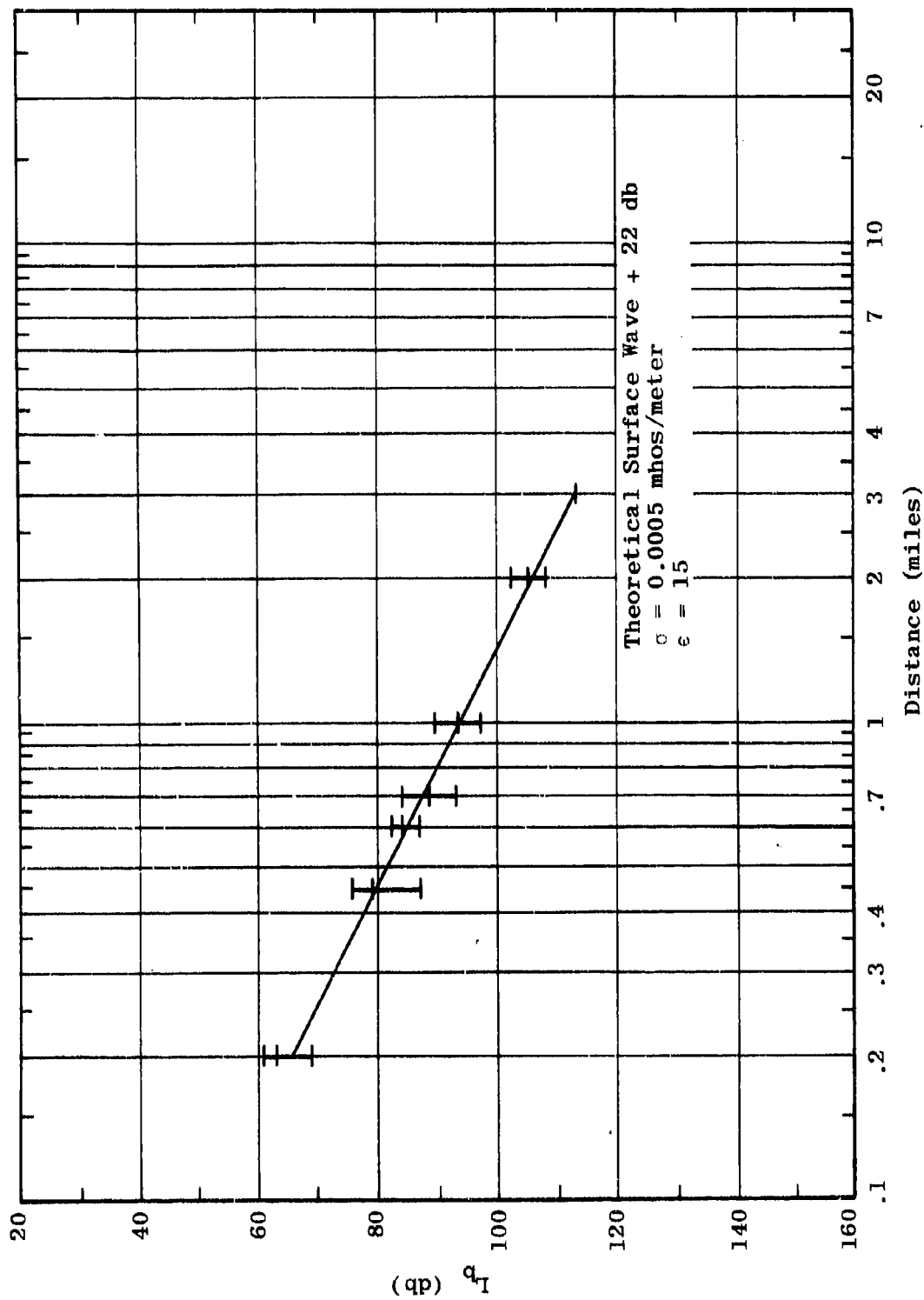


Figure 3.43 Smoothed Fixed-Point Data
 $L_b = F_{A,B}(6.0, 40, V, d, 17)$

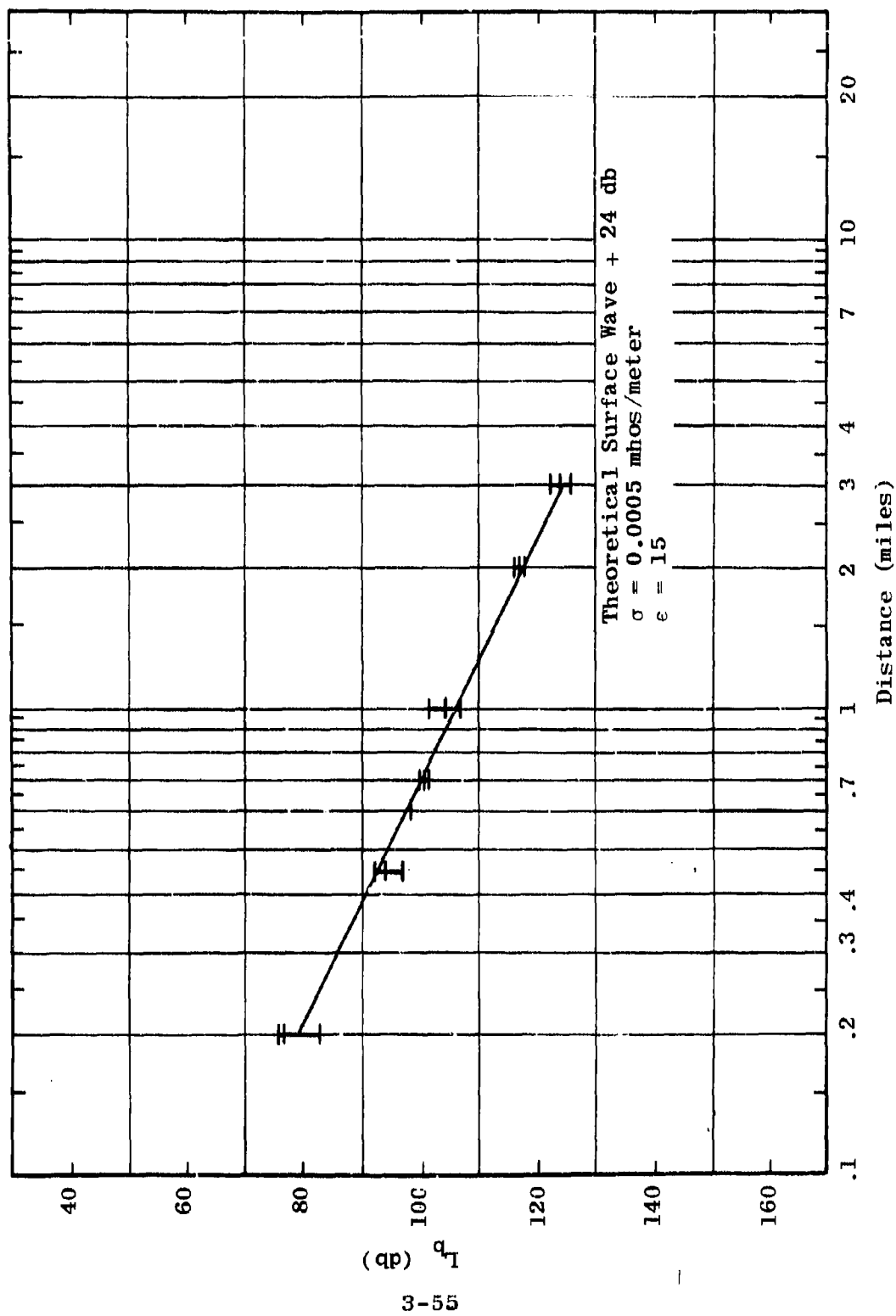


Figure 3.44 Smoothed Fixed-Point Data
 $L_b = F_{A,B}(12.0, 20, V, d, 17)$

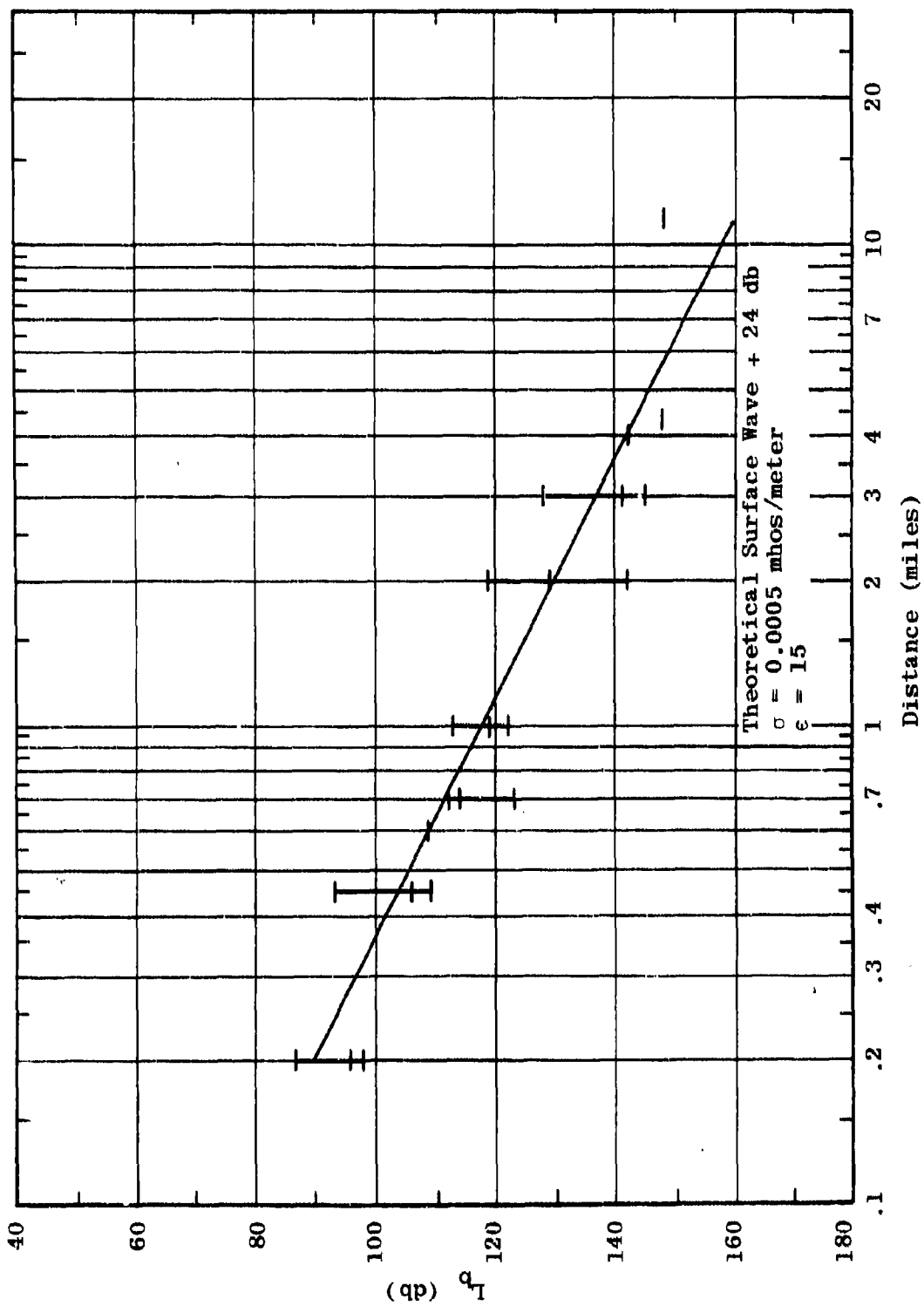


Figure 3.45 Smoothed Fixed-Point Data
 $L_b = F_{A,B}(25.5, 10, V, d, 11)$

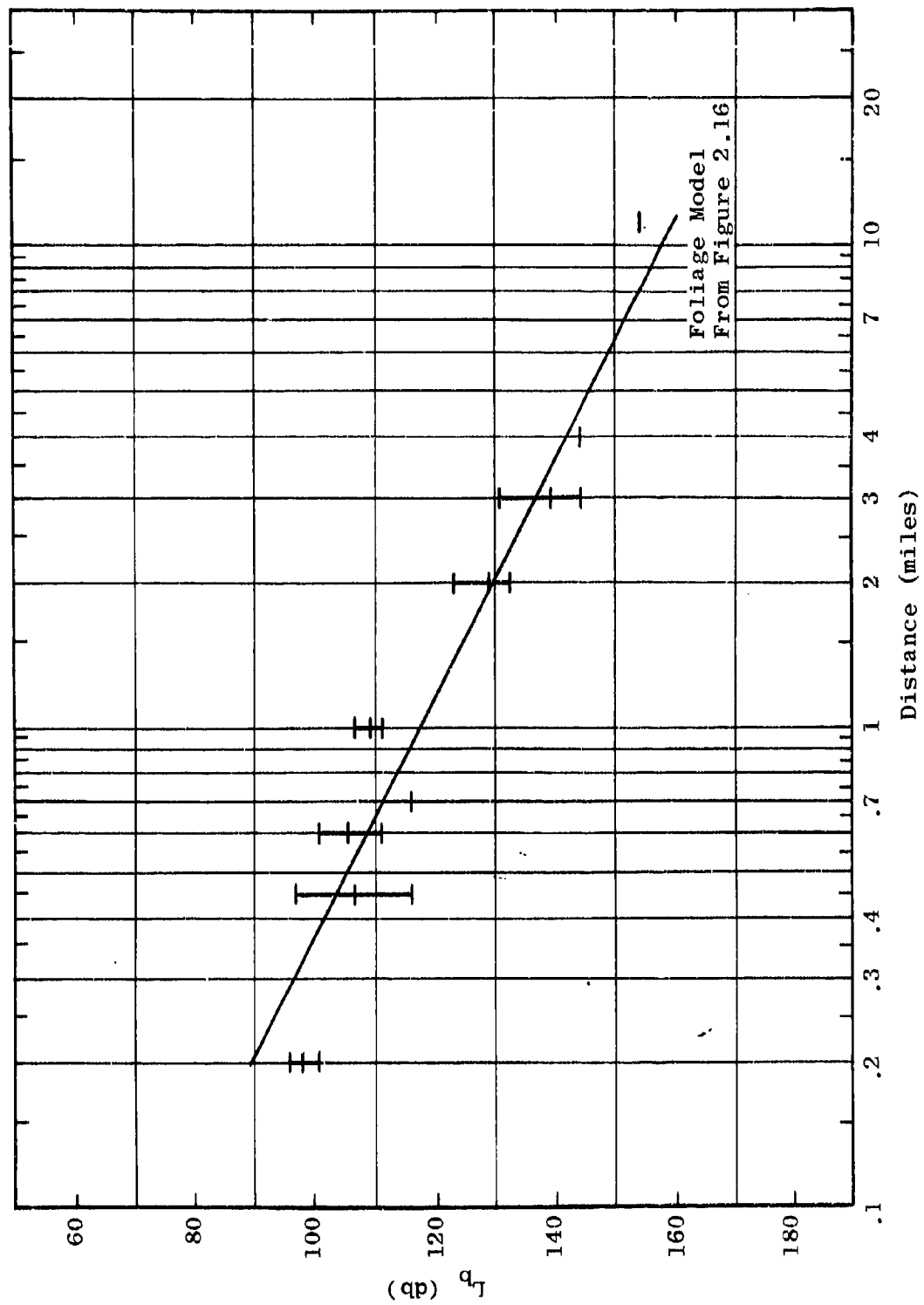


Figure 3.46 Smoothed Fixed-Point Data
 $L_b = F_{A,B}(50.0, 13, V, d, 20)$

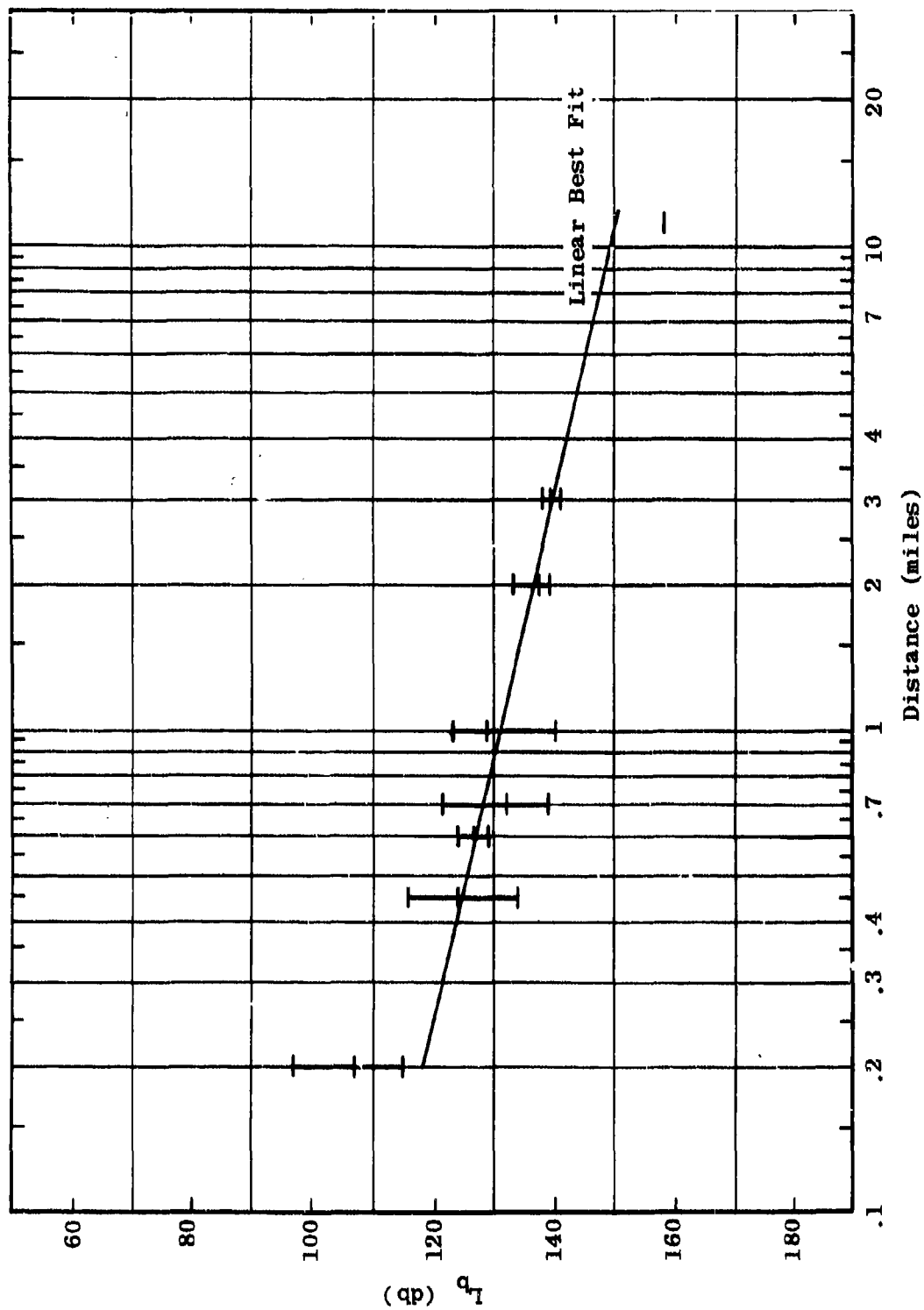


Figure 3.47 Smoothed Fixed-Point Data
 $L_b = F_{A,B}(100.0, 13, V, d, 11)$

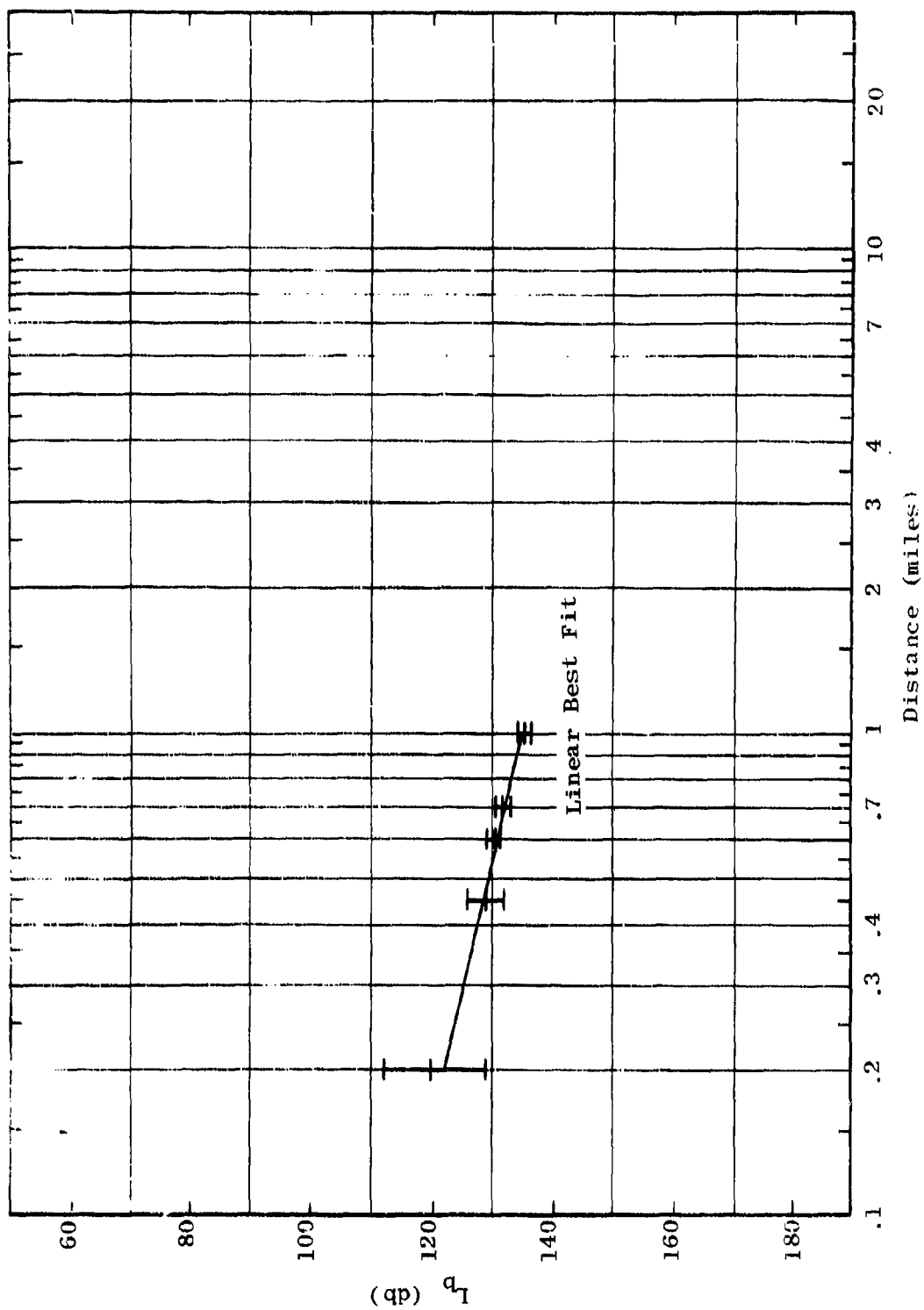


Figure 3.48 Smoothed Fixed-Point Data
 $L_b = F_{A.R.}(250.0, 13. V, d. 11)$

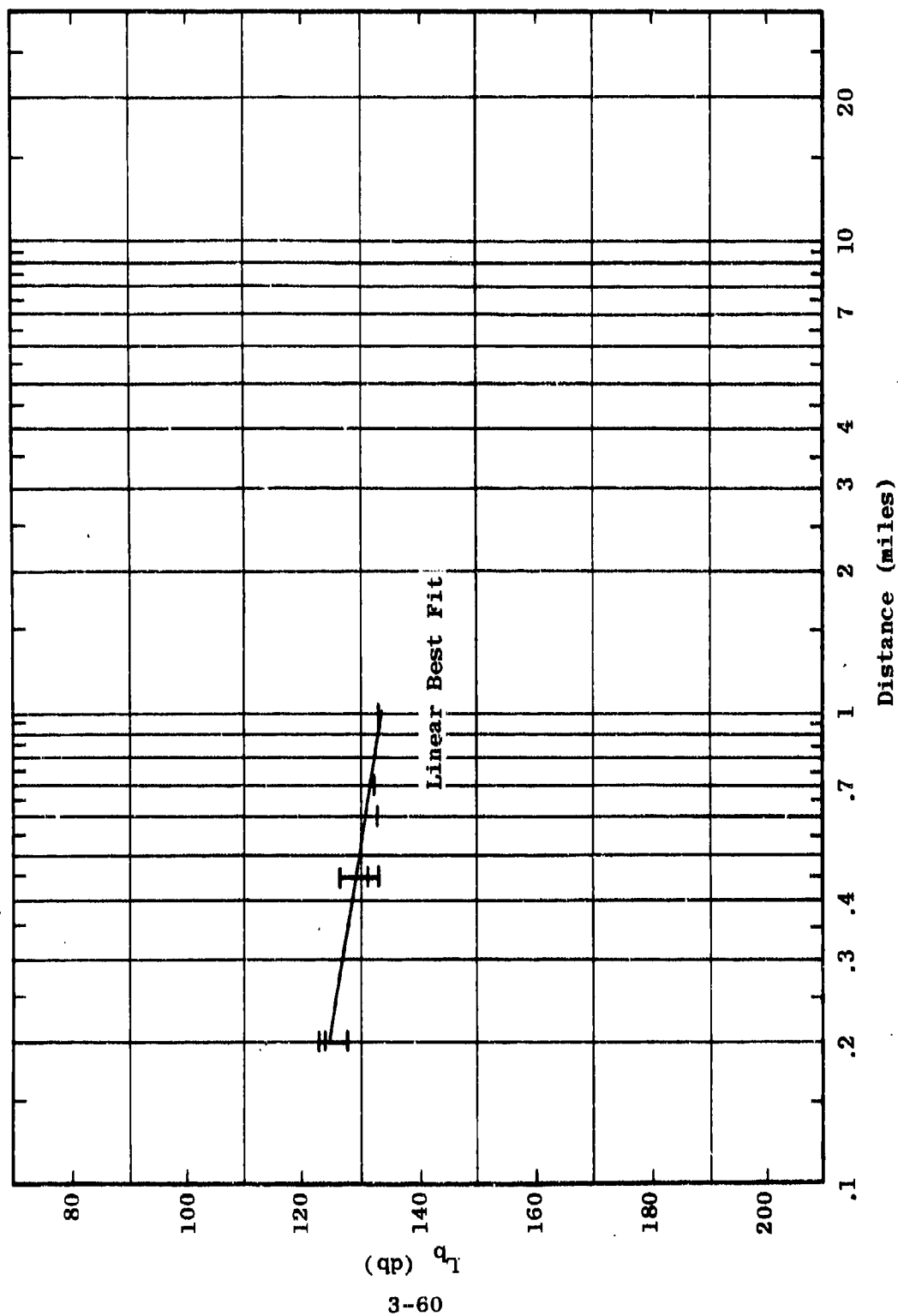


Figure 3.49 Smoothed Fixed-Point Data
 $L_b = F_{A,B}(400.0, 13, V, d, 11)$

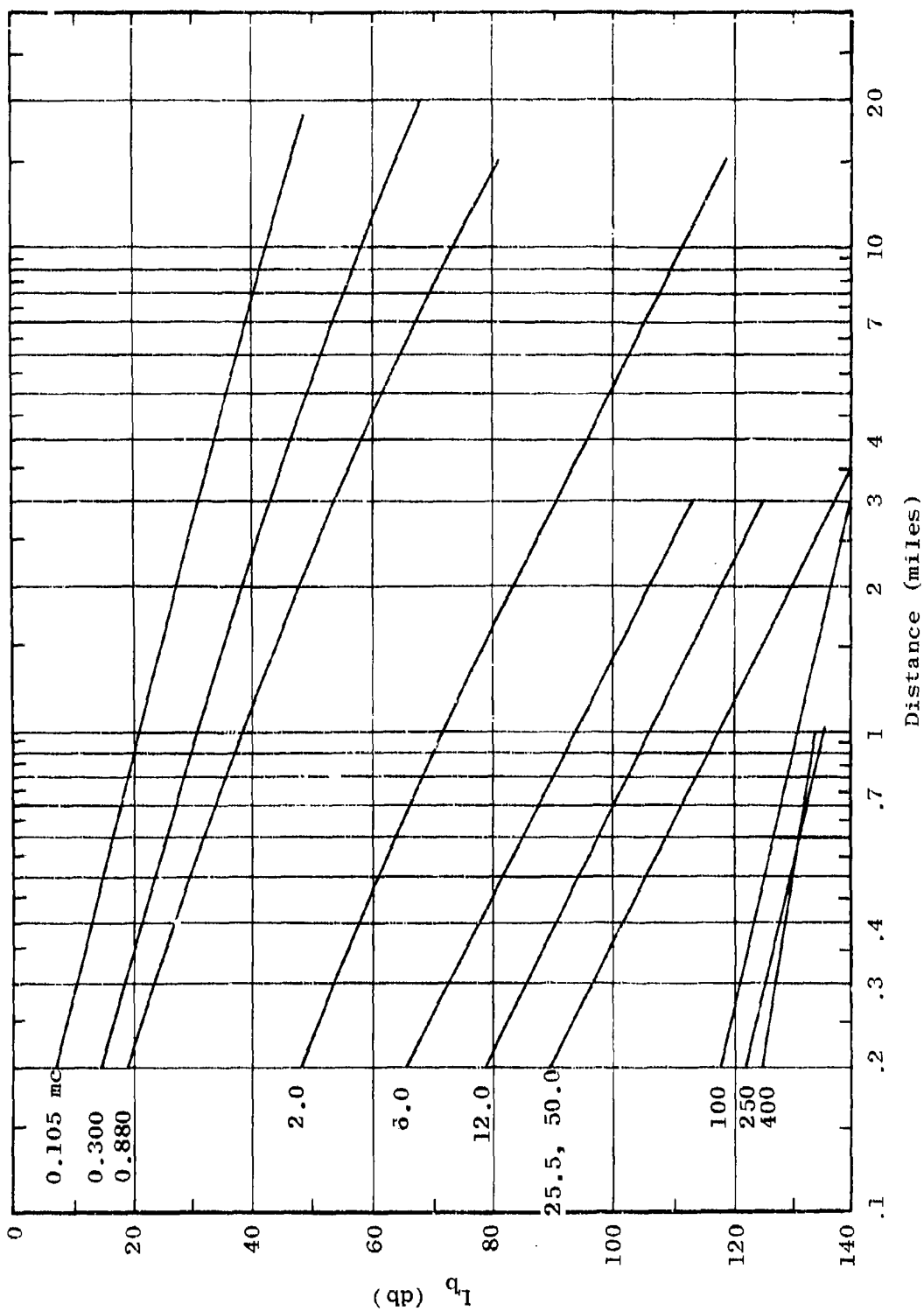


Figure 3.50 Composite of Smoothed Fixed-Point Data, Vertical Polarization, Low Antennas

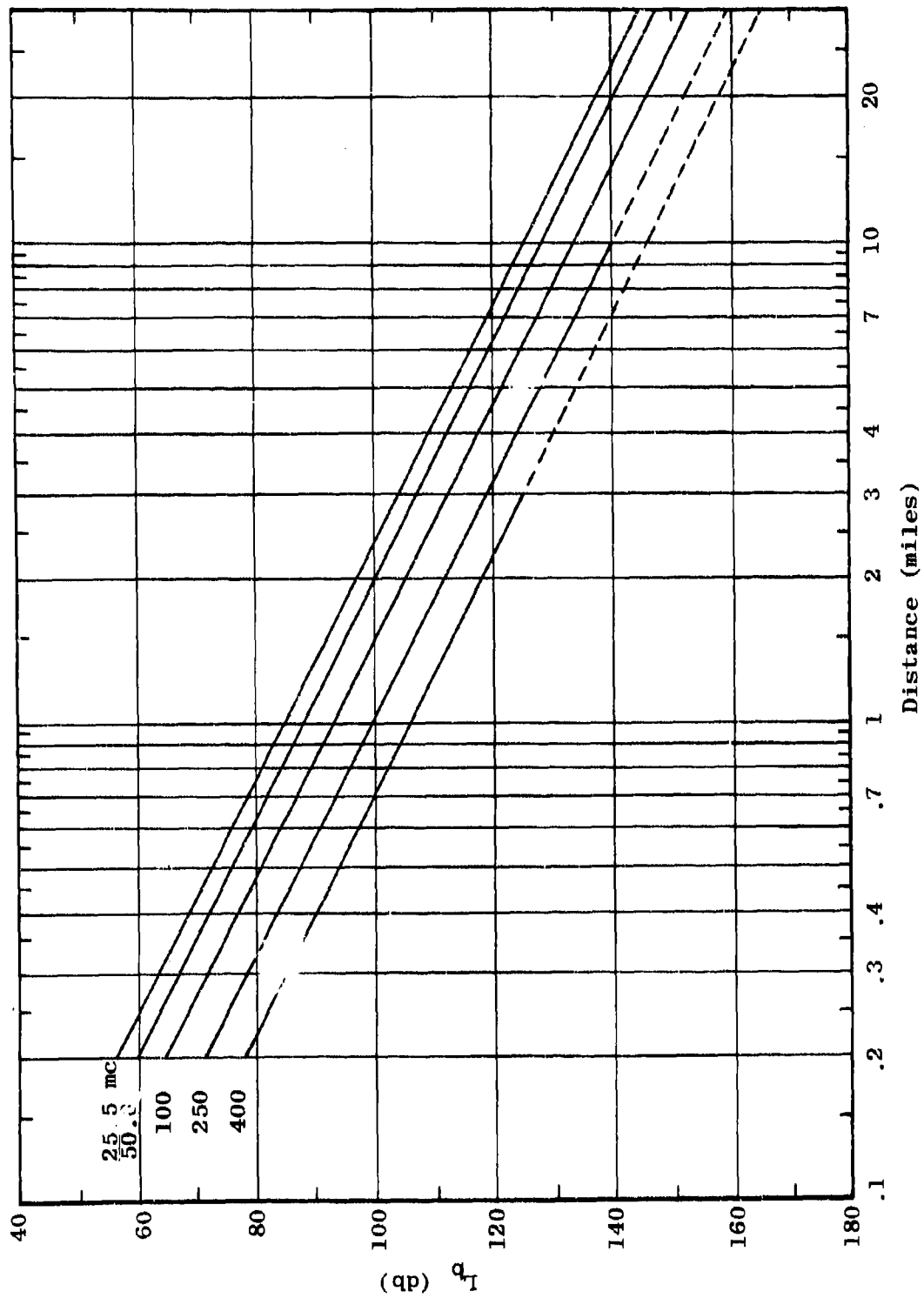


Figure 3.51 Composite of Smoothed Fixed-Point Data, Vertical Polarization, High Antennas

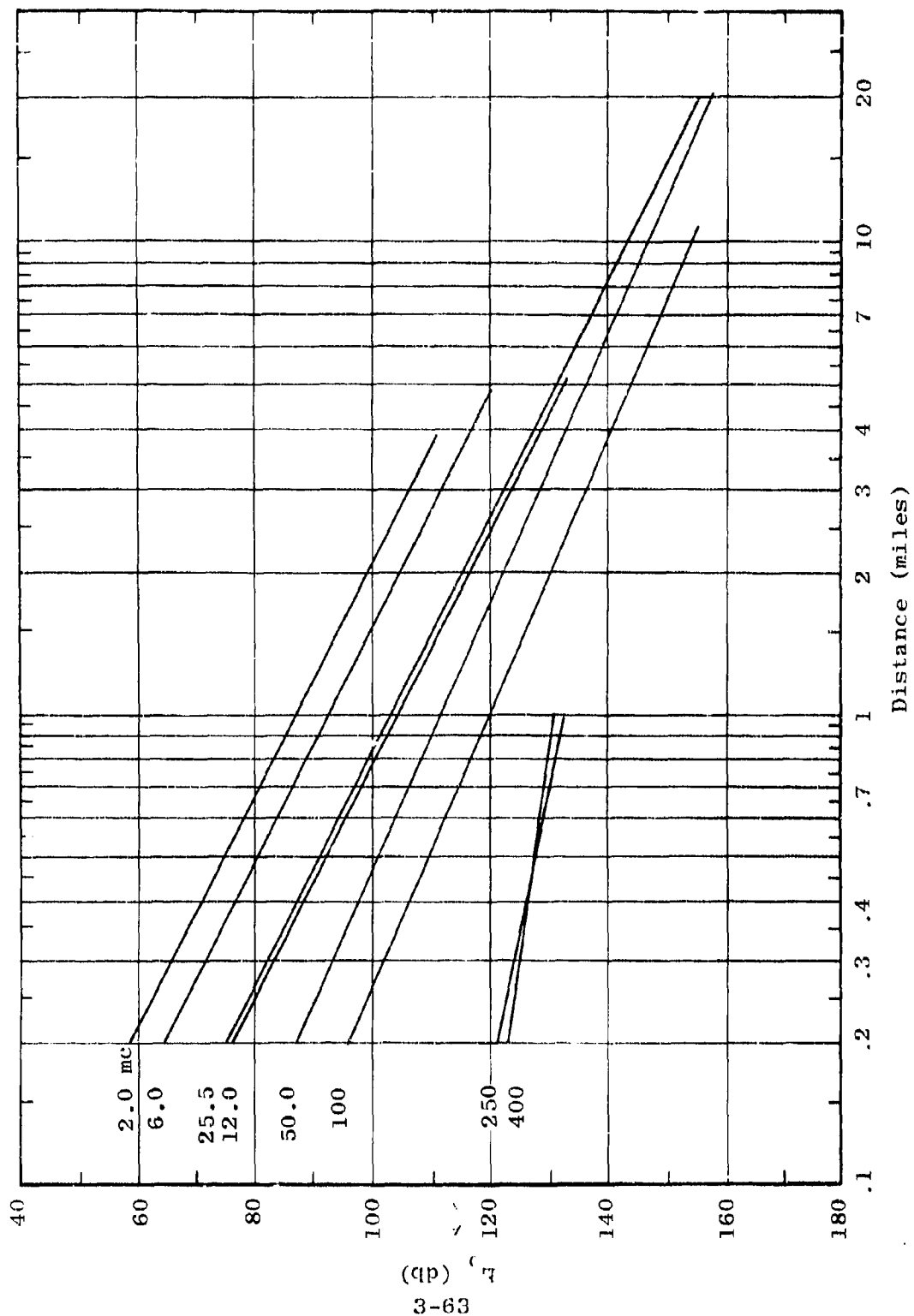


Figure 3.52 Composite of Smoothed Fixed-Point Data,
Horizontal Polarization, Low Antennas

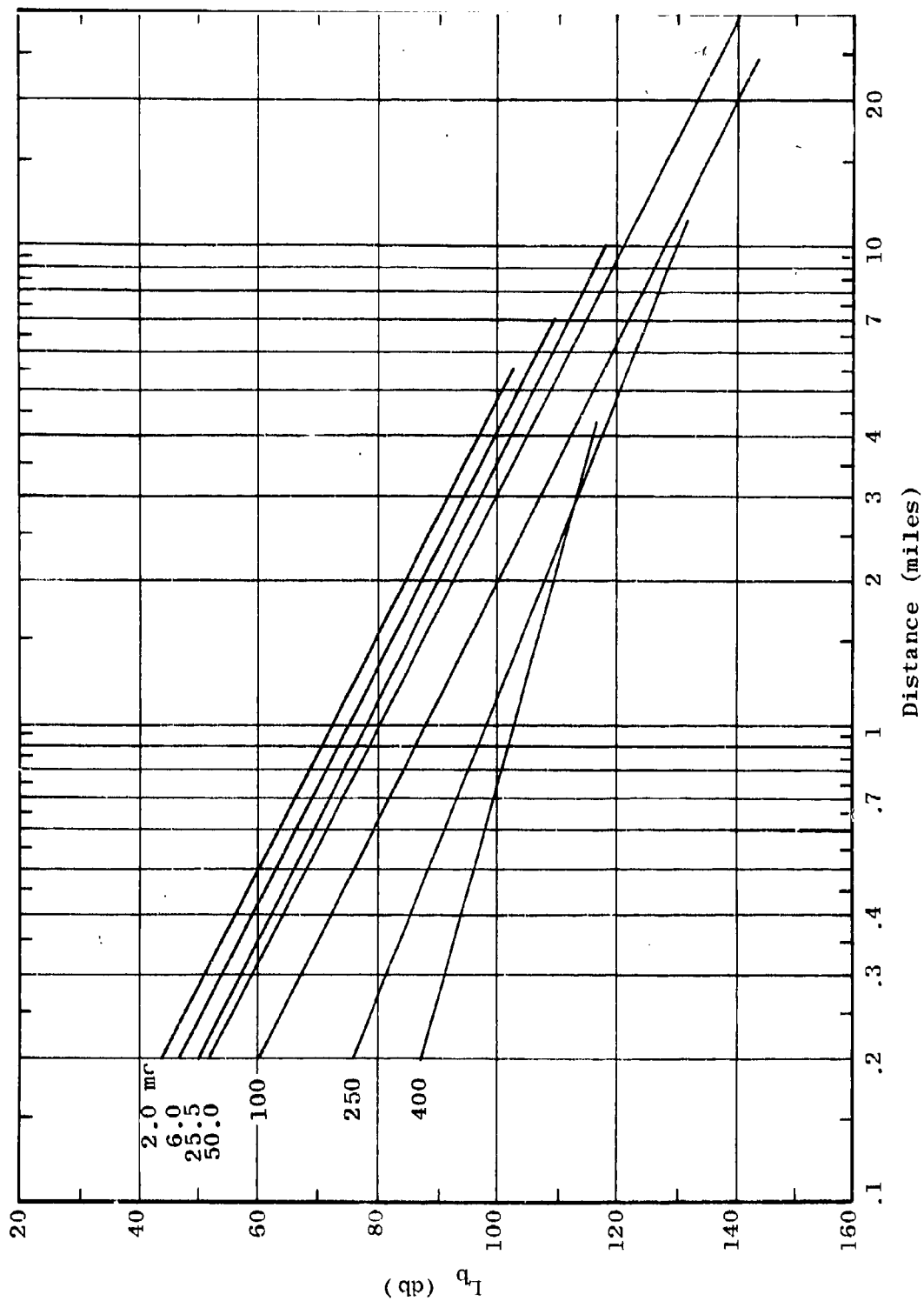


Figure 3.53 Composite of Smoothed Fixed-Point Data, Horizontal Polarization, High Antennas

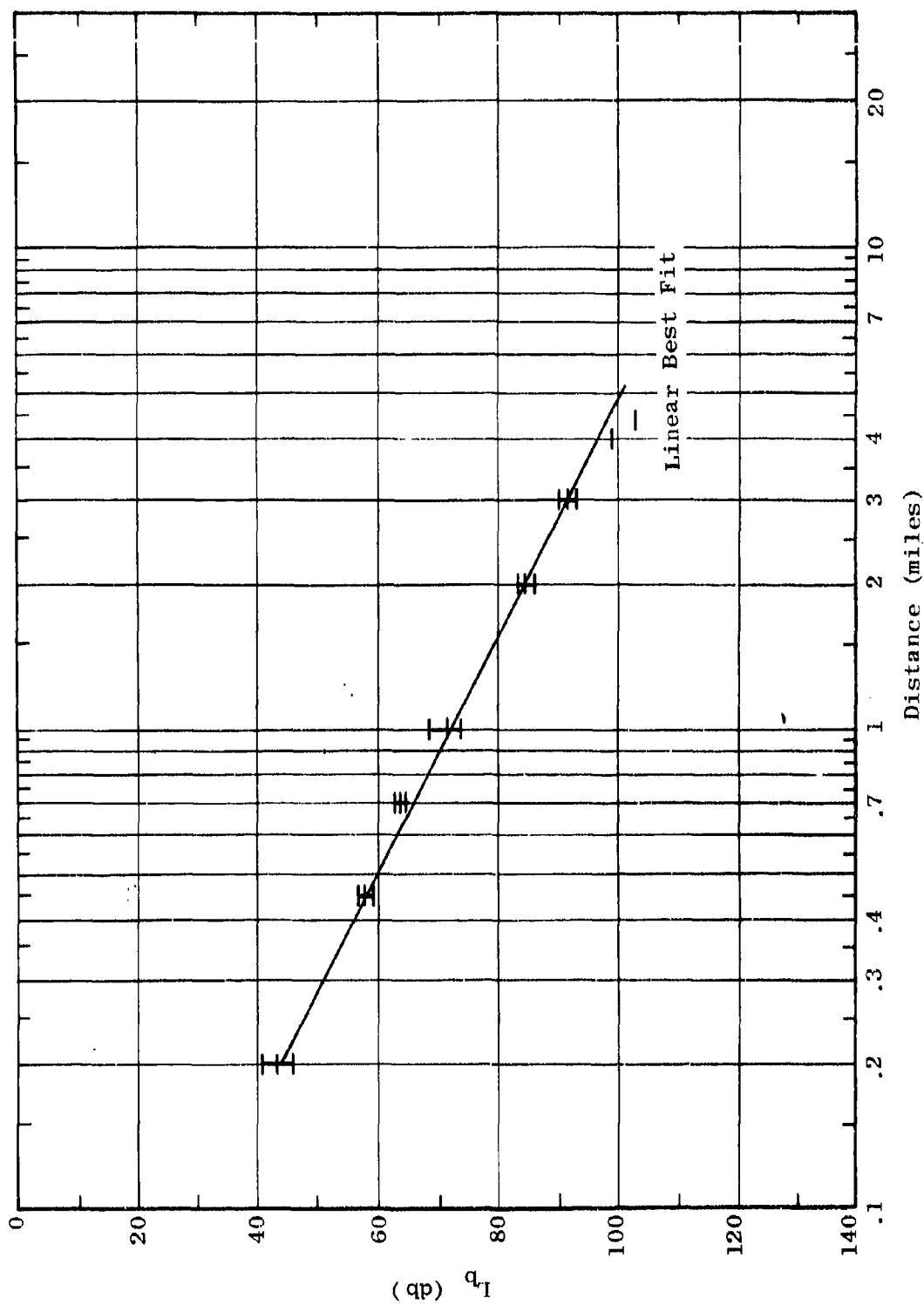


Figure 3.54 Smoothed Fixed-Point Data
 $L_b = F_{A,B}(2.0, 80, H, d, 80)$

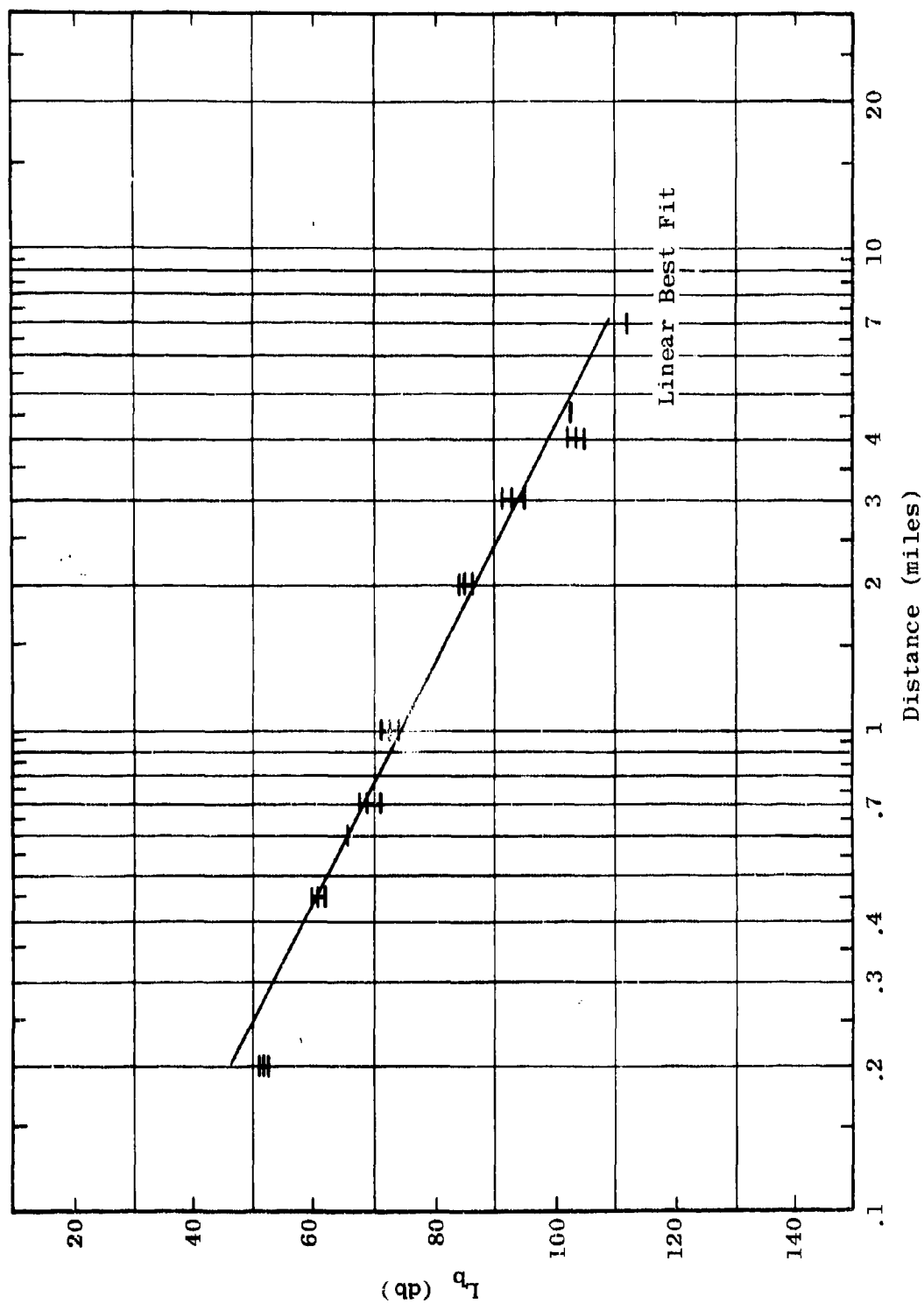


Figure 3.55 Smoothed Fixed-Point Data
 $L_b = F_{A,B}(6.0, 80, H, d, 80)$

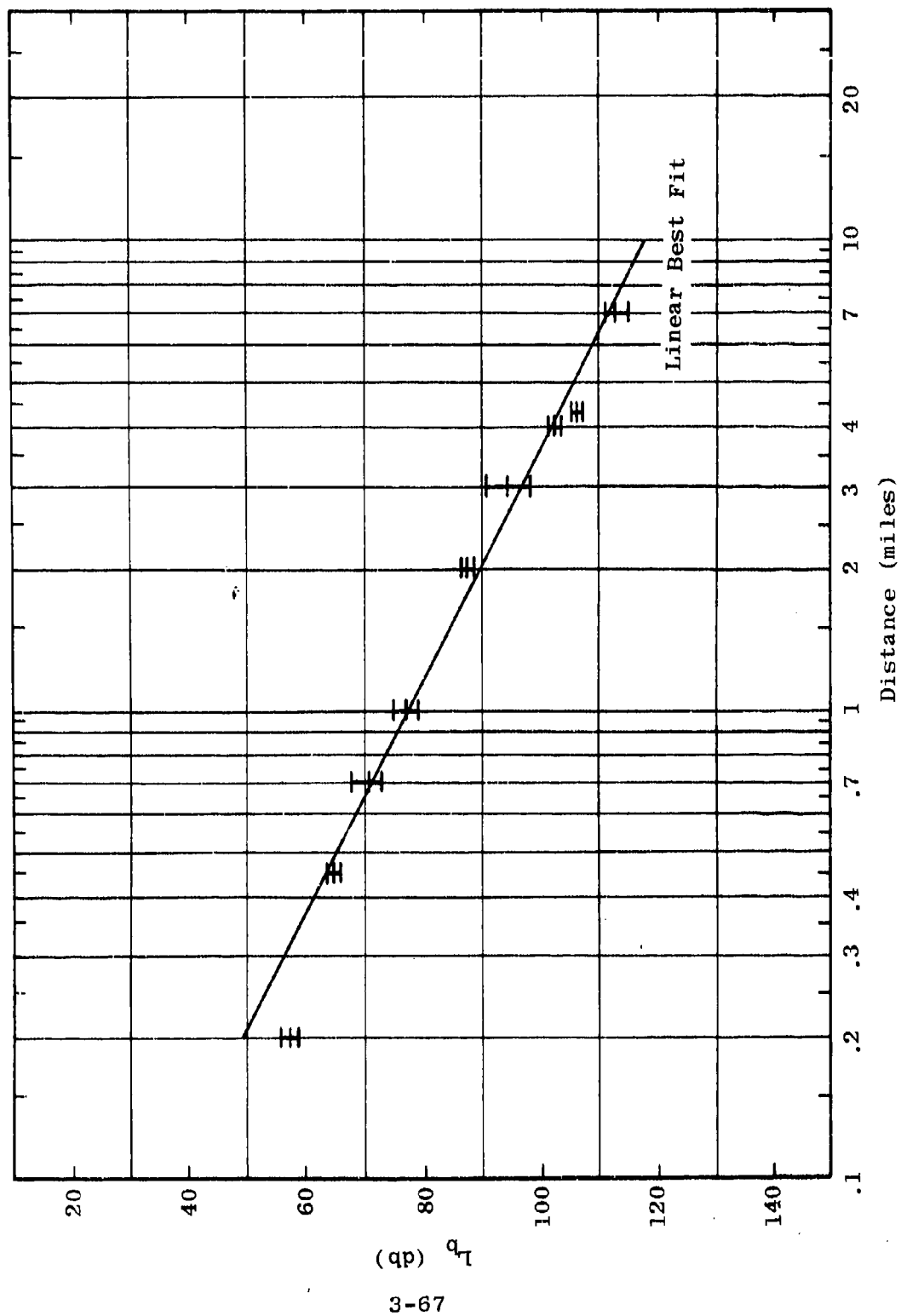


Figure 3.56 Smoothed Fixed-Point Data
 $L_b = F_{A,B}(12.0, 80, H, d, 80)$

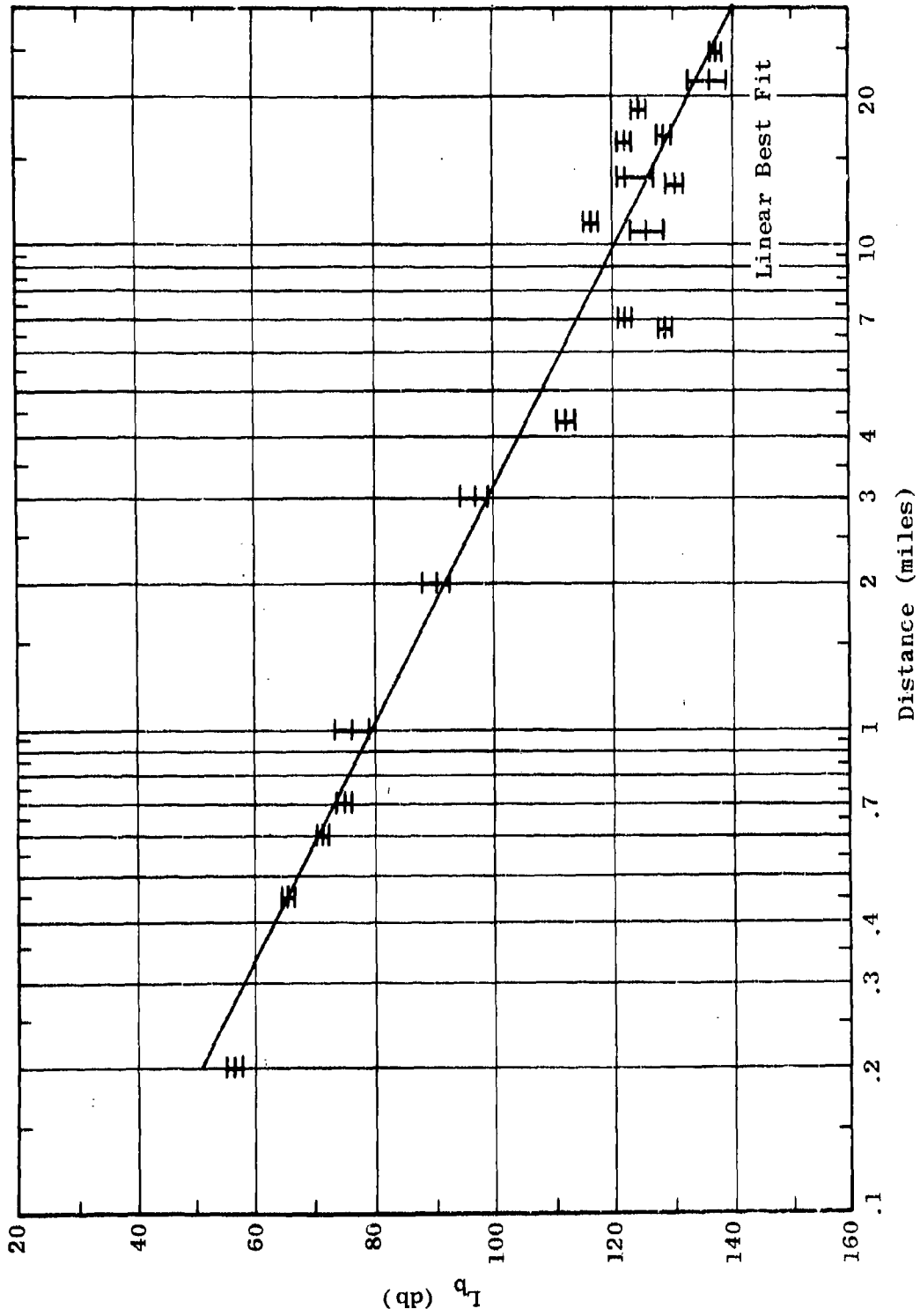


Figure 3.57 Smoothed Fixed-Point Data
 $L_b = F_{A,B}(25.5, 80, H, d, 80)$

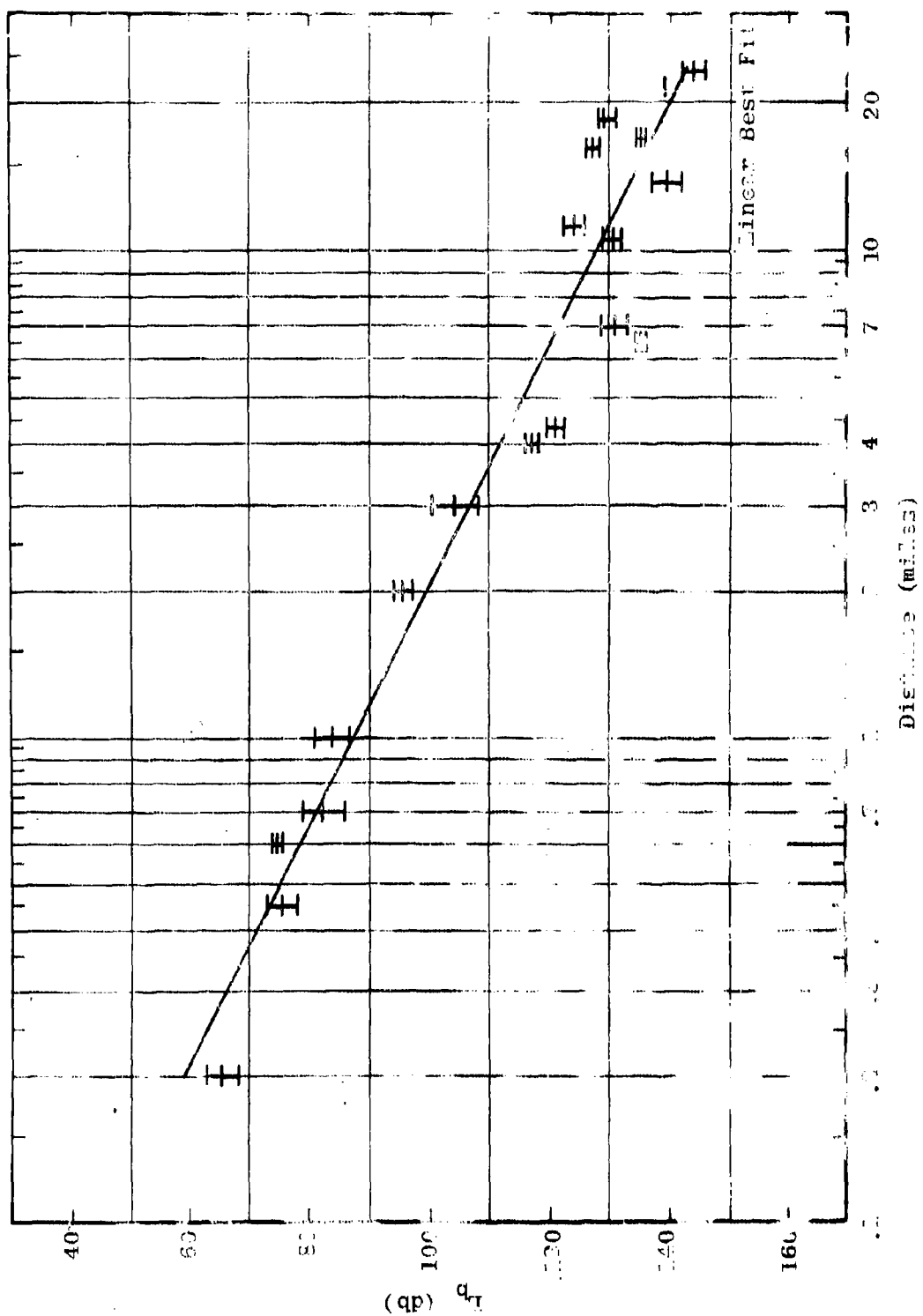


Figure 3.58 - Smoothed Fixed-Point Data
 $L_p = A, B, 50.0, 80, H, 100$

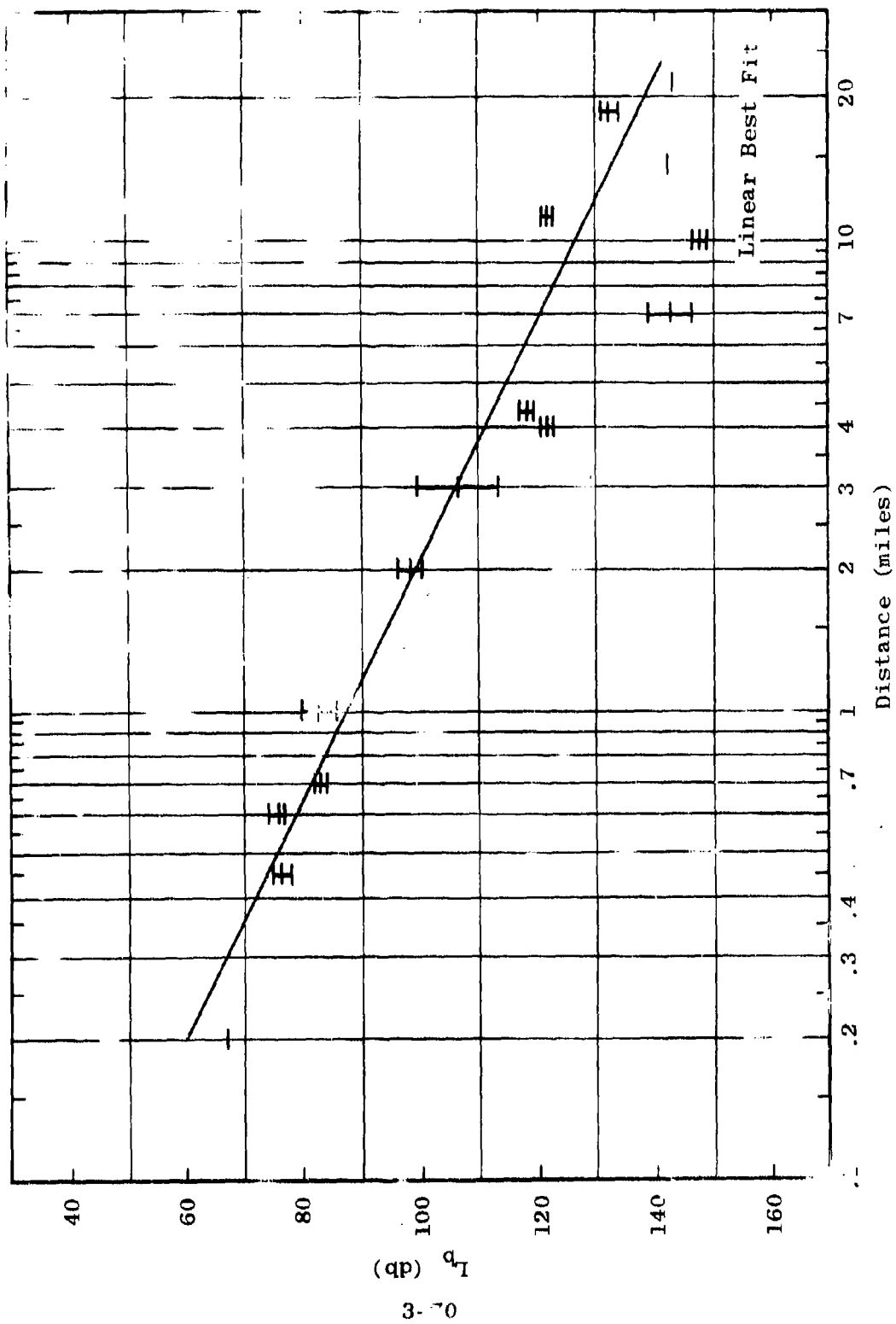


Figure 3.59 Smoothed Fixed-Point Data
 $L_p = F_{A,B}(100.0, 80, H, d, 80)$

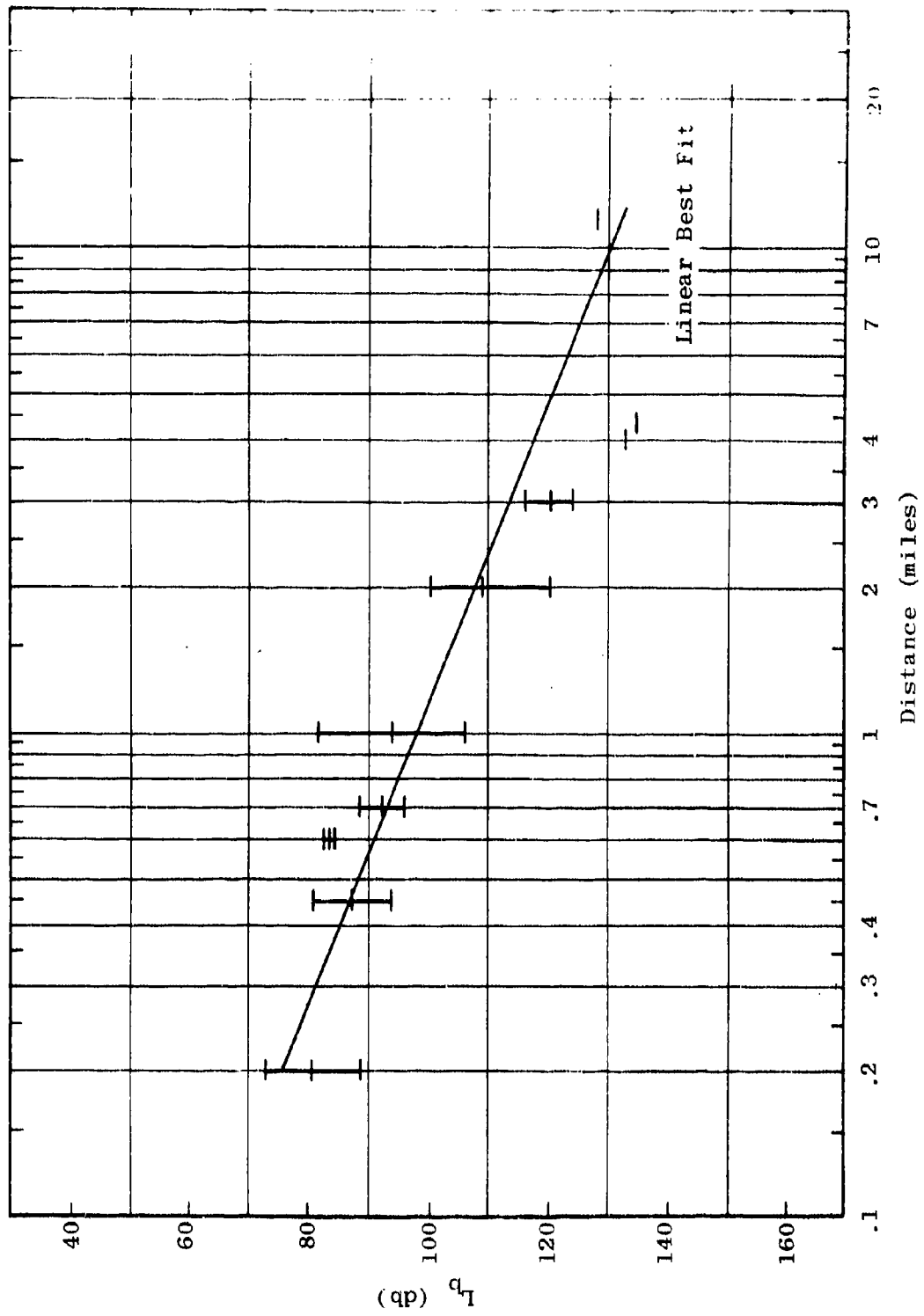


Figure 3.60 Smoothed Fixed-Point Data
 $L_b = F_{A,B}(250.0, 80, H, d, 80)$

(qp) q_1

3-71

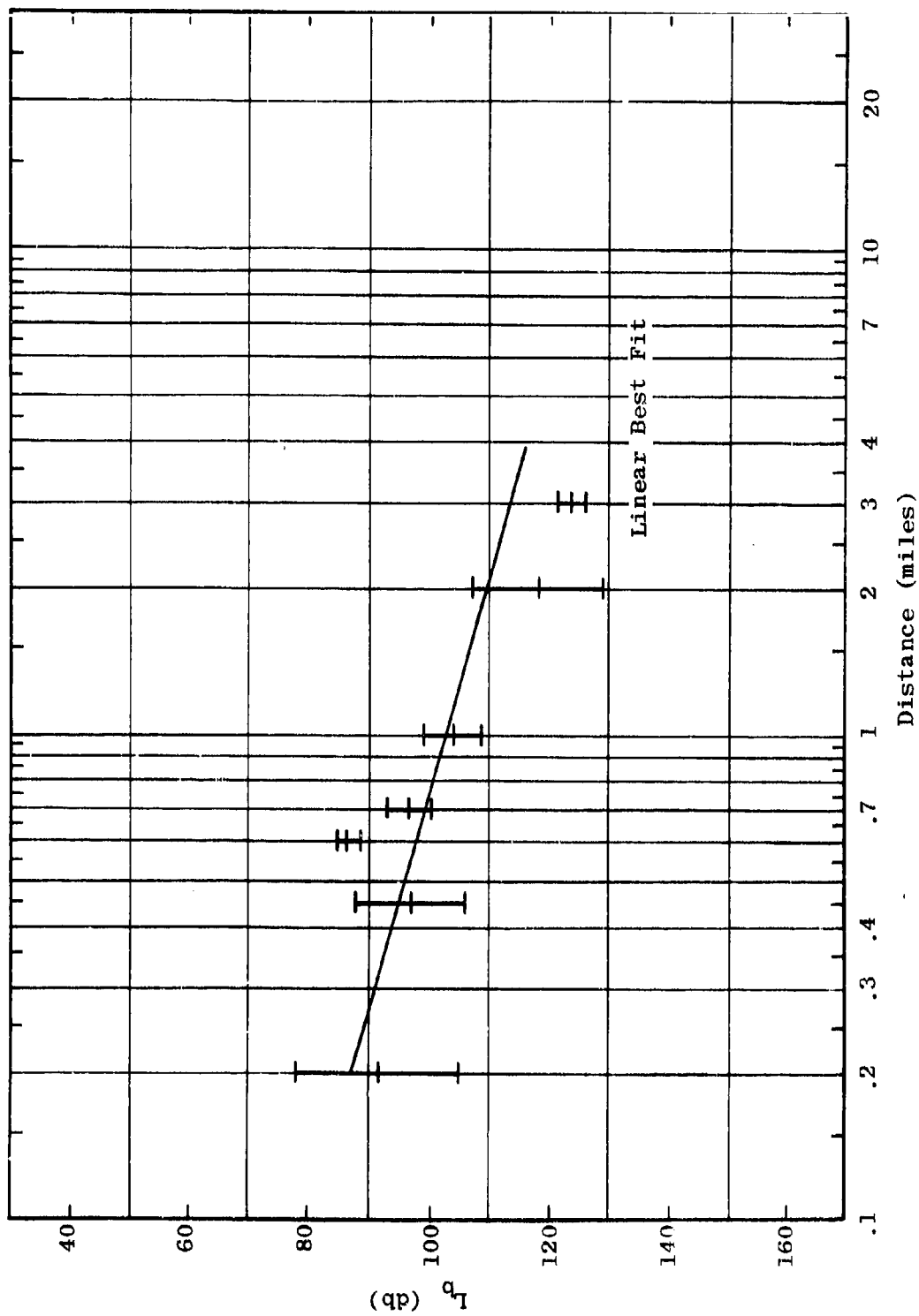


Figure 3.61 Smoothed Fixed-Point Data
 $L_b = F_{A,B}(400.0, 80, H, d, 80)$

range, or polarization. To begin the study, the wet-dry propagation path-loss differences were tabulated. Intuitively, one would expect the path loss to be greater in the wet season than in the dry season. Therefore, the differences were taken so that greater wet-season losses would lead to positive differences, and greater dry-season losses would lead to negative differences.

The tabulated path-loss differences were then grouped in the following manner. Two distinct distance categories were established: short range and long range. The short-range category applies to all path distances from 0.2 mile to 1 mile. The long-range distance category includes all distances greater than 1 mile. The data was also grouped according to antenna heights: low, medium and high. The low antenna category includes all cases for which both antennas have heights of less than 26 feet. The medium antenna category includes all cases in which both antennas were between 26 and 59 feet. The high antenna category includes all cases for which both antennas were higher than 59 feet. All ground-based antennas, regardless of length, were considered to be low antennas. Additional categorizations by frequency and polarization were made. Table 5 gives the number of wet-dry difference samples which were available in each of the categories. In only a few cases were there no samples available at this time. The median wet-dry difference in each of the categories is presented in Table 6. The over-all average difference is given at the bottom of Table 6. The over-all median wet-dry difference varied from about -3 db to about +7 db. The over-all averages were positive, but small indicating that there is a slightly greater loss on the average during the wet season.

Table 5

NUMBER OF SAMPLES USED IN WET-DRY COMPARISON

Freq. (mc)	Antenna Height	Number of Samples			
		Short Range Vert.	Long Range Vert.	Short Range Horiz.	Long Range Horiz.
0.105	Low	52	52	-	-
0.300	Low	52	52	-	-
0.880	Low	65	39	-	-
2	Low	100	38	100	37
6	Low	100	25	88	60
12	Low	100	46	101	65
	Low	24	14	24	23
25.5	Medium	40	34	40	40
	High	40	40	40	40
	Low	12	6	21	21
50	Medium	40	36	40	38
	High	40	40	39	40
	Low	24	9	24	13
100	Medium	40	30	40	30
	High	40	35	40	40
	Low	18	0	11	0
250	Medium	40	12	40	9
	High	40	15	40	20
	Low	6	0	0	0
400	Medium	37	0	18	0
	High	40	18	40	15

Table 6
MEDIAN WET-DRY PATH LOSS DIFFERENCE

Freq. (mc)	Antenna Height	Median Difference (db)			
		Short Range Vert.	Long Range Vert.	Short Range Horiz.	Long Range Horiz.
0.105	Low	-1	0	-	-
0.300	Low	0	0	-	-
0.880	Low	-2	-1	-	-
2	Low	3	2	2	3
6	Low	3	1	0	2
12	Low	0	0	1	2
	Low	1	2	0	1
25.5	Medium	-2	-1	0	1
	High	-1	0	0	1
	Low	-2	0	2	0
50	Medium	0	0	2	0
	High	2	2	2	0
	Low	-1	3	-3	4
100	Medium	0	2	1	1
	High	-1	3	0	1
	Low	0	-	2	-
250	Medium	3	5	7	6
	High	0	2	2	1
	Low	3	-	4	-
400	Medium	-4	-	7	-
	High	1	1	4	2
Average Difference		0.1	1.2	1.8	1.7

The differences for vertical polarization tended to be slightly smaller than for horizontal polarization, particularly at higher frequencies. The wet-dry differences tend to increase with increasing frequency for horizontal polarization but appear to have no consistent variation with frequency for vertical polarization. The difference tends to be slightly higher for the long-range category for vertical polarization. For horizontal polarization, the short-range and long-range differences tend to be approximately the same.

Table 7 gives the standard deviation within each category. The standard deviation is used as a measure of the data spread within each wet-dry difference category. As Table 7 shows, the standard deviations are relatively high, particularly at the higher frequencies.

This analysis suggests that although the data variability is quite high there appears to be only a slight difference between propagation characteristics in the wet season and propagation characteristics in the dry season. The large data variability is to be expected in light of the vehicular results which show that small changes in distance can cause large changes in the observed field. The standard deviations shown in Table 7 are comparable to the standard deviations which have been computed from the vehicular field strength recordings.

Although the data shows that there is no distinctive difference between major seasonal cycles, there could still be some question about the influence of periods of relatively heavy rainfall of propagation loss. In order to gain an insight into the more immediate effects of rainfall,

Table 7
STANDARD DEVIATION OF WET-DRY DIFFERENCE

Freq. (mc)	Antenna Height	Standard Deviation (db)			
		Short Range Vert.	Long Range Vert.	Short Range Horiz.	Long Range Horiz.
0.105	Low	1	2	-	-
0.300	Low	<1	<1	-	-
0.880	Low	2	2	-	-
2	Low	4	4	3	2
6	Low	5	6	2	1
12	Low	1	3	1	1
	Low	2	5	2	2
25.5	Medium	2	4	2	2
	High	4	3	2	2
	Low	4	5	2	3
50	Medium	3	5	2	3
	High	2	2	2	3
	Low	7	3	5	3
100	Medium	4	3	3	2
	High	3	5	1	2
	Low	5	-	4	-
250	Medium	5	3	5	5
	High	5	9	3	2
	Low	3	-	6	-
400	Medium	4	-	6	-
	High	3	5	5	2
Average S.D.		3.3	3.9	3.1	2.3

the following two correlations were attempted. First, the total rainfall in the 24-hour period immediately preceding each measurement was tabulated. Then, the differences in rainfall for the 24-hour period immediately preceding each measurement were correlated with the differences in path loss. This analysis showed that there was no correlation between these two parameters. A similar correlation was attempted using the total rainfall in the 7-day period immediately preceding each measurement. Again, there appeared to be no correlation between total weekly rainfall and propagation loss.

3.4 Height-Gain Profile Summary

In general, basic transmission loss will decrease as the heights of the antennas are increased. This effect is known as height gain. From an operational point of view, it is important to know how the over-all system gain may be improved by elevating one or more of the terminals. In addition, for modeling purposes one of the surest ways to test the validity of a model is to study how well it predicts changes in path loss with antenna height. A rather detailed study of height gain has been made using the large data base now available.

The measurements which are made at fixed receiving locations within the jungle provide a continuous record of loss vs receiving height. A number of heights, ranging from 11 to 80 feet, were chosen for the height-gain study. The median basic transmission loss in each of the height ranges was determined, and that median value was assigned to a nominal receiver height within the sample range. Table 8

Table 8

HEIGHT RANGES USED IN HEIGHT-GAIN STUDY

Nominal Height (ft)	Range Over Which Median was Taken (ft)
11	Fixed
20	17.5 - 23
31	28.5 - 34
42	39.5 - 45
59	56 - 61
79	76 - 81.5

shows the receiving antenna height increments which were used and the nominal receiver height which was assigned to each height increment. The measurement used at 11 feet was a fixed measurement and hence did not have an associated height range.

Since it is very possible that the nature of the height-gain function itself may change as receiving height is increased, the height-gain function is not studied directly, but rather its derivative is studied as a function of receiving antenna height. Further, to make the study as direct as possible, the path-loss data was first normalized to the quantity $20 \log h$ which appeared at the beginning of the study to be the most likely height-gain function.

Tables 9 and 10 summarize the height-gain statistics which were used in the study. Table 9 pertains to vertical polarization and Table 10 pertains to horizontal polarization. The entries in these tables require some

Table 9

NORMALIZED LOSS DIFFERENCES WITH HEIGHT
(Vertical Polarization)

Freq. (mc)	H _t (ft)	L ₁₁ -L ₂₀ (db)		L ₂₀ -L ₃₁ (db)		L ₃₁ -L ₄₂ (db)		L ₄₂ -L ₅₉ (db)		L ₅₉ -L ₇₉ (db)	
		A	B	A	B	A	B	A	B	A	B
25	10	-4	-4	2	3	1	1	0	0	1	1
	40	-5	-1	3	3	1	1	0	0	1	1
	80	-5	-3	3	3	1	1	0	0	0	1
50	13	-1	1	1	1	1	0	2	1	0	1
	40	-1	-1	1	0	1	0	1	1	1	2
	80	1	-5	1	1	0	0	1	2	1	1
100	13	-4	3	0	-1	4	1	4	2	1	3
	40	-1	-1	1	-1	1	1	2	3	2	2
	80	-2	0	1	-1	1	0	3	2	2	2
250	13	-5	-1	1	1	1	4	2	3	5	1
	40	-2	-2	2	2	0	2	4	4	2	2
	80	-1	-2	1	0	1	6	8	3	2	2
400	13	-4	-4	0	1	2	0	4	3	3	4
	40	-2	-4	-2	1	5	5	4	4	2	1
	80	-1	-1	0	1	0	3	4	5	4	1

Table 10

NORMALIZED LOSS DIFFERENCES WITH HEIGHT
(Horizontal Polarization)

Freq. (mc)	H _t (ft)	L ₁₁ -L ₂₀ (db)		L ₂₀ -L ₃₁ (db)		L ₃₁ -L ₄₂ (db)		L ₄₂ -L ₅₉ (db)		L ₅₉ -L ₇₉ (db)	
		A	B	A	B	A	B	A	B	A	B
25	10	0	1	1	0	0	0	-1	0	0	0
	40	-1	1	0	0	0	0	-1	0	0	0
	80	1	1	-1	0	-1	0	0	0	0	-1
50	13	-1	0	-2	-1	-1	-1	0	0	1	0
	40	-1	0	-2	-1	-1	-1	0	-1	0	1
	80	-1	0	-1	-2	-1	-1	0	-1	0	1
100	13	-4	-2	-3	-3	2	1	3	3	1	1
	40	-2	-3	-3	-3	1	1	3	2	-	1
	80	-3	-3	-3	-3	1	0	3	3	0	1
250	13	-4	-4	-2	0	2	4	5	4	3	1
	40	2	-3	0	-1	1	4	0	4	3	2
	80	-2	-1	0	-2	-1	5	6	3	2	3
400	13	-4	-4	0	2	1	-2	2	2	6	2
	40	-2	-2	-1	0	4	1	3	3	3	5
	80	-4	-2	-1	-2	5	5	4	3	4	1

explanation. Frequency, which appears in the extreme left column, runs from 25 mc to 400 mc. The transmitting antenna height appears in the next column. Heights of 13, 40, and 80 feet were used at all frequencies except 25 mc. The next column in the table lists the median basic transmission loss which was observed with a receiver height of 11 feet minus the median basic transmission loss which was observed for the same situation with a nominal receiving antenna height of 20 feet. The A designates data taken in Sector A. The B designates data taken in Sector B. The first data entry under $L_{11}-L_{20}$, Sector A, is -4 db. The -4 represents a difference between the loss observed with a receiving antenna height of 11 feet and the loss with a receiving antenna height of 20 feet on Sector A. The difference has been normalized by taking out the factor $20 \log h$. Hence, if the difference corresponded exactly to $20 \log h_{20}/h_{11}$, the entry in the table would be zero. If the loss fell off more slowly than $20 \log h$ with increasing antenna height, a negative entry in the table would be expected. On the other hand, if the loss fell off more rapidly than $20 \log h$ with increasing antenna height, a positive entry would be expected in the table.

The entries in Table 9 show that the loss, in general, did not change as much between 11 and 20 feet as was expected. However, examination of the next two columns of Table 9 shows that the loss change was more than was expected between 20 feet and 31 feet.

The entries in Table 9 do not represent individual differences but rather the average difference taken over a large number of samples. The different samples which were

averaged to obtain the entries in Table 9 were taken at various distances along each of the two sectors and during both seasons. Table 9 can be used to study height gain as a function of frequency, polarization, transmitting antenna height, receiving antenna height, and sector. A study of the height-gain function with variation in distance has indicated no change in the character of the height-gain function over the distance ranges for which data is available.

Although there are random differences between Sectors A and B, Table 9 shows no consistent difference between these sectors. When the entries in Table 9 are significantly different from zero, there appears to be a dependence, in some cases, on transmitting antenna heights. Comparison of Table 9 and Table 10 indicates that the same general trends apply to both polarizations. For low antenna heights and low frequencies, the decrease in loss with increasing antenna height tends to be less than $20 \log h$. However, for high frequencies and high antenna heights, the decrease in loss with increasing antenna height tends to be greater than $20 \log h$.

In order to study the effects of frequency and antenna height more closely, the data from Tables 9 and 10 has been smoothed. The smoothed results appear in Tables 11 and 12, respectively. The smoothing which resulted in the latter two tables was accomplished by averaging between sectors and averaging over the three transmitting antenna heights. In addition, the abnormal variation seen in Table 9 at 25 mc for the two lowest antenna height ranges was smoothed. This variation is unusual and may be of some interest, but for the purposes at hand the variation is ignored.

Table 11

SMOOTHING OF TABLE 9
(Vertical Polarization)

<u>Freq. (mc)</u>	<u>L₁₁-L₂₀ (db)</u>	<u>L₂₀-L₃₁ (db)</u>	<u>L₃₁-L₄₂ (db)</u>	<u>L₄₂-L₅₉ (db)</u>	<u>L₅₉-L₇₉ (db)</u>
25	-0.5	0	1	0	1
50	-1	1	0	1.5	1
100	-1	0	1.5	3	2
250	-2	1	2	4	2
400	-3	0	2.5	4	2.5

Table 12

SMOOTHING OF TABLE 10
(Horizontal Polarization)

<u>Freq. (mc)</u>	<u>L₁₁-L₂₀ (db)</u>	<u>L₂₀-L₃₁ (db)</u>	<u>L₃₁-L₄₂ (db)</u>	<u>L₄₂-L₅₉ (db)</u>	<u>L₅₉-L₇₉ (db)</u>
25	-0.5	0	0	0	0
50	-0.5	-1.5	-1	0	0.5
100	-3	-3	1	3	1
250	-2	-1	2.5	3.5	2
400	-3	0	2	3	3.5

Table 11 illustrates that for vertical polarization at the lowest heights the decrease in loss from 11 feet to 20 feet is consistently less than would be expected, and the amount of decrease in loss decreases with increasing frequency. For the other height ranges the amount of decrease in loss with increasing height is greater than would be expected and consistently tends to increase with increasing frequency and increasing antenna height.

Since the first two rows in Table 11 are essentially zero, it may be concluded that for vertical polarization, the height gain observed at 25 and 50 mc is essentially the expected logarithmic function. However, Table 11 clearly shows that the height gain at higher frequencies does not follow the expected logarithmic function.

In a similar manner, Table 12 shows that the logarithmic height-gain function is to be expected for the lower frequencies, but that a significant difference seems to exist at the higher frequencies. In order to study the exact nature of the height-gain function, the data from Tables 11 and 12 should be plotted.

Before plotting the data from Tables 11 and 12, it is helpful to denormalize the information by adding the factor $20 \log h$. The denormalized height-gain data is plotted on Figure 3.62 for vertical polarization and on Figure 3.63 for horizontal polarization. The crosses on Figure 3.62 correspond to the height-gain function at 25 mc. The black circles correspond to 50 mc, the white circles to 100 mc, the black squares to 250 mc and the white squares to 400 mc. Note that the plot is in terms of decibels vs a

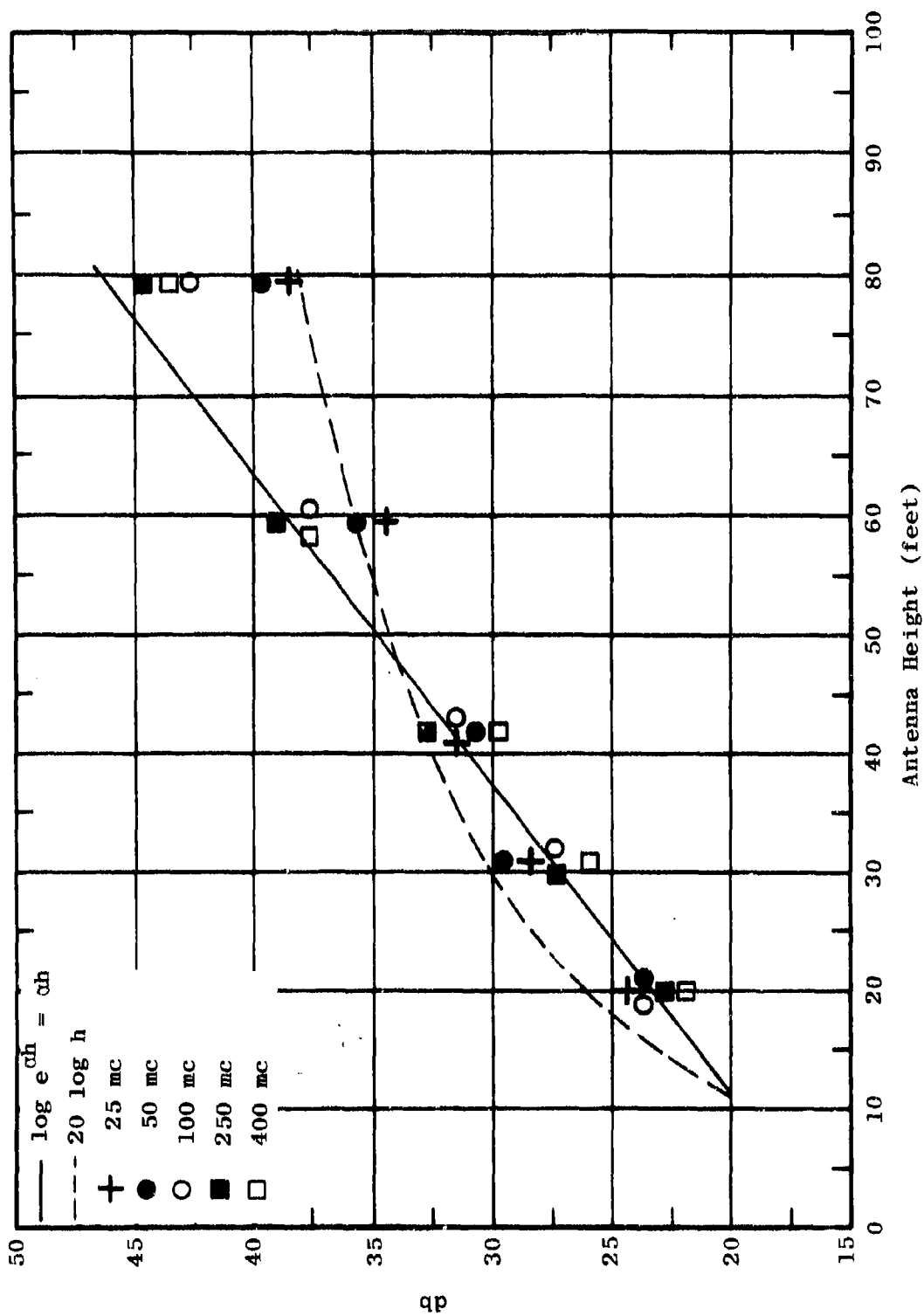


Figure 3.62 Height Gain, Vertical Polarization

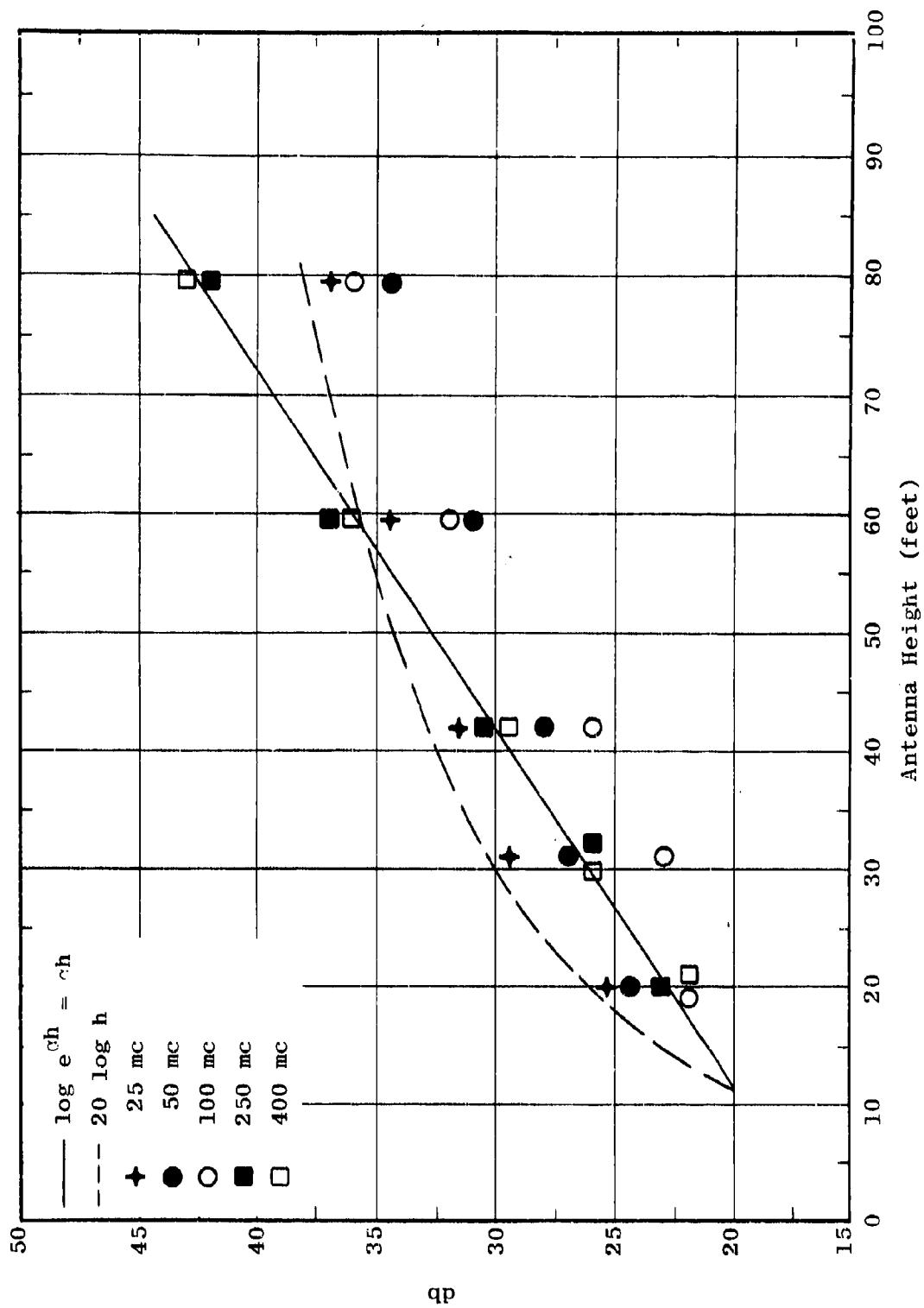


Figure 3.63 Height Gain, Horizontal Polarization

linear scale in height. The solid line drawn on Figure 3.62 corresponds to a constant change in path loss with height. This change corresponds to an exponential change in field strength with height. The dotted curve on Figure 3.62 responds to a logarithmic change in path loss with height.

It can be clearly seen by following the crosses and black circles plotted on Figure 3.62, corresponding to 25 and 50 mc respectively, that this data tends to follow the logarithmic curve. However, for the two highest frequencies, the black squares and the white squares, the data clearly follows the exponential curve (i.e., the solid straight line) for all but the highest elevations, where the height-gain function begins to fall off in the expected logarithmic manner. The circles corresponding to 100 mc follow the straight line in a similar manner but appear to have a very slight tendency toward the logarithmic curve. This means that at the higher frequencies the attenuation characteristic with height tends to be exponential in terms of field strength until the antenna is well clear of the foliage. On the other hand, at the lower frequencies, even when the antenna is submerged in foliage, the height characteristic tends to follow the well-known logarithmic curve.

Figure 3.63 suggests that similar conclusions can be drawn for horizontally polarized transmissions at 250 and 400 mc except that even at the highest elevation there seems to be no fall-off from the exponential curve. At 25 mc, the logarithmic curve is followed reasonably well. However, there appears to be a third, and as yet unexplored, phenomenon in the case of horizontal polarization at 50 and 100 mc.

It is interesting to note that Figure 3.62 seems to indicate that, for vertical polarization and low antenna height, there is a definite change in propagation mechanism between 50 and 100 mc. That is, the characteristics change from exponential to direct in units of field strength or from direct to logarithmic in units of path loss. This rather drastic change in propagation phenomena is consistent with the changes in measured path-loss characteristics which were noted in Figure 3.50. Figure 3.50 pertains to vertical polarization with low antenna heights. A corresponding exhibit, Figure 3.51, pertains to vertical polarization with high antennas. The apparent change in propagation characteristics between 50 and 100 mc does not show up in Figure 3.51 for the high antennas. Again, this observation is consistent with the height-gain results shown in Figure 3.62. Figure 3.62 clearly shows that the height-gain function tends to follow the logarithmic characteristic for all frequencies with vertical polarization at the high antenna elevations.

Does a similar correspondence exist for horizontal polarization? An examination of Figure 3.63 shows that a change in the propagation characteristic between 100 and 250 mc is to be expected for horizontal polarization rather than between 50 and 100 mc as was the case for vertical polarization. Furthermore, the 250 and 400 mc data does not tend toward the logarithmic fall-off at the high heights as was the case for vertical polarization. Therefore, the change in propagation characteristic is expected to occur between 100 and 250 mc for both the low antenna heights and the high antenna heights. Figure 3.52 shows the expected change in propagation characteristics between 100 and 250 mc for the low antenna heights. Figure 3.53 demonstrates that this change in propagation characteristic continues between 100 and 250 mc even for the high antennas.

3.5 Foliage Factor

A foliage factor for frequencies of 25 mc and above appears in Semiannual Report Number 6. The derivation and characteristics of this foliage factor are summarized in Section 2.4 of this report. The derivation was based on a relatively limited data sample and is being re-evaluated in light of the much larger data base available and in light of the height-gain analysis results presented in Section 3.4 of this report. Although the details of the foliage factor are expected to change as a result of this analysis which is currently in progress, the over-all character of that function should remain essentially the same.

It is also important to explore the effects of foliage on propagation for frequencies below 25 mc. Vertical polarization below 25 mc will be considered first.

3.5.1 Vertical Polarization Below 25 mc

The fit of the surface-wave function to measured data is presented in Section 3.2 of this report. It should be noted that in Section 3.2 of this report a distinction is drawn between the terms "surface-wave function" and "theoretical surface-wave path loss values." The theoretical surface-wave values refer to actual surface-wave path-loss curves expected to hold in the absence of foliage. On the other hand, the surface-wave function refers to these theoretical curves displaced vertically by any given db.

Since the surface-wave function appears to match measured data reasonably well at the lower frequencies, it

is logical to explore the hypothesis that the difference between theoretical surface-wave values and the surface-wave function that best fits the measured data is a foliage factor. These differences are plotted on Figure 3.64 as a function of frequency for vertical polarization. The points plotted on Figure 3.64 from 0.105 to 12 mc represent the amount by which theoretical surface-wave curves were moved to obtain a good fit to measured data. Thus, the points plotted on Figure 3.64 for frequencies from 105 kc to 12 mc may be considered as a foliage factor with respect to surface-wave propagation. At 25 mc, there are two points plotted: The lower point corresponds to the difference between surface-wave theory and the measurements made at 25 mc. The upper point corresponds to the foliage factor based on the Egli model as first presented in Semiannual Report Number 6. The points plotted for frequencies of 50 mc and above correspond to the foliage factor which was deduced by using the Egli rough-terrain model.

Although it is by no means certain that the entire effect seen on Figure 3.64 is due to the presence of foliage, for convenience in the present discussion, the effect will be referred to as a foliage effect. The data shown in Figure 3.64 will be analyzed in the three separate groups into which they appear to fall. First, the data at 100, 300 and 880 kc will be referred to as the kc data. The second data grouping, consisting of frequencies from 2 to 25 mc, will be referred to as the HF data. The third grouping, consisting of frequencies from 50 to 400 mc, will be referred to as the VHF data. In analyzing the foliage effect shown in Figure 3.64, it is important to keep in mind the transmitting and receiving antennas which are used

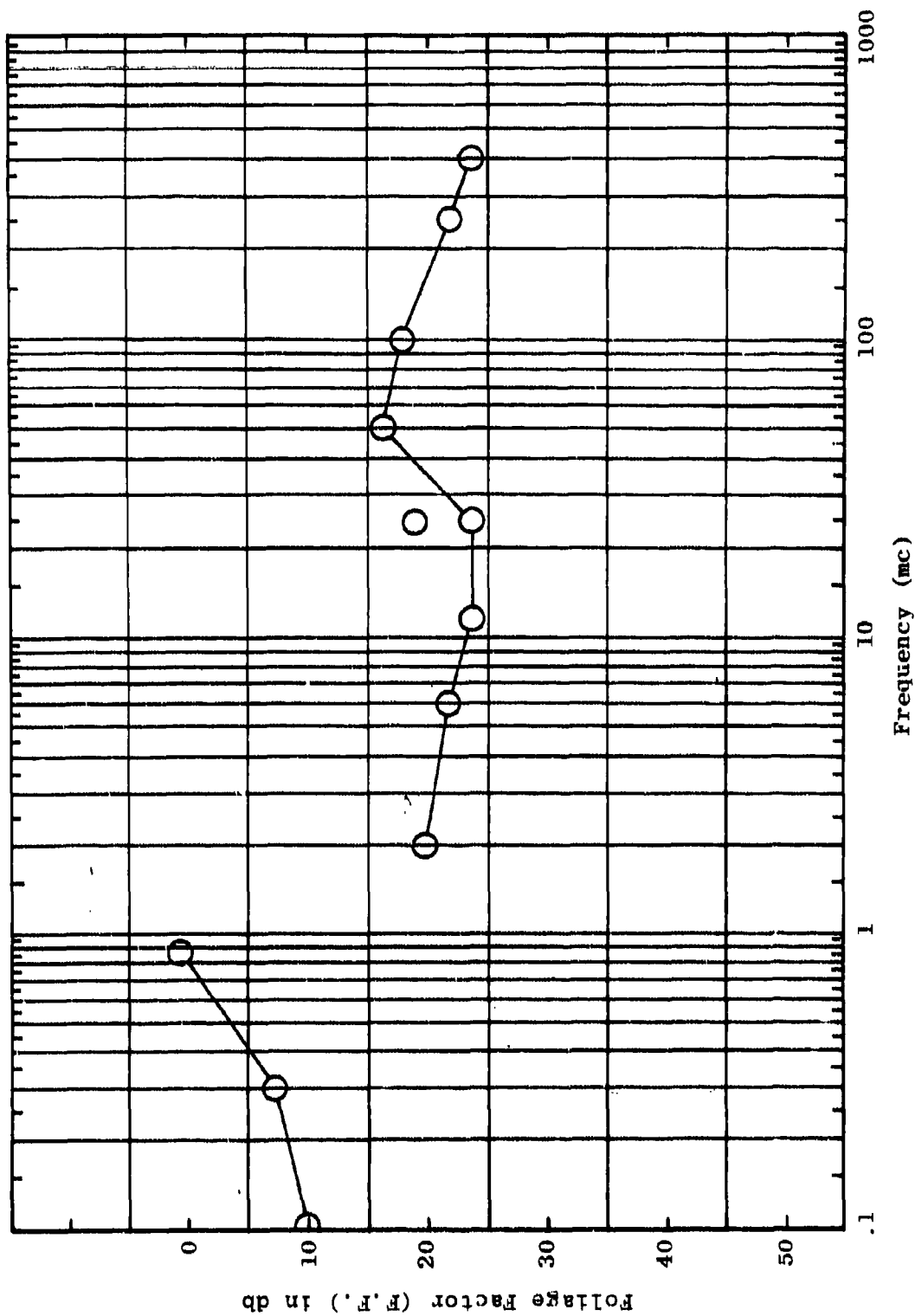


Figure 3.64 Foliage Factor (F.F.) for Vertical Polarization

in each of the frequency ranges. Table 13 provides a summary of the transmitting antennas which were used. For the kc frequencies a ground-based vertical antenna with capacitive top-loading plus a wire-radial ground system is used. This antenna was initially located in the foliage, but the direct effect of the foliage upon the antenna was great enough to prevent loading the antenna. Therefore, the antenna was moved into the base site clearing and is therefore isolated from the foliage by a distance of 100 feet or more. For the high frequencies a vertical antenna without top loading is used and is located in the jungle just beyond the base compound. For frequencies above 25 mc an elevated half-wave dipole is used and is located in the jungle along with the HF antenna. At 25 mc the ground-based vertical antenna and the elevated half-wave dipole antenna are used.

For receiving, loop antennas are used for frequencies up to 25 mc. Vertical half-wave dipole antennas are used for frequencies of 50 mc and above.

In Figure 3.64, the apparent foliage effect decreases with increasing frequency for the kc range, whereas it increases with increasing frequency in the other two frequency ranges. It should be noted further that the rate of increase in the HF range is less than the rate of increase in the VHF range.

The data in Figure 3.64 strongly suggests the presence of two separate foliage effects. One appears to be more of an effect on the antenna in that it is a function of the antenna's proximity to foliage as measured in wavelengths. The other is an effect upon the propagation path

Table 13

TRANSMITTING ANTENNAS

Frequency (mc)	Pol.	Nominal Height (feet)	Description	$20 \log E_1$ (db/ $\mu\text{v}/\text{m}$)
0.105 0.300 0.830	V	80	Ground-based vertical radiator with capacitive top loading and wire radial ground system.	$77.4 + 20 \log I + 20 \log f$ where I = base current in amps f = frequency in megacycles
2	V	80	Ground-based vertical, tuned with BC 939B tuning unit.	$86.4 + 20 \log I$ where I = base current in amps
6	V	40	Ground-based, quarter-wave vertical tuned with modified BC 939B tuning unit.	$91.4 + 20 \log I$ where I = base current in amps
12	V	21	Ground-based vertical antenna cut to $\lambda/4$.	$91.4 + 20 \log I$ where I = base current in amps
15.5	V	10	Ground-based vertical antenna cut to $\lambda/4$.	$72.8 + 10 \log P$ where P = power delivered to antenna in watts

Table 13 (Continued)

Frequency (mc)	Pol.	Nominal Height (feet)	Description	20 Log E_1 (db/ $\mu V/m$)
25.5	V	40 80	Elevated $\lambda/2$ vertical skirted dipole.	72.8 + 10 Log P where P = power delivered to antenna in watts
50 100 250 400	V	13 40 80	Elevated vertical skirted $\lambda/2$ dipole.	72.8 + 10 Log P where P = power delivered to antenna in watts
2 6 12	H	40 80	Horizontal $\lambda/2$ dipole consisting of wire strung between two towers with jumpers to allow change in fre- quency. Center feed with tuned section of 72-ohm twin lead.	91.4 + 20 Log I + 20 Log D where I = input current in amps $\cos(\frac{\pi}{2} \cos \theta)$ $D = \frac{\sin \theta}{\cos(\frac{\pi}{2} \cos \theta)}$ θ = angle between dipole axis and ray to receiving point
25.5 50 100 250 400	H	13 40 80	$\lambda/2$ horizontal dipole mounted on vertical tower.	72.8 + 10 Log P + 20 Log D where P = power delivered to antenna in watts $\cos(\frac{\pi}{2} \cos \theta)$ $D = \frac{\sin \theta}{\cos(\frac{\pi}{2} \cos \theta)}$ θ = angle between dipole axis and ray to receiving point

and is not dependent on the antenna's relative position with respect to foliage. This hypothesis involving two different foliage effects is tentative at this point, but it does explain the phenomenon that is seen in Figure 3.64 and provides a sound basis for further experimentation.

In support of this hypothesis, examine the kc data. The foliage effect decreases with increasing frequency. In this case, the transmitting antenna is somewhat isolated from the foliage in absolute distance terms, but the wavelength is so long at 100 kc that the antenna's effective separation from the foliage in terms of wavelengths is small. At 300 kc, the wavelength has been reduced by one third, and the antenna is effectively three times as far from the foliage as it was at 100 kc. Therefore, any direct influence the foliage may have upon the antenna should decrease at 300 kc. At 880 kc the antenna is effectively nine times farther away from the foliage than it was at 100 kc, and a further decrease in the direct effect of foliage would be expected, which is consistent with what is seen on Figure 3.64.

At 2 mc the transmitting antenna is moved into the foliage where it has an approximate separation distance from the closest foliage of on the order of 10 feet. Therefore, between 880 kc and 2 mc a large increase in the foliage effect would be expected. Such increase is indeed observed. Thus, the evidence is strong in favor of some foliage effect which is intimately dependent upon the separation between antenna and foliage.

In the VHF region the wavelength begins to become small enough so there is no appreciable amount of foliage within the induction field of the antennas. Thus, it would be expected that the phenomenon seen in the VHF region does not exert a significant direct effect upon the antenna. Accordingly, the following hypotheses are posed:

- (1) The apparent foliage effect may be divided into two components: one which depends upon the antenna's proximity to foliage, termed the antenna-to-foliage coupling effect; and one which stems from the foliage effect upon the propagation path, termed the vegetation attenuation effect.
- (2) The antenna-to-foliage coupling effect appears for frequencies in the kc range, but the vegetation attenuation effect does not.
- (3) The vegetation attenuation effect appears for VHF, but the antenna-to-foliage coupling effect does not.
- (4) Both the antenna-to-foliage coupling effect and the vegetation attenuation effect appear for frequencies in the HF range.

On the basis of these hypotheses the following functional relationships can be deduced from the data shown on Figure 3.64.

- (1) The antenna-to-foliage coupling effect is inversely proportional to $4 \log d/\lambda$ where d/λ is the separation distance between antenna and foliage measured in wavelengths.

- (2) The vegetation attenuation effect is directly proportional to $9 \log f_{mc}$ and has a value of zero at 1 mc.

These functions make the kc data consistent with the HF data with the exception of the point at 880 kc. Referring to Figures 3.39, 3.40 and 3.41 in Section 3.3, it can be seen that the fit at 100 kc and 300 kc is very good and that there is not much question about the amount by which the surface-wave function needs to be moved to best fit the data. However, at 880 kc the surface-wave function could be moved as much as 6 db more without significantly affecting the quality of fit. A 6-db increase in the foliage effect at 880 kc would make that point consistent with the remainder of the kc data and the HF data under the above hypotheses.

Under the above hypotheses, there is a slight difference (approximately 4 db) between the antenna-to-foliage coupling effect in the kc region and that in the HF region, indicating that this antenna-to-foliage coupling effect may be a function of the antenna type as well as its proximity to foliage. There is another discontinuity of about 6 db between 25 mc and 50 mc. At this point, dipoles replace loops as receiving antennas and the types of transmitting antennas are also changed.

Considering the hypotheses discussed above, it is recommended that a number of experiments be performed to explore the changes in measured path loss with changes in antenna proximity to foliage for the types of antennas currently used in the measurement program.

3.5.2 Horizontal Polarization

Propagation losses for vertical polarization considerably exceed those expected in the absence of foliage, indicating a significant adverse foliage effect. For horizontal polarization, the opposite is true. The propagation losses observed at 2, 6 and 12 mc were significantly lower than would be expected in the absence of foliage. Table 14 lists the range of measured losses which were observed at 1 mile for horizontal polarization.

Table 14
RANGE OF MEASURED VALUES AT 1 MILE

Freq. (mc)	Range of Observed Loss at 1 Mile (db)			
	Low Antennas Vertical	Low Antennas Horiz.	High Antennas Vertical	High Antennas Horiz.
2	68-73	83-91	67-74	69-74
6	89-97	85-95	86-93	71-74
12	101-107	91-96	92-100	75-79

The vertical polarization losses are also included for comparison purposes. The losses are presented for low antennas and for high antennas. The low antennas for horizontal polarization consist of a 40-foot transmitting antenna and a 17-foot receiving antenna. The high antennas for horizontal polarization consist of an 80-foot transmitting antenna and an 80-foot receiving antenna. For vertical polarization, the low antennas consist of an 80-foot ground-based vertical antenna for transmitting and a receiving loop

7

which is 17 feet above the ground. The high antennas for vertical polarization consist of the same 80-foot transmitting antenna and a receiving loop which is 80 feet from the earth's surface. As Table 14 shows, the losses for horizontal polarization increase with frequency much more slowly than the losses for vertical polarization. The change with frequency is such that for low antennas the horizontal loss is greater than the vertical loss at 2 mc, is roughly comparable to the vertical loss at 6 mc, and is less than the vertical loss at 12 mc. For high antennas the horizontal and vertical losses are comparable at 2 mc, and the vertical losses are lower at 6 and 12 mc.

Table 15 presents the theoretical surface-wave losses to be expected at 1 mile for a low conductivity for the HF region. For comparison purposes, the median observed losses are also presented in Table 15. Table 15 shows clearly that the losses observed for vertical polarization exceed the losses expected in the absence of foliage. However, for horizontal polarization the observed losses are less than those expected in the absence of foliage. The low theoretical losses for horizontal polarization depend upon a cancellation between direct and earth-reflected components. The data shown in Table 15 leads to the hypothesis that the presence of foliage suppresses the cancelling earth-reflected component and therefore permits higher horizontal fields than would be expected.

Table 15
THEORETICAL SURFACE-WAVE VALUES AT 1 MILE

Freq. (mc)	Theoretical Surface-Wave Values* (db)			
	Low Antennas Vertical	Low Antennas Horiz.	High Antennas Vertical	High Antennas Horiz.
2	51 (70)**	97 (87)	51 (70)	97 (71)
6	71 (93)	115 (90)	71 (89)	115 (72)
12	80 (104)	127 (93)	84 (96)	127 (77)

* Conductivity = 0.0005 mho/meter
 $\epsilon_r = 15$

** Values in parentheses are median observed values.

For horizontal polarization at frequencies of 2, 6 and 12 mc no change in loss with height is expected for either the surface-wave or the diffracted fields. However, as Table 15 shows, there is a significant height-gain effect in the measured data. The height gain for horizontal polarization shows a difference of 16 to 18 db between low antennas and high antennas. In the low antenna situation, both the transmitting and receiving antennas are immersed in foliage while with the high antennas both antennas are out of foliage.

The theoretical figures in Table 15 are based on a low conductivity. Table 16 shows how the theoretical losses change at 2, 6 and 12 mc with changes in conductivity. As Table 16 shows, surface-wave losses decrease with increasing conductivity for vertical polarization, whereas surface-wave losses for horizontal polarization increase with increasing

conductivity. To be as consistent as possible with measured results for horizontal polarization, it is necessary to seek theoretical results which are as low as is reasonably possible. Therefore, the tendency toward low conductivities for horizontal polarization is more consistent with measured observations than assuming higher conductivities. Thus, the horizontal data indicates a low conductivity, which is harmonious with the conclusions drawn from the vertical polarization data.

Table 16

THEORETICAL LOSS AS A FUNCTION OF CONDUCTIVITY

Freq. (mc)	Conductivity (mhos/meter)	Theoretical Loss at 1 Mile (db)			
		Low Antennas		High Antennas	
		Vert.	Horiz.	Vert.	Horiz.
2	0.0005	51	96	52	97
	0.01	39	112	41	112
	0.04	38	124	40	124
6	0.0005	71	115	71	115
	0.01	62	123	63	123
	0.04	51	134	57	134
12	0.0005	80	127	84	127
	0.01	78	130	80	131
	0.04	67	140	68	140

4. VEHICULAR DATA

Vehicular measurements provide a detailed picture of the variation in path loss as a function of distance within the foliated environment. As the vehicle proceeds along a path cut through the vegetation, a fifth wheel mechanically drives a strip chart recorder which continuously records the widely varying measured field strengths. Figure 4.1 is a sample of 100-mc data obtained in this way. The radials along which the vehicle moves have markers which indicate radial distance from the transmitter every 0.2 mile from 0.2 mile to 3 miles and every 0.5 mile thereafter. Each time the vehicle passes one of these distance markers, a calibration mark is made on the strip recorder. Since the trails are never exact radials, the actual distance represented on this strip chart is always greater than the indicated radial distance.

Relative field strength is calibrated in terms of db along the vertical scale at the left in Figure 4.1. Figure 4.1 shows an extremely rapid variation superimposed upon a slower variation. The rapid variation becomes less rapid with decreasing frequency and more rapid with increasing frequency. The rapid variation is characteristic of the type of field-strength variation usually observed in the vicinity of foliage. The long-term variation is characteristic of that generally observed over unfoliated rolling terrain.

Vehicular recordings are made along each of the two trail systems for both the wet and dry seasons at each frequency and for each transmitting antenna height and each

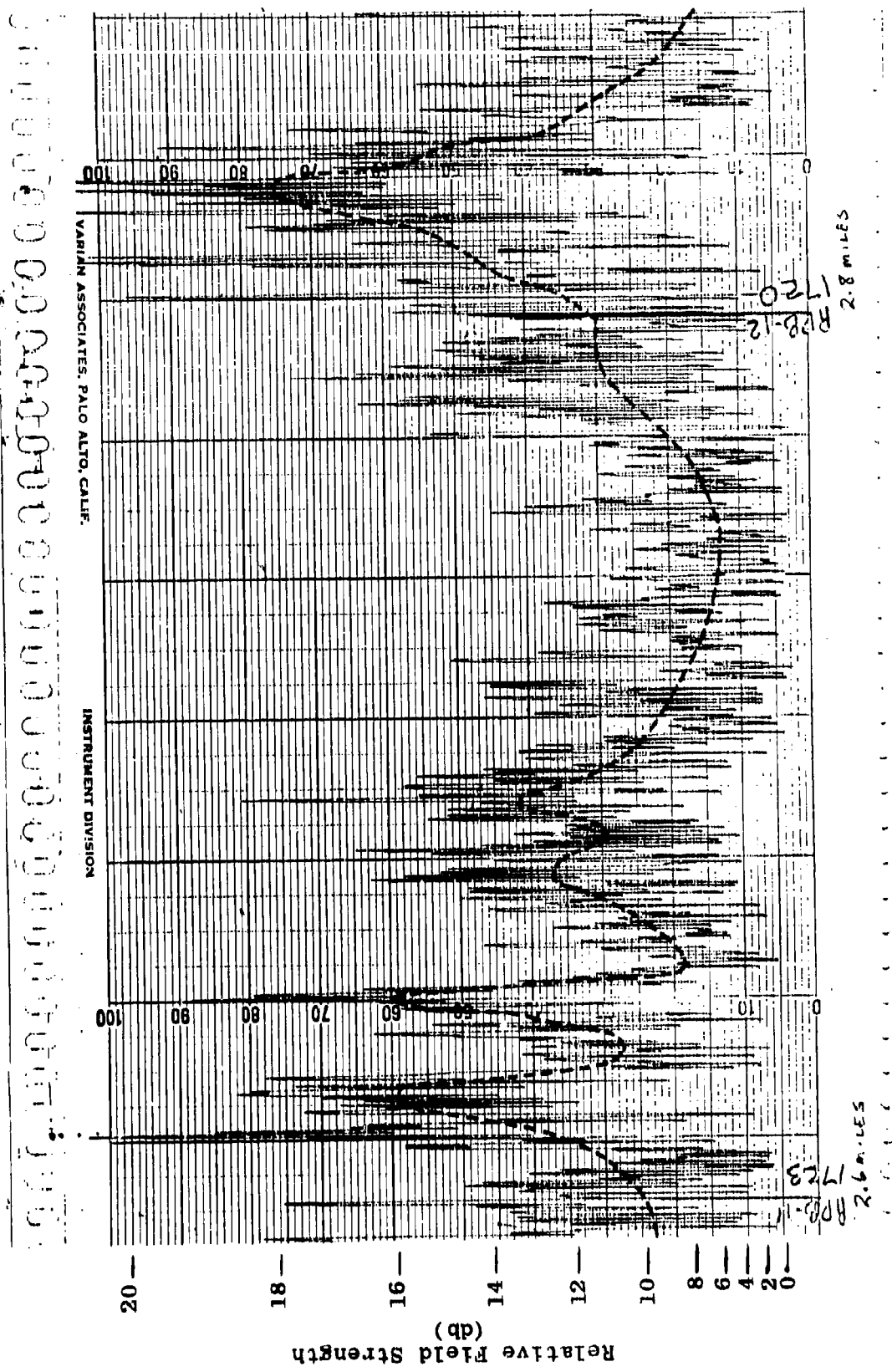


Figure 4.1 Example of Rapid and Slow Variations of Vehicular Data
 $L_b = F_B(100.0, 80, V, d, 7)$

polarization. Thus, it is obvious that a considerable amount of vehicular data is generated. This data is being analyzed in three ways. First, the vehicular recordings are divided into sample intervals. Each sample interval corresponds to the vehicular data which is collected between adjacent calibrated field points. Thus, each sample interval between 0.2 mile and 3 miles corresponds to an increment of 0.2 mile of radial distance. Sample intervals at distances greater than 3 miles correspond to 0.5-mile increments of radial distance. Within each sample interval, the statistical distribution of observed amplitudes is computed. Analyses to date, as indicated in Section 4.3.3 of Semi-annual Report Number 6, suggest that the amplitude statistic in each sampling interval is normally distributed. The standard deviation within each sampling interval varies considerably as distance is increased. However, the over-all tendencies indicate that the average standard deviation tends to increase only slightly as distance is increased. The over-all standard deviation within each sampling interval varies from about 1 to 2 db at 6 mc to between 3 and 7 db at 100 mc.

The second type of analysis being performed on the vehicular data consists of a detailed study of the nature of the rapid and longer-term variations in path loss as a function of distance. The strip recordings show clearly that the rapid variations increase in frequency of occurrence as radio frequency increases. Rough estimates of the distance spacings between adjacent maxima and minima vary from about 20 feet at 25 mc to about 4 feet at 400 mc. To obtain a more accurate picture of these fine-grain variations, it is recommended that some strip chart recordings be made in Thailand with ten times the present resolution. Several

samples of the longer-term variation are presented in Section 4.2 of this report.

The third type of analysis which is being performed on the vehicular data consists of examining the basic transmission loss as a function of distance after the rapid and long-term variations have been smoothed out. Examples of this third type of analysis are presented in the next section.

4.1 L_b vs Distance

The vehicular data provides a large data base for use in the study of basic transmission loss vs distance in foliated areas. This large data base supplements the fixed-point data base, which at the moment consists of approximately 21,000 data samples.

Curves of basic transmission loss vs distance for vertical polarization in Sector A are shown in Figure 4.2. The receiving antennas for these measurements are mounted on the top of the vehicle and are approximately 7 feet above the ground. The transmitting antennas in each case correspond to the lowest transmitting antennas available at each frequency. For frequencies up through 25 mc the antennas were ground-based verticals. For frequencies of 50 mc and above, the antennas were half-wave dipoles whose centers were 13 feet from the ground. An identical family of curves for horizontal polarization is given in Figure 4.3.

It is interesting to compare the fixed-point data with vehicular data. The family of curves based on

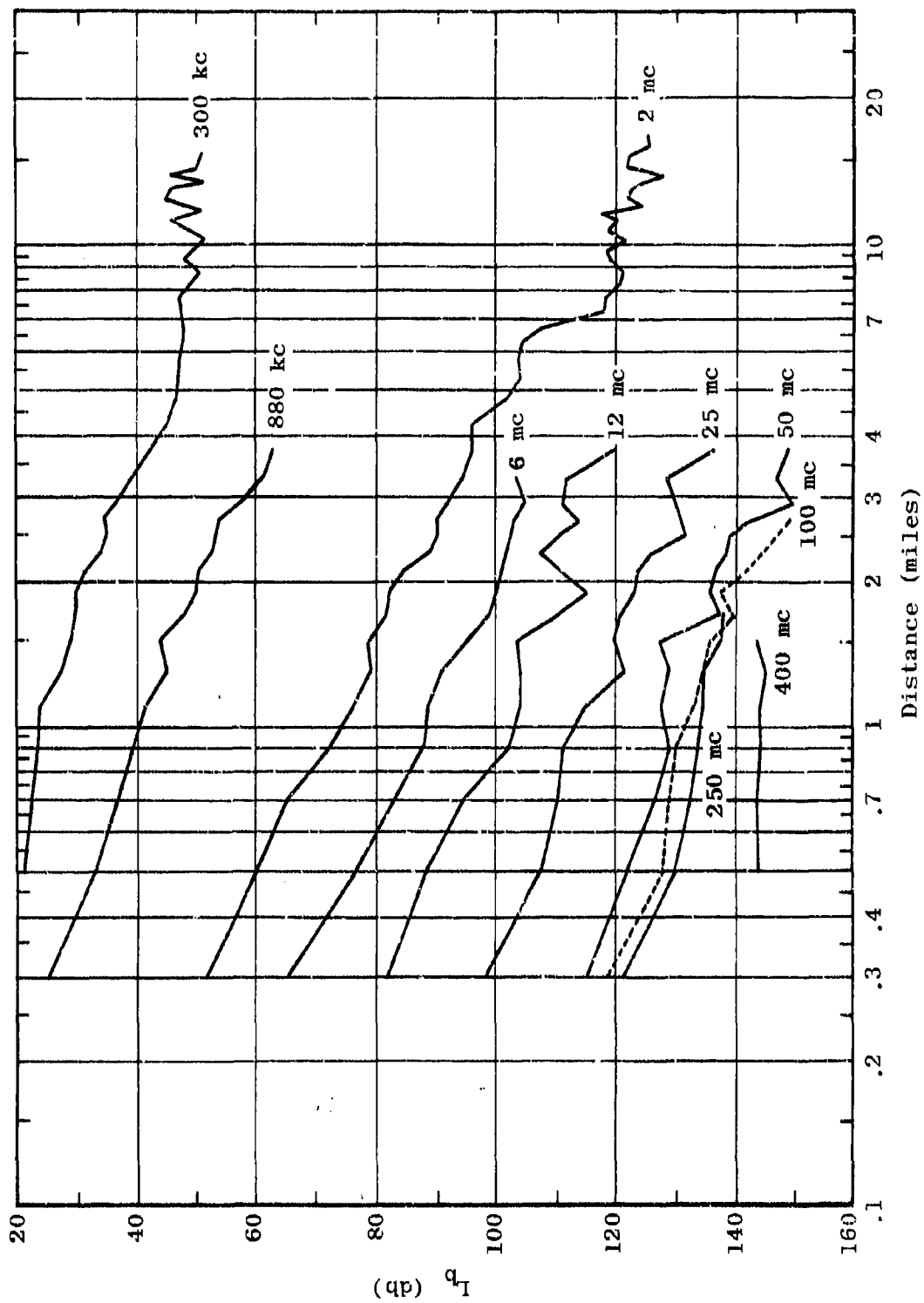


Figure 4.2 Summary of Basic Transmission Loss vs Distance for Vehicular Data.
 $L_b = F_A(f, 13, V, d, 7)$

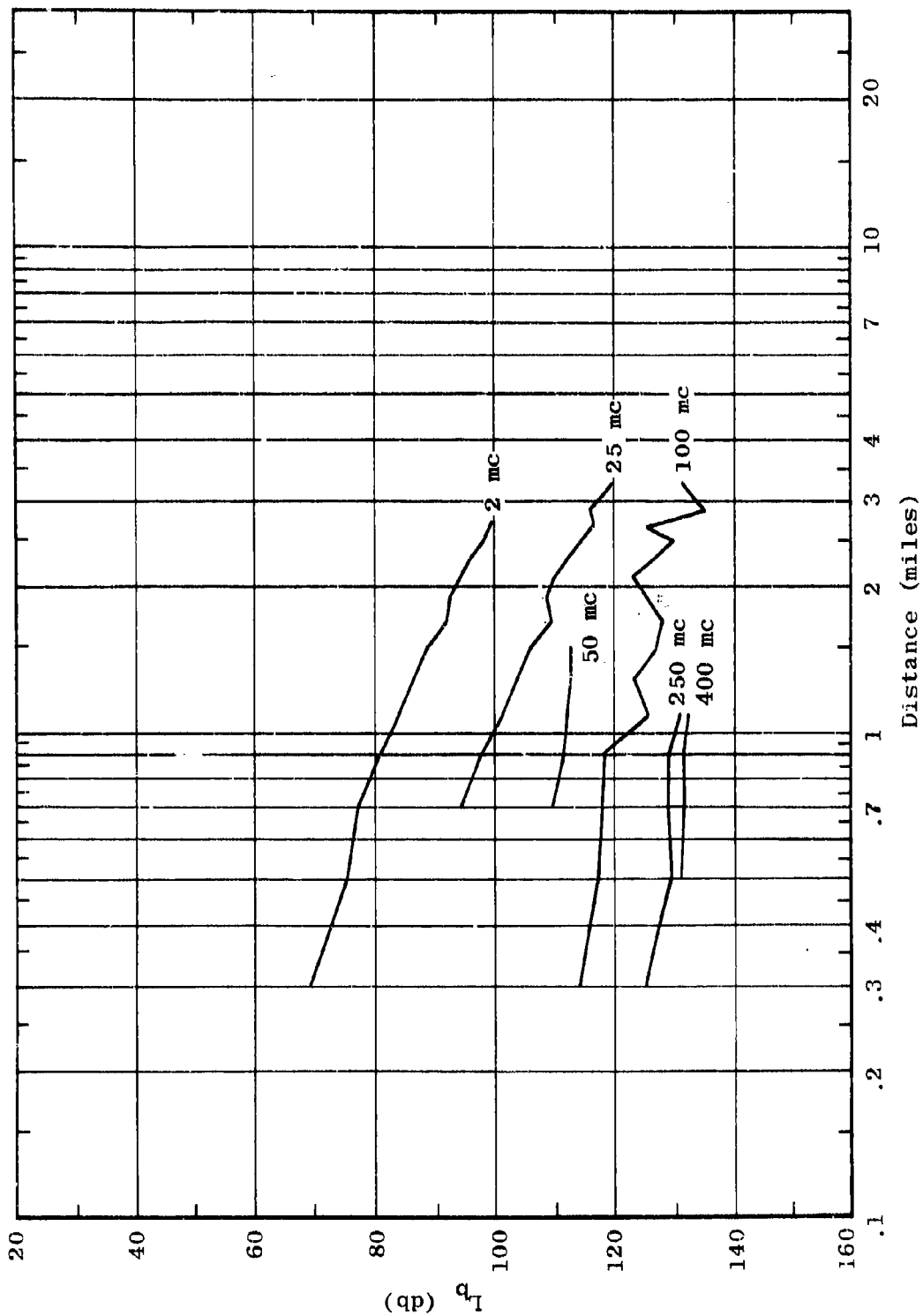


Figure 4.3 Summary of Basic Transmission Loss vs Distance for Vehicular Data
 $L_b = F_A(f, 13, H, d, 7)$

fixed-point data which corresponds to the vehicular data shown in Figure 4.2 is plotted in Figure 3.50. Similarly, Figure 4.3 is to be compared with the data plotted in Figure 3.52. In general, the vehicular data tends to follow the same fall-off with distance as was observed for the fixed-point data. The fixed-point data in Section 3.2 corresponds to a slightly greater receiving antenna height than the vehicular data given in Figures 4.2 and 4.3. Specifically, the receiving antenna height for the fixed-point data is 20 feet and the receiving antenna height for the vehicular data is approximately 7 feet.

At 2 mc for vertical polarization, it can be seen that the fixed-point data and the vehicular data are approximately the same. This observation further confirms the conclusion that there is no height gain for vertical polarization at 2 mc. However, for horizontal polarization, there is a significant difference between the vehicular losses and the fixed-point losses. This confirms the height gain at 2 mc for horizontal polarization which was observed in the fixed-point data. Due to the height gain for horizontal polarization and the lack of height gain for vertical polarization, the basic transmission losses for horizontal and vertical polarizations are more nearly equal in the vehicular data than in the fixed-point data. However, in both cases the losses are greater for horizontal polarization.

At 25 mc, the vehicular data shows that horizontal polarization is better by a margin of 18 db, which is consistent with the conclusions that were drawn from the fixed-point data and is summarized in Section 3.2 of this report. At 100 mc, the vehicular data indicates that horizontal polarization is better by 10 db, a conclusion which is

again consistent with the conclusions drawn from the fixed-point data. At 250 mc, there is only a small difference between horizontal and vertical polarizations for the vehicular data. One inconsistency between vehicular and fixed-point data shows up in the 400-mc vertical data shown in Figure 4.2. In this case, horizontal polarization shows a loss which is 10 db lower than that for vertical polarization at 400 mc. This observation is not consistent with the conclusion that there is very little difference between horizontal and vertical polarization at 400 mc based on fixed-point data. Obviously, the 400-mc data shown in Figure 4.2 is being carefully checked.

The data plotted in Figures 4.2 and 4.3 was obtained by plotting the median values from each of the 0.2- and 0.5-mile data sampling intervals. The variability in the medians is small at the close distances but is great at the farther distances. This observation is consistent with the data variability that is seen in the fixed-point data plotted in Section 3.1 of this report.

A great deal of propagation information can be obtained by studying smoothed curves of the type shown in Figures 4.2 and 4.3. A thorough study of a vehicular recording taken at 100 mc with vertical polarization will be described below.

At 100 mc, for distances greater than 0.2 mile, both the fixed-point data and the vehicular data have indicated a $40 \log d$ increase in loss with distance. The conclusion thus far has been that the significant deviations from this slope are probably due to the effect of distinctive terrain obstacles. The $40 \log d$ increase in loss

suggests a diffraction-type mode across the treetops. Any direct modes at the higher frequencies would be highly attenuated by the presence of foliage. How great is this attenuation? Intuitively, it should be possible to detect some direct but highly attenuated mode, by measuring close enough to the antenna. This direct mode, if it exists, should fall off rapidly with distance until it becomes so weak that the $40 \log d$ mode is able to dominate.

Figure 4.4 is a plot of vehicular data, taken from a radial distance of 0.066 mile (350 feet) to 3 miles. The data was taken with an 80-foot transmitting antenna ($\lambda/2$ dipole) and a vehicular receiving antenna ($\lambda/2$ dipole) mounted about 7 feet above the ground. The frequency is 100 mc, and the polarization is vertical. The rapid and longer-term fluctuations have been factored from the data. The points plotted on Figure 4.4 are derived from measured data, and the solid curve represents a $40 \log d$ increase in loss with increasing distance. As the figure clearly shows, the data follows the $40 \log d$ curve, even as close as 0.066 mile! The deviation from the $40 \log d$ curve for distances greater than 1 mile is expected because of the presence of a terrain obstacle. As the fixed-point data has shown, as distance increased beyond 1 mile, the data fluctuates, but in general follows the $40 \log d$ curve at 100 mc.

The important point here is the $40 \log d$ relationship for the very close distances. This indicates that no direct mode is detectable, even as close to the antenna as 350 feet. It would be interesting to explore the region between 350 feet and the near-field far-field boundary of the antenna, which occurs at a distance of about 5 feet.

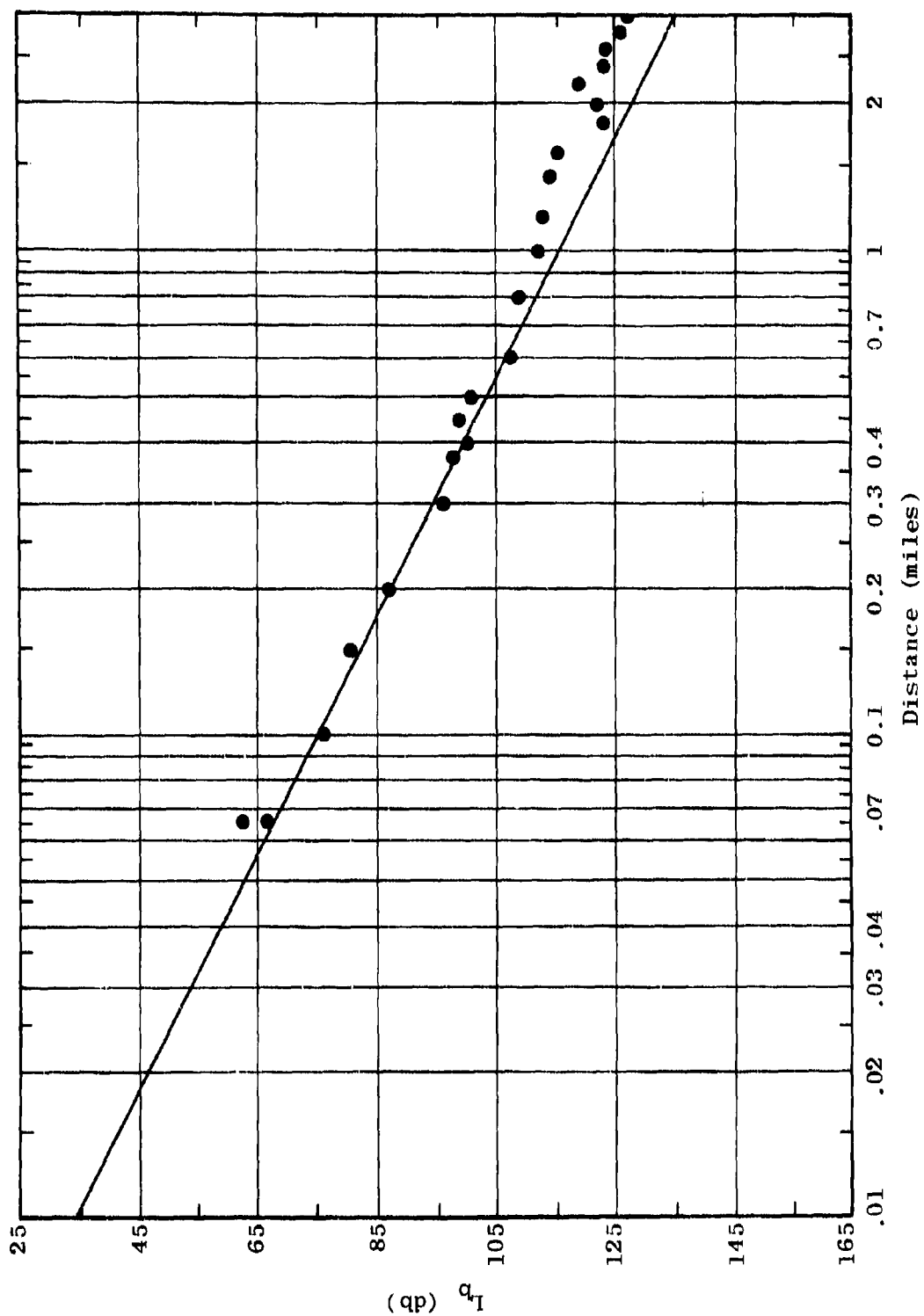


Figure 4.4 Median Basic Transmission Loss Near the Antenna
 $L_b = F_A(100.0, 80, V, d, 7)$

The double point at 0.066 mile is interesting. The lower point (higher loss) was taken on the trail, with foliage continuously present between the transmitting and receiving antennas. The upper point (less loss) was taken at the main gate of the transmitting compound. In this latter case, only about half the distance between the transmitting and receiving antennas is foliated.

4.2 Data Variability

An analysis of the rapid variation of field with small changes in distance is presented in Section 4.3.3 of Semiannual Report Number 6 and is summarized in Section 2.6.1 of this report. Table 17, below, provides a summary of the standard deviations which have been observed in each sampling interval analyzed to date. The standard deviations shown in Table 17 include the effects of both the rapid variation with distance and the less rapid variations with distance. The standard deviations in general vary considerably from one distance to another, but appear to have no consistent trend with increasing distance. The standard deviations tend to increase with increasing frequency and tend to be greater for vertical polarization except at 100 mc.

The total standard deviations, such as those shown in Table 17, are used to find individual standard deviations for the rapid variation and the less rapid, terrain-like variation.

The analysis at 100 mc indicates that the rapid variation (associated with foliage) has a standard deviation of 1 or 2 db. The terrain-induced variation has a standard

Table 17

STANDARD DEVIATION OF VEHICULAR
DATA FOR 13-FOOT TRANSMITTER ON RADIAL A

Pol.	Freq. (mc.)	Standard Deviation for Indicated Distance Interval (mi)															
		0.2 to 0.4	0.4 to 0.6	0.6 to 0.8	0.8 to 1.0	1.0 to 1.2	1.2 to 1.4	1.4 to 1.6	1.6 to 1.8	1.8 to 2.0	2.0 to 2.2	2.2 to 2.4	2.4 to 2.6	2.6 to 2.8	2.8 to 3.0	3.0 to 3.5	3.5 to 4.0
V	0.300	1.3	2.2	0.6	1.1	0.9	1.0	1.0	0.6	0.7	0.7	1.0	1.0	0.8	1.1	1.8	---
V	0.880	1.2	2.4	1.1	1.3	1.3	1.1	3.2	1.3	1.0	1.1	1.1	0.9	1.3	0.8	3.3	2.1
V	2.0	3.7	2.7	1.5	1.2	1.2	0.7	2.4	1.5	---	2.8	0.6	0.4	0.6	0.7	0.9	1.5
V	6.0	2.8	3.2	1.8	1.1	0.8	0.7	1.6	1.1	1.0	1.1	1.2	1.2	1.3	1.2	2.6	---
V	12.0	3.4	4.0	3.1	1.8	1.6	1.3	1.5	2.0	1.4	1.7	1.1	1.8	1.0	1.8	3.1	2.0
V	25.5	4.2	4.3	3.3	3.8	4.1	3.4	4.7	3.4	3.0	3.0	2.6	2.2	2.7	2.9	6.8	3.2
V	50.0	5.0	---	6.4	5.6	6.4	5.3	3.8	3.8	---	3.5	2.4	3.2	2.4	2.6	3.5	1.1
V	100.0	5.7	6.6	4.9	4.6	4.5	3.8	5.3	6.2	4.9	3.7	3.5	2.1	1.8	---	---	---
V	250.0	---	3.7	3.0	2.9	2.3	1.4	---	2.1	---	---	---	---	---	---	---	---
V	400.0	---	1.5	---	1.4	1.3	1.0	1.2	---	---	---	---	---	---	---	---	---
H	25.5	---	---	1.3	1.6	2.4	1.9	2.1	1.7	1.1	1.5	1.6	1.2	1.2	1.1	1.8	1.8
H	50.0	---	---	2.3	1.7	1.2	0.8	1.0	---	---	---	---	---	---	---	---	---
H	100.0	4.7	6.2	7.0	5.5	5.6	4.1	4.3	5.4	4.2	4.5	8.8	4.4	5.4	4.9	5.5	---
H	250.0	3.9	1.2	1.3	1.3	0.6	0.7	---	---	---	---	---	---	---	---	---	---
H	400.0	---	1.1	0.9	0.6	0.5	---	---	---	---	---	---	---	---	---	---	---

deviation which ranges from 0 to 6 db but is most typically about 4 db at 100 mc. Hence, it is seen that, although the foliage variation is rapid, its magnitude at 100 mc is considerably smaller on the average than the longer-term terrain variation.

Figures 4.5A through C provide a plot of the less rapid variation with distance at 100 mc for vertical polarization on Sector A. The distance scale used in Figure 4.5 represents actual trail distance. Table 18 provides a sample of the correlation between actual trail distance from the transmitter compound and radial distance between antennas.

Table 18

RADIAL DISTANCE VS TRAIL DISTANCE

<u>Trail Distance (Miles)</u>	<u>Radial Distance (Miles)</u>
0.030	0.066
0.053	0.066
0.11	0.10
0.16	0.15
0.21	0.20
0.31	0.29
0.32	0.30
0.41	0.37
0.46	0.40
0.53	0.44
0.61	0.50
0.75	0.52
1.03	0.71

In Figure 4.5 the rapid variation has been factored out, leaving only the less rapid variation in loss with distance. As this figure shows, there is only slight variation very close to the transmitting antenna. Then, there is a fairly regular variation out to about 1 mile. Between 1 and 2 miles, there is an unusual variation associated with the distinctive terrain obstacle present at that range. Beyond 2 miles, the variation is relatively regular with a few large peaks or nulls which appear to be associated with major terrain features.

The less rapid variation occurs at a rate of about 350 feet per cycle at 100 mc. The more rapid variation occurs at a rate of about 20 feet per cycle.

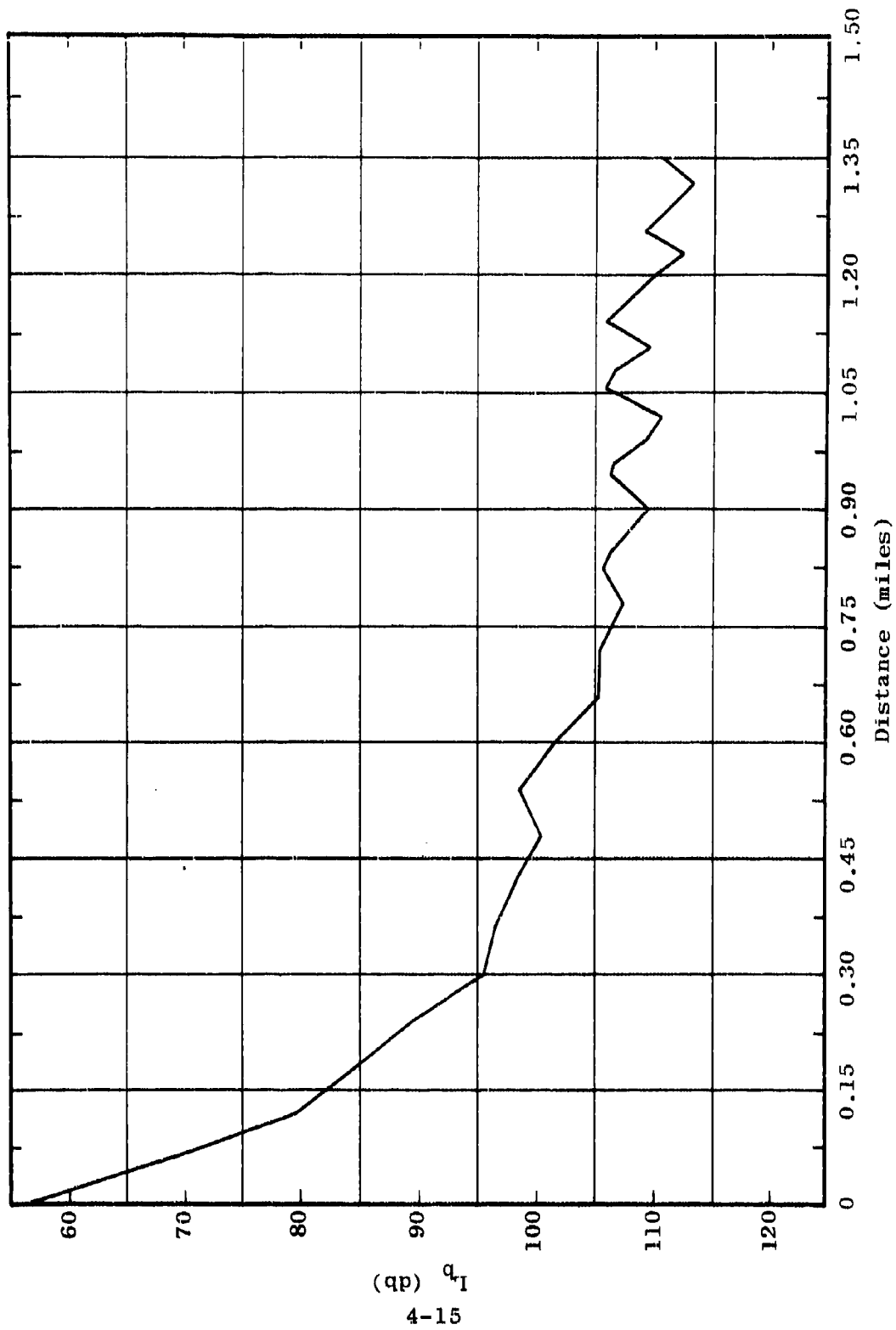


Figure 4.5 (Part A) Median Basic Transmission Loss from Vehicular Data
 $L_b = F_A(100.0, 80, V, d, 7)$

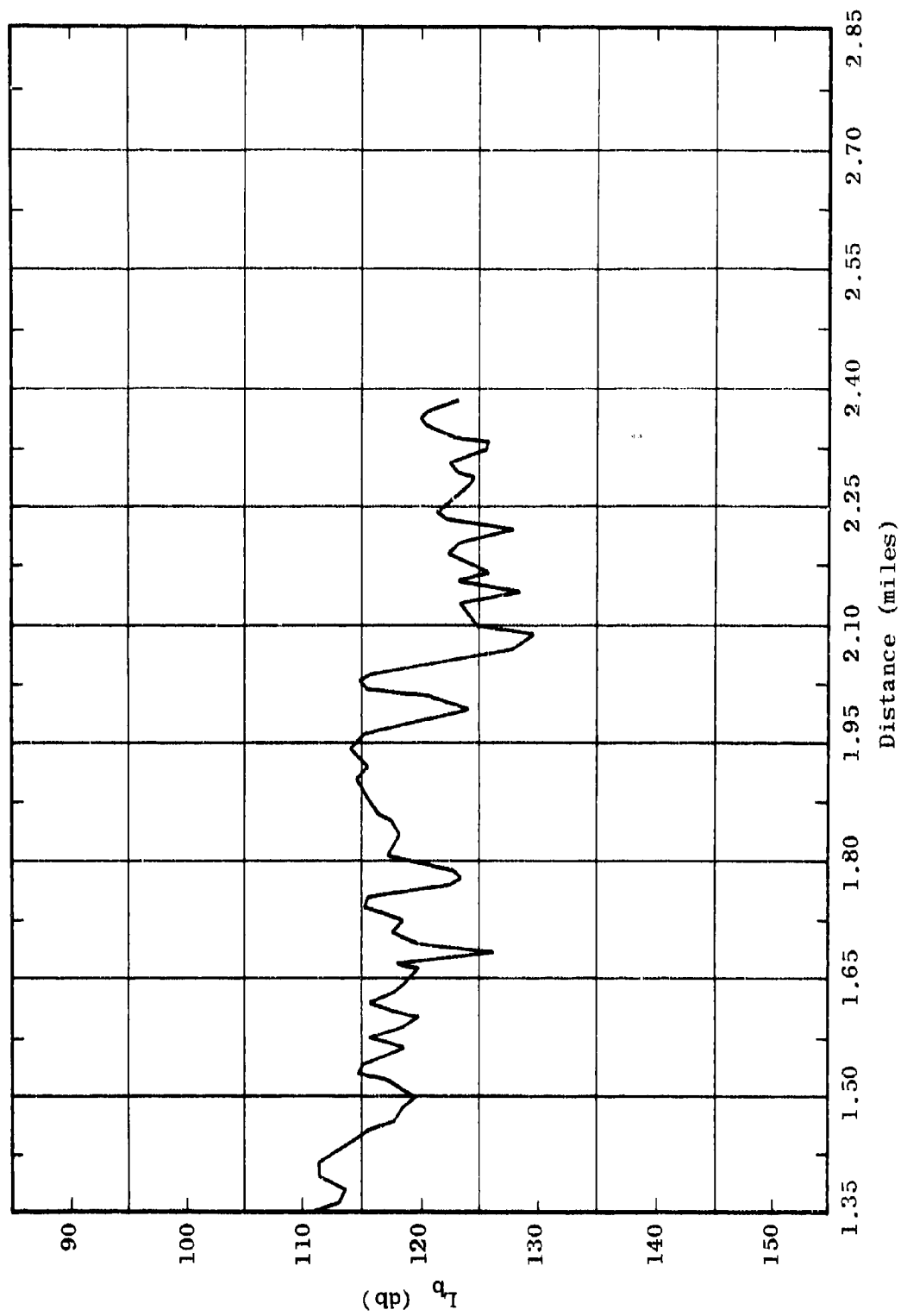


Figure 4.5 (Part B) Median Basic Transmission Loss from Vehicular Data
 $L_b = F_A(100.0, 80, V, d, 7)$

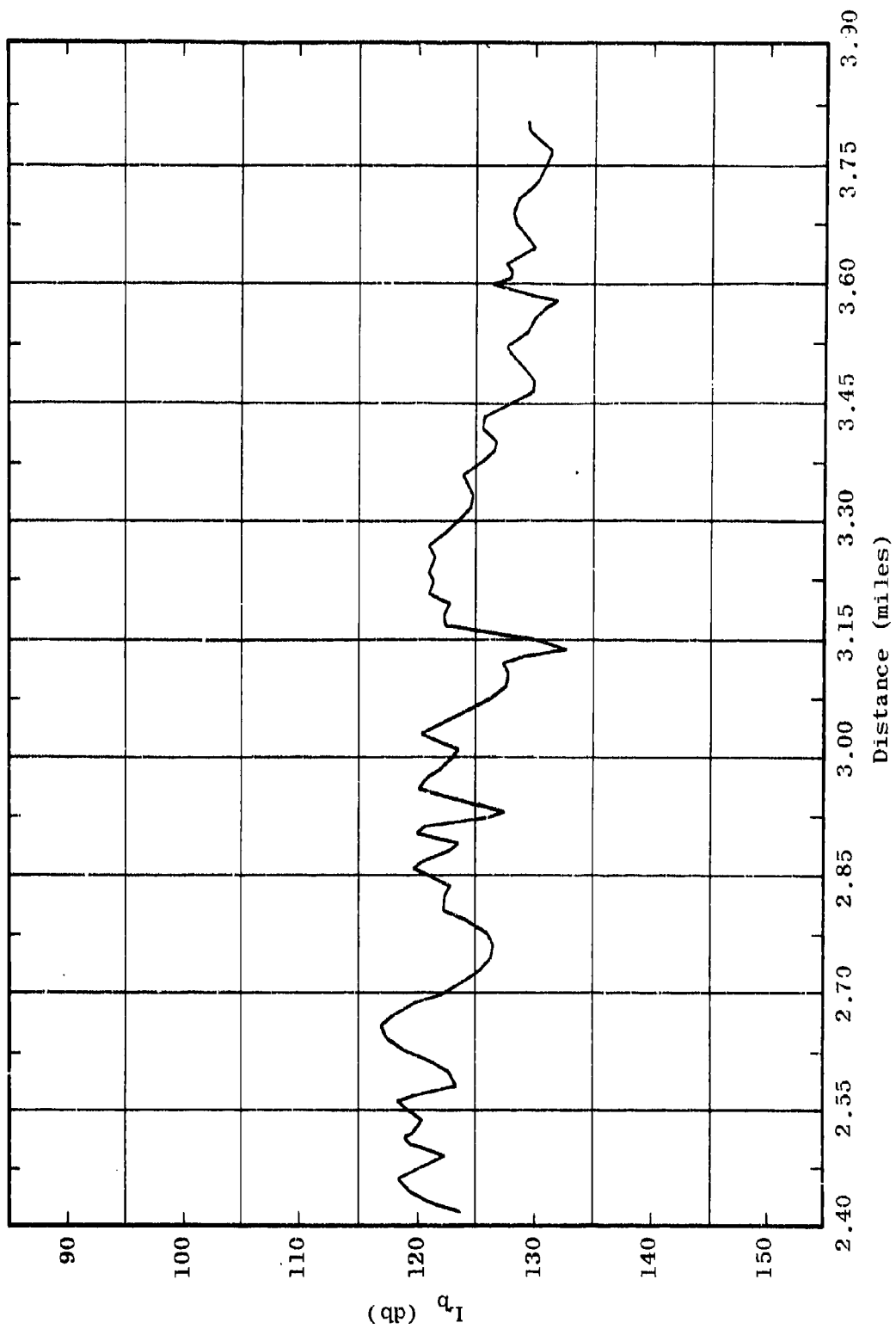


Figure 4.5 (Part C) Median Basic Transmission Loss from Vehicular Data
 $L_b = F_A(100.0, 80, V, d, 7)$

(qp) q_1

5. CLIMATOLOGICAL DATA

The effects of climatic phenomena on radio propagation loss vary as functions of spatial parameters and the time. These effects are generally related to the influence of the climate on the dielectric constant of the atmosphere in the propagation path, and, more indirectly, to its influence on the electrical properties of the ground and vegetation in the path. Also, the degree of these effects will depend upon frequency, the separation distance, and the directivity of the antennas. Although the cause-effect relationships are well understood from a phenomenological view, it is generally not possible to reduce any given practical situation to a mathematically analytical state. Therefore, the study of the influence of the climate on radio path loss must first rely on the techniques of statistical correlation. In order to provide a base of climatic data for an examination of the various correlations between climatic conditions and path loss, climatological data has been taken on a daily basis since the beginning of the measurement program in Thailand.

Data on hand covers the period of February 1964 to November 1965 and represents four types of measurements: (1) wet bulb temperature, (2) dry bulb temperature, (3) barometric pressure, and (4) rainfall. The temperature and pressure readings were made at the base camp three times daily. Rainfall samples were taken three times a day at the base site prior to March 1965, when automatic rain gauge recorders were installed at five different locations in the test area to provide continuous monitoring of the cumulative rainfall.

All rainfall sampling points are either in Sector A or Sector B, where the field strength measurements are taken. Figure 5.1 shows the general locations of the sampling points. The monthly cumulative rainfall at each of the measurement points is shown in Table 19. This table also shows the monthly average rainfall for Sector A and Sector B individually as well as the over-all average for all five measurement points.

The unusually high rainfall recorded at FPB-10 deserves special notice. This recording point is on the north slope of a ridge of a mountain known as Khao Khieo. The mountains and ridge are some 1200 meters above sea level and the recording point is about 440 meters lower. Because the ridge system runs in a northeasterly direction, it effectively shelters the recording site from the prevailing due-east wind in this region. Thus, a low-pressure system can be expected to prevail over the recording point, promoting a high rainfall. The data from this point is also indicative of the wide variation in climatic data that is typical of regions with steep mountains and ridges.

The characterization of the climate in the Pak Chong area for radio propagation purposes presents difficulties in that there is still some uncertainty as to the proper weighting of the FPB-10 samples. Further study of this matter is necessary.

Figure 5.2 presents a comparison of certain significant factors of interest. Only data collected at the base camp was used in this figure. The lower curve gives the monthly cumulative rainfall recorded at the base site,

and the upper curves show monthly averages of the other parameters considered as factors likely to affect path loss.

Averaging values on a monthly basis provides a degree of smoothing suitable for visual comparison. Data similar to that shown in Figure 5.2, but averaged on a weekly basis, was presented in Semiannual Report Number 6. The parameter k , shown in Figure 5.2, is the effective earth's radius as derived from computed values of surface refractivity. Surface refractivity values, in turn, are derived from measurements of atmospheric pressure, wet bulb temperature and dry bulb temperature. Vertical profiles of refractivity for heights ranging from about 70 to 1000 feet have been obtained in the Sector B area. The results of these measurements are presented in Section 7 of this report.

The climatological data presented in Semiannual Report Number 6 and the data in this report are intended to serve basically as a quantitative measure of the climatic parameters with which to study the correlation between variations in these parameters and measured radio path loss. A computerized program to show the correlation between path loss variations and climate changes is under way. Correlations using data on cumulative rainfall as an input are now being made, and the results are summarized in Section 3.3 of this report.

Table 19

CUMULATIVE MONTHLY RAINFALL (INCHES)

Year	Month	Base Site	Sector A		Sector B		Sector A Avg.	Sector B Avg.	Avg. All 5 Meas. Pts.
			Pt. Alfa	FPA-10	FPB-15	FPB-10			
1964	Feb	0.22							
1964	Mar	2.92							
1964	Apr	7.31							
1964	May	11.66							
1964	June	0.23							
1964	July	7.29							
1964	Aug	6.81							
1964	Sept	10.11							
1964	Oct	10.12							
1964	Nov	1.39							
1964	Dec	0.05							
1965	Jan	0.00							
1965	Feb	1.30							
1965	Mar	3.53	1.94*	2.11*	2.71*	1.53*	2.02*	2.12*	2.36*
1965	Apr	3.35	1.40	2.05	2.57	1.20	1.72	1.88	2.11
1965	May	8.88	8.17	10.31	7.02	18.51	9.24	12.76	10.57
1965	June	3.24	5.06	8.02	5.60	32.67	6.54	19.13	10.91
1965	July	2.78	1.65	3.73	2.66	10.60	2.69	6.63	4.28
1965	Aug	6.73	8.75	11.32	9.43	24.09	10.03	16.76	12.06
1965	Sept	11.28	12.88	12.54	14.13	14.27	12.71	14.20	13.02
1965	Oct	5.55	9.62	4.98	5.20	7.61	7.30	6.40	6.59

Note: Unattended recording equipment not available during this period.

Note: Unattended recording equipment not available during this period.

* Data accumulation began March 10, 1965.

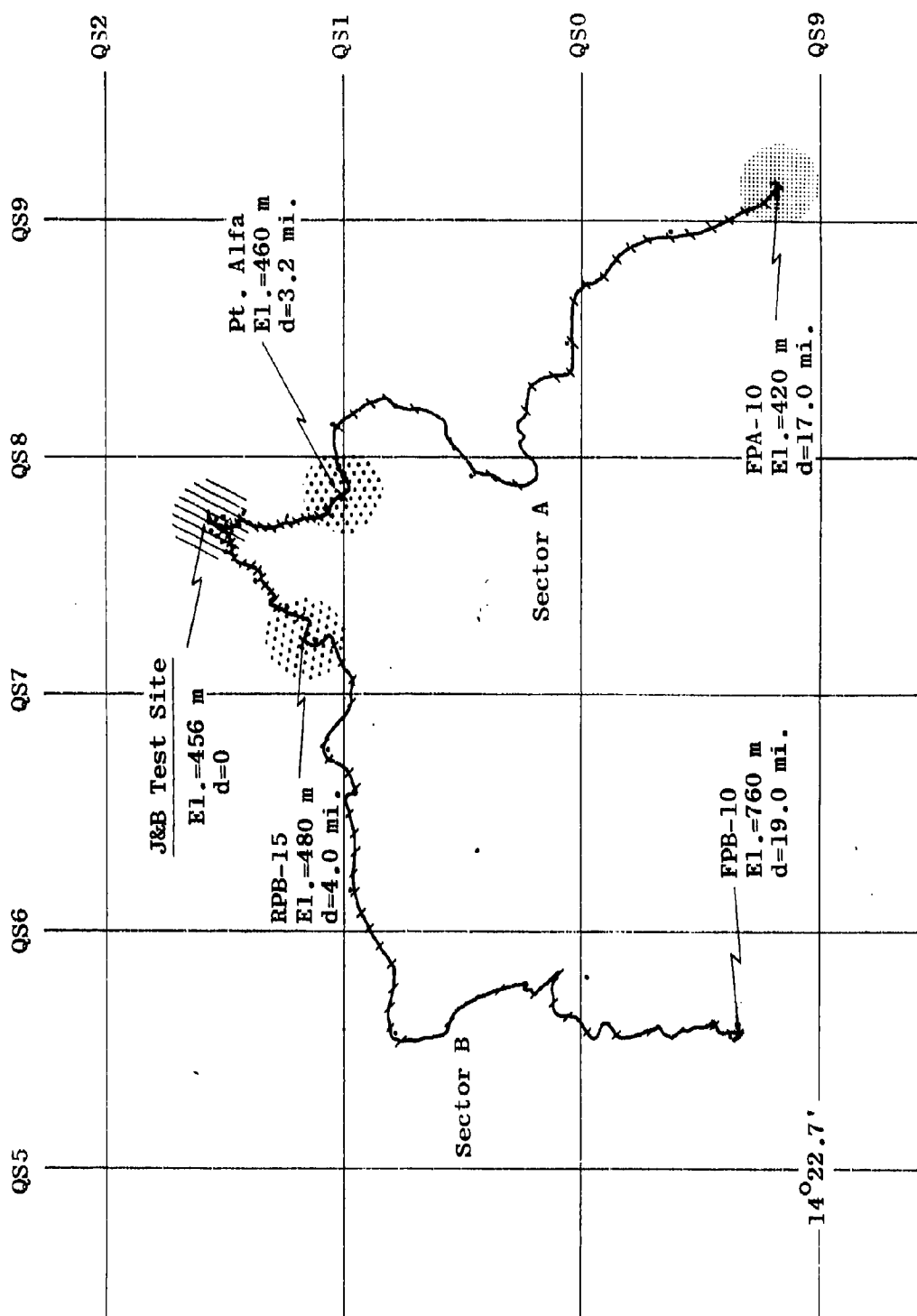


Figure 5.1 Rainfall Measurement Points

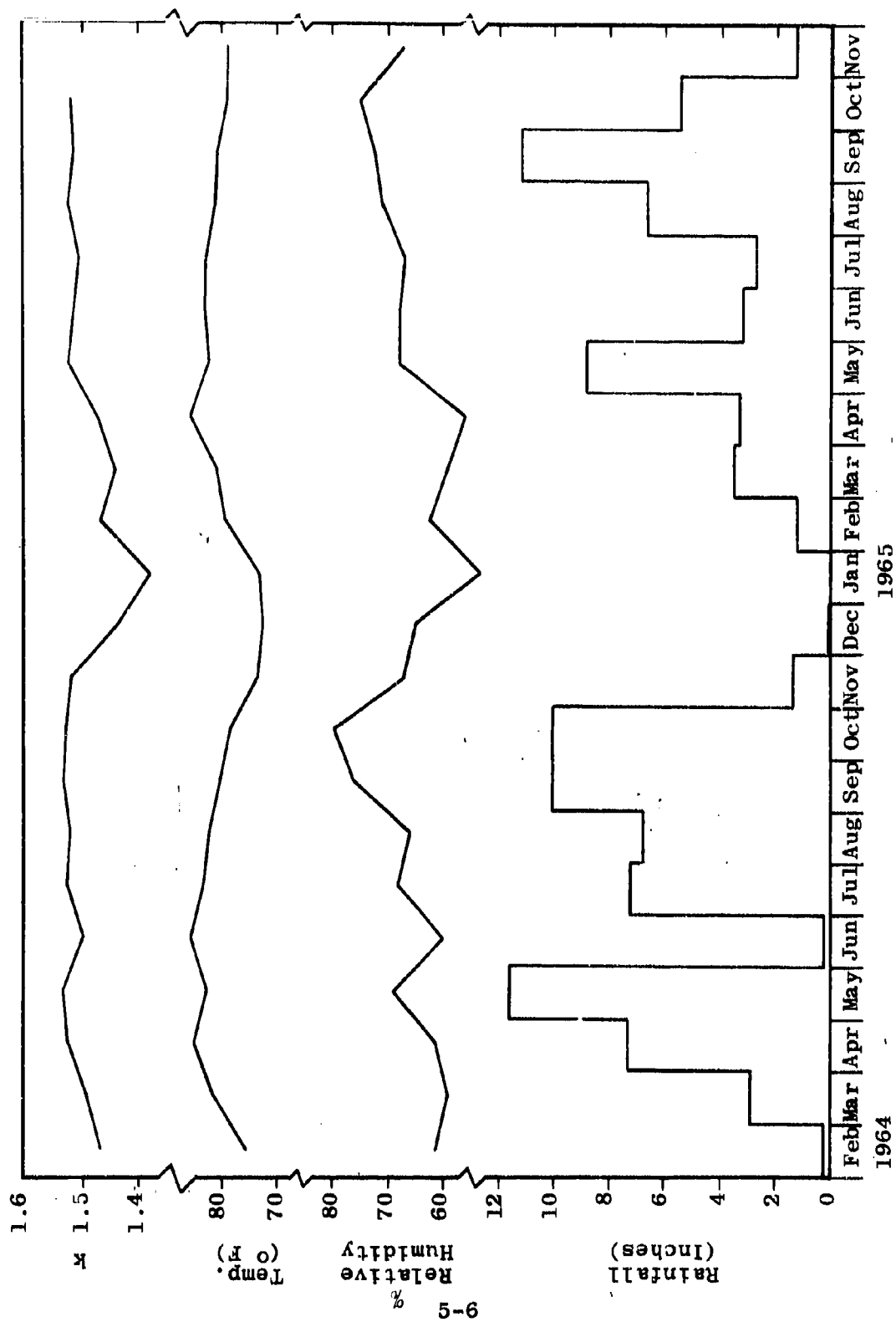


Figure 5.2 Climatological Data

6. 10-GC MEASUREMENT PROGRAM

One phase of the Thailand propagation study program is concerned with measurements in the frequency range from 550 to 10,000 mc. Within this phase, one series of measurements is being conducted to study the transmission loss characteristics for the line-of-sight, point-to-point mode of radio propagation over a well-defined obstacle in the form of a foliated ridge. The results of these measurements are intended to be applied to the design and operation of point-to-point relay systems over heavily vegetated paths.

The second series of measurements has been designed to yield basic data on the propagation of microwaves directly through the jungle vegetation. These measurements are being conducted at about 2.5, 5, and 10 gc. At these frequencies, the high attenuation of the foliage necessarily limits the distance range of these measurements to a few hundred yards. The purpose of these measurements is to study the transmission loss and scattering characteristics that would apply to the performance of short-range microwave systems where at least one terminal is to be operated inside the vegetation.

The techniques and equipments used to make these measurements are described in the 10-gc Primary Field Test Plan and Semiannual Report Number 6. To compare measurements in two different Thailand environments, two areas have been selected. The first area, designated as Area A, is in the vicinity of the main Jansky & Bailey field site near Pak Chong. The second area, designated as Area B, is in southeastern Thailand near the town of Rayong.

The measurements discussed in this section of the report were obtained in Area A. All Area A line-of-sight measurements were completed during this reporting period, and the results of these measurements are summarized in this section. These measurements have been made at frequencies of 0.55, 1, 2.5, 5, and 10 gc.

6.1 Path Characteristics

The line-of-sight path in Area A was selected on the basis of the following specifications:

- (1) First Fresnel zone clearance between receiver and obstacle. Fresnel zones are discussed in Section 6.2.
- (2) A well-defined foliated obstacle approximately equidistant from transmitter and receiver.
- (3) A receiver site which would provide a sufficient number of receiver locations to obtain an adequate range of v values. The parameter v is discussed in detail in Section 6.2.

The paths selected for Areas A and B are shown on a topographical map in Semiannual Report Number 6. The terrain profile for Path A, taken from a detailed map of the area, is shown in Figure 6.1. As shown in this figure, there are two transmitter locations, designated T1 and T2. At the receiving end of the path there are nine receiver locations, designated R1 through R9. The elevation of each receiver and transmitter location relative to the main

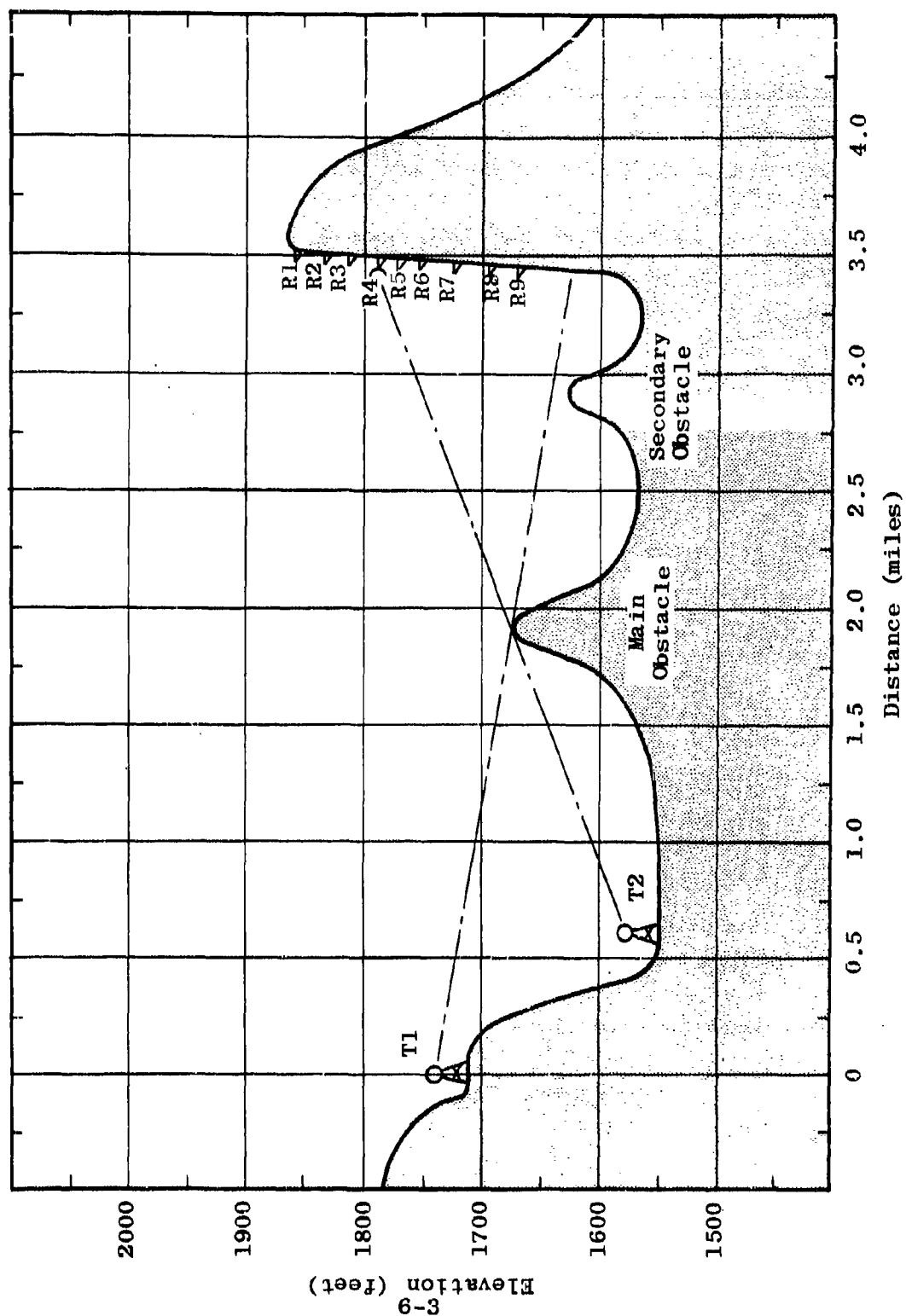


Figure 6.1 Line-of-Sight Profile for Area A

obstacle and also relative to mean sea level is shown in Table 20. These relative elevations were determined by a precision altimeter capable of detecting elevation changes of less than 1 foot.

The transmitter-receiver locations were selected to obtain a wide range of v values as specified in item 3 above. A given transmitter-receiver combination yields a particular value of v . For this same combination, v varies with frequency. Thus, for five test frequencies, two transmitters and nine receivers, a total of 90 values of v is possible. These values are shown in Table 21 for the frequencies being used in the line-of-sight tests. It should be pointed out, however, that tests were not conducted for all v values shown in the table since the power output of the microwave sources was not sufficient to obtain measurements for positive values of v greater than about +2.5.

The amount of loss suffered by diffraction over an obstacle depends to a certain degree upon the shape of the obstacle. Attempts were made to select an obstacle which most closely resembled a knife edge. However, due to the limited number of paths, the obstacle chosen deviates significantly from what would be considered a "perfect" knife edge.

Details of the obstacle are shown in Figure 6.2. The length of the obstacle, in the direction of the line-of-sight rays, is about 547 feet. Cross-sectional cuts are also shown on this figure, along with a plot of the first Fresnel radius at the obstruction. The top of the ridge is covered with fairly dense trees and undergrowth, quite

Table 20

RECEIVER AND TRANSMITTER ELEVATIONS RELATIVE
TO SEA LEVEL AND RELATIVE TO MAIN OBSTACLE

<u>Location</u>	<u>Elevation Above Sea Level (ft)</u>	<u>Elevation Relative to Main Obstacle (ft)</u>
Main Obstacle	1676.0*	0
R1	1860.0	+184.0
R2	1834.1	+158.1
R3	1813.3	+157.3
R4	1789.1	+113.1
R5	1772.8	+ 96.8
R6	1753.6	+ 77.6
R7	1724.0	+ 48.0
R8	1698.6	+ 22.6
R9	1672.4	- 3.6
T1	1738.0	+ 62.0
T2	1578.0	- 98.0

* Elevation of main obstacle includes tree height.

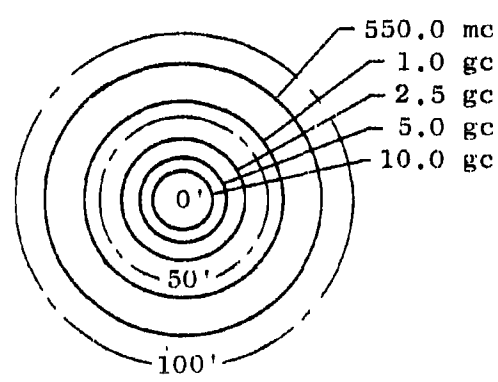
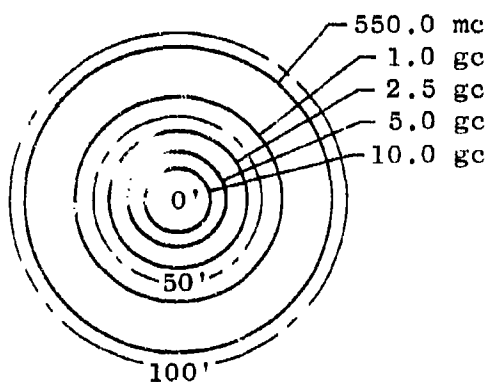
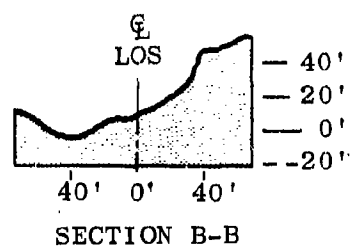
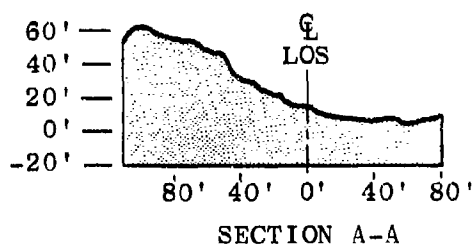
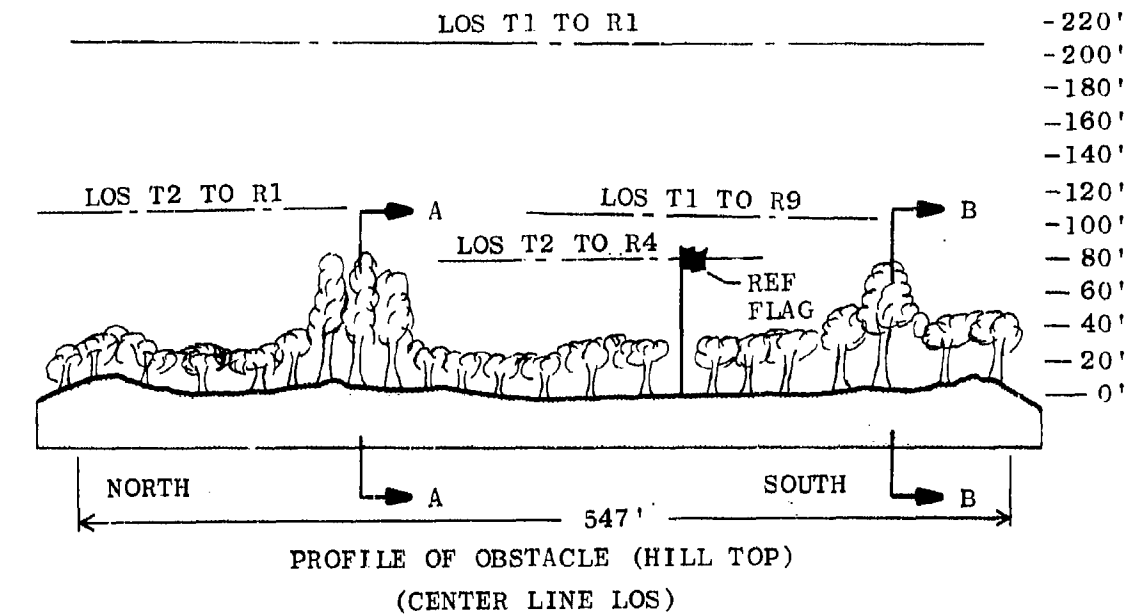
Table 21

PARAMETER V FOR ALL T-R COMBINATIONS

Rec	550 mc		1 gc		2.5 gc		5.0 gc		10.0 gc	
	T1	T2	T1	T2	T1	T2	T1	T2	T1	T2
R1	-2.0	-0.5	-2.7	-0.6	-4.3	-1.0	-6.1	-1.5	-8.6	-2.1
R2	-1.9	-0.3	-2.5	-0.4	-3.9	-0.7	-5.6	-1.0	-7.9	-1.4
R3	-1.7	-0.2	-2.2	-0.3	-3.5	-0.4	-5.0	-0.6	-7.0	-0.9
R4	-1.5	-0.03	-2.0	-0.05	-3.1	-0.07	-4.4	-0.1	-6.2	-0.1
R5	-1.3	-0.2	-1.8	0.2	-2.8	-0.4	-4.0	0.5	-5.6	0.7
R6	-1.2	0.3	-1.6	0.4	-2.5	-0.6	-3.5	0.8	-5.0	1.1
R7	-0.9	0.4	-1.2	0.6	-1.9	-0.9	-2.8	1.3	-3.9	1.8
R8	-0.5	0.7	-0.7	0.9	-1.1	1.5	-1.6	2.1	-2.3	2.9
R9	0.4	0.9	-0.6	1.3	-0.9	2.0	-1.3	2.9	-2.1	4.1

Note: Negative sign denotes line-of-sight clearance.

Positive sign denotes obstructed line-of-sight.



FRESNEL AREAS AT OBSTACLE

Figure 6.2 Physical Characteristics of Obstacle
6-7

similar to the area where short-range vegetated measurements are being conducted. The maximum tree heights in this area are approximately 80 feet. The reference flag shown on top of the obstruction in Figure 6.2 is used as a reference point for determining a v of zero. Notice that the elevation of the reference flag is the same as the largest tree heights. The values of v shown in Table 21 were computed using distance values obtained from a topographical map of the area. The influence of the "non-perfect" obstacle is discussed in Section 6.3, Line-of-Sight Data.

6.2 Theoretical Knife-Edge Diffraction

When the transmission path consists of a single diffracting knife edge, a first Fresnel ellipse can be constructed between each antenna and the single obstruction as shown in Figure 6.3. If terrain between either antenna and the obstruction penetrates this ellipse, the received field will be affected in a somewhat unpredictable fashion.

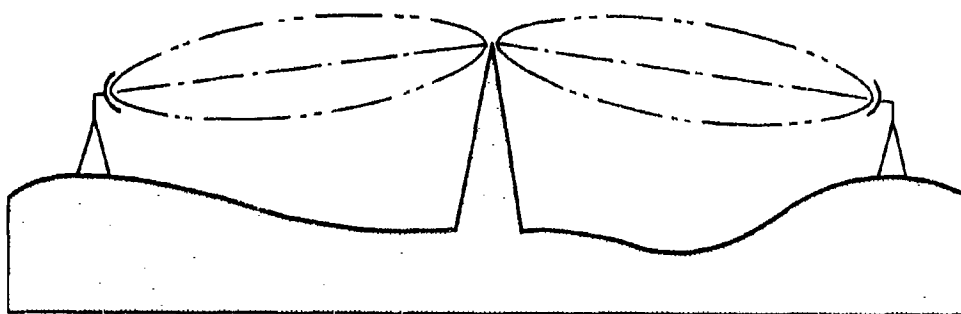


Figure 6.3 Knife-Edge Path with First Fresnel Zone Clearance

To provide a reliable theoretical model for comparison with measured data, the line-of-sight path was selected to provide first Fresnel clearance from both terrain and vegetation at both ends of the path.

For a perfect knife-edge path with Fresnel clearance, the theoretical basic transmission loss is given by

$$L_b = L_{bf} + A(v) \quad (3)$$

where

L_{bf} = free-space basic transmission loss (db)
 $A(v)$ = gain or loss due to diffraction over a perfect knife edge (db)

The function $A(v)$ is defined

$$A(v) = \frac{E}{E_o} \quad (4)$$

where

E = measured field strength at a given point
 E_o = free-space field which would exist at the same point

$A(v)$ can be written in complex form as

$$A(v) = a + jb \quad (5)$$

where a and b can be written in terms of the Fresnel integral as

$$a = \frac{1}{\sqrt{2}} \int_v^{\infty} \cos \frac{\pi v^2}{2} dv \quad (6)$$

$$b = \frac{1}{\sqrt{2}} \int_v^{\infty} \sin \frac{\pi v^2}{2} dv \quad (7)$$

$$v = H \left[\frac{2}{\lambda} \left(\frac{1}{r_1} + \frac{1}{r_2} \right) \right]^{\frac{1}{2}} \quad (8)$$

where

- H = height of obstacle
 - λ = wavelength
 - r_1 = distance between transmitter and obstacle
 - r_2 = distance between receiver and obstacle
- where each of the above has the same units.

The above integrals have been evaluated for a wide range of values of v, and the resultant curve is shown in Figure 6.4. From equation 4 it can be seen that when $A(v) = 0$ E is equal to E_0 , and free-space conditions exist. For increasing negative values of v, the received field oscillates about the free-space field in a damped fashion. Physically, increasing v in the negative direction is accomplished by raising the line-of-sight ray farther and farther above the obstacle from the line-of-sight path. A $v=0$ is obtained

when the obstruction just touches the line-of-sight ray between antennas. Positive values of v are produced when the knife edge obstructs the line-of-sight ray. For these cases, the received field is always less than the free-space field. This region is sometimes referred to as the "shadow" region or in terms of loss as "shadow" loss.

From equation 4, it is noted that $A(v)$ is a complex function whose magnitude and phase depend upon the value of v . Figure 6.4 gives the magnitude $A(v)$ and the phase relationship ϕ . The phase ϕ becomes an important factor when computing the received field with ground reflections but need not be considered for cases where ground reflections do not occur.

To permit easy computation of $A(v)$ with a digital computer, the following approximate expressions have been generated for various ranges of v .⁷

For $-1 \leq v \leq 0$

$$A(v) = 2.78 v'' + 9.95 v + 6.17 \quad (9)$$

For $0 \leq v \leq 3$

$$A(v) = 6.08 - 0.005 v^4 + 0.159 v^3 - 1.7 v^2 + 9.3 v \quad (10)$$

7. C.C.I.R. Study Groups, January 1965, p. III-15.

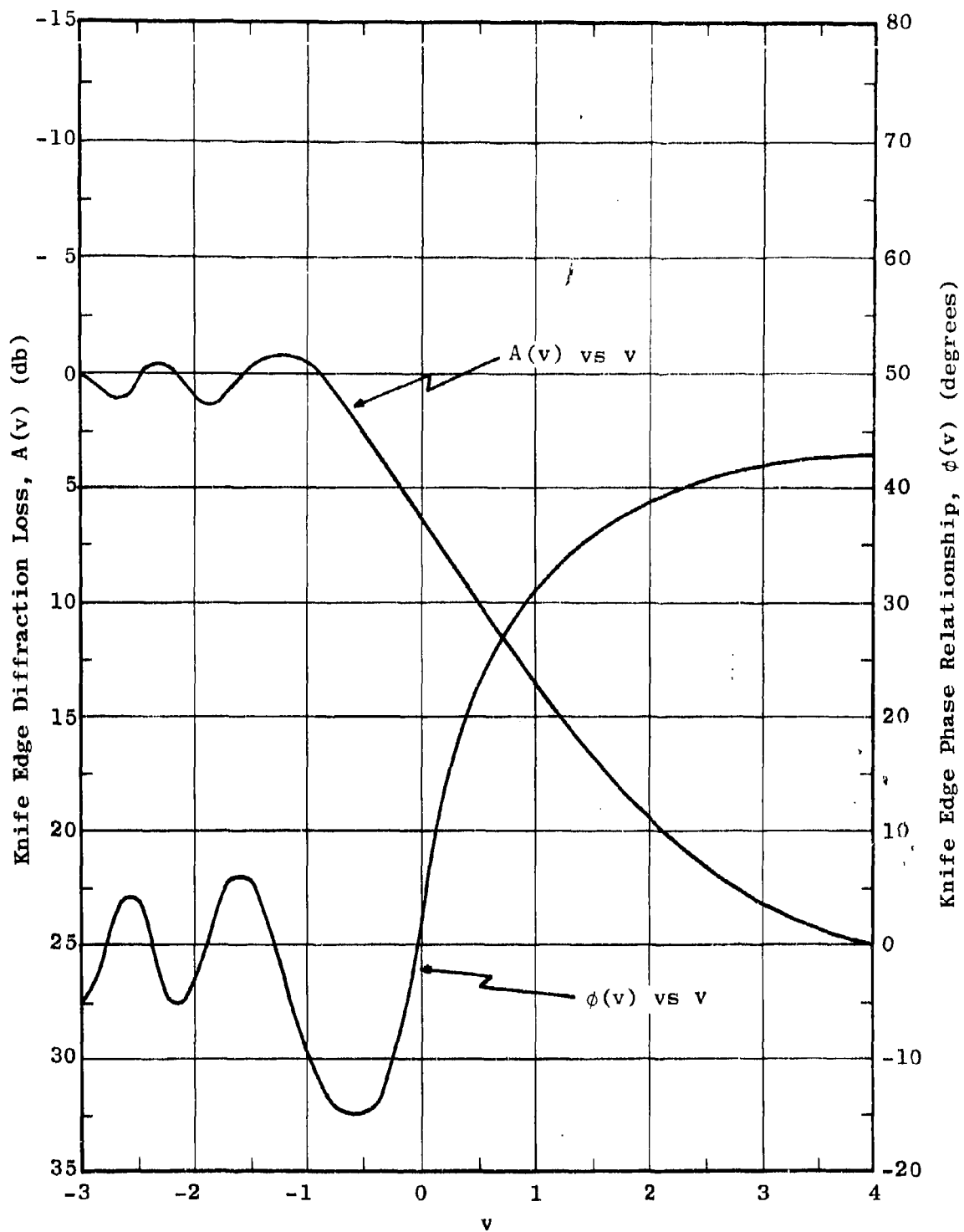


Figure 6.4 $A(v)$ and $\phi(v)$ vs v for Perfect Knife Edge
6-12

For $v > 3$

$$A(v) = 12.953 + 20 \log v \quad (11)$$

6.3 Line-of-Sight Data

The purpose of the line-of-sight test is to determine the effects of foliage on diffraction over an obstacle. Since there is first Fresnel zone clearance at each end of the path, it is assumed, neglecting the small degree of fading, that any deviation of the received field from the theoretical field produced by a perfect knife edge is due to the characteristics of the obstacle itself. Characteristics of the obstacle which are of primary importance are:

(1) foliage on the obstacle, (2) shape of the obstacle, and (3) finite conductivity of the obstacle. The relative importance of the above factors in a real situation is not usually known.

The measured values of $A(v)$ for the five test frequencies are shown in Figures 6.5 through 6.9. Shown also on each graph is the theoretical perfect knife-edge loss.

$A(v)$ measured is obtained as follows.

$$A(v) = L_b(\text{meas}) - L_{bf} \quad (12)$$

where

$L_b(\text{meas})$ = basic transmission loss derived from measurements

L_{bf} = free-space basic transmission loss

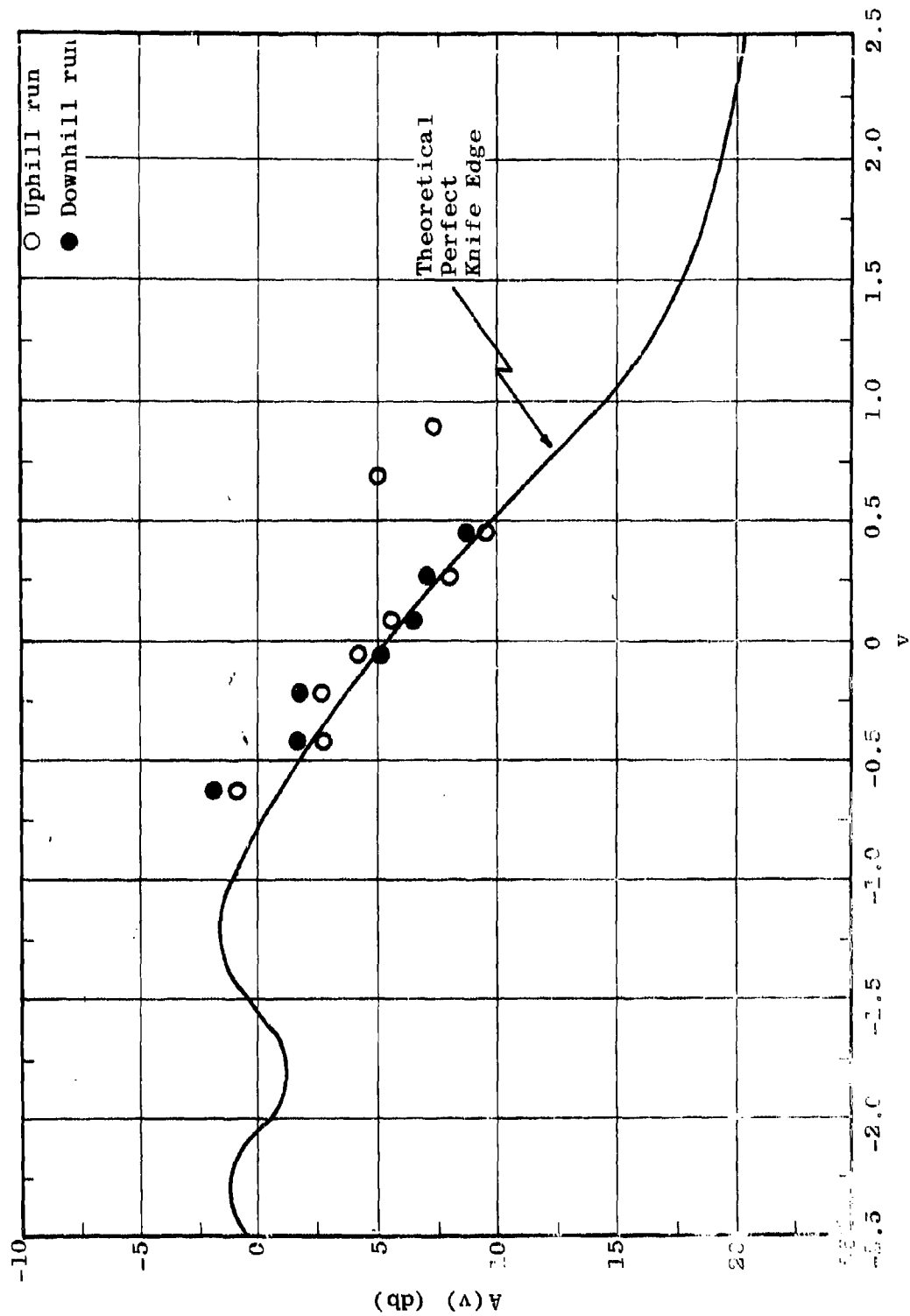


Figure 6.5 Measured Knife Edge Loss at 550 mc

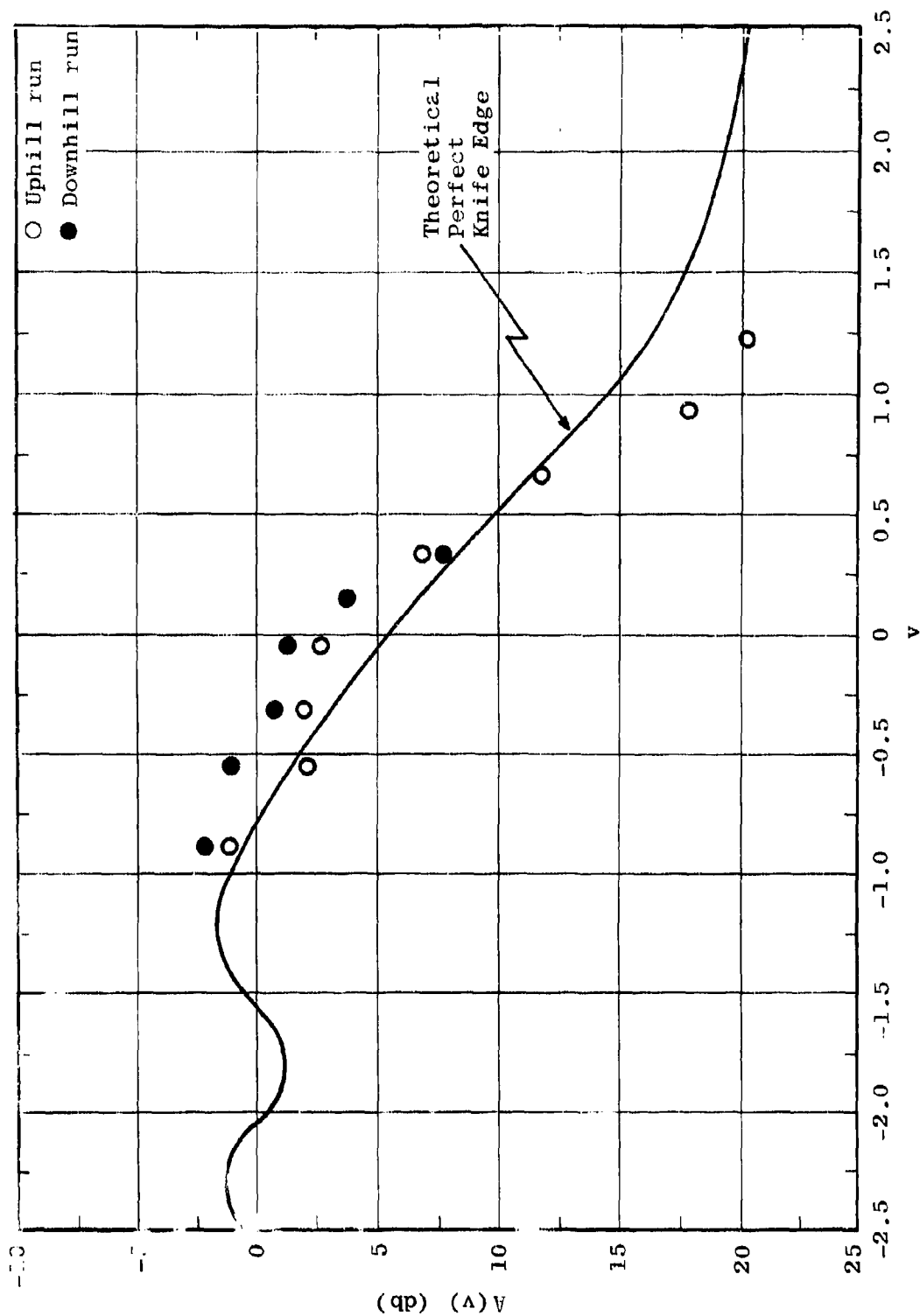


Figure 6.6 Measured Knife Edge Loss at 1.0 gc

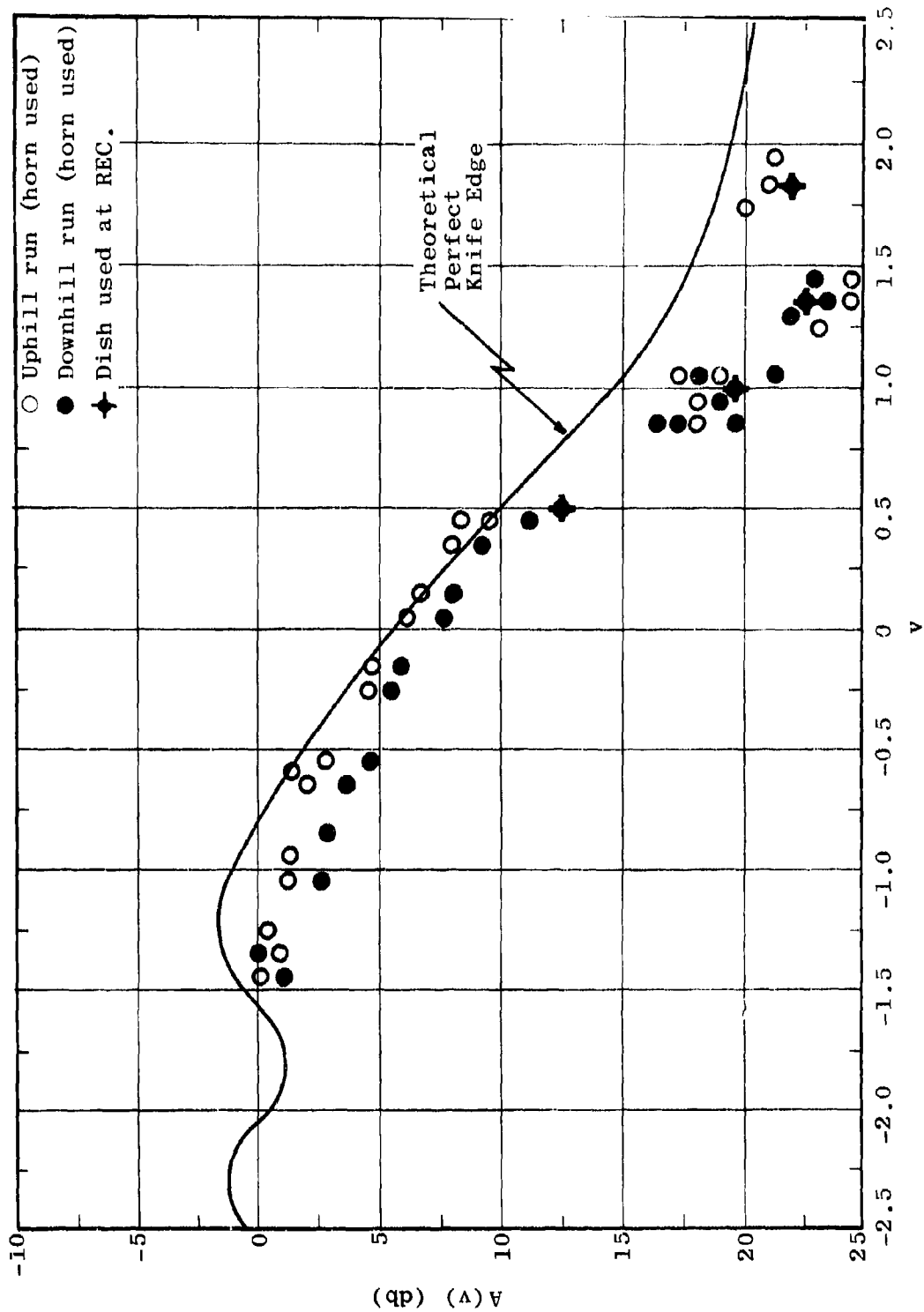


Figure 6.7 Measured Knife Edge Loss at 2.5 gc

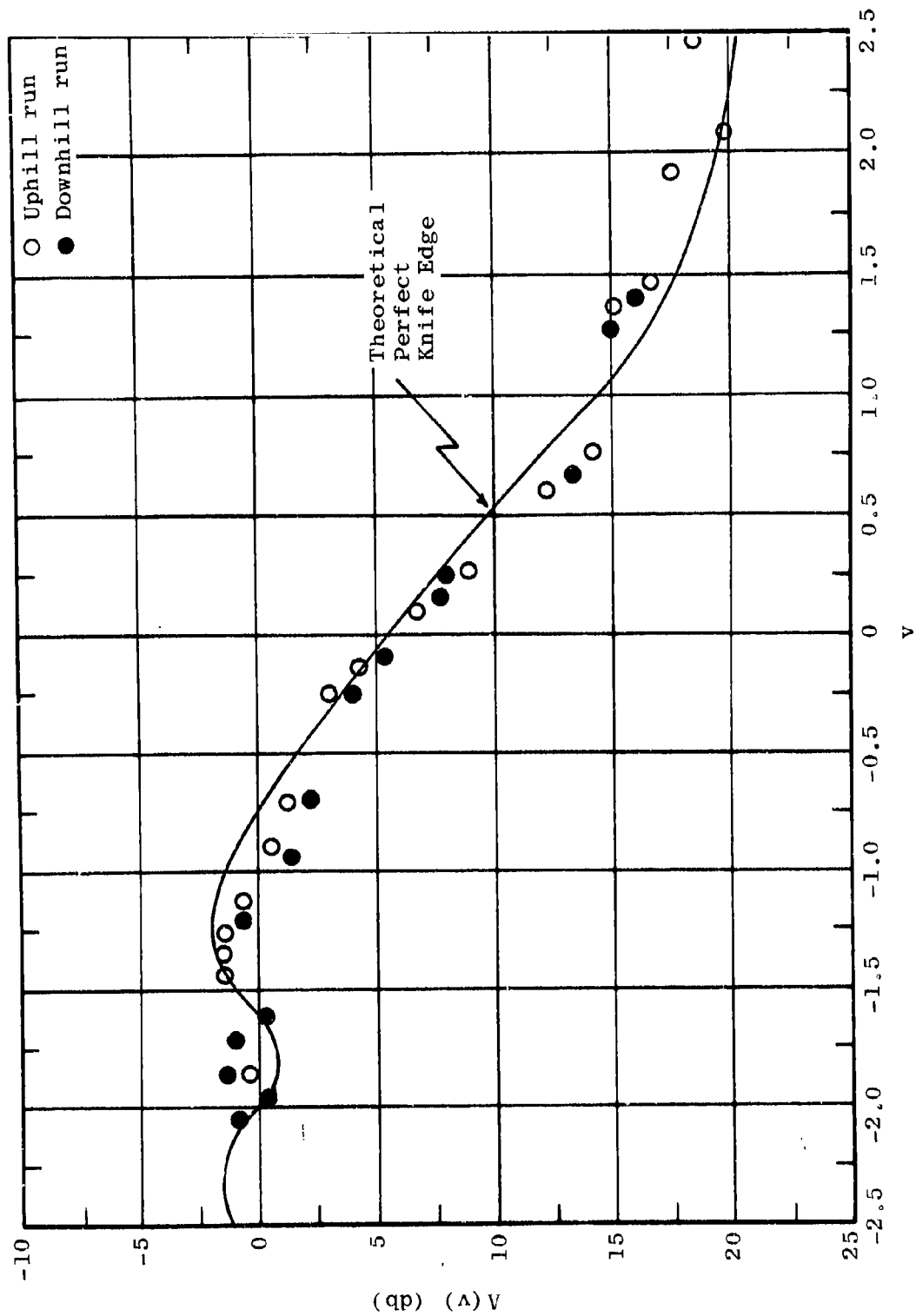


Figure 6.8 Measured Knife Edge Loss at 5.0 gc

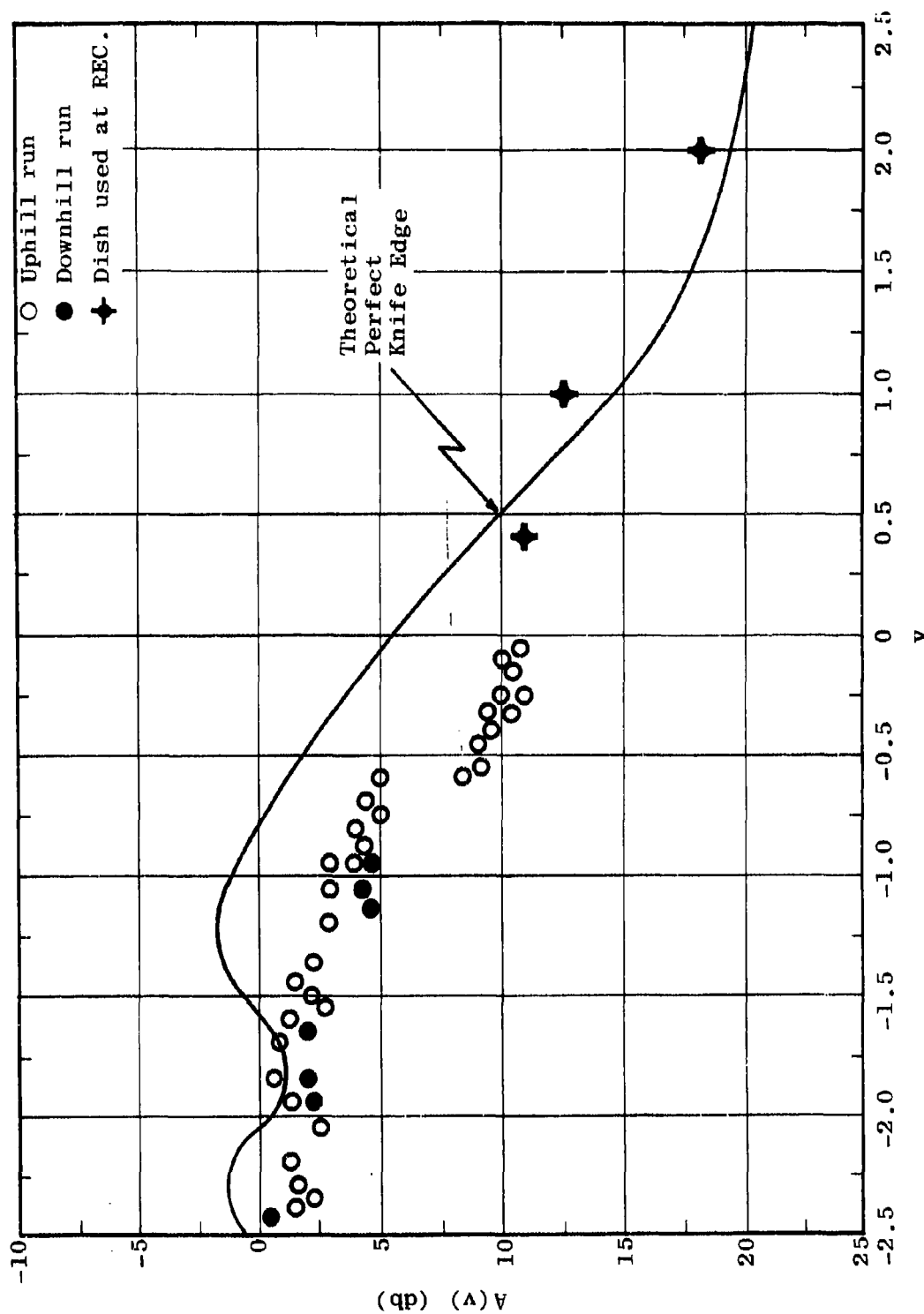


Figure 6.9 Measured Knife Edge Loss at 10.0 gc

and

$$L_{bf} = 36.57 + 20 \log f + 20 \log d \quad (13)$$

where

f = frequency (mc)

d = separation distance (mi)

The significant observation to be made from Figures 6.5 through 6.9 is the close agreement between the theoretical perfect knife-edge loss and the measured knife-edge loss. Since the obstacle used in the line-of-sight path deviated considerably from what would be considered a "perfect" knife edge, it is expected that there would have been even closer agreement if a "more perfect" obstacle had been used.

In conclusion, it can be stated that, although the foliage effects on knife-edge diffraction loss cannot be separated out, the combined loss introduced by all the factors mentioned above is not significant. Thus, the foliage effect itself is insignificant.

6.4 Diurnal Fading Data

Diurnal fading, the variation of signal level over a 24-hour period, is due primarily to changes in atmospheric conditions. In general, the fading range for beyond-the-horizon paths is much greater than for line-of-sight paths, and for either path the fading range ordinarily increases with an increase in either frequency or distance.

In the frequency range of 0.4 to 10 gc, fading considerations are important when designing circuits for a given grade of service. When the fading becomes significant, a common method of injecting fading effects into the reliability equation is to obtain the fading distribution function through measured data. The 10 and 90 per cent points of this function are then used as an input to the reliability equation.

The fading tests in Thailand were conducted over the same path that was used for the obstacle diffraction tests previously discussed. As noted in Figure 6.1, the path length is only about 3 miles. Unfortunately, this distance is not sufficient to provide a significant amount of fading, as noted in Figures 6.10 through 6.12. Output power limitation of the transmitting equipment was the dictating factor in determining separation distance.

Since the degree of fading experienced over the 3-mile path was small, the fading distribution function was not determined. A number of tests were run at each test frequency for different transmitter-receiver combinations. However, since the test results were the same, the results of all the tests are not presented. Figures 6.10 through 6.12 are representative of the data throughout the frequency range.

The basic transmission loss for the fading tests was determined from measurements which were made in the same fashion as the obstacle diffraction tests previously described.

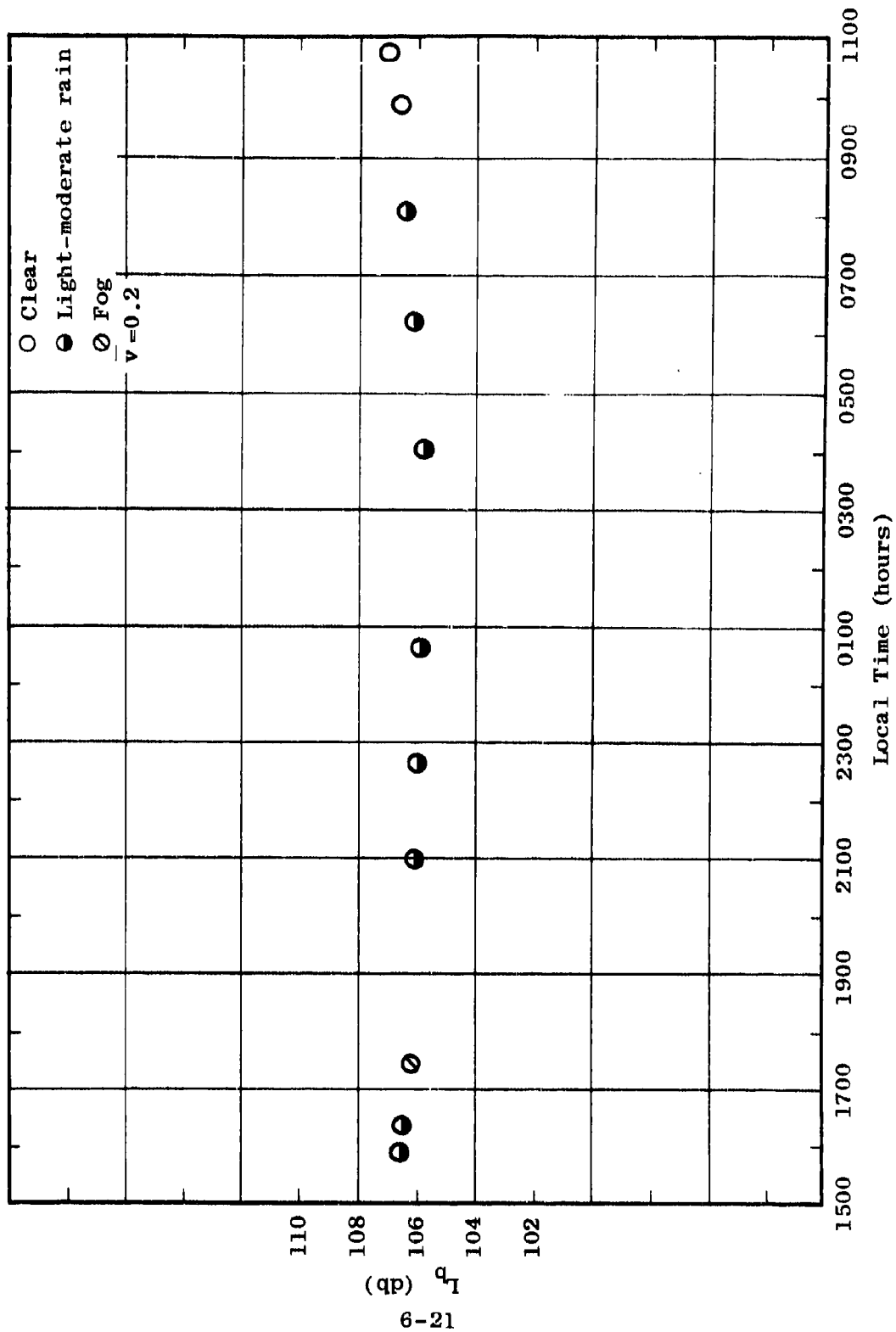


Figure 6.10 Diurnal Variation of L_p at 550 mc

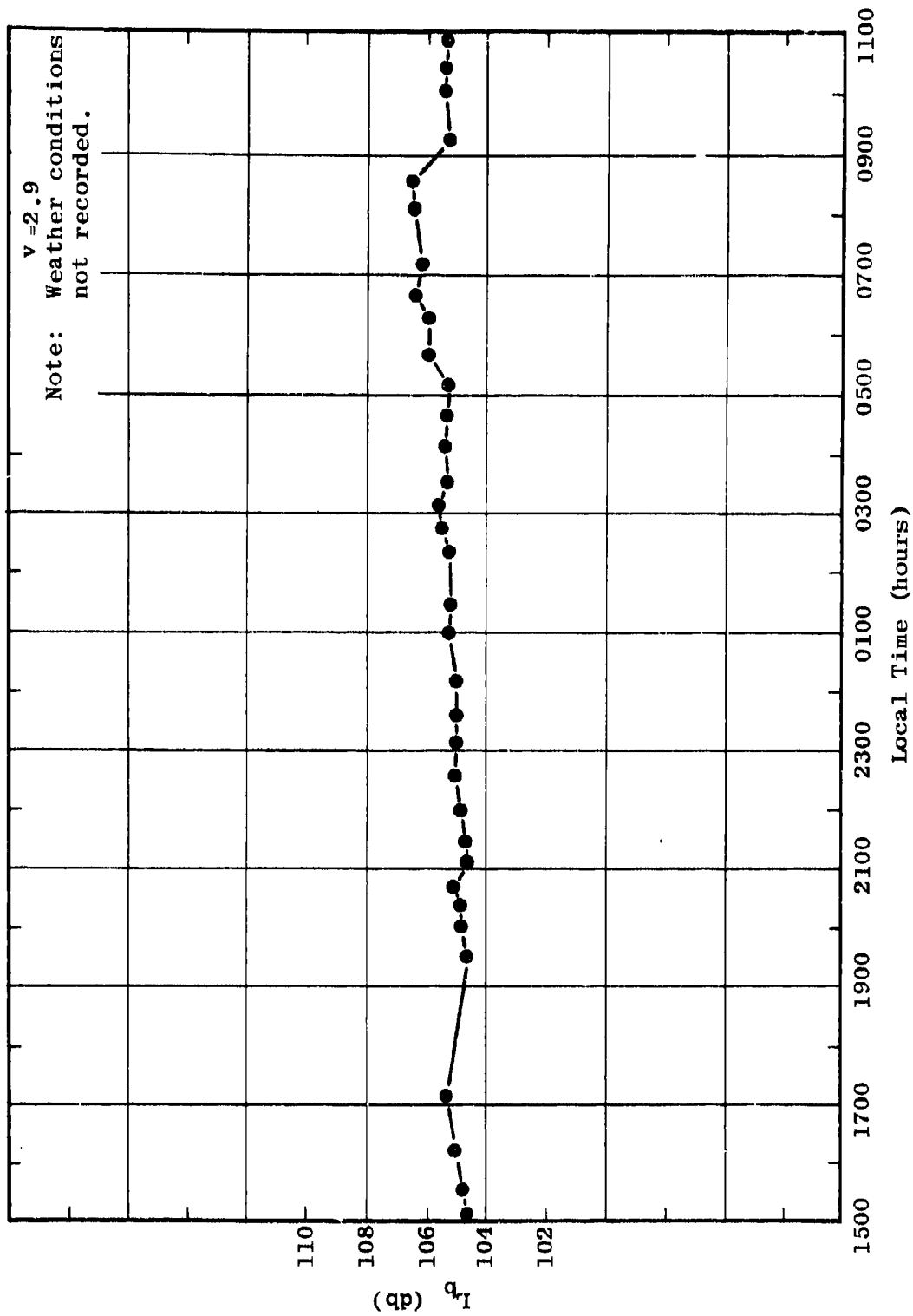


Figure 6.11 Diurnal Variation of L_p at 1.0 gc

The weather conditions that prevailed during the period of the run are shown on some of the fading curves. In some cases, weather conditions varying from clear to heavy rain were encountered with no significant deviation in the received signal. Since attenuation due to rain is known to be significant in the neighborhood of 10 gc, the failure to detect these effects in the tests is assumed to be due to the short path length involved.

6.5 Measurement Equipments and Techniques

The basic measurement setup used in the line-of-sight and diurnal fading tests is shown in Figures 6.13 and 6.14. The use of a signal substitution method at the receiving end of the system reduces the need of calibration factors to a minimum. It is not necessary to calibrate the field strength meter or to obtain antenna factors as was the case in the LF-VHF program. The only factors that must be predetermined are the transmitting and receiving antenna gains.

At the receiving end, the field strength meter is located at a fixed position and is connected to the receiving antenna through a long length of flexible coax. The receiving antenna, power meter and signal source are portable and may be set up at any of the nine receiver platforms.

Basically, the measurements are performed by turning on the system and recording the power meter reading at the transmitter end. At the same time, the receiving antenna is connected to the remote reading field intensity meter and the meter position noted. The receiving antenna

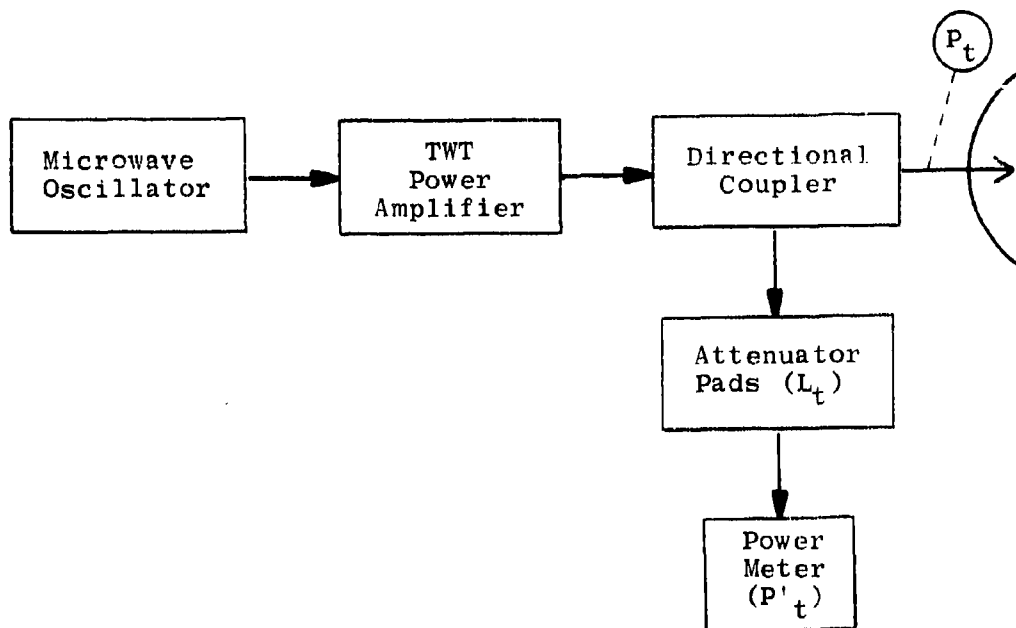


Figure 6.13 Transmitter Basic Block Diagram

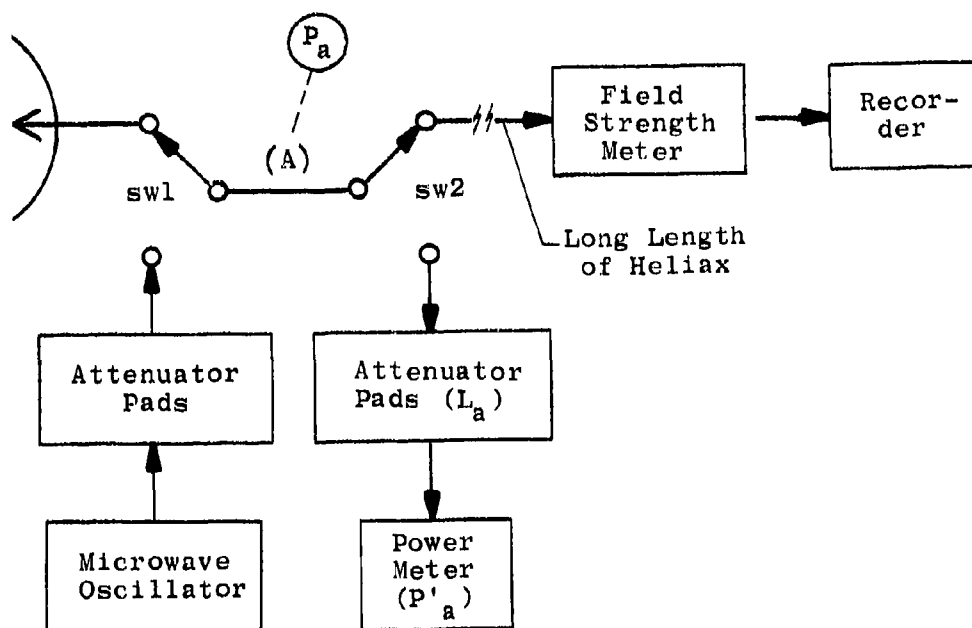


Figure 6.14 Receiver Basic Block Diagram

is then disconnected and the signal source connected to the field intensity meter. The power output of the signal source is then adjusted to obtain the same field strength indication that was previously obtained with the antenna connected. The power output of the signal source is then recorded. This power reading is the same as the power available at Point A of the measurement diagram from the unknown signal.

It is assumed that the power going into the transmitting antenna is totally radiated. This assumption is generally valid at microwave frequencies. The error attributable to this assumption would not exceed 2 db. In some cases, attenuator pads are inserted between the power meter and the transmitting antenna to obtain a reading. For such cases, this attenuation is added to the power meter reading to obtain the power radiated. At the receiver it is sometimes necessary to add attenuation between the signal source and the power meter to obtain the correct indication. This attenuation must likewise be taken into account when determining the power available at Point A of the measurement diagram. By simply knowing P_t , the power radiated; P_a , the power available at Point A; g_t and g_r , the antenna gains, the basic transmission loss can be calculated. Section 6.5.1 outlines the steps to take.

6.5.1 Conversion of Measurements to L_b

The parameters P_a and P_t which were determined by measurement in Section 6.5 are related to system loss by

$$L_b = 10 \log \frac{P_t}{P_a} \quad (14)$$

or

$$L_s(\text{db}) = P_t(\text{dbm}) - P_a(\text{dbm}) \quad (15)$$

where

L_s = system loss (db)

P_t = power delivered to transmitting antenna (dbm)

P_a = power available to receiving system (dbm)

Basic transmission loss is related to system loss
by

$$L_b = L_s + g_t + g_r \quad (16)$$

where

g_t = transmitting antenna gain referenced to
an isotrope

g_r = receiving antenna gain referenced to an
isotrope

The antenna gains were predetermined through separate measurements as outlined in Section 6.5.3.

Combining equations 15 and 16 gives the following equation for converting measured values to basic transmission loss.

$$L_b = P_t - P_a + g_t + g_r \text{ (db)} \quad (17)$$

When the insertion of attenuation is required at the transmitter end or at the receiver end, the general expression for L_b becomes

$$L_b = P'_t + L_t - P'_a + L_a + g_t + g_r \text{ (db)} \quad (18)$$

where

P'_t = power meter reading at transmitter end

L_t = inserted attenuation between power meter and antenna

P'_a = power meter reading at receiver end

L_a = inserted attenuation between power meter and Point A of measurement setup.
(See Figure 6.14.)

6.5.2 Mounting of Antennas

The transmitting antennas at T1 and T2 were mounted on permanent 40-foot towers to obtain a clear first Fresnel zone. At the receiver end, antennas were mounted on permanent wooden platforms at near-ground level. The area surrounding each antenna platform was cleared of foliage. The steepness of the hill then provided a clear first Fresnel zone. A servo-type antenna positioner was used at the transmitter towers to align the main beam. The main beam was sufficiently broad that on-axis alignment was easily obtained through the use of two-way communication between transmitter and receiver sites.

6.5.3 Determination of Antenna Gain

Several methods are available for determining antenna gain at microwave frequencies. The one chosen uses two identical antennas: one for transmitting and one for receiving. The power transmitted and the power received are recorded for any arbitrary separation distance ($d > 2d^2/\lambda$). The gain is then given by

$$G_t = G_r = \left(\frac{4\pi r}{\lambda} \sqrt{\frac{P_r}{P_t}} \right) \quad (19)$$

The test area used for antenna gain measurements was flat and free of reflecting objects. The antennas were mounted sufficiently high on wood towers 180 feet apart to provide first Fresnel zone clearance.

In some cases, different feed antennas are used for the same reflector. Thus, it was necessary to determine the gains of the reflectors by themselves. This was accomplished by first transmitting and receiving with identical antennas, both consisting of a dish fed by a horn. The power received was recorded, and the dish at the receiver removed. Then, the power, received using just the horn, was recorded. The difference in power readings, in db, represented the gain of the dish itself.

6.5.4 Antennas

At the transmitter, a reflector-type antenna was always used. This was not always the case at the receiving

end for the line-of-sight tests. To provide a large number of readings in a relatively short period of time, hand-held horn antennas without reflectors were used. The beamwidths were sufficiently wide that on-axis alignment could be achieved by hand. As a repeatability check, measurements were made both in an uphill and a downhill direction. For transmitting, a TACO model AS-544/U was used at test frequencies of 0.55 and 1.0 gc. This antenna consists of a grid-constructed reflector with a discone feed. For the remaining three test frequencies, an AEL, model APN-110B, consisting of a parabolic reflector with a log periodic feed, was used.

Polarad hand-held horns were used at the receiver. Models CA-M and CA-S were used to cover the frequency range.

6.5.5 Transmitting Equipment

Polarad modular signal sources were used for the microwave source of energy above 1 gc. The following model numbers were used at the test frequencies indicated: 2.5 gc, Model 1206; 5 gc, Model 1207; 10 gc, Model 1208. The power output of these sources varied from 25 mw at 10 gc to 50 mw at 2.5 gc. To boost the power at these frequencies, an AEL, Model T601, TWT amplifier was used. The signal source for the test frequencies of 0.55 and 1.0 gc was a Science Metrics Model ED 1241 UHF power oscillator. Since the power output of this device is 40 watts, no amplification was needed.

A Narda directional coupler was used to sample the power output of the signal sources. The following Narda

models were used at the test frequencies indicated: 0.55 and 1 gc, Model 3020; 2.5 gc, Model 3022; 5 and 10 gc, Model 3004-20. The power sensing device was an HP 478A thermistor mount. The power indicating device was an HP 431B power meter.

The frequency stability of the power sources was monitored by noting the output current variation of the oscillators. Retuning was carried out when the current variation exceeded a specified value. This method of monitoring eliminated the need of a transfer oscillator and frequency counter.

The output of the directional coupler connected directly to the transmitting antenna through a short length of Heliac coax cable.

6.5.6 Receiving Equipment

As described in Section 6.5, a signal substitution method of measurement is used at the receiving end of the path. To provide the power source for the known signal, the same Polarad oscillators described in the transmitter section above were used. Also, the power measuring equipment was identical to that employed at the transmitter. Attenuation capability was provided by fixed, Weinschel coaxial attenuators of 3, 6, 10 and 20 db.

For test frequencies from 1 to 10 gc an NF-112 field strength meter was used as the receiving device. Four tuning units, T1 through T4, were used to cover this

frequency range. For the test frequency at 0.55 gc, an NF-105 receiver with tuning unit, T3, was used.

For the 24-hour fading tests a continuous strip chart was made of the received signal. The recorder used was a Varian model G-11A.

7. REFRACTIVITY MEASUREMENTS

At microwave frequencies, the absolute value of path loss depends to a certain degree upon the vertical refractivity profile. The degree of dependence generally increases with both frequency and separation distance. It follows then that a change in the refractivity gradient can produce a change in the path loss. The magnitude of the path loss variation depends upon frequency, separation distance and severity of the change in gradient.

To obtain knowledge of the behavior of the refractivity gradient in a tropical environment, such as Thailand, two types of profiles are being obtained: in-foliage profiles from 10 to 80 feet (treetop level) and out-of-foliage profiles from about 70 to 1000 feet. In-foliage measurements, which are made for every 10-foot incremental change in elevation, will be used to determine if the presence of foliage affects the refractivity for elevations up to treetop level. Out-of-foliage measurements are intended to provide refractivity profiles in a tropical environment for elevations from treetop level to about 1000 feet. This type of data is useful in designing reliable microwave circuits.

Sufficient measurements are being made to provide diurnal and seasonal variations of the refractivity profiles. In an attempt to determine if there is a correlation between the diurnal fading of signal strength and the refractivity gradient, these tests were conducted at the same time as the diurnal fading tests mentioned previously. However, since no pronounced fading was observed in the field strength, no correlation analysis was made.

7

Since the analysis of the refractivity data has just begun, the measurement results presented in this section represent only a small segment of the over-all picture to eventually be presented. The following sections describe the measurement setup and present sample diurnal plots of the out-of-foliage refractivity profile.

7.1 Measurement Setup, In-Foliage Measurements

In-foliage measurements were conducted at a location very close to the present J&B base site. To obtain the 10- to 80-foot profile, the sensing equipment was attached to a telescoping tower identical to the ones being used to obtain vertical field-strength profiles. Readings were taken every 10 feet as the tower was raised and, also, as it was being lowered. The approximate time taken to complete a profile in one direction was about 30 minutes. This resulted in a reading about once every four minutes. The sensing equipment consisted of thermistors, one for sensing dry-bulb temperature and the other for sensing wet-bulb temperature. The wet-bulb thermistor was mounted in a "wet-sock" and air forced across by a battery-operated fan.

The dry-bulb thermistor was exposed to the ambient environment. The resistances of the two thermistors then varied in accordance with the temperatures of the two environments. A resistance bridge located on the ground and connected to the sensors by wires was used to determine the thermistor resistance and, hence, through calibration curves, the wet- and dry-bulb temperatures. A waiting period was required at each successive elevation level to allow the wet-bulb resistance to stabilize.

Profiles from about 70 to 1000 feet were obtained at a clearing near the T2 transmitter tower shown in Figure 6.1. The equipment used was an AN/UMQ-4 wiresonde set. The vehicle for housing the sensing equipment is a lighter-than-air device with lift surfaces attached. Thus, when flown with a wind, lift is obtained through two mechanisms.

The vehicle is connected by light cable to a play-out reel stationed on the ground. The cable is marked in length so that cable payout at any time is known. The height of the vehicle above ground is determined by noting the cable payout and measuring the elevation angle by the use of a clinometer at the mooring point. Greater precision in height determination could possibly have been obtained by using two clinometers at separate locations. However, the lack of cleared space in the area precluded the use of this technique. Clinometer readings were obtained during darkness by installing a light source aboard the vehicle.

Resistance bridge readings were obtained in a fashion identical to that described for the in-foliage measurements. Wires leading from the vehicle along the mooring cable to ground were used to connect the thermistor sensors to the bridge reading device.

Weather conditions, such as rain or lack of wind, often prevented the obtaining of a complete profile or, in some cases, the obtaining of any profile.

7.3 Sample Diurnal Plots

Two sample refractivity profiles showing diurnal variations are shown in Figures 7.1 and 7.2. Each plot is composed of data taken during four separate time blocks. Ideally, time blocks of constant duration with constant spacing between time blocks are desirable. However, due to weather limitations, time block consistency was impossible to maintain. The time blocks chosen for each of the sample plots consist primarily of two daytime blocks and two nighttime blocks.

For each time block, data was obtained as the wire-sonde was raised and again as it was lowered. The spread in the data, as observed on the sample plots, for a given time-block results from the time lapse between the increasing elevation run and the decreasing elevation run. The diurnal spread of the data is observed by noting the variation of the refractive index for the four time periods shown.

The preliminary observation that can be drawn from the sample plots is that the vertical refractivity seems to decrease with elevation in a fairly linear fashion when several time blocks are combined. The spread of the data appears to increase with a decrease in elevation.

A theoretical linear gradient is shown on the two sample plots. This gradient is a portion of the NBS standard atmosphere model⁸ for elevations up to 1 kilometer. This gradient is determined by the following expression.

8. B. R. Bean and G. D. Thayer, "A Model Radio Refractivity Atmosphere," NBS Report 5576; July 1958.

$$N = N_s + \Delta N(h-h_s) \quad (20)$$

where

N_s = surface value of refractivity

ΔN = $-7.32 \exp. (0.005577 N_s)$

h_s = height of earth's surface above mean sea level (feet)

h = height of point of interest above mean sea level (feet)

The value of N_s was determined by selecting a point which appeared to fit the data best. This, in turn, dictated ΔN , or the slope of the linear gradient.

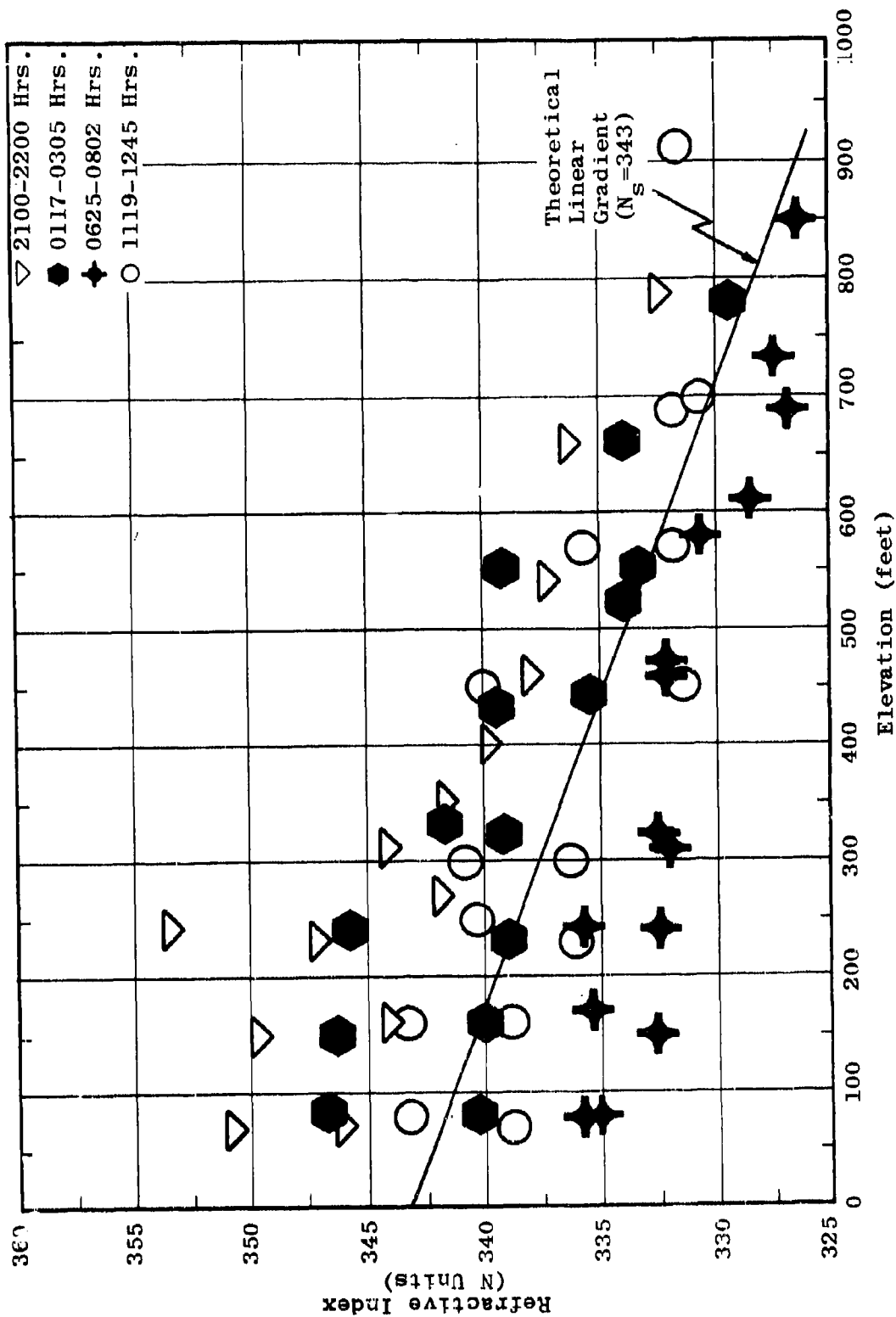


Figure 7.1 Diurnal Variation of Refractivity Profile (30-31 July 1965)

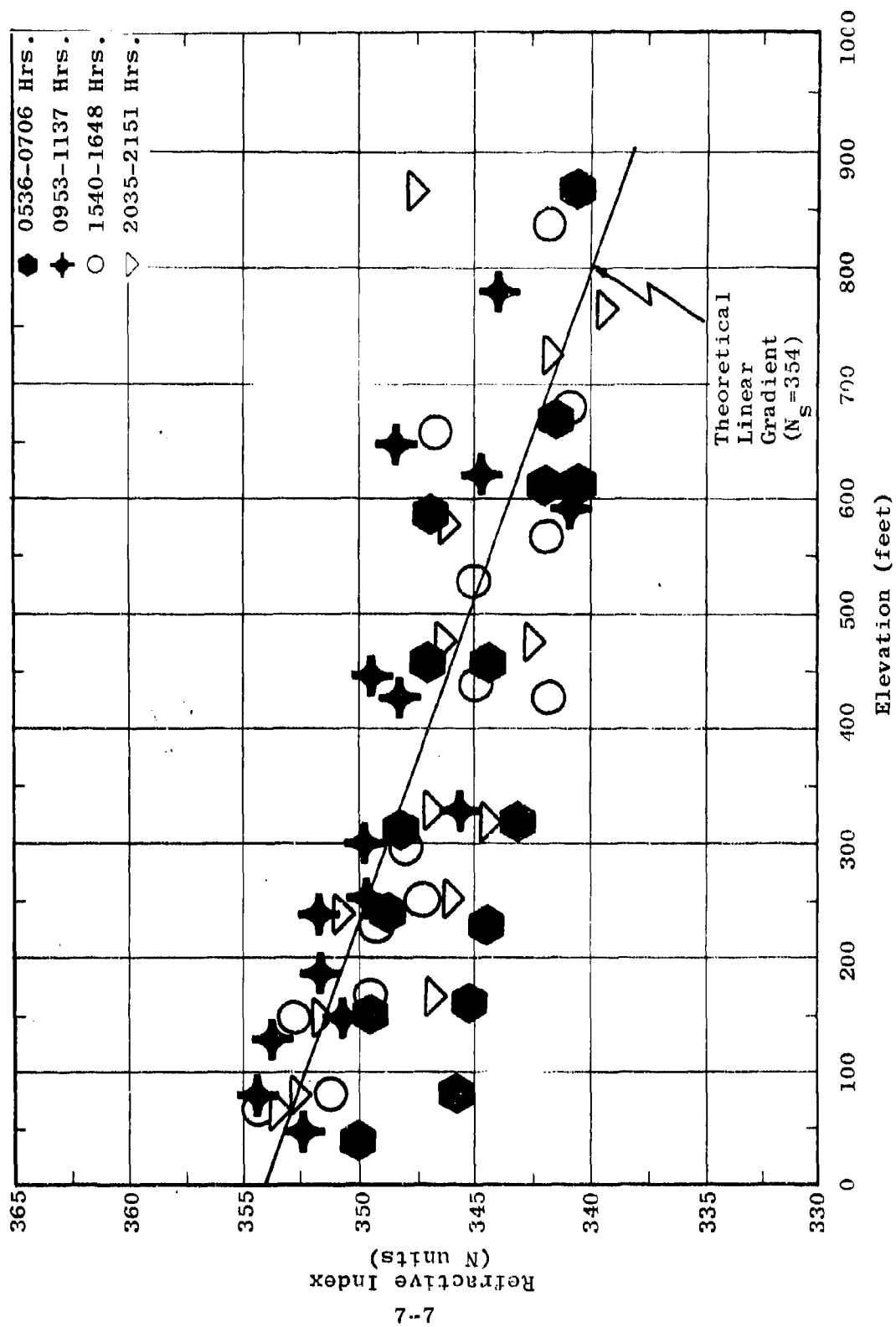


Figure 7.2 Diurnal Variation of Refractivity Profile (1-2 August 1965)

8. MEETINGS AND CONFERENCES

15 July 1965. Colonel Thomas W. Doeppner, Communications Program Manager, OSD/ARPA Field Unit, Vietnam, met with Atlantic Research personnel at the Principal Laboratories to be briefed on the over-all aims and general technical aspects of the Tropical Propagation Program.

20 July 1965. Messrs. L. G. Sturgill, Project Director, and K. G. Heisler, Project Engineer - Propagation, met at Fort Monmouth, New Jersey, with Messrs. Robert Kulinyi and Howard Kitts of USAECOM to review a pre-draft of Semi-annual Report Number 6.

23 August 1965. Jansky & Bailey personnel presented a review of the Tropical Propagation Research Program before ARPA and USAECOM representatives at the Pentagon. Program progress was outlined and tentative technical conclusions obtained from the data analysis were presented and discussed.

26 August 1965. ARPA and J&B personnel met at the Pentagon to plan and discuss a site survey to find a suitable location for Area 2 for the propagation measurements.

The technical data produced under this program is of interest to personnel of various government agencies concerned with radio propagation in tropical environments as well as to personnel of other organizations engaged in government-sponsored research in this field. In response to approved requests from such agencies and personnel, J&B has presented several technical briefings on the program,

concentrating on the audience's particular area of interest. During the month of August, these conferences have included a discussion at Aberdeen, Maryland, with representatives of TECOM; and briefings at the Principal Laboratories for Dr. Joseph deBettencourt and Mr. Carson Tsao of the Raytheon Corporation; Messrs. Irvin Page, Samuel George and Isaac Fuller of the Naval Research Laboratory; and Dr. James Chisholm and Mr. Louis A. DeRosa of Lincoln Labs.

1 September 1965. Mr. Howard L. Kitts of USAECOM met with J&B personnel in Alexandria for discussions of the 10-gc program.

13 September 1965. Mr. Lester G. Sturgill, Project Director, met with ARPA personnel at the Pentagon to discuss plans for a forthcoming site survey in Thailand with ARPA and USAECOM personnel.

24 September 1965. Mr. Robert Kulinyi of USAECOM met with J&B personnel at the ARC Principal Laboratories for a further discussion of plans for the Thailand site survey.

15 October 1965. Mr. Howard L. Kitts of USAECOM met with Jansky & Bailey personnel in Alexandria for a project review.

16 November 1965. Messrs. Frank T. Mitchell, Jr., Jansky & Bailey Research and Engineering Division Director; and Kenneth G. Heisler, Project Engineer - Propagation; met at Fort Monmouth with Major Alexander Sidon, COR, USAECOM-Thailand; and Lt. Col. John Valenti and Messrs. Robert Kulinyi, Howard Kitts, and Ron Herring, all of USAECOM; to discuss technical planning of the forthcoming Stanford Research

Institute XELEDOP measurements at the J&B test site.

17 November 1965. Messrs. Frank T. Mitchell, Jr., Jansky & Bailey Research and Engineering Division Director; L. G. Sturgill, Project Director; and K. G. Heisler, Project Engineer - Propagation; met with ARPA and USAECOM personnel at the Pentagon to discuss the results of the site survey trip to Thailand to select a potential second propagation test area.

19 November 1965. Major Percy Collom, OSD/ARPA RDFU Communications Project Officer; Major Alexander Sidon, COR, USAECOM - Thailand; and Messrs. Robert Kulinyi and Ron Herring, both of USAECOM; met at Atlantic Research Corporation Principal Laboratories with Messrs. Mitchell, Sturgill, and Heisler to discuss the results of a joint survey in Thailand to select the second area for the basic propagation measurements. Other technical aspects of the program were also reviewed.

10 December 1965. Mr. C. W. Bergman, of the Defense Research Corporation, met with project personnel at the Principal laboratories to discuss Semiannual Report Number 6. Also, aerial photographs of the Pak Chong area were loaned to Mr. Bergman for further stereographic study of the vegetation and terrain of this area.

19 December 1965. Messrs. L. G. Sturgill, Project Director; K. G. Heisler, Project Engineer - Propagation; and J. P. Kallenborn, Engineer; presented a seminar-type discussion of the program at the Institute for Telecommunications Sciences and Aeronomy, Boulder, Colorado. The purpose of these ITSA discussions is to exchange technical information and coordinate the various aspects of radio propagation

research, including the field under investigation in the
Tropical Propagation Research Program.

9. PROJECT PERSONNEL

The following personnel contributed to the program effort during the interval covered by this report:

R. W. Ayers	Field Technician
W. A. Backus	Engineer
S. L. Bailey	Vice President, Atlantic Research Corporation
R. F. Bass	Field Engineer
K. E. Bodle	Field Technician
R. S. Boswell, Jr.	Technician
J. E. Bruns	Engineer
C. O. Conway	Field Technician
H. R. Cozzens	Field Administrator, Thailand
R. H. Dawson	Field Technician
T. J. Deebel	Field Technician
J. E. Dodge	Engineer
L. L. Engle, Jr.	Data Technician
J. M. Fallon	Engineer
A. E. Goddard	Field Engineer
J. J. Grant, IV	Assistant Project Engineer, Thailand
R. W. Gross	Assistant Project Engineer, Thailand
E. M. Hake	Data Technician
K. G. Heisler	Project Engineer, Propagation
J. P. Kallenborn	Engineer
E. J. Knowles	Data Technician
C. R. Kocherhans	Field Technician
A. J. Kosko	Field Engineer
G. V. Lucha	Assistant Project Engineer, Thailand
Standish Marriott	Engineer
F. T. Mitchell, Jr.	Division Director
W. B. Munson	Engineer

J. D. O'Neale	Engineer
E. O. Parham	Field Technician
L. V. Pellettier	Assistant to Project Director
J. E. Pratt	Field Technician
D. L. Prisaznick	Engineer
S. M. Ragan	Engineer
R. J. Richey	Technician
R. G. Robertson	Field Engineer
W. C. Roehr, Jr.	Field Engineer
N. J. Schairer	Project Engineer, Instrumentation
W. P. Seneker	Engineer
L. G. Sturgill	Project Director
C. B. Sykes	Project Engineer, Thailand
I. A. Townsend	Data Technician
A. B. Wakelin	Technician
R. L. Weddle	Data Technician
Leslie Wengel	Technician
J. A. Wyand	Engineer
K. E. Zasowski	Field Technician

Appendix A
VEGETATION SURVEY REPORT
by
Edward N. Gladish
Forestry Consultant
Atlantic Research Corporation

INTRODUCTION

This report summarizes a survey of prospective locations for a second area for conducting radio propagation research measurements in Thailand.

The survey, which was concerned with the vegetation characteristics of the areas considered, was conducted jointly by the author and representatives of ARPA, USAECOM, the Royal Thai Government and Atlantic Research Corporation between 26 October and 16 November 1965. The author, with the invaluable assistance of Amnuay Kaosingha, Forester, ARPA RDFU-T, concentrated on the vegetation measurements while the other members of the party explored access, ownership and future land-use considerations.

Briefly, with the measurements at the present site at Pak Chong nearing completion, the purpose of the survey was to find a suitable second test measurement area in Thailand with significantly different vegetation characteristics from those at Pak Chong. This report describes basic procedures followed, sites surveyed, and data collected, and compares the vegetation characteristics of Pak Chong with those of a prospective second measurement area in southern Thailand.

GENERAL

Vegetation has long been recognized as a factor affecting radio propagation. More specifically, within present knowledge, total density and height characteristics of a forest are considered to be the primary vegetation features of interest in radio propagation. Accordingly, the survey was undertaken to quantitatively characterize the vegetation of prospective sites.

Comparisons of the radio propagation measurements made in two significantly different vegetation environments will thus provide quantitative knowledge of the effects of various types of vegetation on radio propagation.

The two methods used in the quantitative characterization of the forests surveyed were the relatively new concept of biomass, and classification according to tree density by canopy height.

The biomass concept, introduced by Dr. Lee T. Burcham of ARPA, is based on estimates of the total quantity of plant material per unit land area, usually expressed in terms of tons of plant material per acre. The estimate of forest biomass is an especially suitable tool for comparing prospective radio propagation sites because it provides a quantitative measure of the total vegetation of a tree or a group of trees. The relationship between tree diameter and biomass has been developed on an empirical basis and may be inexact in the absolute sense. However, the concept of biomass is used in radio propagation work in a relative sense and, for these purposes, is entirely sound.

Within these concepts, the primary purpose of the site survey was to find a second area in Thailand where the biomass factor is at least twice that of the Pak Chong area and where the trees are significantly taller. Other important considerations included topography, climate, and area size. It should be noted that the Pak Chong area has a biomass index of 1276 tons per acre. The site, classified as a "wet-dry" forest, consists of very dense second growth, vines, and occasional old-growth trees. Present conditions indicate that this area has probably been logged, burned, and possibly cultivated in the past. More detailed information on the vegetation characteristics of this site and a comparison of these characteristics with those of four plots in another area in Thailand are presented later in this appendix.

Nine locations, distributed over a very wide area of Thailand, were considered during the survey. Specific data on the eight which were considered unsatisfactory for this program is given at the end of this appendix.

AREA RECOMMENDED

The most promising area for a second site was found on the southwest coast of Thailand, between Trang and Satun, 3 miles north of the village of Ban U-Dai, about 40 miles west of Songkhla. The precise location of the area, as can be seen from the reduced portion of the Thai Welfare Department map included in this appendix, is 7°00' N and 99°55' E.

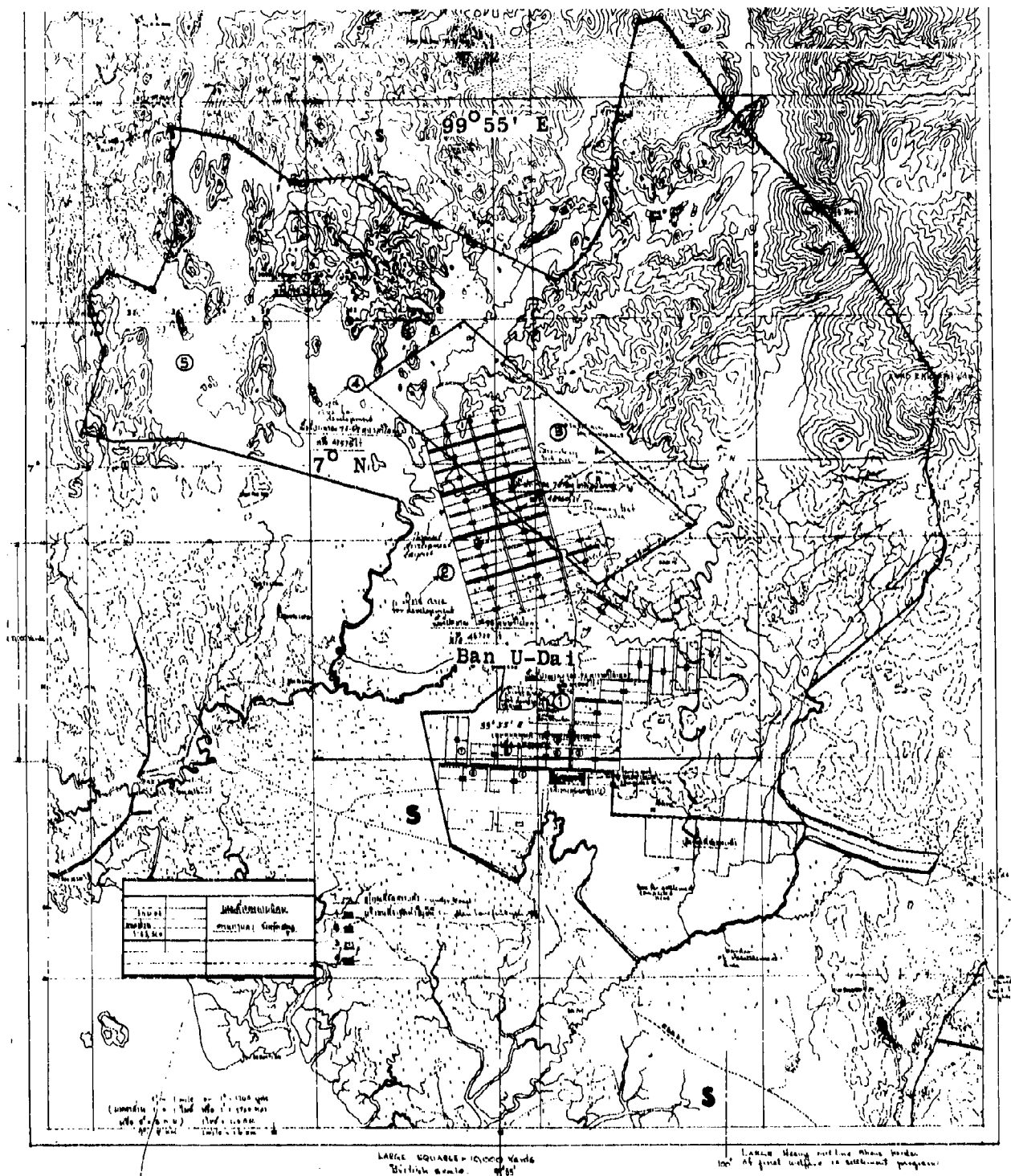


Figure A.1 Map of Proposed Measurement Location

This area is virtually inaccessible tropical rain forest. Four 400-square-meter plots at this site were chosen for measurement after several low-level inspection flights over the area and subsequent ground observation. Detailed information on each plot is presented in tabular form later in this appendix.

Three different forest types can be visually distinguished in the area on the basis of differences of tree density and tree height:

The first type, covering about 50 per cent of the area, is characterized by tree density and tree height in which the detailed measurements described later in this report were made. This type, therefore, becomes a reference with respect to these vegetation parameters. Within this forest type, the following tropical rain forest species were found to be common:

- Ficus spp.
- Hopea spp. (Takientrai)
- Areca spp.
- Dipterocarpus spp.
- Parkia spp.
- Calophyllum spp.
- Salacca
- Bamboos
- Rattan
- Vines
- Epiphytes

The second type covers approximately 30 per cent of the site. It has a higher density of very tall trees and is richer in palms than the first type. This type is in the northeastern corner of the area.

The third type consists of trees that are shorter than those in the first type and appears to contain fewer palms. This type is found in the south central portion of the area.

After the sampling sites were initially chosen by low-level inspection flights and later verified by ground observation, the location of four specific plots was determined by compass and tape computation, and trees on each plot were numbered consecutively. Although data from the RDFU-T Forestry Inventory Project indicates that areas 10 meters by 30 meters are adequate for sampling variations in tree diameter and height class in Thailand forests, plots 10 meters by 40 meters were used in this survey to conform with the sampling previously done at Pak Chong.

The following data was gathered for the four plots at Ban U-Dai:

- (1) Diameter at breast height (d.b.h.) of the trees to a minimum of 5 cm.
- (2) Height of trees, by Abney level instrument.
- (3) Canopy levels.
- (4) Upper canopy density.
- (5) Number of trees.

The vegetation characteristics of the potential site at Ban U-Dai and those of the Pak Chong site are compared in Table 1A.

Table 1A
SUMMARY OF VEGETATIVE CHARACTERISTICS
OF TWO SITES IN THAILAND

Characteristics	Unit	Location	
		Ban U-Dai	Pak Chong
Biomass	Relative Index	3086	1276
Total Trees	Per Acre	609	362
Height Class			
6-16 m	Trees/Acre	434	290
17-29 m	Trees/Acre	74	62
30-50 m	Trees/Acre	81	10
Vines	Vines/Acre	20	-
Upper Canopy Density	% Crown Cover	60-80%	20%

As can be seen, the biomass index at Ban U-Dai is more than twice that at the Pak Chong site. The average number of trees per acre at Ban U-Dai is 609, as opposed to 362 at Pak Chong.

The most distinctive characteristics of the Ban U-Dai site are the numbers and heights of the trees on the upper canopy (30-50 meters): 81 per acre at Ban U-Dai as opposed to 10 per acre at Pak Chong. When viewed vertically, the crowns of these upper canopy trees cover an estimated 60-80 per cent of the ground at Ban U-Dai; less than 20 per cent of the ground is covered by crowns of trees of this height at Pak Chong, as noted in Semiannual Report Number 6.

* From data collected by Forest Inventory Project (RDFU-T)

Table 2A

TREE DENSITY BY CANOPY HEIGHT CLASS - BAN U-DAI

Plot* Number	(1) Upper Level Canopy 30 - 50 m	(2) Second Level Canopy 17 - 29 m	(3) Third Level Canopy <17 m	Vines >5 cm d.b.h.	Total
2	10	6	19	3	38
3	10	8	49	2	69
4	5	7	61	1	74
<hr/>					
Avg/Plot	8.0	7.3	43.0	2.0	
Avg/Acre	81	74	434	20	609

* .400 square meters

Table 3A
TREE DENSITY BY CANOPY HEIGHT CLASS - PAK CHONG

Plot* Number	(1) Upper Level Canopy 30 - 50 m	(2) Second Level Canopy 17 - 29 m	(3) Third Level Canopy <17 m	Vines >5 cm d.b.h.	Total
1	0	1	34	-	35
2	0	0	36	-	36
3	0	8	23	-	31
4	3	13	17	-	33
5	1	13	20	-	34
5a	2	8	35	-	45
6	1	7	27	-	35
7	1	1	38	-	40
8	1	4	28	-	33
<hr/>					
Avg/Plot	1	6	28.8		
Avg/Acre	10	62	290		362

* 400 square meters except Plots 4 and 5a (600 square meters).
Data from Plots 4 and 5a proportionately reduced for uniformity.

The shading effect of this dense overstory at Ban U-Dai produces a ground cover that contrasts noticeably with that at Pak Chong. The extremely dense ground cover at Pak Chong consists of shrubs, herbs, and vines, whereas the ground cover at Ban U-Dai is composed of suppressed small trees (averaging 434 per acre), and moderately dense small shrubs. Rattan and bamboo are found occasionally in small sunlit openings.

CLIMATIC DATA

Data from the Meteorological Department of the Thai Navy (1956) indicates that precipitation in this area exceeds 50 mm in all months except January and February, when the average is slightly less than 50 mm. The long-term records during these two months show a variation from a few mm to several hundred mm per month. The data also indicates that this area receives precipitation from both northwest and southeast monsoons.

The Ban U-Dai area is in that section of Thailand with the highest average relative humidity (80-85 per cent). The annual evaporation is 800-1000 mm. The average monthly temperature is 26°-28° C for all months except December and June, when it averages 24°-26° C. The tall dense vegetation in this area would appear to be a product of this warm, wet climate.

FIELD DATA AND CALCULATIONS FOR FOUR PLOTS AT BAN U-DAI

Plot 1

<u>Tree No.</u>	<u>Girth (cm)</u>	<u>d.b.h. (cm)</u>	<u>Biomass</u>	<u>Canopy Level</u>	<u>Misc.</u>
1	41	13.0	1,140	3	
2	80	25.5	5,090	1	
3	18	5.7	188	3	
4	27	8.6	485	3	
5	18	5.7	188	3	
6	55	17.5	2,120	2	
7	15	4.8	122	3	
8	47	15.0	1,600	2	
9	20	6.4	188	3	
10	15	4.8	122	3	
11	82	26.1	5,625	1	
12	22	7.0	270	3	
13	176	55.9	34,000	1	
14	31	9.9	620	3	
15	20	6.4	188	3	
16	15	4.8	122	3	
17	17	5.4	122		Vine
18	21	6.7	270		Vine
19	27	8.6	485		Vine
20	25	8.0	360	3	
21	31	9.9	620	3	
22	28	8.9	485	3	
23	45	14.3	1,350	3	
24	36	11.5	770	3	
25	33	10.5	620	3	
26	81	25.8	5,625	2	
27	15	4.8	122	3	
28	219	69.7	57,000	1	
Total			119,897		

The accuracy of measuring the boundaries of this plot is in question because of difficulties with the measuring tape. Therefore, although the measured data is given above, the biomass index has not been used for calculations in Tables 1A and 2A.

Plot 1

Location...

From northerly edge of grass opening 3 kilometers northwest of Ban U-Dai run N 40° E 250 meters, then N 80° E, cross meandering stream, 300 meters to plot. Topography - flat.

Notes...

Canopy of very large tree (taller than 50 meters) just east of plot boundary shades portion of plot. This shaded portion is taken up with rattan (Dae monocrops). Nearby snag was found to be 80 cm d.b.h. and 45 meters in height.

Plot 2

<u>Tree No.</u>	<u>d.b.h. (in.)</u>	<u>d.b.h. (cm)</u>	<u>Biomass (kg)</u>	<u>Height (m)</u>	<u>Canopy Level</u>	<u>Misc.</u>
1	26.0	66.0	50,000		1	
2	2.5	6.4	188	7	3	
3	13.6	34.5	10,800		1	
4	6.4	16.3	1,830		2	
5	12.5	31.8	9,250		1	
6	7.8	19.8	3,050		2	
7	30.5	77.5	71,350		1	
8	6.2	15.7	1,830			Vine
9	4.5	11.4	770	10	3	
10	3.0	7.6	360	10	3	
11	12.5	31.8	9,250		1	
12	3.6	9.1	485	8	3	
13	17.9	45.5	20,600		1	
14	3.3	8.4	360	7	3	
15	20.7	52.8	30,050		1	
16	2.7	6.9	270			Vine
17	2.9	7.4	270	11	3	
18	3.6	9.1	485			Vine
19	4.5	11.4	770	15	3	
20	3.2	8.1	360	10	3	
21	5.2	13.2	1,140	19	2	
22	2.7	6.9	270	8	3	
23	4.2	10.7	770	14	3	
24	8.9	22.6	4,230		2	
25	14.2	36.1	12,300		1	
26	19.8	50.3	26,200		1	
27	3.0	7.6	360	10	3	
28	5.7	14.5	1,350		3	
29	15.5	39.4	14,800		1	
30	4.8	12.2	920	13	3	
31	5.0	12.7	1,140	14	3	
32	2.1	5.3	122		3	
33	5.2	13.2	1,140		3	
34	2.4	6.1	188	8	3	
35	2.5	6.4	188	8	3	
36	8.3	21.1	3,450		2	
37	3.5	8.9	485	12	3	
38	12.2	31.0	8,600		2	Leaning
Total			289,981			

Plot 2

Trees Per Acre...

38/400 square meters x 10.1 = 384 trees/acre

Location...

From Plot 1 run N 80° E along Thai Welfare Department survey line 450 meters to plot location. Creek borders easterly edge of plot. Plot oriented north-south direction. Topography - flat.

Notes...

Intense rain prevented accurate height measurements. Upper canopy estimated at 30-45 meters in height with 60-70 per cent density. Species include Hopea, Dipterocarpus, Parkia, and Calophyllum.

Plot 3

<u>Tree No.</u>	<u>d.b.h. (in.)</u>	<u>d.b.h. (cm)</u>	<u>Biomass (kg)</u>	<u>Height (m)</u>	<u>Canopy Level</u>	<u>Misc.</u>
1	9.9	25.1	5,090	13	3	
2	4.2	10.7	770	13	3	
3	6.5	16.5	1,830	16	3	
4	19.6	49.8	26,200	20+	1	Upper Canopy
5	2.5	6.4	188	7	3	
6	5.0	12.7	1,140	14	3	
7	2.2	5.6	188	7	3	
8	3.7	9.4	620	16	3	
9	8.6	21.8	3,840	20+	2	
10	4.9	12.4	920	16	3	Areca Palm
11	3.5	8.9	485	10	3	
12	3.4	8.6	485			Vine
13	7.2	18.3	2,400	20+	2	
14	2.9	7.4	270	9	3	
15	15.2	38.6	14,800		1	
16	3.1	7.9	360			Vine
17	2.1	5.3	122	8	3	
18	2.8	7.1	270	10	3	
19	8.4	21.3	3,450		2	
20	2.9	7.4	270	12	3	
21	3.0	7.6	360	9	3	
22	2.0	5.1	122	7	3	
23	3.1	7.9	360	10	3	
24	3.5	8.9	485	6	3	
25	25.0	63.5	44,400	20+	1	
26	4.2	10.7	770	16	3	
27	2.6	6.6	270	10	3	
28	2.7	6.9	270	10	3	
29	3.0	7.6	360	12	3	
30	15.0	38.1	13,900	20+	1	
31	5.9	15.0	1,600	20+	2	
32	2.0	5.1	122	7	3	
33	2.1	5.3	122	9	3	
34	2.0	5.1	122	6	3	
35	3.9	9.9	620	11	3	
36	2.0	5.1	122	8	3	
37	2.2	5.6	188	12	3	
38	27.4	69.6	57,000	20+	1	Dead
39	6.9	17.5	2,120	16	3	
40	3.3	8.4	360	14	3	

(Table is continued on next page.)

Plot 3 (continued)

<u>Tree No.</u>	<u>d.b.h. (in.)</u>	<u>d.b.h. (cm)</u>	<u>Biomass (kg)</u>	<u>Height (m)</u>	<u>Canopy Level</u>	<u>Misc.</u>
41	5.1	12.9	1,140	16	3	
42	3.0	7.6	360	10	2	
43	5.6	14.2	1,350	17	2	
44	3.6	9.1	485	13	3	
45	2.2	5.6	188	6	3	
46	18.9	48.0	23,900	20+	1	
47	3.4	8.6	485	9	3	
48	7.6	19.3	2,740		2	
49	18.5	47.0	22,700		1	
50	3.9	9.9	620	12	3	
51	2.3	5.8	188	9	3	
52	3.7	9.4	485	14	3	
53	3.8	9.7	620	6	3	
54	2.2	5.6	188	6	3	
55	6.3	16.0	1,830	14	3	
56	5.5	14.0	1,350	16	3	
57	6.8	17.3	2,120		2	
58	2.0	5.1	122		3	
59	4.1	10.4	620	15	3	
60	7.3	18.5	2,400	19	2	
61	4.5	11.4	770	9	3	
62	2.5	6.4	188	8	3	
63	11.8	30.0	7,900		1	
64	11.3	28.7	7,300		1	
65	11.3	28.7	7,300		1	
66	4.7	11.9	920	13	3	
67	4.1	10.4	620	14	3	
68	2.3	5.8	188	7	3	
69	2.2	5.6	188	6	3	
Total			276,636			

Plot 3

Trees Per Acre...

69/400 square meters x 10.1 = 697 trees/acre

Location...

From Plot 1 run N 80° E along Thai Welfare Department survey 250 meters to plot location. Plot is oriented in east-west direction adjacent to survey post 2. Southerly aspect with 5 per cent slope.

Notes...

Two upper level canopy trees near plot were 151 and 150 feet tall. Other upper level trees on plot were 145 and 153 feet tall.

Upper canopy 35-50 meters consisting of:

Hopea spp.
Dipterocarpus spp.
Parkia spp.
Calophyllum.

Middle canopy 20-35 meters.

Lower canopy less than 20 meters, mostly less than 15 meters consisting of:

Sapplings	Salacra
Palms	Wallchiana
Bamboo	Areca
Vines	

Plot 4

<u>Tree No.</u>	<u>d.b.h. (in.)</u>	<u>d.b.h. (cm)</u>	<u>Biomass (kg)</u>	<u>Height (m)</u>	<u>Canopy Level</u>	<u>Misc.</u>
1	21.1	53.6	31,300	42.8	1	NW corner
2	3.7	9.4	485		3	
3	5.2	13.2	1,140		3	
4	3.0	7.6	3 360		3	Vine
5	3.3	8.4	360		3	
6	3.8	9.7	620		3	
7	3.5	8.9	485		3	
8	2.9	7.4	270		3	
9	2.2	5.6	188		3	
10	2.6	6.6	270		3	
11	8.1	20.6	3,450	18	2	
12	2.6	6.6	270		3	
13	32.2	81.8	81,700		1	Hopea
14	21.2	53.8	31,300		1	Ficus
15	2.0	5.1	122		3	
16	5.0	12.7	1,140		2	
17	5.3	13.5	1,140		3	
18	2.6	6.6	270		3	
19	2.7	6.9	270		3	
20	8.3	21.1	3,450	17	2	
21	2.1	5.3	122		3	
22	4.0	10.2	620	7	3	
23	2.7	6.9	270		3	
24	2.5	6.4	188	6	3	
25	4.3	10.9	770	10	3	
26	7.8	19.8	3,050	17	2	
27	2.8	7.1	270		3	
28	3.5	8.9	485		3	
29	3.0	7.6	360	7	3	
30	3.6	9.1	485		3	
31	12.0	30.5	7,900	>30	1	
32	2.9	7.4	270		3	
33	5.2	13.2	1,140		3	
34	4.1	10.4	620		3	
35	2.5	6.4	188	6	3	
36	23.9	60.7	41,200	>30	1	On Trail
37	2.1	5.3	122		3	
38	2.1	5.3	122		3	
39	2.5	6.4	188		3	
40	4.5	11.4	770		3	

(Table is continued on next page.)

Plot 4 (continued)

<u>Tree No.</u>	<u>d.b.h. (in.)</u>	<u>d.b.h. (cm)</u>	<u>Biomass (kg)</u>	<u>Height (m)</u>	<u>Canopy Level</u>	<u>Misc.</u>
41	3.2	8.1	360		3	Vine
42	5.8	14.7	1,600	17	2	
43	2.1	5.3	122		3	
44	11.1	28.2	6,750		1	
45	5.7	14.5	1,350		2	
46	16.3	41.4	16,450	30+	1	Hopea
47	3.1	7.9	360		3	Takientrai
48	2.1	5.3	122		3	
49	2.3	5.8	188		3	
50	2.5	6.4	188		3	
51	7.1	18.0	2,400		2	
52	3.7	9.4	485		3	
53	7.5	19.1	2,740		2	
54	2.2	5.6	188		3	
55	3.7	9.4	485		3	
56	2.9	6.1	188		3	
57	7.6	19.3	2,740		2	
58	2.1	5.3	122		3	
59	4.3	10.9	770		3	
60	4.1	10.4	620		3	
61	3.5	8.9	485		3	
62	4.3	10.9	770		3	
63	3.4	8.6	485		3	
64	2.5	6.4	188		3	
65	4.7	11.9	920		3	
66	6.7	17.0	2,120		2	
67	2.1	5.3	122		3	
68	2.5	6.4	188		3	
69	2.7	6.9	270		3	
70	3.0	7.6	360		3	
71	4.2	10.7	770		3	
72	4.2	10.7	770		3	
73	8.0	20.3	3,050	20	2	
74	3.0	7.6	360		3	
Total			266,816			

Plot 4

Trees Per Acre...

74/400 square meters x 10.1 = 747 trees/acre

Location...

From northerly edge of grass opening 3 kilometers northwest of Ban U-Dai run N 40° E 240 meters, then due north 480 meters to plot location. Topography flat, plot oriented east-west direction.

Notes...

Typical under-level-canopy tree in northwest corner of plot measured 141 feet tall. Heavy shade from 70-80 per cent density upper canopy results in light undergrowth.

Upper canopy 25-50 meters consisting of:

Hopea spp.
Ficus spp.
Parkia spp.
Calophyllum

Middle canopy 10-20 meters.

Lower canopy less than 10 meters consisting of:

Bamboo
Rattan

OTHER AREAS CONSIDERED BUT FOUND UNSUITABLE

The sites listed below were also considered but for a variety of reasons were found unsuitable for the measurements planned for the second area.

1. Fifty kilometers northwest of Surat Thani (latitude $9^{\circ}30'$, longitude 99°) in southern Thailand.

Access: Good with jeep trail 5 miles from railroad.

Topography: Rolling 5-10 per cent, sharp ridges nearby.

Size: 2 miles - marginal
10 miles - not uniform, considerable logging and agriculture.

Biomass: Probably twice that of Pak Chong.

Weather: Thai weather data indicates two months below 50 mm.

Conclusion: Useful area not large enough.

2. Fifty kilometers southwest of Surat Thani (latitude 9° , longitude 99°) in southern Thailand.

Conclusion: Useful area not large enough due to agriculture and logging activities.

3. Surat Thani (latitude 9° , longitude 100°) in south-central Thailand.

Weather: Thai climatic data indicates all months average 50 or more mm.

Conclusion: Useful area not large enough.

4. Phatthalung-Trang area (latitude $7^{\circ}15'$, longitude 100°) in southern Thailand near ARPA Plots 114, 116, and 117.

Access: Very good - along Phatthalung-Trang road.

Topography: Rolling to flat with adjacent mountain.

Size: Inadequate, less than 1 mile.

Biomass: More than twice that of Pak Chong.

Weather: Thai climatic data indicates one month or less below 50 mm.

Conclusion: Useful area not large enough.

5. Kao Pong Chanuam area (12 miles south of J&B Pak Chong site).

Access: Some trails in area.

Topography: Rolling 5-25 per cent broken.

Size: 2 miles - ample vegetation but rough terrain
10 miles - broken terrain

Biomass: Upper canopy appears significantly denser than Pak Chong, lower canopy visible in many areas.

Weather: Thai weather data indicates three months below 50 mm.

Conclusions: Biomass probably significantly different than that of Pak Chong.
Terrain not suitable.

6. Rayong area (latitude $13^{\circ}15'$, longitude $101^{\circ}50'$) in southeastern Thailand.

Access: Some jeep trails in area.

Topography: Very flat and uniform, less than 5 per cent. Easily best site from terrain aspect.

Size: 2 miles - ample
10 miles - ample

Biomass: Only slightly more than that of Pak Chong. Probably not all-wet rainforest, trees appear to be showing stress. Many vines in openings - average canopy canopy (upper) about 40 per cent density. Very uniform area with little logging.

Weather: Thai weather data indicates three months below 50 mm - vegetation looks at least this dry.

Conclusions: Biomass lower than that of Ban U-Dai.
Not all-wet.

7. Pattani-Vale area (latitude $6^{\circ}30'$, longitude $101^{\circ}30'$).

Conclusion: Thai weather and topo maps indicate that this would be a potential test area, but land-use maps indicate that most flat areas are under intensive agriculture.

8. Northern Thailand.

Conclusion: Available vegetative and climatic data combined with field observation indicate that desired conditions probably do not exist in northern Thailand.

REFERENCES

1. Christensen, Kelley, Anan Nalampoon, and Sommart Sukhawong, Environmental Description 1 of the Jansky & Bailey Test Site at Khao Yai, Thailand, 66-015 Joint Thai - U. S. Military Research and Development Center; January 1966.
2. H. C. T. Whale, "Ground Aerials," M. Sc. Thesis; 1945.
3. J. W. Herbstreit and W. Q. Crichlow, "Measurement of Factors Affecting Jungle Radio Communications," Office of Chief Signal Officer, Operational Research Branch, ORB-2-3; November 1943.
4. J. J. Egli, "Radio Propagation Above 40 mc Over Irregular Terrain," Proc IRE; October 1957.
5. K. A. Norton, et al., "The Use of Angular Distance in Estimating Transmission Loss and Fading Range for Propagation Through a Turbulent Atmosphere Over Irregular Terrain," Proc. IRE; October 1955.
6. P. L. Rice, et al., "Transmission Loss Predictions for Tropospheric Communication Circuits," NBS Technical Note 101, Vol. I; May 7, 1965.
7. C.C.I.R. Study Groups, January 1965, p. III-15.
8. B. R. Bean and G. D. Thayer, "A Model Radio Refractivity Atmosphere," NBS Report 5576; July 1958.

Unclassified

Security Classification

DOCUMENT CONTROL DATA - R&D		
(Security classification of title, body of abstract and indexing annotation must be entered when the overall report is classified)		
1. ORIGINATING ACTIVITY (Corporate author) Atlantic Research Corporation Jansky & Bailey Research and Engineering Department Shirley Highway at Edsall Road Alexandria, Virginia 22314		2a. REPORT SECURITY CLASSIFICATION Unclassified 2b. GROUP
3. REPORT TITLE Tropical Propagation Research (U)		
4. DESCRIPTIVE NOTES (Type of report and inclusive dates) Semiannual Report Number 7, 1 July 1965 - 31 December 1965		
5. AUTHOR(S) (Last name, first name, initial) Sturgill, L. G., and Staff		
6. REPORT DATE January 1966	7a. TOTAL NO. OF PAGES 251	7b. NO. OF REFS 8
8a. CONTRACT OR GRANT NO. DA 36-039 SC-90889 b. PROJECT NO. AMC Code #5621-11-919-01-13 c. AMC Sub Task #1P620501 A 4480113 d. pertaining to ARPA Order #371		9a. ORIGINATOR'S REPORT NUMBER(S) 9b. OTHER REPORT NO(S) (Any other numbers that may be assigned this report)
10. AVAILABILITY/LIMITATION NOTICES Qualified requesters may obtain copies of this report from DDC. DDC release to CRSTI not authorized.		
11. SUPPLEMENTARY NOTES Report on experimental studies of RF propagation in tropically vegetated environments.	12. SPONSORING MILITARY ACTIVITY U. S. ARMY ELECTRONICS COMMAND FORT MONMOUTH, NEW JERSEY	
13. ABSTRACT This is the seventh semiannual report on a research program involving theoretical and experimental studies of the propagation of radio waves in tropically vegetated environments. The over-all purpose of this program is to provide basic information about radio propagation phenomena that can be used to improve communications equipment and techniques for military forces in Southeast Asia and other areas with similar environments. The first comprehensive series of measurements of propagation and environmental data has been obtained in a "wet-dry" tropically vegetated area in Thailand in the vicinity of the town of Pak Chong. Propagation measurements have been made at discrete test frequencies in the 100-kc to 10-gc range. (U) A major portion of this program is concerned with the collection and analysis of basic data on radio propagation in relation to the physical characteristics of the natural environment that influence propagation losses. These characteristics include terrain features, climate, vegetation, and radio noise. The quantitative effects of the environment upon radio propagation losses are being studied through correlation analysis. The information thus obtained will be used to develop a comprehensive model that will permit practical predictions of range performance of tactical mobile communications equipment in any tropical environment. (U) The field measurements originally planned in the 100-kc to 425-mc frequency range at Pak Chong were essentially completed during this reporting period. This report summarizes the results of these measurements and presents certain tentative conclusions which can be drawn from the work thus far. (U) A part of the field measurement program, not yet completed, has been devoted to measurements of line-of-sight propagation in the 400-mc to 10-gc frequency range over a well-defined, vegetated obstacle. This report presents the initial results of these measurements, including results from conjunctive measurements of the radio refractive index profile which were made with a balloon-borne wiresonde system. (U)		

DD FORM 1 JAN 64 1473

Unclassified
Security Classification

Unclassified
Security Classification

KEY WORDS	LINK A		LINK B		LINK C	
	ROLE	WT	ROLE	WT	ROLE	WT
Propagation Techniques Tropical Environment SEA - Southeast Asia Thailand - SEA Path Loss Climatology - Rainfall, Temperature, Barometric Pressure Antenna Height Transmission Distance						

INSTRUCTIONS

1. **ORIGINATING ACTIVITY:** Enter the name and address of the contractor, subcontractor, grantee, Department of Defense activity or other organization (*corporate author*) issuing the report.

2a. **REPORT SECURITY CLASSIFICATION:** Enter the overall security classification of the report. Indicate whether "Restricted Data" is included. Marking is to be in accordance with appropriate security regulations.

2b. **GROUP:** Automatic downgrading is specified in DoD Directive 5200.10 and Armed Forces Industrial Manual. Enter the group number. Also, when applicable, show that optional markings have been used for Group 3 and Group 4 as authorized.

3. **REPORT TITLE:** Enter the complete report title in all capital letters. Titles in all cases should be unclassified. If a meaningful title cannot be selected without classification, show title classification in all capitals in parenthesis immediately following the title.

4. **DESCRIPTIVE NOTES:** If appropriate, enter the type of report, e.g., interim, progress, summary, annual, or final. Give the inclusive dates when a specific reporting period is covered.

5. **AUTHOR(S):** Enter the name(s) of author(s) as shown on or in the report. Enter last name, first name, middle initial. If military, show rank and branch of service. The name of the principal author is an absolute minimum requirement.

6. **REPORT DATE:** Enter the date of the report as day, month, year; or month, year. If more than one date appears on the report, use date of publication.

7a. **TOTAL NUMBER OF PAGES:** The total page count should follow normal pagination procedures, i.e., enter the number of pages containing information.

7b. **NUMBER OF REFERENCES:** Enter the total number of references cited in the report.

8a. **CONTRACT OR GRANT NUMBER:** If appropriate, enter the applicable number of the contract or grant under which the report was written.

8b, 8c, & 8d. **PROJECT NUMBER:** Enter the appropriate military department identification, such as project number, subproject number, system number, task number, etc.

9a. **ORIGINATOR'S REPORT NUMBER(S):** Enter the official report number by which the document will be identified and controlled by the originating activity. This number must be unique to this report.

9b. **OTHER REPORT NUMBER(S):** If the report has been assigned any other report numbers (either by the originator or by the sponsor), also enter this number(s).

10. **AVAILABILITY/LIMITATION NOTICES:** Enter any limitations on further dissemination of the report, other than those

imposed by security classification, using standard statements such as:

- (1) "Qualified requesters may obtain copies of this report from DDC."
- (2) "Foreign announcement and dissemination of this report by DDC is not authorized."
- (3) "U. S. Government agencies may obtain copies of this report directly from DDC. Other qualified DDC users shall request through _____."
- (4) "U. S. military agencies may obtain copies of this report directly from DDC. Other qualified users shall request through _____."
- (5) "All distribution of this report is controlled. Qualified DDC users shall request through _____."

If the report has been furnished to the Office of Technical Services, Department of Commerce, for sale to the public, indicate this fact and enter the price, if known.

11. **SUPPLEMENTARY NOTES:** Use for additional explanatory notes.

12. **SPONSORING MILITARY ACTIVITY:** Enter the name of the departmental project office or laboratory sponsoring (paying for) the research and development. Include address.

13. **ABSTRACT:** Enter an abstract giving a brief and factual summary of the document indicative of the report, even though it may also appear elsewhere in the body of the technical report. If additional space is required, a continuation sheet shall be attached.

It is highly desirable that the abstract of classified reports be unclassified. Each paragraph of the abstract shall end with an indication of the military security classification of the information in the paragraph, represented as (TS) (S) (C) or (U).

There is no limitation on the length of the abstract. However, the suggested length is from 150 to 225 words.

14. **KEY WORDS:** Key words are technically meaningful terms or short phrases that characterize a report and may be used as index entries for cataloging the report. Key words must be selected so that no security classification is required. Identifiers, such as equipment model designation, trade name, military project code name, geographic location, may be used as key words but will be followed by an indication of technical context. The assignment of links, rules, and weights is optional.

Unclassified
Security Classification

SUPPLEMENTARY

INFORMATION

AD-486 499
Atlantic Research
Corp., Alexandria, Va.
Jansky and Bailey
Research and
Engineering Div.
Semiannual rept. no.
7, 1 Jul-31 Dec 65.
Jan 66
Contract DA-36-039-
SC-90889

No Foreign without
approval of Army
Electronic Command,
Fort Monmouth, N. J.

No limitation

USARV 147,
14 Mar 69